THE DYNAMIC REGULATION OF INTESTINAL STEM CELLS BY NOTCH SIGNALING

by

Alexis J. Carulli

A dissertation submitted in partial fulfillment
of the requirements for the degree of
Doctor of Philosophy
(Molecular and Integrative Physiology)
in The University of Michigan
2014

Doctoral Committee:

       Professor Linda C. Samuelson, Chair
       Professor Deborah L. Gumucio
       Associate Professor Ivan Maillard
       Professor Juanita L. Merchant
       Associate Professor Santiago Schnell
       Assistant Professor Yatrik M. Shah

This thesis is dedicated to my grandparents, Ben and Josephine Avimeleh
My thoughts turn to you at the most unexpected times
You are loved and greatly missed

ACKNOWLEDGEMENTS

TABLE OF CONTENTS

LIST OF FIGURES

LIST OF TABLES

ABSTRACT

THE DYNAMIC REGULATION OF INTESTINAL STEM CELLS BY NOTCH SIGNALING

by

Alexis J. Carulli

Chair: Linda C. Samuelson

The intestinal epithelium has one of the fastest cellular turnover rates in the body. To keep up with the constant demand for newly differentiated absorptive and secretory cells, the intestinal crypt contains a highly active intestinal stem cell (ISC) compartment. Presently, two populations of ISCs are thought to exist: the active crypt base columnar stem cell (CBCC) and slower-cycling quiescent stem cells (QSCs). Both populations of ISCs must be regulated to maintain intestinal homeostasis as well as accommodate cellular needs during times of intestinal growth, altered nutritional status, injury and repair. The Notch signaling pathway is one of many molecular messengers used to regulate these processes. Previous studies determined that Notch plays crucial roles in regulating differentiated cell fate, proliferation and CBCC survival. My thesis work has focused on understanding the specificity and kinetics underlying Notch regulation of CBCCs.

First, I used transgenic animal models to probe the specificity of Notch receptors in regulating intestinal homeostasis by conditionally deleting the Notch1 (N1) and/or Notch2 (N2) receptors in the intestinal epithelium. I discovered that N1 is the dominant Notch receptor regulating cell fate decisions, as deletion of N1 but not N2 led to a marked increase in secretory cell

production. Additionally, I showed that N1 is important for stem cell maintenance, as N1 deletion resulted in a loss of approximately half of the CBCC population. Furthermore, I determined that N1 is required for post-irradiation intestinal recovery, an important discovery that has clinical implications for targeted anti-Notch drugs as cancer treatments.

Our lab has shown that long-term (chronic) pharmacologic Notch inhibition with the drug Dibenzazepine (DBZ) leads to decreased CBCCs and decreased transit-amplifying (TA) cell proliferation, but the mechanism behind these changes was unknown. To approach these questions, I utilized a single dose of DBZ (acute treatment) to track the consequences of Notch inhibition on stem cells over time. Surprisingly, while acute DBZ did result in decreased CBCC number it also led to increased TA proliferation rather than the decreased proliferation observed with chronic DBZ. Like chronic DBZ, acute DBZ was sufficient to initiate a secretory cell differentiation program, suggesting that the increased proliferative cells were secretory progenitors. I devised a discrete compartmental mathematical model of the intestinal crypt to test several hypotheses to reconcile the proliferation differences observed with acute and chronic Notch inhibition. The model favored a mechanism where Notch signaling regulates both the symmetry of CBCC division into TA cells, as well as repopulation of the CBCC compartment, presumably by activation of QSCs. Further work investigating the role of Notch inhibition on QSCs suggests that Notch regulation of CBCC replacement is through regulation of the CBCC niche rather than direct regulation of QSCs.

In summary, my thesis work has further probed the role of Notch in intestinal epithelial homeostasis and CBCC maintenance. I show that loss of Notch signaling leads to a dynamic shift of CBCCs into the TA cell compartment and that N1 is the key receptor regulating these changes.

CHAPTER 1

INTRODUCTION[*]

Adult stem cells are crucial for maintaining proper function and repair of gastrointestinal tissues. The small intestinal epithelium is a complex tissue composed of a number of distinct differentiated cell types that must be continually replenished from rapidly dividing intestinal stem cells (ISCs) housed in the proliferative crypt region (Figure 1-1). The organized structure of the crypt as well as the fast rate of regeneration have made the intestine an ideal model for studying stem cell biology. ISC research not only aims to advance our understanding of stem cell physiology, but also to provide insight into intestinal pathologies. As ISCs are thought to drive intestinal and colorectal cancers[1, 2], understanding how aberrant stem cell regulation initiates such processes is a major interest in the field. Additionally, ISCs are required for epithelial repair after intestinal damage, such as exposure to irradiation and chemical mutagens[3-7]. Thus, investigating the repair response is important for managing radiation therapies and environmental exposures as well as developing treatments for intestinal disease. Finally, ISC tissue engineering provides hope for regenerative therapies that can treat lost or damaged intestinal tissue[8-10]. For all of these

---

[*] *Note this chapter is an expansion of the following published review article:*

Carulli AJ, Samuelson LS, and Schnell S. Unraveling intestinal stem cell behavior with models of crypt dynamics. Integrative Biology 2014; 6:243-57.
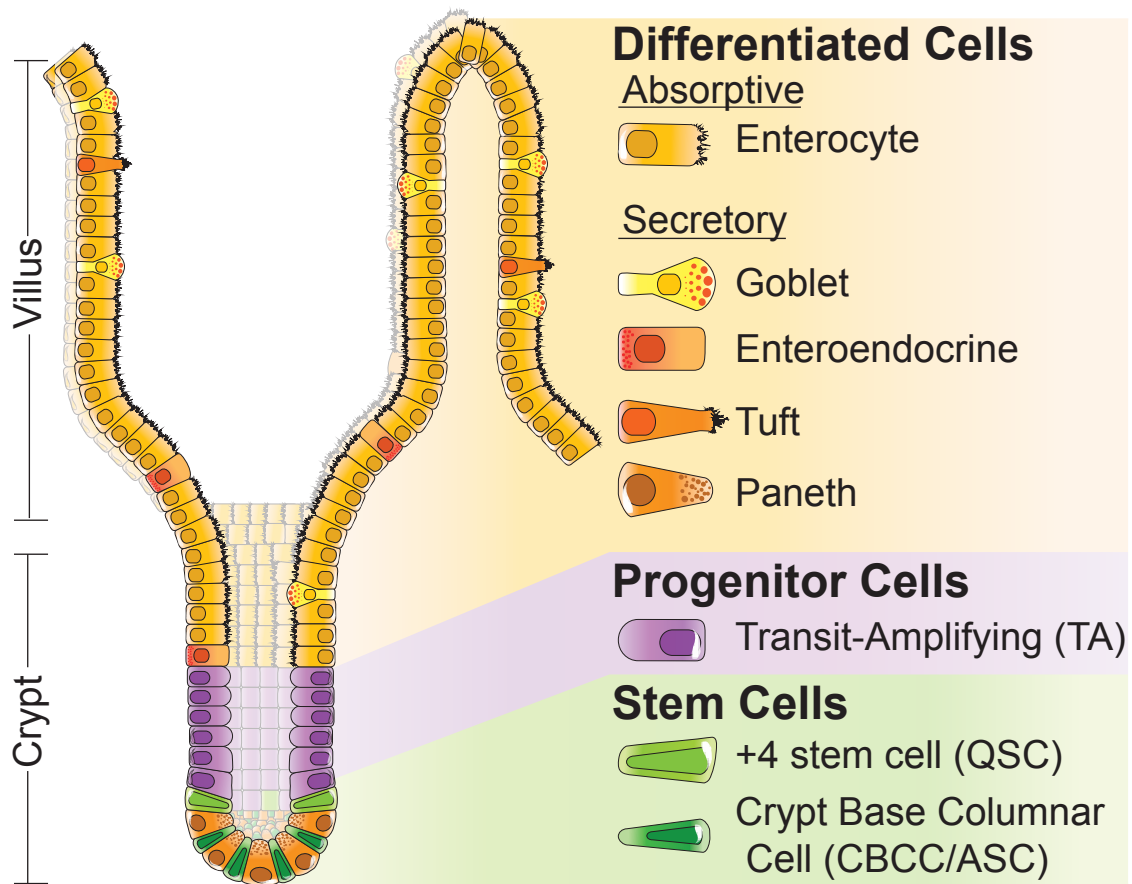
Figure 1-1. Intestinal epithelial structure and cell composition. The intestinal epithelium is organized into crypt and villus regions, with the stem and progenitor zone localized in the crypt. Current models favor the existence of two stem cell populations, the +4 stem cell and the crypt base columnar cell (CBCC), which are thought to be quiescent and active stem cells, respectively. Transit-amplifying (TA) progenitors arise from the stem cell compartment and differentiate into absorptive enterocytes or secretory goblet, enteroendocrine, tuft, or Paneth cells. Most of the differentiated cell populations migrate up the villi, but, uniquely, the Paneth cells move downward and reside between the CBCCs.

reasons, the impetus to unravel this cell's identity, function, and regulation remains a priority.

One of the greatest areas of interest in ISC biology is discovering the regulatory networks that modulate stem cell function. The Notch signaling pathway is a conserved cell-cell signaling pathway that is crucial throughout early development and organogenesis, as well as maintenance of many adult tissues[11, 12]. In the intestine, Notch has proven to be an essential regulator of proliferation, differentiated cell fate, and, importantly, stem cell maintenance[13-18]. Our understanding of how Notch regulates ISCs, however, is limited. Thus, the goal of this thesis is to present new investigation into the mechanisms behind Notch-regulated ISC homeostasis. Using transgenic mouse models, pharmacologic intervention, irradiation damage modalities and *in silico* mathematical modeling, the chapters ahead explore the sensitive dynamics of Notch regulation and the interconnection between ISCs and transit-amplifying (TA) progenitor cells.

To properly introduce these themes, Chapter 1 introduces three broad topics: (1.1) the history and current understanding of intestinal stem and progenitor cells and the genes that define and regulate them, (1.2) the Notch signaling pathway, (1.3) current efforts in mathematical modeling of the intestinal crypt. Finally, the chapter concludes with an overview of the experimental approaches and main findings obtained in this thesis (1.4).

1.1: INTESTINAL STEM AND PROGENITOR CELLS

A Historical Debate

There has been much debate over the location and identity of the ISC. Early studies suggested that the ISC was located approximately 4 cell positions from the base of the crypt, commonly referred to as the "+4 cell"[3, 19, 20]. Alternatively, it was proposed that crypt base columnar cells (CBCCs), small undifferentiated cells intercalated between the Paneth cells at the base of the

crypt, were the true ISCs[21, 22]. The prevailing theory today suggests that there are two stem cell populations in the intestine: an active stem cell (ASC) that is responsible for the bulk of proliferation and crypt maintenance, and a quiescent or reserve stem cell (QSC) that divides more slowly and is important for replenishing ASCs during crypt recovery after injury[6, 23, 24]. Recent findings, however, have called this two stem cell system into question, and thus a definitive catalog of ISC populations remains an active area of investigation[7, 25-27].

Early stem cell markers

Clearly, the way to reconcile the +4/CBCC cell debate was to identify a reliable marker that would allow for visualization, isolation and genetic manipulation of ISCs. The first method that allowed visualization of putative stem cells was retention of a radioactive tritiated thymidine label[21]. These "label retaining cells" (LRCs) localized to the +4 position of the crypt and were thought to be stem cells due to their long-lived nature, although no functional data was obtained to validate this hypothesis[3].

The development of *Vil1* promoter constructs capable of expression in all intestinal epithelial cells, including stem and progenitor cells, allowed the genetic manipulation of ISCs in transgenic mice for the first time[28, 29]. The capability to manipulate ISCs continues to be widely utilized to probe gene function for intestinal development or disease; however, the widespread *Vil1*-promoted transgene expression did not allow specific identification or manipulation of ISCs.

The first more specific molecular marker of ISCs was the RNA-binding protein Musashi-1, which was shown by antibody staining to be expressed in the same location as LRCs[30]. Musashi-1 is also expressed in CBCCs and lower crypt TA cells[31], which has limited its usefulness as a tool to manipulate specific stem cell populations. In 2007, the Wip1 phosphatase was shown to be expressed in ISCs and to regulate apoptosis and tumor formation at the stem cell level[1]. *In situ* hybridization and protein expression primarily localized Wip1 to the +4 position, but abundant CBCC labeling was observed as well, which has restricted its use as a specific stem cell marker[1].

Lgr5 marks CBCCs

In a landmark paper published in 2007, the leucine-rich-repeat–containing G-protein–coupled receptor 5 (*Lgr5)*, was found to be a specific marker of CBCCs[32]. The Clevers group functionally demonstrated that LGR5^{+} cells were stem cells capable of producing all of the mature cell types of the intestine[32]. This conclusion was achieved through lineage tracing, a technique that allows permanent activation of a reporter gene in a cell and all of its progeny and is the gold standard for defining a stem cell *in vivo*[33]. In addition, isolated LGR5^{+} cells were subsequently shown to produce intestinal enteroids, intestine-like tissue grown in perpetuity *in vitro*, another indication of this cell's stem-like function[34]. Importantly, activation of Wnt signaling in the LGR5^{+} cell population showed progressive formation of intestinal adenomas, a feature expected of aberrantly regulated stem cells[2]. Thorough quantitative studies have demonstrated that LGR5^{+} cells are highly proliferative, cycling approximately every 24 hours[32, 35]. This rate of proliferation confirms that if the LGR5^{+} CBCC is not the only stem cell population in the gut, it certainly is doing the bulk of the work, and thus has been indisputably considered the ASC. Notable additional markers subsequently identified for the ASC population include *Ascl2*[36], *Olfm4*[37], *Smoc2*[25], and *Sox9*[5, 38] (Figure 1-2) although a multi-scale stem cell signature analysis identified countless others[25].

The +4 cell as a quiescent stem cell

Although the LGR5^{+} CBCC had been established as the ASC, a surge of additional studies surfaced that continued to support the idea of a stem cell population that resides approximately in the +4 position. Immunostaining and lineage tracing studies identified a number of putative markers of this population including *Bmi1*[39, 40], *Lrig1*[41], *mTert*[42] and *Hopx*[43] (Figure 1-2). Of note, the gene *Dclk1* has been cited numerous times in the literature as a putative +4 stem cell marker[24, 44]; however other studies reported that *Dclk1* marks tuft cells, a differentiated cell type found in the stomach and intestine, rather than stem
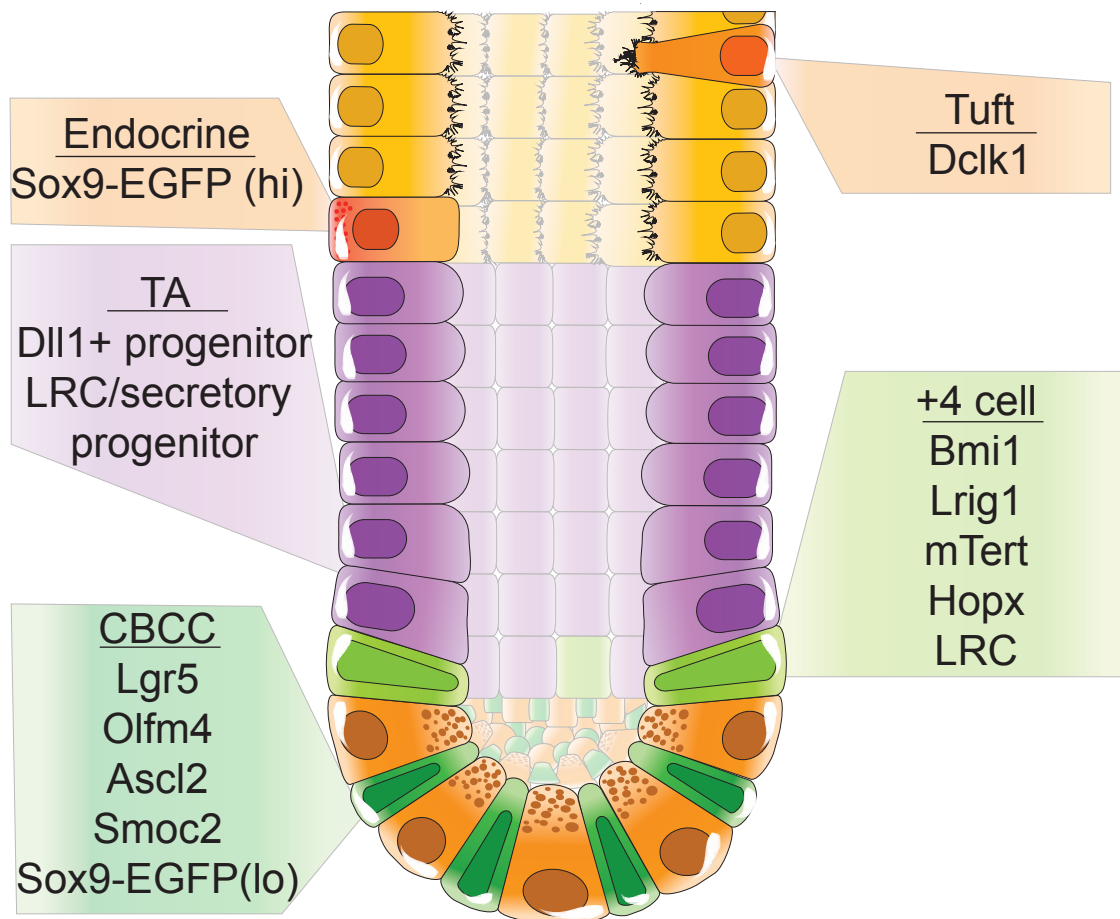
Figure 1-2. Intestinal stem cell markers. Molecular and functional markers that have been described for various proposed stem cell and potential stem cell populations. Of note, both TA cells and +4 cells have been shown to be Label Retaining Cells (LRCs). Sox9-EGFP ¬has been shown to mark both CBCCs and clonogenic enteroendocrine cells, depending on the level of EGFP expression. The gene Dclk1 has been proposed to be a stem cell marker, but it has also been shown to be a specific marker of differentiated tuft cells. It is possible that there is an independent +4 cell population that is also marked with Dclk1, but this has not been verified by lineage tracing.

cells[45-47]. Interestingly, recent lineage tracing studies showed that *Dclk1* might additionally mark tumor stem-like cells[48], although a new tumor expression study suggests that this might not extend to human intestinal cancers[49]. Although it is still unclear exactly what cells express *Dclk1*, it is likely that this gene is not useful for marking normal ISCs.

Similar to the *Lgr5* studies, the +4 cell lineage tracing experiments demonstrated that these markers were present in a stem cell population that was able to produce all of the differentiated intestinal cell types. Additionally, Wnt-activated LRIG1$^+$ cells showed even more aggressive adenoma formation than in the comparable LGR5 studies, again suggesting that these cells harbored stem-like function[41]. As opposed to ASCs, however, many of these cells were shown to cycle more slowly, furnishing the idea that these markers were identifying a QSC population[39, 41-43].

It is important to note that Potten's original studies did not suggest that the +4 cell was a quiescent cell population. Rather, it was thought that, like ASCs, this cell cycled approximately once per day and that the property of label retention was due to retention of an "immortal strand" of DNA that protected stem cells from accumulating mutations during DNA replication[23]. This hypothesis is highly controversial and has been challenged by several groups[50, 51]. In particular, Escobar et al.[50] combined mathematical modeling with careful pulse-chase labeling experiments to show that stem cells randomly sort their chromosomes. These findings further bolster the idea that the label retaining property of the +4 population is due to the cell being a long-lived, slower-cycling stem cell.

One predicted function of a QSC population is to act as a reserve stem cell compartment. This feature was demonstrated in a number of studies that showed activation of QSCs in the post-irradiation injury setting[5, 6, 43]. Additionally, specific ASC ablation with diphtheria toxin led to activation of BMI1$^+$ cells to generate differentiated intestinal epithelial cells. These QSCs appear to replace LGR5$^+$ cells, thus repopulating the depleted ASC pool[6, 40]. Similarly, isolated BMI1$^+$ cells were shown to create enteroids *in vitro* that ultimately contained

LGR5[+] ASCs[6]. Interestingly, ablation of BMI1^{+} cells with diphtheria toxin results in complete epithelial collapse, suggesting that, unlike ASCs, these cells are indispensible for epithelial homeostasis[39].

Together, these findings support a two-stem cell paradigm in the gut: the LGR5^{+} cell is the ASC that divides every day and supports homeostasis under normal conditions and the +4 cell is the QSC that usually divides slowly and only occasionally contributes to homeostasis at baseline. In an injury setting the QSCs are activated and expanded and allow for crypt repopulation and repair of the ASC pool.

Overlapping markers: the QSC dispute

Despite the abundant lineage tracing data that supports the idea that *Bmi1* and other +4 genes mark QSCs, there continues to be doubt that these cells are truly an independent stem cell population. Much of the argument originates from studies that find putative QSC markers to be expressed in ASCs. Sorted ASCs were shown to express high levels of *Bmi1* mRNA[36] and an independent study showed that ASCs expressed higher levels of *Lrig1* than any other cell in the epithelium[52]. A robust transcriptomic and proteomic approach that aimed to elucidate a definitive stem cell signature for the ASC showed that many QSC markers, including *Bmi1*, *mTert*, *Hopx*, and *Lrig1*, are not only expressed in the ASC, but single molecule transcript counting showed mRNA expression was located throughout the crypt rather than in a localized +4 cell population[25, 26]. To make matters more complex, Munoz et al.[25] was unable to replicate the lineage tracing data of Capecchi and colleagues[39] which showed that BMI1^{+} cells were predominantly located in the +4 position. Additionally, they observed that lineage tracing from BMI1^{+} cells occurred with similar kinetics as the ASC lineage tracing, calling into question the quiescent nature of this cell population[25]. Consequently, a molecular marker that uniformly and specifically marks +4 cells remains to be identified.

Transit-amplifying cells

Like most adult tissue stem cells, ISCs do not directly form the differentiated cell types of the intestine; rather, they contribute to an intermediate progenitor pool. These cells are referred to as transit- or transiently-amplifying (TA) cells because they divide approximately every 12-18 hours, 4-6 times prior to fully differentiating into the various epithelial lineages, fundamentally amplifying the population in the crypt[20, 53, 54]. Figure 1-3 shows the TA cell compartment and unanswered questions associated with this cell population. As TA cells divide it is assumed that they become committed to specific lineages and cell types, finally leading to mitotically-inactive fully mature absorptive or secretory cells as they migrate out of the crypt. The specific timing and nature of these differentiation events and how they might affect TA clonogenicity is largely unknown.

Early mutagenic marking studies showed that multipotent progenitors exist as well as progenitors committed to a single differentiated cell type[33]. It is well established that a binary decision occurs between absorptive and secretory cell fates, which is largely controlled by the Notch signaling pathway, however it is unclear exactly when and how this occurs[55]. Some studies suggest that this is the first decision of TA cells[13]. Others report that the specific type of secretory lineage is first determined, but that this differentiation trajectory can be aborted if the cell is later specified to be an absorptive cell[56]. Some studies have identified an intermediate cell with both Paneth and goblet cell features, which might suggest that these cells share a common progenitor[13, 57], although other studies describe a common Paneth/endocrine precursor[7]. Clearly, a definitive lineage fate map in the gut is still forthcoming. Additionally, it is unknown during which round of TA cell division these decisions take place. A paucity of specific markers or functional assays for different TA progenitors cells has been a stumbling block for progress on these fronts. Some markers like *Msi1*[30] and *Prom1*[58, 59] have been proposed, but these label both stem and progenitor cells,
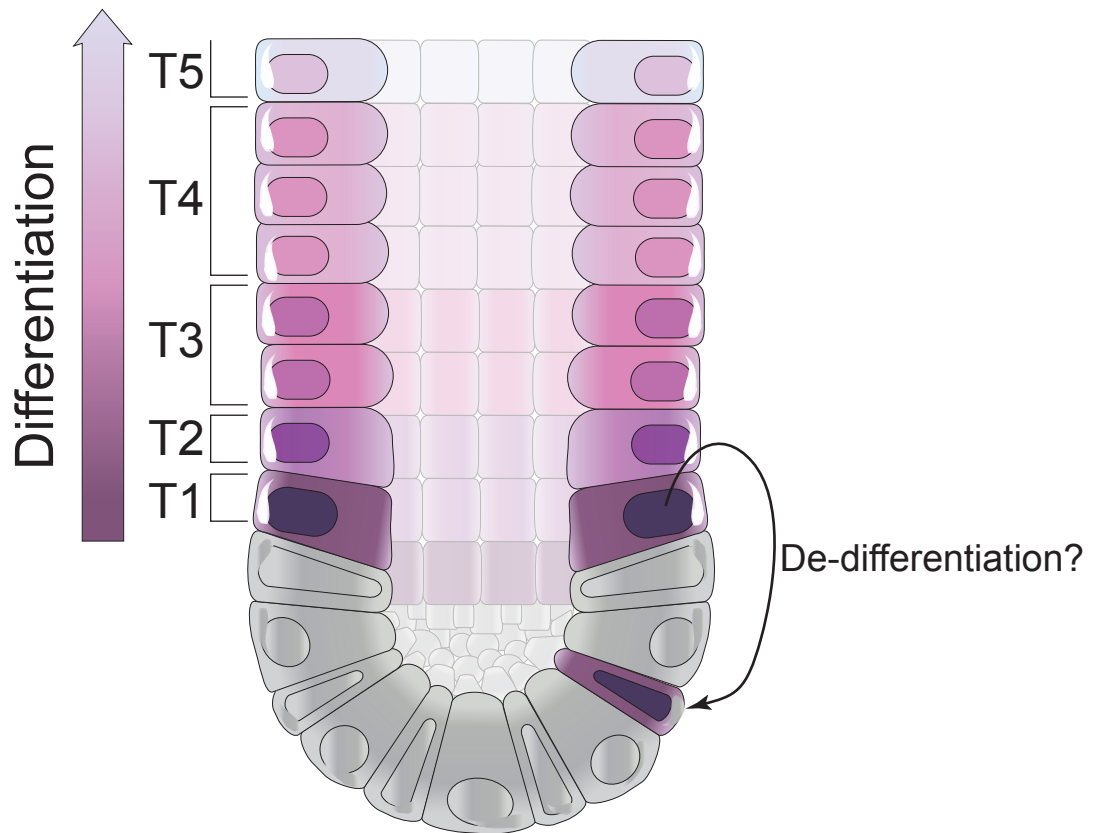
Figure 1-3. TA cell amplification and clonogenicity. Schematic of the TA cell compartment. Left: The TA cells are thought to divide 4-6 times, but the exact number and regulation of TA cell divisions is not known. Five rounds of division (T1-T5) are illustrated above with increasing numbers of cells in each subsequent division. TA cells are thought to become more differentiated during each division, but the details of this process are not well understood. Right: a TA cell is shown to de-differentiate and replace a lost CBCC (curved arrow). Exactly which TA cells possess clonogenicity is unknown.

and it is uncertain whether they differentially label TA subpopulations. Additionally, *Ngn3* marks TA cells that are fated to become endocrine cells[60], but this only applies to a small subset of the TA population. In Chapter 3, I use the gradient of GFP expression that exists in the crypt of the *Lgr5-GFP* mouse model to differentiate between stem cells and TA cells.

TA cells are facultative stem cells

Studies by Potten[20,61] indicate that TA cells possess potential stem cell capabilities in the event that the stem cells are lost or damaged. Irradiation studies suggest that the first two rounds of TA cell division possess some regenerative capacity[20]. Later TA divisions, however, were shown to have lost this capability, suggesting that this property is either cell age- or crypt location-dependent[20].

Recently, a cell expressing the Notch ligand *Dll1* was identified as a multi-potent progenitor cell that was definitively not a stem cell, as evidenced by its lack of robust lineage tracing and inability to form enteroids *in vitro*[27]. Interestingly, this cell population was shown to gain stem-like function by Wnt stimulation *in vitro* and crypt damage *in vivo*[27]. This study further supports the idea that early TA progenitors possess plasticity and can act as potential stem cells. Interestingly, other studies have shown a subpopulation of enteroendocrine cells in the crypt that co-express stem cell markers and seem to function as stem cells *in vitro* and *in vivo*[5, 62, 63]. This raises the possibility that committed TA cells or even fully differentiated cells may possess stem-like potential.

Recently, Winton and colleagues[7] returned to the approach of label retention to isolate and manipulate QSCs. In this study, LRCs were defined as non-Paneth cells in the crypt that retained a YFP label for 10+ days[7]. Isolation of these cells by FACS followed by transcriptome profiling showed that these LRCs were a distinct subpopulation of LGR5^{+} cells that expressed both secretory cell and stem cell markers. Using a clever split Cre construct and dimerization agent, Buczacki et al.[7] was able to lineage trace from LRCs and found that these cells contributed exclusively to differentiated Paneth and endocrine cell populations, a

property consistent with a bipotential secretory cell progenitor. Interestingly, with ASC injury the LRCs gained full clonogenic capacity and were shown to lineage trace into all differentiated cell populations[7]. This study supports the idea that there is not a dedicated population of QSCs, but rather a population of semi-differentiated progenitor cells that can act as a reserve stem cell population in the event of ASC loss.

Neutral drift dynamics and epigenomics

Many believe that stem cell identity is not cell-intrinsic, but rather a consequence of the local signaling environment, or niche, such that any cell within the niche will have stem-like properties. One heavily-studied aspect of crypt biology that has fueled this belief is the process of crypt monoclonality, where heterogeneous crypts, presumably fed by many stem cells, become derived from a single stem cell over time[35, 64, 65]. The Winton and Clevers groups have independently investigated this process by modeling the rate it takes for a lineage trace to encompass an entire crypt[35, 64]. These studies conclude that this occurs through neutral competition of stem cell progeny for niche space, or neutral drift[35, 64]. This finding implies that the progeny of a stem cell division event are not one stem and one non-stem daughter cell, but rather two identical cells that are only further defined by the niche available to them.

A recent study by the Shivdasani lab comparing epigenetic signatures of ISCs, secretory and absorptive progenitor cells, and differentiated cells showed that the genomes of these populations are largely primed to express the same transcripts[66]. The conclusion of this study extends the implications of the neutral drift dynamics findings to suggest that most cells in the crypt are able to interconvert depending on the niche signals available, and that lineage-defining decisions are not permanent changes[66].

In contrast, a recent report by the Kaestner lab also investigating the epigenetic changes that occur during intestinal differentiation came to different conclusions[67]. They find that DNA methylation by the DNMT1 methyltransferase is required for proper intestinal epithelial differentiation by repressing enhancers

involved in stemness[67]. The two studies together could suggest that epigenetic regulation is important for cell fate decisions and differentiation but that genomic flexibility remains to allow interconversion depending on niche signals.

Niche signaling pathways

Several signaling pathways are known to be important for intestinal epithelial homeostasis, and many of these have been implicated in forming and sustaining the stem cell niche (Figure 1-4).

Wnt signaling is important for stem cell establishment in the developing intestine, as well as crypt development during the postnatal period[68, 69]. In the adult intestine, Wnt responsive cells are stimulated by soluble ligands that are released from both the surrounding mesenchymal cells as well as crypt epithelial cells, leading to a Wnt activity gradient from crypt to villus[42, 69]. Wnt signal is required for stem and TA progenitor cell proliferation and has been implicated in regulating aspects of cell differentiation[70], likely through cross-talk with the Notch signaling pathway[69]. R-spondins are a family of proteins that potentiate the Wnt signal in the presence of Wnt ligand[71]. LGR5 itself is the receptor for RSPO1 and is thus inextricably linked to the level of Wnt signal that reaches the stem cell nucleus[72-74]. Indeed, exogenous WNT and RSPO are required for growth of *in vitro* enteroids[34, 75]. Interestingly, ASCs and QSCs appear to have different requirements for Wnt signaling, as ASCs depend on Wnt for survival, but BMI1$^+$ QSCs appear to be unaffected by Wnt repression[6]. Of note, aberrant Wnt signaling is observed in almost all cases of colorectal and intestinal cancers[68, 76].

The Notch signaling pathway plays a critical role in controlling lineage specification of differentiated cells in the intestinal epithelium; i.e. active Notch signaling leads to the formation of the absorptive lineage while absence of Notch results in secretory cell types[55]. Notch regulates intestinal proliferation, as blocking Notch reduces proliferation[18, 77] and Notch activation has been shown to increase proliferating cell number[17, 78]. In addition, Notch was recently shown to be essential for maintenance of ASC number and function[13]. Together these studies suggest Notch may be distinctly required for ASC maintenance and for
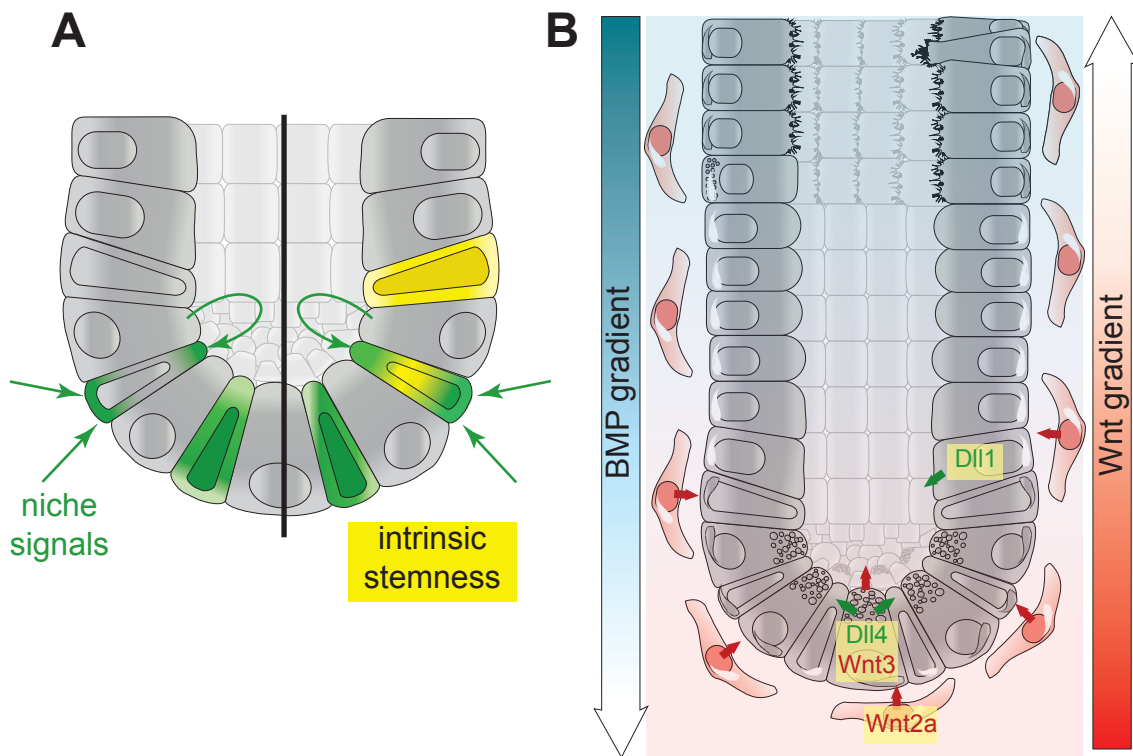
Figure 1-4. The stem cell niche. (A) An illustration of two opposing theories regarding the role of the stem cell niche. Left: The niche (green arrows) completely specifies the stem cell. Right: the niche partially specifies a cell that possesses certain features of intrinsic stemness (yellow). Only cells that acquire both extrinsic and intrinsic signals become stem cells. (B) Signaling pathways implicated in niche specification. Activation of the Bone Morphogenetic Pathway (BMP) occurs at a gradient that is higher in the villi and lower in the crypts. Conversely, Wnt activity is highest in the crypts. The Wnt gradient is established by secretion of Wnt ligands both from the mesenchymal myofibroblasts (WNT2a) as well as from epithelial cells. WNT3, in particular, is expressed in Paneth cells. The Notch signaling pathway is also critical for niche specification. Notch ligand presentation must occur from adjacent cells, and there is evidence that Paneth cells present DLL4, and that a subset of secretory progenitors express DLL1. It is unclear if other TA cell populations can present Notch ligand to stem cells.

TA cell fate. A more detailed description of the Notch signaling pathway will follow in section 1.2.

Other signaling pathways shown to be involved in intestinal homeostasis and development include Bone Morphogenetic Protein (BMP), Hedgehog, Hippo, Eph/Ephrin, and Epidermal Growth Factor (EGF)/ErbB. Many of these pathways play important roles in stem cell function and are likely contributing to the niche[69]. Briefly, BMP signaling occurs in a gradient in the epithelium, with the highest signal in the villi and the lowest at the base of the crypt[79]. Lower signaling levels are also associated with expression of the antagonist Noggin in the crypt region[79]. BMP appears to limit crypt formation and stem cell number as repression of the pathway with excessive Noggin results in aberrant crypt formation and tumors[80, 81]. Eph/Ephrin signaling is required for normal Paneth cell localization[82], which might have critical implications in niche formation as discussed below. The EGF pathway is important for regulating different cellular functions, including proliferation and differentiation, and has been shown to be important for the intestinal adaptation response post-resection[83]. The putative QSC marker LRIG1 is a negative regulator of EGF signaling[84, 85], which is consistent with the quiescent nature of these cells[41, 52]. Of note, recombinant EGF and BMP antagonist Noggin are growth factors required for enteroid culture[34, 75].

It is believed that many of these essential signals originate from the myofibroblasts in the mesenchyme underlying the epithelial basement membrane[86]. Recent studies, however, have challenged this mesenchyme-centric hypothesis. Evidence in a number of different tissues supports a model where stem cell progeny may also play an important role in defining the stem cell niche[87].

The Paneth cell as niche

Paneth cells secrete antimicrobial peptides and are thought to have a role in regulating host-microbial interactions[88]. Unlike other differentiated cells, which migrate up the villi and are sloughed off the tip on the order of 3-5 days, Paneth

cells migrate down to the base of the crypt, where they persist for approximately 3 weeks[89], perhaps longer[90]. In this position Paneth cells are in close association with CBCCs and thus have recently been implicated in specifying the stem cell niche. Over 80% of the CBCC surface area is in contact with neighboring Paneth cells[91]. As some niche signals, like Notch pathway components, are dependent on cell-cell interaction, the Paneth cell is the ideal candidate for ligand presentation. Indeed, expression-profiling studies suggest that Paneth cells express Notch, Wnt, and EGF ligands[91]. Additionally, the formation of epithelial-only enteroids supports the idea that mesenchymal signals may not be essential for niche formation[34]. In fact, LGR5$^+$ cell/Paneth cell doublets increased enteroid formation efficiency over 10-fold higher than LGR5$^+$ cells alone[91].

Opponents of this theory cite that these *in vitro* culturing techniques rely on a large number of growth factors for successful enteroid formation. As mentioned above, these include a BMP antagonist, Notch ligand, EGF, WNT3a and the Wnt potentiator RSPO1, as well as a synthetic basement membrane-like matrix; all factors that could be provided by the mesenchyme or other adjacent epithelial cells *in vivo*[34]. Additionally, several studies have shown that genetic deletion of Paneth cells does not have deleterious effects on the intestine[92-94]. Furthermore, colonic stem cells appear to function similarly to small intestinal ASCs but the colon does not contain Paneth cells, although a study by Rothenberg et al.[95] identified cKit$^+$ cells that may function like Paneth cells to support stem cells in the colon.

A recent study by the Clevers group[96] indicated that mesenchymal Wnt signals may in fact play an essential role. The study showed that a Wnt ligand secreted from the Paneth cell, WNT3, is essential for *in vitro* enteroid growth but deletion of *Wnt3 in vivo* does not affect homeostasis[96]. They identified WNT2B as a mesenchymal Wnt signal that could compensate for the lost WNT3 signal[96]. These results may explain why genetic models that lack Paneth cells may form a normal stem cell compartment. It is therefore very likely that a combination of epithelial and mesenchymal signals determine the stem cell niche.

A full understanding of the niche is critical for advances in *in vitro* tissue engineering technology. It is hoped that the use of *in vitro* systems will quicken the pace of discovery and allow more detailed signaling and mechanistic data to be discovered. Additionally, the use of human organoids is anticipated to allow easier translation of these findings into the human health context[97-99]. Since current enteroid culturing conditions employ undefined components like Matrigel, which are unlikely to ever receive FDA approval[100], all necessary external signaling and growth factors will need to be delineated before moving forward with applied clinical approaches.

Irradiation and stem cells

Irradiation-induced intestinal damage has been a widely used methodology for studying stem cell biology. As noted above, many QSC markers have been defined by their activation and expansion in the post-irradiation setting. Still, there is some debate over exactly how different ISC populations respond to irradiation damage. Originally, Potten described his +4 population as exquisitely sensitive to irradiation, dying at doses as low as 1Gy[3, 101]. This may suggest that the more recently discovered QSCs are not marking the same population, as they are not sensitive to low doses of irradiation. Additionally, although it was thought that ASCs were destroyed by moderate doses (8-12Gy), one report shows that some LGR5$^+$ stem cells not only survive irradiation treatment, but also possess enhanced non-homologous end joining to repair double-stranded DNA breaks caused by the damage[4].

Furthermore, combination of irradiation with diphtheria toxin-induced LGR5$^+$ cell ablation showed that ASC-deficient intestine can recover when less than 6Gy is applied, but doses above this threshold resulted in permanent intestinal damage[102]. Interestingly, ASC-deficient crypts were still able to mount a post-irradiation proliferative response, but crypt-fission activity and crypt organization was lost leading to intestinal architecture collapse[102]. This suggests that QSCs are still activated with irradiation damage, but the crypt cannot properly recover without ASCs.

Recently, LGR5^{+} cells were shown to express the receptor ROBO1 and its ligand SLIT2[103]. Treating mice with recombinant SLIT2 and the Wnt agonist RSPO1 leads to an increase in the number of LGR5^{+} stem cells, and surprisingly protects the intestine from chemoirradiation treatment[104]. This is further evidence that ASCs are required for irradiation recovery, and is a promising therapeutic avenue for protecting against irradiation damage.

Additionally, the Notch signaling pathway has been implicated in providing radioresistance in cancer stem cells, and Notch blockade improved the therapeutic response to radiation treatment[105]. This suggests that normal stem cells with Notch activity, like ISCs, likely have multiple mechanisms to resist radiation damage. In Chapters 2 and 3 I show continued evidence that Notch is required for ASC maintenance, as numerous forms of Notch inhibition result in inability to recover from irradiation.

Tamoxifen and stem cells

Most of the data that has been compiled in the field and reviewed above has been dependent on reporter activation in transgenic mouse model systems. These inducible Cre transgenics have revolutionized mouse genetics by allowing both temporal and spatial regulation of a gene of interest. Sensitive temporal control is achieved by fusion of the Cre recombinase to a modified ligand-binding domain of the estrogen receptor (CreER[T] and CreER[T2]), such that Cre is only translocated to the nucleus to induce recombination in the presence of synthetic estrogen antagonists[106-108]. The tamoxifen-inducible Cre/Lox system is essential for conditional activation of reporter genes in stem cells, but also allows for specific deletion or expression of a gene of interest.

Alarmingly, a new study calls into question experiments that have utilized tamoxifen as a method to activate stem cell lineage tracing. This study showed that tamoxifen alone was sufficient to induce apoptosis of both LGR5^{+} and LGR5^{-} cells located near the +4 region[109]. Previously tamoxifen had been shown to cause parietal cell apoptosis in the gastric epithelium, but this is the first report linking tamoxifen to stem cell damage[110]. In this study, apoptosis was a key

factor leading to lineage tracing from LGR5^{+} cells, as tracing events were strikingly reduced in genetic models that block apoptosis[109]. These results suggest that the LGR5^{+} cell might not be the true ASC after all, but rather a dependable replacement for loss of the true stem cell located at the +4 position. Interestingly, the evidence suggests that this highly-tamoxifen sensitive cell population is the same low-dose irradiation-sensitive population described in Potten's early studies[109].

In response to this finding, Winton and colleagues investigated the effect of high and low tamoxifen doses on stem cell clonality[111]. In contrast to the above report, they found no tamoxifen-dependent changes in clone number or size and concluded that tamoxifen was unlikely to cause stem cell death[111]. Because tamoxifen usage is ubiquitous in the field, it is clear that more research needs to be done to reconcile these findings.

Non-transgenic applications of ISC research

A chief goal of ISC research is to directly apply what is learned to treat human diseases. Since many of the approaches used in animal models rely on complicated transgenics that would be infeasible to replicate in humans, there is great interest in developing non-transgenic methods to identify and separate stem cells that could be used in the clinical setting.

One widely-used approach is antibody staining of human specimens to determine biomarkers for diagnosis and prognosis of diseases. Accordingly, many ISC markers have recently been associated with colon cancer progression and outlook. *LGR5* expression, for instance, is increased in tumors compared to normal neighboring tissue[112, 113] and higher levels of *LGR5* are linked with chemotherapy resistance[114]. Expression of *OLFM4* was shown to differentiate between serrated sessile lesions and other colorectal cancer types[115] as well mark cancers associated with improved survivability[116]. The QSC marker *BMI1* also displays increased expression in colorectal tumors[117] and higher levels of *BMI1* are associated with worse outcomes[118].

Aside from merely identifying the presence of stem cell markers in human tissues, there is great interest in actually isolating ISCs from patients to analyze, expand, or modify *ex vivo*. One method that has been attempted to achieve this is side population sorting, a technique that separates populations of cells that have low retention of a dye, like Hoescht, with fluorescence-activated cell sorting (FACS). This system was first discovered in hematopoietic stem cells[119, 120] and relies on the expression of the ABCG2 efflux transporter, which has been found to distinguish a number of different tissue stem cells[121]. The Henning group has adapted this approach to investigate ISC populations[122]. They have found that there are two groups of side population sorted cells, an upper side population and lower side population[122]. The upper side population was found to contain a large percentage of proliferating cells as measured by incorporation of the thymidine analog 5-ethynyl-2´-deoxyuridine (EdU). In contrast, the lower side population had almost no EdU uptake and is thus presumed to be a quiescent population. Combined studies using the *Lgr5-GFP* mouse demonstrated that the LGR5$^+$ cells were almost exclusively localized in the upper side population. Transcript analysis of the populations showed expression of both ASC and QSC markers in the upper side population, which is not surprising due to the overlap in marker expression discussed above. In contrast, the quiescent lower side population was enriched with QSC markers. Thus, this technique is a promising way to separate different ISC populations based on cycling rate rather than marker expression that can easily be applied to human tissue.

ISCs: a work in progress

In summary, although much has been discovered about ISCs, many questions and controversies continue to divide the field. The largest dispute concerns the existence and function of QSCs and how these cells may overlap with ASCs and progenitor cells. Other questions include regulation of ISC number, required niche signals and their origin, and ISC injury response. This thesis addresses many of these themes by investigating the specific Notch receptors required for stem cell maintenance (Chapter 2), ASC and TA plasticity

(Chapter 3-4), and the requirement of Notch for post-irradiation epithelial recovery (Chapter 2-3).

1.2: THE NOTCH SIGNALING PATHWAY

A direct cell contact pathway

As shown in Figure 1-5, Notch signal requires the interaction of two neighboring cells, a signal-receiving cell that expresses the transmembrane Notch receptor and a signal-sending cell, which expresses a transmembrane Notch ligand. In mammals there are 4 Notch receptors (Notch1-4) and 5 ligands (Delta-like1,3,4, Jagged1-2)[123], all of which have variable temporal-spatial expression. Successful interaction of receptor and ligand results in the Notch intracellular domain (NICD) being released and transmitted to the nucleus where it can activate target gene transcription. No secondary messengers are generated by the signal and the Notch receptor is destroyed in the process[124], thus generating a short-lived transcriptional signal to instill Notch effects.

Notch receptor activation and regulation

The Notch receptor undergoes many modifications and enzymatic cleavage events along the path to activation, which can modulate Notch signaling. In the ER, glycosylation of the Notch extracellular domain (NECD) occurs, catalyzed by the enzyme *O*-fucosyltransferase (*O*-FUT), which adds a fucose moiety and acts as a chaperone for the receptor[125, 126]. Additional fucose and glucose modifications subsequently occur in the trans-Golgi network mediated by Fringe proteins[127]. In mammals there are three Fringe proteins: Lunatic, Manic and Radical Fringe, which have varied and non-redundant activity in a number of tissues[128]. The accumulated number and location of glycosylation events function to alter receptor-ligand interactions[124]. In fact, two independent

21
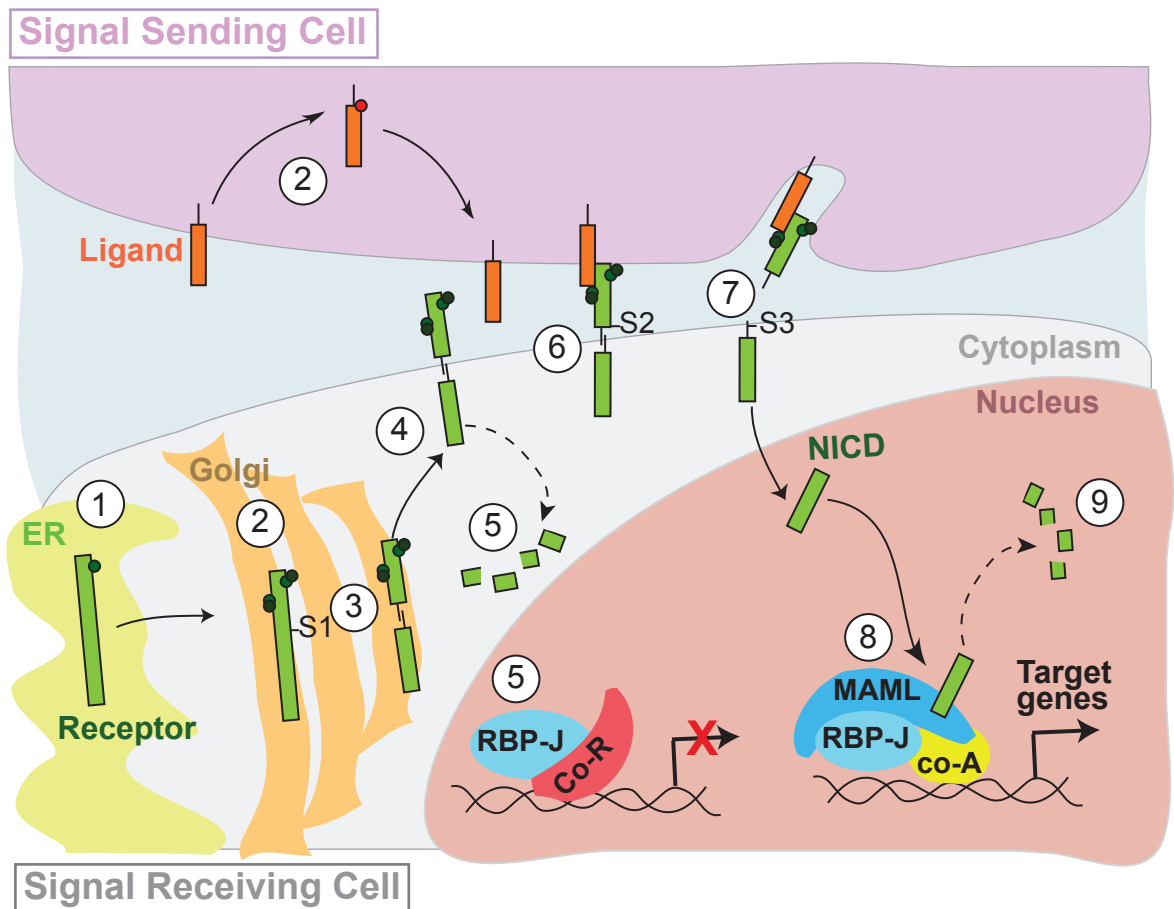
Figure 1-5. The Notch Signaling Pathway. (1) The immature Notch extracellular domain (NECD) is fucosylated in the ER by O-FUT. (2) Further glycosylation of NECD occurs in the Golgi by FRINGE proteins. Meanwhile, ubiquitin modifications by MINDBOMB result in ligand recycling and maturation. (3) FURIN-mediated S1 cleavage of the receptor results in mature Notch intracellular domain (NICD) and NECD. (4) The mature receptor is trafficked to the membrane chaperoned by O-FUT. (5) In the absence of ligand activation, ITCH mediates degradation of Notch receptor. Meanwhile, in the nucleus RBP-J associates with co-repressors blocking transcription of Notch target genes. (6) Binding of receptor and ligand exposes the S2 site, which is cleaved by ADAM proteases, releasing NECD. (7) NECD is trans-endocytosed with ligand by the signal-sending cell. S3 cleavage is catalyzed by the gamma-secretase complex. NICD is released from the membrane. (8) NICD translocates into the nucleus where it binds to a co-regulatory complex activating transcription of Notch target genes. (9) The Notch signal is terminated by CDK8 through NICD phosphorylation and degradation.

groups used hybrid receptor constructs composed of mis-matched NICD/NECD pairs to demonstrate that differences in Notch receptor activity is primarily attributed to NECD interactions[129, 130], underscoring the importance of these post-translational modifications.

While the immature Notch receptor is in the Golgi, it undergoes its first proteolytic cleavage event, S1. This furin-mediated enzymatic cleavage results in the separation of the NICD and NECD to form a mature heterodimer[131]. The receptor is then trafficked to the membrane and, after interaction with ligand, two more cleavage events take place. S2 cleavage is catalyzed by ADAM metalloproteases and results in shedding of the NECD[132]. NECD remains associated with the ligand and is endocytosed by the signal-sending cell. It is thought that the tension of endocytosis leads to receptor conformational changes allowing S2 site exposure and successful recruitment of ADAM proteases[133]. In the intestine ADAM10 has been shown to be the protease responsible for this cleavage event[134]. The final cleavage, S3, is performed by the gamma-secretase complex, which releases NICD from the membrane to enter the nucleus[135].

Once in the nucleus, NICD associates with a protein complex, including the DNA-binding protein RBP-J and the transcriptional activator MAML, to activate target gene transcription[136]. Alternatively, when NICD is not in the nucleus, RBP-J associates with a co-repressor complex ensuring target gene inactivation[123]. The duration of the Notch signal is relatively short, as NICD has a limited half-life[137]. Interaction with the co-activation complex leads to CDK8 recruitment and phosphorylation, which quickly targets NICD for ubiquitin ligase-mediated degradation[137].

Additional regulatory mechanisms

Like the receptors, Notch ligands require post-translational modifications for proper activation. This involves ubiquitination, endocytosis, and recycling back on the membrane, a process initiated by the Neuralized and Mindbomb family of E3-ubiquitin ligases[138, 139]. Absence of this step leads to ligand endocytosis and degradation[138].

Notch receptors are also actively endocytosed and degraded when not engaged by ligand. ITCH, DTX1 and DTX2 are E3 ligases that ubiquitinate receptors to incite lysosomal degradation[140]. Additionally, NUMB, an endocytic adaptor protein, functions to remove Notch from the membrane and associates with a number of different factors to promote receptor degradation[11, 141]. NUMB is segregated asymmetrically into daughter cells and is thought to regulate cell fate switches and asymmetric stem cell division[124].

Notch patterning mechanisms

Notch is critical for patterning throughout development. This is accomplished by several different mechanisms: lateral inhibition, lineage decisions, and boundary development[142]. The variety of outcomes offered by these patterning mechanisms allow this simple pathway to play key roles in the development or homeostasis of almost every organ or tissue system. A comprehensive list has been compiled by Andersson et al.[11] and has been summarized in Table 1-1.

Notch target genes

Despite its fundamental role in development and homeostasis only a few Notch target genes have been well characterized. These consist of the HES and HEY (or HERP) families of basic helix-loop-helix (bHLH) transcription factors[143]. bHLH proteins can function as both transcriptional activators or transcriptional repressors, but the HES/HEY family members function primarily as repressors[143]. In many cases this leads to repression of differentiation factors and cell cycle inhibitors. In the intestine, for instance, HES1 blocks the transcription of *Atoh1*, the transcription factor linked to secretory cell fate[18, 78, 144, 145] as well as the cyclin-dependent kinase inhibitors *p27^{Kip1}* and *p57^{Kip2}* [16, 146-148]. Other tissue specific target genes have been identified, such as *c-Myc* in developing and leukemic T cells[149, 150], and we have identified the ASC-marker *Olfm4* to be a direct Notch target in the intestine[13]. Although Notch regulates many important

Table 1-1. Notch regulation in multiple tissue systems*

Organ/Tissue	Processes regulated
Brain	Balance between gliogenesis and neurogenesis, stem cell maintenance, neuroepithelial cell polarity
Breast	Alveolar development, luminal cell fate, regulation basal cell proliferation
Craniofacial	Palate morphogenesis, tooth development
Ear	Defines sensory epithelium, hair cell and supporting cell fate
Esophagus	Regulates epithelial homeostasis
Eye	Fiber cell differentiation, lens development
Heart	Cardiac patterning
Hematopoietic system	Hematopoiesis, balance of B-cell/T-cell development, myeloid homeostasis
Intestine	Regulates proliferation vs. differentiation, stem cell maintenance
Kidney	Defines podocytes and proximal tubules
Limbs	Digit morphogenesis
Liver	Ductal plate formation, intrahepatic bile duct morphogenesis
Lungs	Tracheal branching morphogenesis
Muscle	Regulates satellite cell transition to myogenic precursors and myoblasts
Neural crest	Cardiac patterning, Schwann cell proliferation, melanocyte stem cell maintenance
Pancreas	regulates endocrine cell differentiation, endocrine precursor maintenance, inhibits terminal differentation of acinar cells, controls epithelial branching
Pituitary	Regulates growth and proliferation. Specifies malanotropes and gonadotropes
Placenta	Fetal angiogenesis, maternal circulatory and spongiotrophoblast development
Prostate	Epithelial differentiation, branching morphogenesis, stromal survival
Sex organs and germ cells	Leydig progenitor cell maintenance, spermatogenesis, ooctyle growth
Skin	Cell adhesion, proliferation, hair follicale differentiation and homeostasis
Spine/pinal cord/somites	Somite segmentation
Spleen	Generation of T lineage-restricted progenitors and marginal zone B-cells, CD8 dendritic cell homeostasis
Stomach	Luminal and glandular cell fate switch
Thymus	Thymic morphogenesis, gamma delta T-cell differentiation
Thyroid	Regulates cell number, differentiation and endocrine function of thryrocytes and C-cells
Vasculature	Arteriovenous specification, endothelial and vascular smooth muscle differentiation, blood vesssel sprouting and branching

* Table contents paraphrased from Andersson et al, 2011. Specific references are listed therein

Red text indicates tissues where Notch is implicated in stem and progenitor cell maintenance as published in Andersson et al. Blue text is additional information from VanDussen et al., 2012

processes in numerous tissues, surprisingly few target genes have been described. Identification of Notch target genes that mediate key cellular responses in the intestine will be an important future goal to understand the mechanism of action.

A new study in developing and leukemic T cells suggests that Notch transcriptional regulation may occur at a superenhancers, increasing promoter permissiveness at a large number of loci[151]. This may explain how Notch regulates widespread transcriptional programs with only a few known direct target genes.

Notch components in the intestine

Notch signaling has been shown to play fundamental roles in intestinal homeostasis, and many efforts have been made to define the Notch components expressed in this tissue. *In situ* hybridization (ISH) has been employed to map receptor, ligand and target gene expression. *Notch1* and *Notch2* appear to be the primary receptors expressed in the epithelium[152], although studies publishing expression patterns have reported inconsistent results. In one study, *Notch1* was shown to be expressed throughout the crypt while *Notch2* expression was found only in a few cells[153]. Other reports have shown ISH results with much broader *Notch2* crypt expression[14]. *Notch3* and *Notch4* expression are present in the intestine but are confined to the mesenchymal tissue[152, 153]. A mesenchymal component of *Notch1* has also been identified[153]. Notch ligands *Jag1*, *Dll1*, and *Dll4* are all expressed in the intestinal epithelium, specifically localized to the crypt region[152, 153]. Finally, *Hes1, 5, 6,* and *7* are all expressed in the crypt epithelium, although *Hes5* was also found in the mesenchyme[152].

Notch intestinal function uncovered with inhibition studies

Genetic and pharmacologic Notch inhibitory models and their intestinal phenotypes are listed in Table 1-2. In summary, inhibition of the pathway results in a profound transformation of the intestinal epithelium from predominantly absorptive enterocytes to secretory cells[15, 16, 18, 27, 154, 155]. This occurs due to de-

Table 1-2. Intestinal phenotypes of Notch inhibition models

	Category	Gene/Target	S*	P^	Additional Findings	Reference
GENETIC MODELS	Nuclear Effector	f-RBP-J	↑	↓	weight loss, death	Van Es et al., 2012; Riccio et al., 2008
		Rosa26-LSL-dnMAML	↑	↓		Dempsey, unpublished
	Receptor/ Ligand	f-N1			No phenotype	Riccio et al., 2008
		f-N2			No phenotype	
		f-N1 + f-N2	↑	↓	weight loss, death	
		f-N1	↑		weight loss, decreased stem cells	Chapter 2
		f-Dll1	↑		mild phenotype	Pellegrinet et al., 2011
		f-Dll4			no phenotype	
		f-Jag1			no phenotype	
		f-Dll1+f-Dll4	↑	↓	weight loss, death, decreased stem cells	
		f-Dll1+f-Jag1	↑		mild phenotype	
	Receptor/ ligand processing	f-ADAM10	↑	↓		Dempsey, unpublished
		f-Mindbomb	↑	↓	mislocalized Paneth cells	Koo et al., 2009
		f-Pofut1	↑	↓		Guilmeau et al., 2008
	Target gene	f-Hes1	↑		precociuos Paneth cell differentiation	Jensen et al., 2000; Suzuki et al., 2005
PHARMACOLOGIC AGENTS	chronic DBZ	gamma-secretase complex	↑	↓	weight loss, death, decreased stem cells	Milano et al., 2004; Van Es et al., 2005 ;
	acute DBZ		↑	↑	decreased stem cells	Chapter 3
	α-N1	N1	↑	↓	mild phenotype, toxicity with irradiation	Wu et al., 2010; Tran et al., 2013; Chapter 2
	α-N2	N2			no phenotype	Wu et al., 2010
	α-N1 + α-N2	N1+N2	↑	↓	weight loss, death, decreased stem cells	Wu et al., 2010; Tran et al., 2013; Chapter 2
	α-Dll1	Dll1			no phenotype	Chapter 2
	α-Dll4	Dll4			no phenotype	Ridgeway et al., 2006, Chapter 2
	α-Dll1 + α-Dll4	Dll1 + Dll4			no phenotype	Tran et al., 2013, Chapter 2

* S = secretory cell abundance

^ P = epithelial proliferation

repression of *Atoh1*, as discussed above. While some studies have suggested that only goblet cells are aberrantly formed with Notch inhibition, our lab and others have shown that all secretory lineages are increased including goblet, Paneth, enteroendocrine, and tuft cells[13, 148, 154]. In addition to cell lineage specification, these Notch inhibition also results in decreased epithelial proliferation[15, 16, 18, 154, 155]. Finally, pharmacologic inhibition by dibenzazepine (DBZ) treatment or genetic inhibition by *Dll1/Dll4* deletion showed loss of ASCs cells, suggesting a role for Notch in stem cell maintenance[13, 15].

Notch redundancy in the intestine

Since multiple Notch receptors and ligands are expressed in the crypt there has been interest in determining if these factors are functioning in specific cell populations or if they play distinct roles in the epithelium. To determine which Notch receptors function in ISCs, mouse genetic reporter models have been engineered to activate a reporter gene in cells undergoing active Notch signaling (Table 1-3). These Cre reporter mice have shown that both *Notch1* and *Notch2* are expressed in a stem cell population[14]. However, *Notch2* tracing occurred at a much lower frequency than *Notch1*[14], which could indicate that *Notch2* is present in a more rare stem cell population, like a QSC, although construct mosaicism could also lead to this phenotype.

NOTCH1 and NOTCH2 were shown to be functionally redundant since genetic deletion of either receptor reportedly had no phenotype[16]. Other studies contested that *Notch1* deletion has a mild secretory cell phenotype compared to pan-deletion[155, 156]. My work in Chapter 2 extends these findings to show that Notch1 is the primary receptor regulating both secretory cell fate decisions and stem cell maintenance.

Similar questions of redundancy have been addressed for epithelial Notch ligands. While DLL1, DLL4, and JAG1 are all expressed in the crypt, only combined deletion of *Dll1* and *Dll4* results in a severe secretory hyperplasia phenotype[15]. This suggests that DLL1 and DLL4 are the main ligands

Table 1-3. Notch reporter models

Gene Construct	Finding	Reference
NIP-Cre (N1-ICD replaced by CreER^{T2})	Fully labeled crypts/vili indicate that N1 actiity occurs in stem cells	Vooijs et al., 2007, Pellegrinet et al., 2011
N1-CreER^{T2}	Fully labeled crypts/vili indicate that N1 is expressed in stem cells	Fre et al., 2011
N2-CreER^{T2}	Rare fully labeled crypts/vili indicate that N2 is expressed in some stem cells	Fre et al., 2011
Dll1-GFP-ires-CreER^{T2}	Short-lived secretory cell clones indicate Dll1 is expressed in secretory progenitor cells. Lineage tracing post-irradiation suggest that Dll1+ precursors revert back to stem cells with injury	Van Es et al., 2012

responsible for cell fate and stem cell maintenance, and that their function is largely redundant.

Notch in disease

Mutations in the Notch signaling pathway genes are associated with a number of human diseases, including T-cell acute lymphoblastic leukemia (T-ALL) (*Notch1*), CADASIL (*Notch3*), Alagille syndrome (*Jag1, Notch2*), Hajdu-Cheney syndrome (*Notch2*) and serpentine fibula polycystic kidney syndrome (*Notch2*)[157]. Additionally, alterations in Notch signaling have been associated with intestinal diseases, including inflammatory bowel diseases[158, 159] and colon cancer[160-162]. Thus, Notch is a promising therapeutic target for disease. Since Notch is required for many tissue systems, a perfectly refined understanding of the effect of Notch activation or inhibition in targeted systems will need to be achieved. A large focus of this thesis, discussed in Chapter 2, is to understand the requirement of NOTCH1 and NOTCH2 in the intestine, which will be important information for treatment regimes targeted in the gut or delivered systemically.

1.3: MATHEMATICAL MODELING OF THE INTESTINAL CRYPT

A powerful system

Mathematical and computational models are immensely powerful tools that can be used to probe biological systems in ways that may be very difficult to address experimentally. First, models can be used to test several parallel hypotheses to help narrow down the most likely biological explanation, which can be validated by *in vivo* analysis. New experimental findings can then be implemented into the model, and reiterations can relay new questions. Repeated refining of the model through coupled experimentation can lead to the identification of the key mechanisms underlying the behavior of the system as a whole.

Modeling has long been used as a method to investigate cellular mechanisms of intestinal crypt homeostasis, tumorigenesis, and injury. The full potential of these models was not realized, however, due to the limited availability of stem cell markers to identify the location and numbers of ISCs as well functional assays to validate the models *in vivo*. Much progress has been made on these fronts, resulting in a recent resurgence in modeling efforts to study ISC function and crypt dynamics.

Modeling has been critical for understanding the viability of the immortal strand hypothesis as well as neutral drift dynamics. Additional modeling approaches have been used to understand cell-cell adhesion, flow, and migration within the crypt[163, 164], which is important for understanding how stem cell progeny migrate out of the crypts as well as how Paneth cells travel to the base.

Modeling stem cell number

In light of the continued ASC/QSC dispute, there is no agreed upon number of total stem cells in the crypt. Interestingly, even the number of ASCs continues to be debated. Snippert et. al[35] calculated the number of stem cells/crypt to be 14 +/- 2 cells. This was based on counting the number of GFP-labeled LGR5^{+} cells intercalated between Paneth cells at the base of the crypt. More recent studies have challenged the idea that mere expression of *Lgr5* defines an ASC. The Winton lab has taken a stem cell marker-independent functional approach to define stem cells and has found that the number of stem cells per crypt is closer to six[111]. Additionally, this method identified that the rate of functional stem cell turnover much lower than previously predicted[111]. With these new data, Kozar et al.[111] re-modeled the neutral drift dynamics from the Clevers data set as well as their own experimental data. They found that their new parameters fit both sets of data better than the previously tested values[111]. This study provided further evidence for neutral drift dynamics in the crypt while also challenging the accepted values for stem cell number and cell cycle rates. This example demonstrates one of the most important strengths of modeling approaches: the ability to test publicly available data sets and possibly draw new

conclusions as more information from biological study is discovered and subsequently implemented in the modeling process.

Types of crypt models

Apart from the specific mathematical analyses used in these models, there are two broad modeling approaches that have been applied in this field: spatial models and compartmental models. Spatial models use a geometric lattice, algorithm or boundary conditions to organize individual cells in space. These models typically consider both crypt physical forces and cell-cell interactions and have recently been reviewed by De Matteis[165]. Compartment models, on the other hand, utilize the unique cellular organization of the intestine, with proliferating stem and progenitor cells at the base of the crypts and most differentiated cells migrating up the villi, to group cell lineages into discrete cell population compartments for analysis.

A recent trend in crypt modeling is to try to incorporate everything that is known about the crypt, including crypt geometry, migration, stem cell division, niche signals, differentiation, and other factors into one comprehensive model[166, 167]. While these models have been able to seemingly replicate many experimental outcomes, these efforts must be interpreted with caution, as these models are created to fill a set of known outcomes and are often filled with assumptions that cannot be validated experimentally. Models of this nature typically have rule-based algorithms that depend on cell location and identity to determine cell behavior. With all of the ambiguity surrounding the existence and function of QSCs, TA cell plasticity and required niche signals, it is premature to develop these types of comprehensive models of the crypt. For instance, a computational model of the crypt by Pin et al.[167] defines QSCs as the same population as ASCs, but located higher up the crypt in a different Wnt gradient. While this is an interesting hypothesis, current data, summarized above, cannot determine if QSCs are an independent population, a subset of LGR5$^+$ cells, or progenitor cells.

An alternate approach would be to tackle narrow questions to limit the amount of assumptions in the model. Compartmental models, which look at different cell lineages in the intestine as separate independent compartments, are ideally suited to answer many of the questions that dominate the ISC field. Depending on the specific question being asked, these compartments can be made as nuanced or broad as desired. For instance, we can consider a model with a stem cell compartment that is inclusive of all types of stem cells, or we can define compartments more specifically and designate ASC, QSC, and facultative TA cells as separate stem cell compartments. The advantage of this approach is that models can be developed to what is known at present and updated as more definitive information about stem cell populations becomes known. The benefit of working with such a model is that the simple design allows for addressing very specific questions.

In Chapter 4 I utilize compartmental modeling to investigate stem cell dynamics in a system of acute Notch inhibition. To provide credence for using this technique, in the following section, I discuss in detail compartmental models that have successfully investigated various aspects of crypt homeostasis and tumorigenesis[168], crypt recovery post-irradiation[169], and crypt development[170]. I discuss the impact these models have made on the field and compare the various techniques employed. Finally, I discuss how compartmental modeling can be used to answer some of the lingering questions remaining in the ISC biology field.

Compartmental models of homeostasis and tumorigenesis

The level of cellular proliferation and turnover in the intestine is quite remarkable. In humans, an estimated 10^{11} cells are shed and replaced every day[171]. Colon cancer remains the third most prevalent and third most deadly cancer[172], thus, appreciating how normal proliferation is kept in check is essential for understanding when these processes go awry and lead to tumor formation. Early theories proposed that tumor initiation could be mediated by mutations that led to increased cellular proliferation of immortal stem cells[173]. Fearon and

Vogelstein[174] contextualized these mutations with their genetic model for tumor initiation in the colon, characterized as a systematic acquisition of mutations: both activation of oncogenes and loss of tumor suppressors. More recently, modeling of colorectal tumors showed that as tumors grow they become more heterogeneous as new mutations are acquired[175, 176]. This heterogeneity implies that more than one treatment approach is needed to eradicate the tumor. Modeling has also been used to directly determine how therapies should be applied. For example, a model of colon cancer carcinogenesis and tumor response to irradiation has been developed to better tune dosing of radiation therapy[177].

In 1995, Tomlinson and Bodmer[178] probed the mechanisms through which mutations act to incite tumor initiation with their computational model of crypt homeostasis and tumorigenesis. This simple model divided the crypt into 3 compartments: stem cells, semi-differentiated cells, and fully-differentiated cells, with cell populations determined by the rates of death, differentiation, renewal, and removal (Figure 1-6). The model was simplified to assume that all cell divisions occurred synchronously and updated at each subsequent generation. This study[178] explored normal cell division as well as the resulting effect on cellular homeostasis when changing the rates of cells undergoing death or differentiation in each compartment. The findings were striking: under normal conditions, this model found that there are very stringent parameters that must be met in order for steady-state to be reached; small perturbations in rates of death, differentiation, or renewal led to exponential growth or decay. Importantly, the model[178] suggested that alterations in stem cell number that lead to tumorigenesis might be through mechanisms other than simply increased stem cell proliferation rate, highlighting that it is not necessarily the mechanism of a tumorigenic mutation that is of key importance, but the crypt compartment that is affected.

Several models have been adapted from the general framework of the Tomlinson and Bodmer[178] study. In particular, Johnston and colleagues[168] aimed to improve the model by eliminating synchronous division as a simplification to
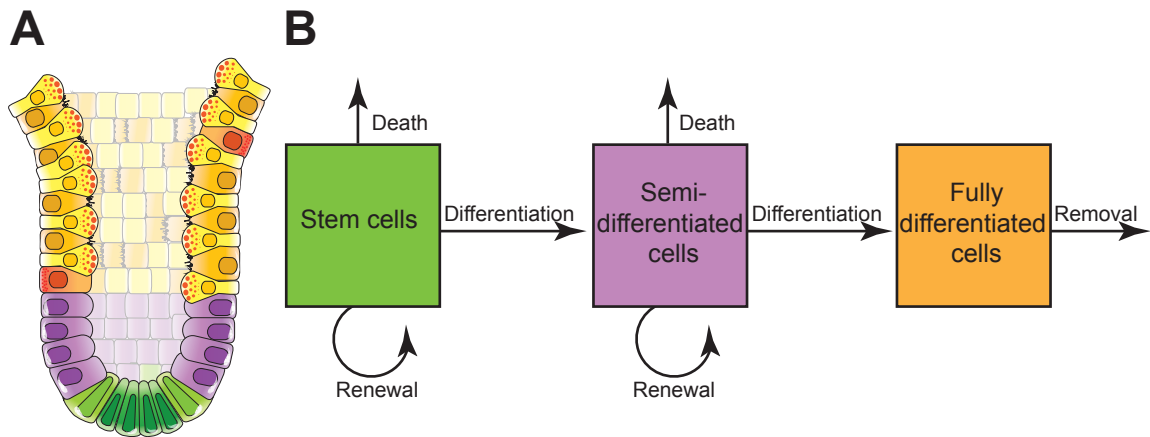
Figure 1-6. **A compartmental model of crypt homeostasis and tumorigenesis.** (A) An illustration of the colonic crypt as modeled by Johnston et al. Unlike the small intestine the colon does not have villi nor traditional Paneth cells. (B) Compartmental model diagram adapted from Figure 1 of Johnston et al.[167]. Cell populations include stem cells, semi-differentiated cells and fully differentiated cells. Cell flows into and out of the compartments are indicated by arrows and are defined by rates of death, differentiation, and renewal from the stem and semi-differentiated compartments. There is no renewal in the fully differentiated compartment and cells leave by removal.

more closely match crypt physiology. To do this they created two different revisions of the model: an "age-structured model" using partial differential equations that takes into account asynchronous cell divisions and a "continuous model" using ordinary differential equations (ODEs) that looks at the average cell population over time. In the age-structured model they explored the effect of cells in each compartment being in different stages of the cell cycle prior to undergoing renewal, differentiation, or death at certain time points. The resultant population of semi-differentiated cells from a crypt that started with all cells at the same point of the cycle was compared to one that started with an evenly distributed age profile. Since this resulted in similar populations, they concluded that it was unnecessary to specifically follow each cell's age, and validated the use of the continuous model to study this system.

Johnston et al.[168], like the Tomlinson and Bodmer model[178], found that both the age-structured and continuous models were "structurally unstable", that is they reach stable steady-state cell populations only at very precise parameter values. Any deviation from these values results in exponential growth or decay of the crypt. In the intestine, unbounded growth would be equivalent to tumorigenesis and decay would result in eventual crypt loss. Due to this complication, Johnston et al.[168] sought to test feedback mechanisms to model the steady-state that occurs in the actual crypt during homeostasis. Two alternative feedback models were tested, "linear feedback" and "saturating feedback". In the linear feedback model, logistic growth of the stem cell population was implemented leading to a limited population size. In this case, tuning the parameters below a certain point resulted in exponential decay, but unlike the model without feedback, no set of parameters resulted in exponential growth. Effectively, the linear feedback model creates a crypt that is incapable of initiating tumors no matter how many mutations are accumulated that change cell renewal and differentiation rates, unless the mutation compromised the feedback mechanism.

In the saturating feedback model[168], rather than limiting total population size, feedback was incorporated to only limit the rate of differentiation. With this

feedback, three states of stem cell population growth were possible: crypt extinction, homeostasis, and exponential growth. Thus, the saturating feedback model establishes a simple model to explore the initiation and growth kinetics in tumorigenesis associated with multiple mutation acquisition. Alterations in the rate of renewal, differentiation, and death due to genetic mutations would change the governing rate parameters, leading to altered steady-state populations.

Several studies have confirmed that the Johnston et al.[168] model predicts experimental findings in tumorigenesis[179, 180]. Additionally, there have been adaptations of the model for colon cancer and other systems. For example, one study maintained the general framework of the model but included telomere length as a parameter that was regulated by location in the stem cell niche[181]. In another study[182], the Johnston et al.[168] scaffold was used to build a model for hematopoiesis and treatment of Chronic Myeloid Leukemia (CML). This study[182] tested synchronized discrete, age-structured, and continuous models with feedback mechanisms to determine that modulating growth factor signaling through the use of tyrosine kinase inhibitors should be able to cure CML by regulating CML progenitor cell populations.

A compartmental crypt post-irradiation model

As discussed above, irradiation leads to severe intestinal damage. In fact, understanding both early and late injury responses has been a key interest in the field[183]. Additionally, acute irradiation damage has been used as a mechanism to study pathways involved in intestinal recovery, and, as mentioned above, has been a key tool in studying activation of QSCs. The acute irradiation response can be distilled into two stages. Initially, there is crypt apoptosis, mitotic arrest, and a decrease in both crypt and villus cell numbers[184, 185]. Next, there is a robust rebound "overshoot" in population before homeostasis is re-established[184]. Paulus et al.[169] aimed to create a model that would faithfully replicate the post-irradiation recovery to test their hypothesis that the damage control response resided solely in the stem cell compartment. They engineered a compartmental

model of the crypt to map the effect of the post-irradiation response on stem and TA cell populations (Figure 1-7).

Prior to the publication of Paulus et al.[169], several models had been designed to describe the intestinal response to irradiation. Many of these attempts were fueled by the observation that irradiation injury leads to shortened villi prior to crypt expansion and proliferative cell surge[184]. This was first investigated in the compartmental model by Sato et al.[186], which posited that irradiation-induced changes to cell number and proliferation were generated from a feedback mechanism where villus damage sends signals to the crypts to regenerate. One complication with this hypothesis was the observation of subtle changes in the crypt prior to the onset of villar atrophy, suggesting that not all of the effects originated from a villus feedback mechanism[187].

Paulus et al.[169] challenged the idea that the irradiation recovery response had any aspect of villus-to-crypt feedback. Rather, they hypothesized that all cellular consequences could be traced back to changes in the stem cell compartment. Their study tested whether a stem cell-centric response could replicate the experimental findings in cell number, labeling index (incorporation of a tritiated thymidine label), and mitotic index in the post-irradiation recovery. To begin their model, they drew from a comprehensive data set that included 35 time points after various irradiation doses from 2.5-12Gy. In these experiments, mice were administered tritiated thymidine 40 minutes prior to sacrifice, and ileal crypts were scored for labeling index and mitotic activity on histological sections.

Paulus et al.[169] used an agent-based approach, a computational model where cells are modeled as autonomous decision-making entities called agents that behave according to a set of rules defined from experimental observations of the phenomenon under investigation. Unlike many agent-based models that align cells to a geometrical lattice, this model situated the cells into one of six compartments: stem cells (A), four TA cell compartments (T1-T4) and differentiated cells (D) (Figure 1-7A). Each compartment contained sub-compartments allocated to specific portions of the cell cycle (Figure 1-7B). Movement of cells from one compartment to the next was based on two
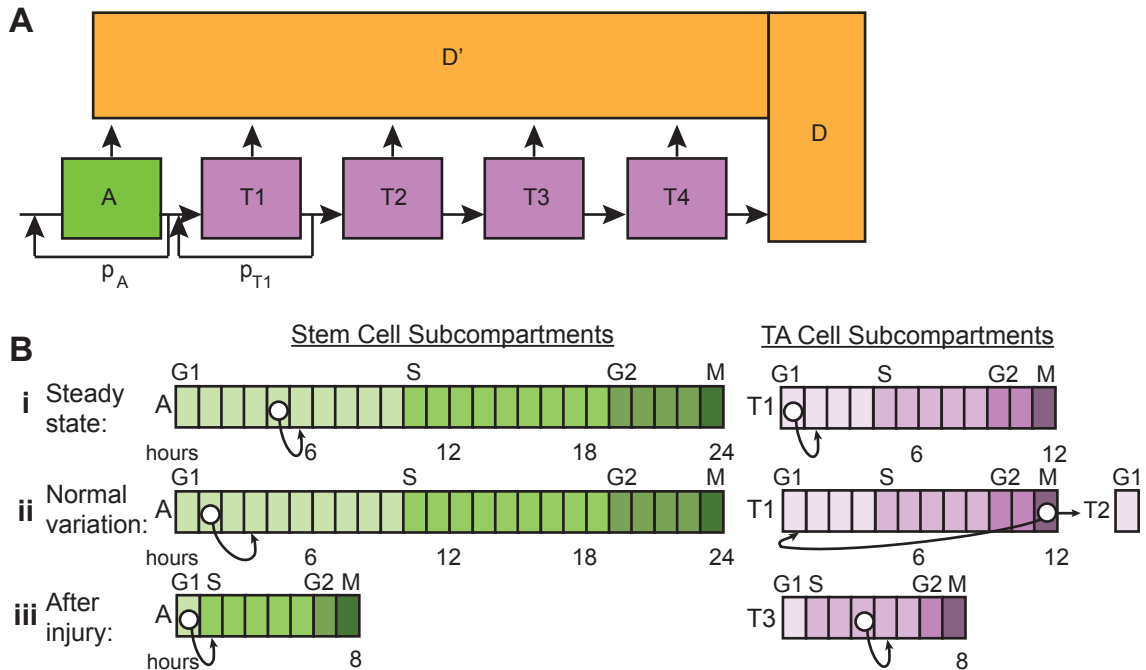
Figure 1-7. A compartmental model of crypt post-irradiation recovery. (A) Diagram of the cell population compartments of the crypt post-irradiation model adapted from Figure 2 of Paulus et al.[168]. Cell populations include stem cells (A), TA cells (T1-T4), differentiated cells (D), and previously proliferative cells that stopped cycling due to irradiation injury (D'). Cells move from one compartment to the next after completing the cell cycle. Cells in A and T1 can re-enter their compartment with the probability p_A and p_{T1}, respectively. (B) Diagram of different cell cycle subcompartments are shown. (i) Subcompartments during steady state when the cell cycle time is 24 hours for A and 12 hours for T compartments. Cells (white circles) advance to the next subcompartments every hour of the simulation. For clarity we have included G1, S, G2 and M phases of the cell cycle, but the lengths of G2 and M that were used during the Paulus et al.[168] simulation was not made clear in the manuscript. (ii) Normal stochasticity in the model. Cell cycle time was allowed to vary slightly for each individual cell. This variation was limited to the G1 compartment and was achieved by skipping a subcompartment. Renewal in the A and T1 compartment was accomplished by re-entering the first G1 subcompartment after completing M phase. (iii) Alteration in subcompartments after maximal irradiation injury, where cell cycle lengths are decreased to 8 hours.

regulated processes during the simulation: cell cycle time and self-maintenance probability; all other parameters were held constant. During the simulations, cell cycle time was very highly regulated based on experimental findings: 24 hours for stem cells and 12 hours for TA cells during steady-state; but after irradiation injury, cell cycle for both populations was shortened, with a minimum cell cycle time of 8 hours. Additionally, the number of stem cells in the crypt influenced stem cell cycle time, while TA cells were not regulated in this fashion. The model also embraced the idea of TA cells as potential stem cells, although it is assumed that only T1 cells have self-renewal capabilities. Therefore, after completing the cell cycle, cells in the A and T1 compartments either moved to the next compartment or re-entered the same compartment with the probabilities p_A and p_{T1}.

Paulus et al.[169] used data from administration of 8Gy irradiation to fit their parameters: cell death, "irreversible proliferative inhibition" i.e. removal of previously proliferative cells to a non-proliferative compartment (D'), mitotic delay, cell numbers, cell cycle times, and villus transit time. With these parameters, they were able to replicate the observed labeling index and cell numbers, including the expected overshoot in population, simply by regulating cell cycle time and self-maintenance probability. To validate their model, they changed the initial values to match the observed cell numbers after 2.5Gy and 12Gy irradiation, and again were able to replicate the labeling index and overshoot populations observed after these levels of irradiation damage.

The Paulus et al.[169] model served its goal to debunk the idea that the irradiation-response is a villus feedback mechanism. More recent studies have made it clear that the acute post-irradiation response is a crypt-centric process fueled by stem cell proliferation[5, 39]. Interestingly, although some stem cells undergo apoptosis after irradiation, a recent study showed that surviving ASCs possess radioresistance by activating DNA-damage repair processes[4]. Additionally, a recent study investigating lineage tracing of SOX9-EGFP during post-irradiation showed a marked increase in SOX9-EGFP low cells (which are thought to be CBCCs), but also found increased numbers of SOX9-EGFP high

cells (which are thought to be differentiated enteroendocrine cells[5].) This finding suggests that more mature cells can de-differentiate to replace lost stem cells, not just the T1 compartment as proposed by Paulus et al.[169].

A compartmental model of stem cell expansion during development

In the adult intestine, stem cell divisions must result, on average, in one stem cell and one TA cell in order to maintain homeostasis. This is usually termed asymmetric stem cell division, since the two daughter cells are of different lineages. Asymmetric division is one of the defining characteristics of stem cells as it allows for self-renewal[188, 189]. However, stem cells must also possess the ability to divide symmetrically to increase numbers in development and after injury[190]. This property is especially crucial as the intestine grows in length and develops crypts during postnatal development.[191]

There have been a number of mathematical models probing the question of stem cell symmetry in adult tissues. Clayton et al.[192] devised the first model of this kind for the mammalian epidermis, demonstrating that stem cells had flexibility in cell division symmetry. Their probabilistic model of clone labeling concluded that adult skin stem cells were undergoing asymmetric division 84% of the time and symmetric division 16% of the time[192]. In the intestine, mathematical models of stem cell symmetry have come to slightly different conclusions. As mentioned above, neutral drift studies have suggested that stem cell division results in two equipotential daughter cells, which compete for spots in the niche. Essentially this means that stem cell divisions never truly occur asymmetrically, rather that population asymmetry occurs via stochastic availability of niche positions[35, 64]. While these studies call into question asymmetric division, they do indicate precedence for symmetric division in the intestine, the mechanism assumed to be essential for stem cell expansion.

Itzkovitz et al.[170] aimed to answer the question of exactly how shifts between asymmetric and symmetric stem cell division can create a mature crypt in the developing intestine in the optimal, or shortest, amount of time. The main question the group focused on was if there were multiple types of cell division

occurring simultaneously or if all cells completed similar types of division during the same window of time. This compartmental model defined two cell populations: stem cells and non-stem cells. Differentiated cell populations were not directly addressed, however non-stem cell extrusion was included as a possible outcome of cell division. The system is defined by a set of stochastic ODEs where the state variables are the population of stem cells and non-stem cells. The parameters include rates of stem cell and non-stem cell division, as well as extrusion from the non-stem cell compartment. The number of cells are governed by the probabilities that each compartment will undergo symmetric or asymmetric cell division.

Since more than one type of symmetric stem cell division is addressed in the model, a shorthand nomenclature is used for this discussion: symmetric (S) or asymmetric (A), with a number indicating stem cell (1) or non-stem cell (2) progeny (Figure 1-8). The authors[170] started with the assumption that development of mature intestine occurred with a certain probability of S1 and A stem cell divisions, but no S2 division. They next utilized optimal control theory[193] to determine the probabilities of each of these division events to take the initial population of cells at birth to the population of cells in the mature crypt in the least time possible. As the immature gut contains only a short supply of differentiated cells at birth[191, 194], the authors rationalized that time was the driving force for creating a mature crypt.

By solving for minimal time, they found that all stem cells would always divide the same way at the same time, either S1 or A, never mixed[170]. With this criteria, there are two options for behavior, 1) cells will always divide the same way with no transition to another type of symmetry or 2) cells can switch which type of symmetry they undergo one or multiple times until maturation is achieved. The authors found that in order to reach mature crypts in the minimal amount of time symmetry would need to switch once and only once during development. Thus if the stem cells started with S1 division they would all switch to A division and continue dividing asymmetrically until the mature crypt was established. Alternatively, stem cells could begin with A division and switch to S1. This type of
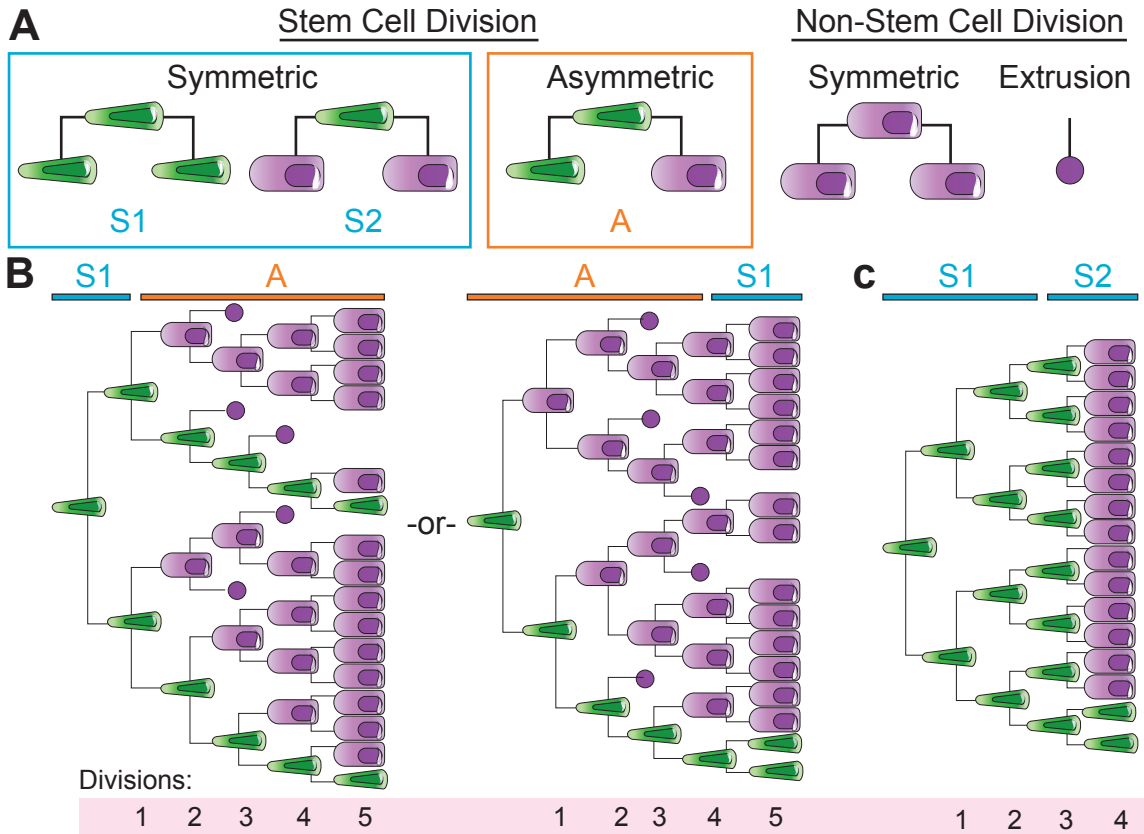
Figure 1-8. A compartmental model of crypt development. This figure has been adapted from Figure 3 of Itzkovitz et al.[169] (A) Definitions of types of stem and non-stem cell divisions. Stem cells can undergo two types of symmetric division, S1 and S2, or asymmetric division, A. Non-stem cells always divide symmetrically or are extruded from the crypt. (B) Depiction of the two types of "bang-bang" model outcomes. The rounds of division have been limited to 5 for clarity. The left cell lineage tree shows bang-bang division that shows a switch from S1 stem cell division to A division. The right lineage tree shows A division preceding S1 division. (C) Depiction of the "overshoot" model where stem cells undergo S1 division followed by S2 division. The final cell composition is the same as the bang-bang models, but it only takes 4 rounds of divisions instead of 5 to achieve this.

control mechanism containing a single on/off switch in behavior is referred to as "bang-bang control"[195, 196].

Next, the authors[170] embraced the idea that stem cells could divide symmetrically into two non-stem cells (S2 division) (Figure 1-8). Strikingly, they found that if S1 divisions occurred for the duration of crypt development, with the last round of divisions switching to S2, they could also achieve mature crypt populations, without any A divisions. Importantly, this approach led to overshooting the mature crypt stem cell population, before attaining normal levels. Interestingly, this "overshoot" model resulted in mature crypt formation in less time than with bang-bang control (Figure 1-8).

Itzkovitz et al.[170] then investigated *in vivo* their "bang-bang" vs. "overshoot" control findings. They used *Lgr5 in situ* hybridization to visualize stem cells and performed a kinetic analysis to measure proliferation rates. First, they found that the proliferation rate of stem cells and non-stem cells was maximal during crypt development, which was in accordance with their prediction for attaining mature crypts in minimal time. In fact, they measured stem cell cycle time (15.7 hours) to be essentially the same as TA cell time (16.9 hours), a marked decrease from the normal adult stem cell cycle time (22.4 hours). They were able to feed these proliferation rates back into their model to determine that the type of "bang-bang" control that would be favored is S1 division followed by A division. Additionally, their *Lgr5 in situ* data showed that developing crypts were initially filled, almost exclusively, with stem cells, and only later contained non-stem cell progeny, nicely corroborating this prediction. Importantly, they did observe *Lgr5*⁻ non-stem cell progeny prior to the last round of division, which surprisingly favored the less efficient "bang-bang" model over the "overshoot" model. Finally, they performed lineage tracing studies that showed that they never observed S2 division, suggesting that the "overshoot" mechanism did not occur. Interestingly, this is in direct contrast to the findings in adult intestines, where S2 division is predicted to frequently occur[35, 64]. This inconsistency could point to a difference in the regulation of stem cell symmetry specifically during development or could call these earlier results into question.

The Itzkovitz et al.[170] model exemplifies the importance of closely linking mathematical modeling efforts with *in vivo* validation. Had they only relied on their modeling data they may have assumed that the mechanism of crypt development was the "overshoot" model since it reached maturity in less time than the "bang-bang" control model.

Although only recently published, the work by Itzkovitz et al.[170] has spurred investigation into the discrepancy it introduced regarding the absence of S2 division in the developing intestine. Hu et al.[197] reported both *in vivo* and modeling data suggesting that stem cell symmetry shifts from strict asymmetry (via A division) to population symmetry (via stochastic S1 and S2 division) with intestinal maturation. This report suggests that Itzkovitz et al.[170] and the adult modeling studies by Lopez Garcia et al.[64] and Snippert et al.[35] could be correct and that stem cell symmetry is dependent on tissue age.

A comparative look at crypt compartment models

While the theoretical models discussed above share the feature of analyzing the intestinal epithelia as compartmental populations, the compartments that they utilize and the mathematical/computational approach that they employ are very different: Johnston et al.[168] applied ODEs and partial differential equations, Paulus et al.[169] embraced an agent-based model, and Itzkovitz et al.[170] used a stochastic ODE system. These differences emphasize the versatility of the compartment modeling approach; many different types of questions can be addressed simply by restructuring the compartments and altering the theoretical framework. Since each approach is best suited to a specific type of system, it is wise to carefully consider which method will best answer the anticipated questions. There are strengths and weaknesses for each of these approaches.

Johnston et al. model. The Johnston model[168] comes to the conclusion that an ODE-derived "continuous" model is the simplest and most appropriate model of crypt homeostasis, and that changes in the rate parameters can be modulated to model both homeostasis and the process of tumorigenesis. Since

ODE models look at averages of cells over time, they assume that the cells in the system are uniform and that cell number is very large. Additionally, neither ODE nor partial differential equation models can resolve changes in small cell numbers that occur rapidly or transiently. While the number of cells in the intestinal crypt range in the several hundred, the number of stem cells is estimated to be 6 to 14 per crypt[35, 111]. This population number is too small to be well-described with a deterministic ODE model. When there are very small numbers like this, small random variations in stem cell number due to asymmetric vs. symmetric stem cell division can only be accurately captured with stochastic models. This does not invalidate the model, but does limit the questions that the model can answer. For example, this model would be inappropriate to probe post-irradiation recovery where the changes in stem cell number change very quickly.

Another weakness is that this model treats the TA, or semi-differentiated cell population, essentially as a stem cell population, which does not reflect crypt physiology. In order to appropriately capture the limited cell divisions in the TA compartment this model would need to use discrete equations or an agent-based system.

Paulus et al. model. The Paulus et al.[169] model of crypt post-irradiation recovery takes a unique approach. They treat cells as individual agents, but distribute the cells into compartments and follow each one through sub-compartments that reflect cell cycle time. One of the strengths of an agent-based approach is that all cells are accounted individually so the model allows for small cell numbers and rapid changes in cell populations. One of the disadvantages of agent-based models is that they have arbitrary physical units, which need to be explicitly defined *a priori* to interpret the simulation results with the experimental findings[198]. Unlike most agent-based models, however, the Paulus et al.[169] model is free from a geometrical lattice and cells are not influenced by the behavior of neighbors. Although individual cell interactions cannot be resolved in a model like this, population-level behavior can be inferred. For instance, the probability that a T1 cell can re-enter the T1 compartment is dependent on the population of stem

cells in the A compartment. This approach could be used to ask questions about homeostasis or tumorigenesis, and would be informative to probe the interaction between different stem cell populations.

Itzkovitz et al. model. The Itzkovitz et al. model[170] used a stochastic ODE system to model the probabilities of symmetric or asymmetric stem cell division during the process of crypt development. One of the assumptions this approach makes is that the mechanisms controlling crypt development are optimized to take the shortest amount of time biologically possible. This is a stringent feature that leads to the conclusion that stem cell divisions occur via "bang-bang" control. If time were not the determining factor, the optimal control theory would be the wrong approach to take. A strength of this model is it was validated *in vivo,* and the model clearly helped to inform the appropriate experiments to perform in this respect. This is one of the most important aspects of these types of models: the ability to inform biological experiments to test mechanisms regulating the complex process of epithelial cell homeostasis.

Weaknesses of this model include failure to address that the developing intestine does not receive all of the mature niche signals[199]. Since the niche is changing as crypt expansion occurs, it is possible that the rates of division intrinsic to the stem cell population could change throughout the process. They also assume that the crypt starts with one stem cell and zero TA cells, which does not account for any immature proliferative cells that may be located in the intervillus zone. The timing for TA cell appearance has not been critically determined, but cells expressing differentiated cell markers are apparent in prenatal intestine and intestinal function to absorb nutrients is essential upon birth, so differentiated cell populations must occur before crypts mature[191]. Finally, Itzkovitz et al.[170] determined that there is a shift from stem cells dividing symmetrically to asymmetrically during crypt maturation. Notably, their *in vivo* studies determined that Paneth cells were not responsible for this shift because the timing occurred prior to Paneth cell maturation[170]. One option they did not address is whether signaling for the shift could occur through immature Paneth cell precursors, which have not been well defined in the immature intestine.

Immature intestine contains cells that express Paneth-like markers, which may provide signals to the developing ISCs to regulate their behavior. If the process of ISC maturation is totally independent from Paneth-like cell development, then it will be important to identify which signal may control this process during intestinal development.

Future directions for modeling intestinal dynamics

The models that have been discussed above utilized a compartmental framework to investigate the mechanisms of tumorigenesis, post-irradiation recovery, and development. All of these models have been able to answer specific questions about their system, and Paulus et al.[169] and Itzkovitz et al.[170] validated their models with *in vivo* data. Itzkovitz et al.[170] went even further to use their model to design new experimental approaches and used those results to further refine their model. We believe that similar techniques can be used to tackle some of the lingering questions that remain in the field of stem cell biology.

1) How is stem cell number regulated? Modulations of several signaling pathways as well as various injury models have dramatic effects on stem cell numbers in the crypt. Some of these perturbations can result in loss of all CBCCs or reduction to a single stem cell. After recovery, stem cell populations return to normal, approximately 16 CBCCs/crypt. Compartmental modeling of stem cell populations in normal conditions compared to models of unbounded growth, can provide insights into exactly what signals are necessary for regulation of stem cell number. Use of CBCC markers like the Lgr5-GFP-CreERT2 mouse[32] can be used to validate stem cell numbers in different conditions. Compartmental models can also help to answer the questions of whether all ASCs are equal or if there are subpopulations even within the Lgr5$^+$ stem cell population. This would simply require sub-compartmentalizing these cells. Because a model like this would be working with very small numbers it would be best to use a stochastic model or an agent-based design to track cells individually.

2) Are ISCs completely defined by the niche? A compartmental model investigating this aspect of stem cell biology could distinguish between two

possibilities: all cells are potential stem cells if they are exposed to niche signals or only cells possessing intrinsic stemness can become stem cells once they are in the niche. Like the Paulus et al.[169] model this could be achieved by a subcompartment approach, where the large compartments would be niche and not niche, and the smaller compartments would be the cell populations. Total cell population censes would be measured with the inclusion of a intrinsically programmed cell compartment compared to a compartment that contained equipotential potential stem cells.

3) Is there a dedicated QSC population? A compartmental model testing this question would need to address whether QSCs are always in existence, or whether they only arise during times of injury by de-differentiation of TA and differentiated cell populations. If QSCs are a true population then crypts containing these cells would have a slightly higher cell population than a crypt where QSCs are actually cells with other functions. Very refined cell counting *in vivo* would be required to determine if this additional cell compartment exists.

4) What is the nature of the TA compartment? A model of TA cells could investigate the stringency of the number of divisions that these cells undergo. Proliferating cell numbers during homeostasis, injury, and post-injury could be utilized to determine if TA cells have an intrinsic division limit, or if the number of divisions is externally regulated. Although there are no specific markers for TA cells, TA cell number can be approximated by subtracting the number of stem cells from the total number of cells that proliferate during a 12-hour window.

There are a number of other ways that these questions can be approached, combining *in vivo* and modeling techniques. A spatial model that takes into account crypt size boundaries as a regulatory mechanism, for instance, might best answer the stem cell number question. This would be combined with very careful measurements of crypt circumference to determine if stem cell number/crypt varies based on crypt size.

Regardless of the specific modeling method used, the key issue is to keep the models focused and modest. By limiting the number of parameters in the system, we have the best chance to validate and refine the models

experimentally. This generates small-scale models that can be very powerful in generating new testable questions. Ideally, these smaller scale models would also be useable by non-experts, which would allow for more utilization of the combined *in vivo*/*in silico* approach and would fuel further advancement of the field.

1.4: THESIS OVERVIEW

The thesis research that I have undertaken has focused on how the Notch signaling pathway regulates stem cell dynamics. I have approached this question using mouse models of pharmacologic inhibition, and genetic inhibition or activation of the pathway and focusing on the temporal consequences of Notch inhibition.

In Chapter 2, I investigate the specificity of Notch receptors in intestinal epithelial differentiation and stem cell maintenance with genetic models of *Notch1* and *Notch2* deletion. I discovered that NOTCH1 is the main receptor controlling differentiation in the intestinal epithelium as deletion of *Notch1* alone results in secretory cell hyperplasia and stem cell loss. Additionally in Chapter 2, I use a Notch activation model to understand how constitutive Notch signaling affects the intestinal epithelial proliferation and differentiation profiles. To assess this I utilized the *Villin-CreER^{T2}* x *Rosa26-LSL-NICD-nGFP* model, which leads to expression of activated NICD in the intestinal epithelium. In this system I found that proliferation is increased, and that all types of differentiated cells are decreased. This is important since earlier works suggested that Notch activation results in an increase in the absorptive lineage at the expense of secretory cells[17, 78].

In Chapter 3 I investigate the short-term dynamics of stem cells after Notch signaling is turned off, by using an acute DBZ model. Since chronic Notch inhibition is typically associated with decreased proliferation and increased secretory cells, I was surprised to find that acute DBZ led to a both increased proliferation and increased secretory cell production, as well as decreased

CBCCs. I hypothesized that a Notch-dependent change in stem cell symmetry could explain both the proliferation and stem cell phenotypes observed in both chronic and acute Notch inhibition, and used a compartmental mathematical model to test this hypothesis. Furthermore, since CBCC loss is associated with QSC activation, I use a post-irradiation DBZ model and genetic deletion of Notch in QSCs (*Bmi1-Cre^{ER}* x *floxed-Rbp-j*) to determine if Notch is required for QSC activation.

In Chapter 4, I build and test a discrete compartmental model of the intestinal crypt for the purpose of testing our stem cell symmetry hypothesis. I found that stem cell symmetry could explain our chronic and acute DBZ proliferation findings, but only in the context of Notch-dependent stem cell repopulation.

Finally, in Chapter 5 I put my work in the context of the field and demonstrate how these findings have provided important insights in ISC biology. I end with future directions and propose experimentation to further understand Notch receptor function in niche specification and ISC dynamics.

REFERENCES

1. Demidov ON, Timofeev O, Lwin HN, Kek C, Appella E, Bulavin DV. Wip1 phosphatase regulates p53-dependent apoptosis of stem cells and tumorigenesis in the mouse intestine. Cell stem cell 2007;1:180-90.
2. Barker N, Ridgway RA, van Es JH, van de Wetering M, Begthel H, van den Born M, Danenberg E, Clarke AR, Sansom OJ, Clevers H. Crypt stem cells as the cells-of-origin of intestinal cancer. Nature 2009;457:608-11.
3. Potten CS. Extreme sensitivity of some intestinal crypt cells to X and gamma irradiation. Nature 1977;269:518-21.
4. Hua G, Thin TH, Feldman R, Haimovitz-Friedman A, Clevers H, Fuks Z, Kolesnick R. Crypt base columnar stem cells in small intestines of mice are radioresistant. Gastroenterology 2012;143:1266-76.
5. Van Landeghem L, Santoro MA, Krebs AE, Mah AT, Dehmer JJ, Gracz AD, Scull BP, McNaughton K, Magness ST, Lund PK. Activation of two distinct Sox9-EGFP-expressing intestinal stem cell populations during crypt regeneration after irradiation. American journal of physiology. Gastrointestinal and liver physiology 2012;302:G1111-32.
6. Yan KS, Chia LA, Li X, Ootani A, Su J, Lee JY, Su N, Luo Y, Heilshorn SC, Amieva MR, Sangiorgi E, Capecchi MR, Kuo CJ. The intestinal stem cell markers Bmi1 and Lgr5 identify two functionally distinct populations. Proceedings of the National Academy of Sciences of the United States of America 2012;109:466-71.
7. Buczacki SJ, Zecchini HI, Nicholson AM, Russell R, Vermeulen L, Kemp R, Winton DJ. Intestinal label-retaining cells are secretory precursors expressing Lgr5. Nature 2013;495:65-9.
8. Grikscheit TC, Siddique A, Ochoa ER, Srinivasan A, Alsberg E, Hodin RA, Vacanti JP. Tissue-engineered small intestine improves recovery after massive small bowel resection. Annals of surgery 2004;240:748-54.
9. Spence JR, Mayhew CN, Rankin SA, Kuhar MF, Vallance JE, Tolle K, Hoskins EE, Kalinichenko VV, Wells SI, Zorn AM, Shroyer NF, Wells JM. Directed differentiation of human pluripotent stem cells into intestinal tissue in vitro. Nature 2011;470:105-9.
10. Yui S, Nakamura T, Sato T, Nemoto Y, Mizutani T, Zheng X, Ichinose S, Nagaishi T, Okamoto R, Tsuchiya K, Clevers H, Watanabe M. Functional engraftment of colon epithelium expanded in vitro from a single adult Lgr5(+) stem cell. Nature medicine 2012;18:618-23.
11. Andersson ER, Sandberg R, Lendahl U. Notch signaling: simplicity in design, versatility in function. Development 2011;138:3593-612.
12. Liu J, Sato C, Cerletti M, Wagers A. Notch signaling in the regulation of stem cell self-renewal and differentiation. Current topics in developmental biology 2010;92:367-409.
13. VanDussen KL, Carulli AJ, Keeley TM, Patel SR, Puthoff BJ, Magness ST, Tran IT, Maillard I, Siebel C, Kolterud A, Grosse AS, Gumucio DL, Ernst

SA, Tsai YH, Dempsey PJ, Samuelson LC. Notch signaling modulates proliferation and differentiation of intestinal crypt base columnar stem cells. Development 2012;139:488-97.

14.   Fre S, Hannezo E, Sale S, Huyghe M, Lafkas D, Kissel H, Louvi A, Greve J, Louvard D, Artavanis-Tsakonas S. Notch lineages and activity in intestinal stem cells determined by a new set of knock-in mice. PloS one 2011;6:e25785.

15.   Pellegrinet L, Rodilla V, Liu Z, Chen S, Koch U, Espinosa L, Kaestner KH, Kopan R, Lewis J, Radtke F. Dll1- and dll4-mediated notch signaling are required for homeostasis of intestinal stem cells. Gastroenterology 2011;140:1230-1240 e7.

16.   Riccio O, van Gijn ME, Bezdek AC, Pellegrinet L, van Es JH, Zimber-Strobl U, Strobl LJ, Honjo T, Clevers H, Radtke F. Loss of intestinal crypt progenitor cells owing to inactivation of both Notch1 and Notch2 is accompanied by derepression of CDK inhibitors p27Kip1 and p57Kip2. EMBO Rep 2008;9:377-83.

17.   Stanger BZ, Datar R, Murtaugh LC, Melton DA. Direct regulation of intestinal fate by Notch. Proc Natl Acad Sci U S A 2005;102:12443-8.

18.   van Es JH, van Gijn ME, Riccio O, van den Born M, Vooijs M, Begthel H, Cozijnsen M, Robine S, Winton DJ, Radtke F, Clevers H. Notch/gamma-secretase inhibition turns proliferative cells in intestinal crypts and adenomas into goblet cells. Nature 2005;435:959-63.

19.   Kaur P, Potten CS. Circadian variation in migration velocity in small intestinal epithelium. Cell and tissue kinetics 1986;19:591-9.

20.   Potten CS. Stem cells in gastrointestinal epithelium: numbers, characteristics and death. Philosophical transactions of the Royal Society of London. Series B, Biological sciences 1998;353:821-30.

21.   Cheng H, Leblond CP. Origin, differentiation and renewal of the four main epithelial cell types in the mouse small intestine. V. Unitarian Theory of the origin of the four epithelial cell types. The American journal of anatomy 1974;141:537-61.

22.   Bjerknes M, Cheng H. The stem-cell zone of the small intestinal epithelium. I. Evidence from Paneth cells in the adult mouse. The American journal of anatomy 1981;160:51-63.

23.   Potten CS, Gandara R, Mahida YR, Loeffler M, Wright NA. The stem cells of small intestinal crypts: where are they? Cell proliferation 2009;42:731-50.

24.   Lund PK. Fixing the breaks in intestinal stem cells after radiation: a matter of DNA damage and death or DNA repair and regeneration. Gastroenterology 2012;143:1144-7.

25.   Munoz J, Stange DE, Schepers AG, van de Wetering M, Koo BK, Itzkovitz S, Volckmann R, Kung KS, Koster J, Radulescu S, Myant K, Versteeg R, Sansom OJ, van Es JH, Barker N, van Oudenaarden A, Mohammed S, Heck AJ, Clevers H. The Lgr5 intestinal stem cell signature: robust expression of proposed quiescent '+4' cell markers. The EMBO journal 2012;31:3079-91.

26. Itzkovitz S, Lyubimova A, Blat IC, Maynard M, van Es J, Lees J, Jacks T, Clevers H, van Oudenaarden A. Single-molecule transcript counting of stem-cell markers in the mouse intestine. Nature cell biology 2012;14:106-14.

27. van Es JH, Sato T, van de Wetering M, Lyubimova A, Nee AN, Gregorieff A, Sasaki N, Zeinstra L, van den Born M, Korving J, Martens AC, Barker N, van Oudenaarden A, Clevers H. Dll1+ secretory progenitor cells revert to stem cells upon crypt damage. Nature cell biology 2012;14:1099-104.

28. Pinto D, Robine S, Jaisser F, El Marjou FE, Louvard D. Regulatory sequences of the mouse villin gene that efficiently drive transgenic expression in immature and differentiated epithelial cells of small and large intestines. The Journal of biological chemistry 1999;274:6476-82.

29. Madison BB, Dunbar L, Qiao XT, Braunstein K, Braunstein E, Gumucio DL. Cis elements of the villin gene control expression in restricted domains of the vertical (crypt) and horizontal (duodenum, cecum) axes of the intestine. The Journal of biological chemistry 2002;277:33275-83.

30. Potten CS, Booth C, Tudor GL, Booth D, Brady G, Hurley P, Ashton G, Clarke R, Sakakibara S, Okano H. Identification of a putative intestinal stem cell and early lineage marker; musashi-1. Differentiation; research in biological diversity 2003;71:28-41.

31. Kayahara T, Sawada M, Takaishi S, Fukui H, Seno H, Fukuzawa H, Suzuki K, Hiai H, Kageyama R, Okano H, Chiba T. Candidate markers for stem and early progenitor cells, Musashi-1 and Hes1, are expressed in crypt base columnar cells of mouse small intestine. FEBS letters 2003;535:131-5.

32. Barker N, van Es JH, Kuipers J, Kujala P, van den Born M, Cozijnsen M, Haegebarth A, Korving J, Begthel H, Peters PJ, Clevers H. Identification of stem cells in small intestine and colon by marker gene Lgr5. Nature 2007;449:1003-7.

33. Bjerknes M, Cheng H. Multipotential stem cells in adult mouse gastric epithelium. American journal of physiology. Gastrointestinal and liver physiology 2002;283:G767-77.

34. Sato T, Vries RG, Snippert HJ, van de Wetering M, Barker N, Stange DE, van Es JH, Abo A, Kujala P, Peters PJ, Clevers H. Single Lgr5 stem cells build crypt-villus structures in vitro without a mesenchymal niche. Nature 2009;459:262-5.

35. Snippert HJ, van der Flier LG, Sato T, van Es JH, van den Born M, Kroon-Veenboer C, Barker N, Klein AM, van Rheenen J, Simons BD, Clevers H. Intestinal crypt homeostasis results from neutral competition between symmetrically dividing Lgr5 stem cells. Cell 2010;143:134-44.

36. van der Flier LG, van Gijn ME, Hatzis P, Kujala P, Haegebarth A, Stange DE, Begthel H, van den Born M, Guryev V, Oving I, van Es JH, Barker N, Peters PJ, van de Wetering M, Clevers H. Transcription factor achaete scute-like 2 controls intestinal stem cell fate. Cell 2009;136:903-12.

37. van der Flier LG, Haegebarth A, Stange DE, van de Wetering M, Clevers H. OLFM4 is a robust marker for stem cells in human intestine and marks a subset of colorectal cancer cells. Gastroenterology 2009;137:15-7.

38. Gracz AD, Ramalingam S, Magness ST. Sox9 expression marks a subset of CD24-expressing small intestine epithelial stem cells that form organoids in vitro. American journal of physiology. Gastrointestinal and liver physiology 2010;298:G590-600.

39. Sangiorgi E, Capecchi MR. Bmi1 is expressed in vivo in intestinal stem cells. Nature genetics 2008;40:915-20.

40. Tian H, Biehs B, Warming S, Leong KG, Rangell L, Klein OD, de Sauvage FJ. A reserve stem cell population in small intestine renders Lgr5-positive cells dispensable. Nature 2011;478:255-9.

41. Powell AE, Wang Y, Li Y, Poulin EJ, Means AL, Washington MK, Higginbotham JN, Juchheim A, Prasad N, Levy SE, Guo Y, Shyr Y, Aronow BJ, Haigis KM, Franklin JL, Coffey RJ. The pan-ErbB negative regulator Lrig1 is an intestinal stem cell marker that functions as a tumor suppressor. Cell 2012;149:146-58.

42. Montgomery RK, Carlone DL, Richmond CA, Farilla L, Kranendonk ME, Henderson DE, Baffour-Awuah NY, Ambruzs DM, Fogli LK, Algra S, Breault DT. Mouse telomerase reverse transcriptase (mTert) expression marks slowly cycling intestinal stem cells. Proceedings of the National Academy of Sciences of the United States of America 2011;108:179-84.

43. Takeda N, Jain R, LeBoeuf MR, Wang Q, Lu MM, Epstein JA. Interconversion between intestinal stem cell populations in distinct niches. Science 2011;334:1420-4.

44. May R, Riehl TE, Hunt C, Sureban SM, Anant S, Houchen CW. Identification of a novel putative gastrointestinal stem cell and adenoma stem cell marker, doublecortin and CaM kinase-like-1, following radiation injury and in adenomatous polyposis coli/multiple intestinal neoplasia mice. Stem cells 2008;26:630-7.

45. Gerbe F, Brulin B, Makrini L, Legraverend C, Jay P. DCAMKL-1 expression identifies Tuft cells rather than stem cells in the adult mouse intestinal epithelium. Gastroenterology 2009;137:2179-80; author reply 2180-1.

46. Saqui-Salces M, Keeley TM, Grosse AS, Qiao XT, El-Zaatari M, Gumucio DL, Samuelson LC, Merchant JL. Gastric tuft cells express DCLK1 and are expanded in hyperplasia. Histochemistry and cell biology 2011;136:191-204.

47. Bjerknes M, Khandanpour C, Moroy T, Fujiyama T, Hoshino M, Klisch TJ, Ding Q, Gan L, Wang J, Martin MG, Cheng H. Origin of the brush cell lineage in the mouse intestinal epithelium. Developmental biology 2012;362:194-218.

48. Nakanishi Y, Seno H, Fukuoka A, Ueo T, Yamaga Y, Maruno T, Nakanishi N, Kanda K, Komekado H, Kawada M, Isomura A, Kawada K, Sakai Y, Yanagita M, Kageyama R, Kawaguchi Y, Taketo MM, Yonehara S, Chiba

T. Dclk1 distinguishes between tumor and normal stem cells in the intestine. Nature genetics 2013;45:98-103.

49. Femia AP, Dolara P, Salvadori M, Caderni G. Expression of LGR-5, MSI-1 and DCAMKL-1, putative stem cell markers, in the early phases of 1,2-dimethylhydrazine-induced rat colon carcinogenesis: correlation with nuclear beta-catenin. BMC cancer 2013;13:48.

50. Escobar M, Nicolas P, Sangar F, Laurent-Chabalier S, Clair P, Joubert D, Jay P, Legraverend C. Intestinal epithelial stem cells do not protect their genome by asymmetric chromosome segregation. Nature communications 2011;2:258.

51. Schepers AG, Vries R, van den Born M, van de Wetering M, Clevers H. Lgr5 intestinal stem cells have high telomerase activity and randomly segregate their chromosomes. The EMBO journal 2011;30:1104-9.

52. Wong VW, Stange DE, Page ME, Buczacki S, Wabik A, Itami S, van de Wetering M, Poulsom R, Wright NA, Trotter MW, Watt FM, Winton DJ, Clevers H, Jensen KB. Lrig1 controls intestinal stem-cell homeostasis by negative regulation of ErbB signalling. Nature cell biology 2012;14:401-8.

53. Cheng H, Leblond CP. Origin, differentiation and renewal of the four main epithelial cell types in the mouse small intestine. I. Columnar cell. The American journal of anatomy 1974;141:461-79.

54. Barker N, van de Wetering M, Clevers H. The intestinal stem cell. Genes & development 2008;22:1856-64.

55. van der Flier LG, Clevers H. Stem cells, self-renewal, and differentiation in the intestinal epithelium. Annu Rev Physiol 2009;71:241-60.

56. Bjerknes M, Cheng H. Intestinal epithelial stem cells and progenitors. Methods in enzymology 2006;419:337-83.

57. Troughton WD, Trier JS. Paneth and goblet cell renewal in mouse duodenal crypts. The Journal of cell biology 1969;41:251-68.

58. Snippert HJ, van Es JH, van den Born M, Begthel H, Stange DE, Barker N, Clevers H. Prominin-1/CD133 marks stem cells and early progenitors in mouse small intestine. Gastroenterology 2009;136:2187-2194 e1.

59. Zhu L, Gibson P, Currle DS, Tong Y, Richardson RJ, Bayazitov IT, Poppleton H, Zakharenko S, Ellison DW, Gilbertson RJ. Prominin 1 marks intestinal stem cells that are susceptible to neoplastic transformation. Nature 2009;457:603-7.

60. Jenny M, Uhl C, Roche C, Duluc I, Guillermin V, Guillemot F, Jensen J, Kedinger M, Gradwohl G. Neurogenin3 is differentially required for endocrine cell fate specification in the intestinal and gastric epithelium. The EMBO journal 2002;21:6338-47.

61. Cai WB, Roberts SA, Potten CS. The number of clonogenic cells in crypts in three regions of murine large intestine. International journal of radiation biology 1997;71:573-9.

62. Schonhoff SE, Giel-Moloney M, Leiter AB. Neurogenin 3-expressing progenitor cells in the gastrointestinal tract differentiate into both endocrine and non-endocrine cell types. Developmental biology 2004;270:443-54.

63. Sei Y, Lu X, Liou A, Zhao X, Wank SA. A stem cell marker-expressing subset of enteroendocrine cells resides at the crypt base in the small intestine. American journal of physiology. Gastrointestinal and liver physiology 2011;300:G345-56.

64. Lopez-Garcia C, Klein AM, Simons BD, Winton DJ. Intestinal stem cell replacement follows a pattern of neutral drift. Science 2010;330:822-5.

65. Fletcher AG, Breward CJ, Jonathan Chapman S. Mathematical modeling of monoclonal conversion in the colonic crypt. Journal of theoretical biology 2012;300:118-33.

66. Kim TH, Li F, Ferreiro-Neira I, Ho LL, Luyten A, Nalapareddy K, Long H, Verzi M, Shivdasani RA. Broadly permissive intestinal chromatin underlies lateral inhibition and cell plasticity. Nature 2014;506:511-5.

67. Sheaffer KL, Kim R, Aoki R, Elliott EN, Schug J, Burger L, Schubeler D, Kaestner KH. DNA methylation is required for the control of stem cell differentiation in the small intestine. Genes & development 2014;28:652-64.

68. Gregorieff A, Clevers H. Wnt signaling in the intestinal epithelium: from endoderm to cancer. Genes & development 2005;19:877-90.

69. Crosnier C, Stamataki D, Lewis J. Organizing cell renewal in the intestine: stem cells, signals and combinatorial control. Nat Rev Genet 2006;7:349-59.

70. Pinto D, Gregorieff A, Begthel H, Clevers H. Canonical Wnt signals are essential for homeostasis of the intestinal epithelium. Genes Dev 2003;17:1709-13.

71. de Lau WB, Snel B, Clevers HC. The R-spondin protein family. Genome biology 2012;13:242.

72. Carmon KS, Gong X, Lin Q, Thomas A, Liu Q. R-spondins function as ligands of the orphan receptors LGR4 and LGR5 to regulate Wnt/beta-catenin signaling. Proceedings of the National Academy of Sciences of the United States of America 2011;108:11452-7.

73. de Lau W, Barker N, Low TY, Koo BK, Li VS, Teunissen H, Kujala P, Haegebarth A, Peters PJ, van de Wetering M, Stange DE, van Es JE, Guardavaccaro D, Schasfoort RB, Mohri Y, Nishimori K, Mohammed S, Heck AJ, Clevers H. Lgr5 homologues associate with Wnt receptors and mediate R-spondin signalling. Nature 2011;476:293-7.

74. Glinka A, Dolde C, Kirsch N, Huang YL, Kazanskaya O, Ingelfinger D, Boutros M, Cruciat CM, Niehrs C. LGR4 and LGR5 are R-spondin receptors mediating Wnt/beta-catenin and Wnt/PCP signalling. EMBO reports 2011;12:1055-61.

75. Sato T, Stange DE, Ferrante M, Vries RG, Van Es JH, Van den Brink S, Van Houdt WJ, Pronk A, Van Gorp J, Siersema PD, Clevers H. Long-term expansion of epithelial organoids from human colon, adenoma, adenocarcinoma, and Barrett's epithelium. Gastroenterology 2011;141:1762-72.

76. White BD, Chien AJ, Dawson DW. Dysregulation of Wnt/beta-catenin signaling in gastrointestinal cancers. Gastroenterology 2012;142:219-32.

77. Crosnier C, Vargesson N, Gschmeissner S, Ariza-McNaughton L, Morrison A, Lewis J. Delta-Notch signalling controls commitment to a secretory fate in the zebrafish intestine. Development 2005;132:1093-104.

78. Fre S, Huyghe M, Mourikis P, Robine S, Louvard D, Artavanis-Tsakonas S. Notch signals control the fate of immature progenitor cells in the intestine. Nature 2005;435:964-8.

79. Scoville DH, Sato T, He XC, Li L. Current view: intestinal stem cells and signaling. Gastroenterology 2008;134:849-64.

80. Batts LE, Polk DB, Dubois RN, Kulessa H. Bmp signaling is required for intestinal growth and morphogenesis. Developmental dynamics : an official publication of the American Association of Anatomists 2006;235:1563-70.

81. Haramis AP, Begthel H, van den Born M, van Es J, Jonkheer S, Offerhaus GJ, Clevers H. De novo crypt formation and juvenile polyposis on BMP inhibition in mouse intestine. Science 2004;303:1684-6.

82. Batlle E, Henderson JT, Beghtel H, van den Born MM, Sancho E, Huls G, Meeldijk J, Robertson J, van de Wetering M, Pawson T, Clevers H. Beta-catenin and TCF mediate cell positioning in the intestinal epithelium by controlling the expression of EphB/ephrinB. Cell 2002;111:251-63.

83. Warner BW, Erwin CR. Critical roles for EGF receptor signaling during resection-induced intestinal adaptation. Journal of pediatric gastroenterology and nutrition 2006;43 Suppl 1:S68-73.

84. Gur G, Rubin C, Katz M, Amit I, Citri A, Nilsson J, Amariglio N, Henriksson R, Rechavi G, Hedman H, Wides R, Yarden Y. LRIG1 restricts growth factor signaling by enhancing receptor ubiquitylation and degradation. The EMBO journal 2004;23:3270-81.

85. Laederich MB, Funes-Duran M, Yen L, Ingalla E, Wu X, Carraway KL, 3rd, Sweeney C. The leucine-rich repeat protein LRIG1 is a negative regulator of ErbB family receptor tyrosine kinases. The Journal of biological chemistry 2004;279:47050-6.

86. Lahar N, Lei NY, Wang J, Jabaji Z, Tung SC, Joshi V, Lewis M, Stelzner M, Martin MG, Dunn JC. Intestinal subepithelial myofibroblasts support in vitro and in vivo growth of human small intestinal epithelium. PloS one 2011;6:e26898.

87. Hsu YC, Fuchs E. A family business: stem cell progeny join the niche to regulate homeostasis. Nature reviews. Molecular cell biology 2012;13:103-14.

88. Darmoul D, Ouellette AJ. Positional specificity of defensin gene expression reveals Paneth cell heterogeneity in mouse small intestine. The American journal of physiology 1996;271:G68-74.

89. Cheng H, Merzel J, Leblond CP. Renewal of Paneth cells in the small intestine of the mouse. The American journal of anatomy 1969;126:507-25.

90. Ireland H, Houghton C, Howard L, Winton DJ. Cellular inheritance of a Cre-activated reporter gene to determine Paneth cell longevity in the

murine small intestine. Developmental dynamics : an official publication of the American Association of Anatomists 2005;233:1332-6.

91. Sato T, van Es JH, Snippert HJ, Stange DE, Vries RG, van den Born M, Barker N, Shroyer NF, van de Wetering M, Clevers H. Paneth cells constitute the niche for Lgr5 stem cells in intestinal crypts. Nature 2011;469:415-8.

92. Garabedian EM, Roberts LJ, McNevin MS, Gordon JI. Examining the role of Paneth cells in the small intestine by lineage ablation in transgenic mice. The Journal of biological chemistry 1997;272:23729-40.

93. Durand A, Donahue B, Peignon G, Letourneur F, Cagnard N, Slomianny C, Perret C, Shroyer NF, Romagnolo B. Functional intestinal stem cells after Paneth cell ablation induced by the loss of transcription factor Math1 (Atoh1). Proceedings of the National Academy of Sciences of the United States of America 2012;109:8965-70.

94. Kim TH, Escudero S, Shivdasani RA. Intact function of Lgr5 receptor-expressing intestinal stem cells in the absence of Paneth cells. Proceedings of the National Academy of Sciences of the United States of America 2012;109:3932-7.

95. Rothenberg ME, Nusse Y, Kalisky T, Lee JJ, Dalerba P, Scheeren F, Lobo N, Kulkarni S, Sim S, Qian D, Beachy PA, Pasricha PJ, Quake SR, Clarke MF. Identification of a cKit(+) colonic crypt base secretory cell that supports Lgr5(+) stem cells in mice. Gastroenterology 2012;142:1195-1205 e6.

96. Farin HF, Van Es JH, Clevers H. Redundant sources of Wnt regulate intestinal stem cells and promote formation of Paneth cells. Gastroenterology 2012;143:1518-1529 e7.

97. Finkbeiner SR, Spence JR. A Gutsy Task: Generating Intestinal Tissue from Human Pluripotent Stem Cells. Digestive diseases and sciences 2013.

98. Kovbasnjuk O, Zachos NC, In J, Foulke-Abel J, Ettayebi K, Hyser JM, Broughman JR, Zeng XL, Middendorp S, de Jonge HR, Estes MK, Donowitz M. Human enteroids: preclinical models of non-inflammatory diarrhea. Stem cell research & therapy 2013;4 Suppl 1:S3.

99. Guezguez A, Pare F, Benoit YD, Basora N, Beaulieu JF. Modulation of stemness in a human normal intestinal epithelial crypt cell line by activation of the WNT signaling pathway. Experimental cell research 2014.

100. Polykandriotis E, Arkudas A, Horch RE, Kneser U. To matrigel or not to matrigel. The American journal of pathology 2008;172:1441; author reply 1441-2.

101. Marshman E, Booth C, Potten CS. The intestinal epithelial stem cell. BioEssays : news and reviews in molecular, cellular and developmental biology 2002;24:91-8.

102. Metcalfe C, Kljavin NM, Ybarra R, de Sauvage FJ. Lgr5(+) stem cells are indispensable for radiation-induced intestinal regeneration. Cell stem cell 2014;14:149-59.

103. Zhou WJ, Geng ZH, Spence JR, Geng JG. Induction of intestinal stem cells by R-spondin 1 and Slit2 augments chemoradioprotection. Nature 2013;501:107-11.

104. Wang G, Li Y, Wang XY, Han Z, Chuai M, Wang LJ, Ho Lee KK, Geng JG, Yang X. Slit/Robo1 signaling regulates neural tube development by balancing neuroepithelial cell proliferation and differentiation. Experimental cell research 2013;319:1083-93.

105. Wang J, Wakeman TP, Lathia JD, Hjelmeland AB, Wang XF, White RR, Rich JN, Sullenger BA. Notch promotes radioresistance of glioma stem cells. Stem cells 2010;28:17-28.

106. Feil R, Brocard J, Mascrez B, LeMeur M, Metzger D, Chambon P. Ligand-activated site-specific recombination in mice. Proceedings of the National Academy of Sciences of the United States of America 1996;93:10887-90.

107. Feil R, Wagner J, Metzger D, Chambon P. Regulation of Cre recombinase activity by mutated estrogen receptor ligand-binding domains. Biochemical and Biophysical Research Communications 1997;237:752-757.

108. Koitabashi N, Bedja D, Zaiman AL, Pinto YM, Zhang M, Gabrielson KL, Takimoto E, Kass DA. Avoidance of transient cardiomyopathy in cardiomyocyte-targeted tamoxifen-induced MerCreMer gene deletion models. Circulation research 2009;105:12-5.

109. Zhu Y, Huang YF, Kek C, Bulavin DV. Apoptosis differently affects lineage tracing of Lgr5 and Bmi1 intestinal stem cell populations. Cell stem cell 2013;12:298-303.

110. Huh WJ, Khurana SS, Geahlen JH, Kohli K, Waller RA, Mills JC. Tamoxifen induces rapid, reversible atrophy, and metaplasia in mouse stomach. Gastroenterology 2012;142:21-24 e7.

111. Kozar S, Morrissey E, Nicholson AM, van der Heijden M, Zecchini HI, Kemp R, Tavare S, Vermeulen L, Winton DJ. Continuous clonal labeling reveals small numbers of functional stem cells in intestinal crypts and adenomas. Cell stem cell 2013;13:626-33.

112. Pitule P, Vycital O, Bruha J, Novak P, Hosek P, Treska V, Hlavata I, Soucek P, Kralickova M, Liska V. Differential expression and prognostic role of selected genes in colorectal cancer patients. Anticancer research 2013;33:4855-65.

113. McClanahan T, Koseoglu S, Smith K, Grein J, Gustafson E, Black S, Kirschmeier P, Samatar AA. Identification of overexpression of orphan G protein-coupled receptor GPR49 in human colon and ovarian primary tumors. Cancer biology & therapy 2006;5:419-26.

114. Hsu HC, Liu YS, Tseng KC, Hsu CL, Liang Y, Yang TS, Chen JS, Tang RP, Chen SJ, Chen HC. Overexpression of Lgr5 correlates with resistance to 5-FU-based chemotherapy in colorectal cancer. International journal of colorectal disease 2013;28:1535-46.

115. Sentani K, Sakamoto N, Shimamoto F, Anami K, Oue N, Yasui W. Expression of olfactomedin 4 and claudin-18 in serrated neoplasia of the colorectum: a characteristic pattern is associated with sessile serrated lesion. Histopathology 2013;62:1018-27.

116. Seko N, Oue N, Noguchi T, Sentani K, Sakamoto N, Hinoi T, Okajima M, Yasui W. Olfactomedin 4 (GW112, hGC-1) is an independent prognostic marker for survival in patients with colorectal cancer. Experimental and therapeutic medicine 2010;1:73-78.

117. Kim JH, Yoon SY, Kim CN, Joo JH, Moon SK, Choe IS, Choe YK, Kim JW. The Bmi-1 oncoprotein is overexpressed in human colorectal cancer and correlates with the reduced p16INK4a/p14ARF proteins. Cancer letters 2004;203:217-24.

118. Li DW, Tang HM, Fan JW, Yan DW, Zhou CZ, Li SX, Wang XL, Peng ZH. Expression level of Bmi-1 oncoprotein is associated with progression and prognosis in colon cancer. Journal of cancer research and clinical oncology 2010;136:997-1006.

119. Spangrude GJ, Johnson GR. Resting and activated subsets of mouse multipotent hematopoietic stem cells. Proceedings of the National Academy of Sciences of the United States of America 1990;87:7433-7.

120. Wolf NS, Kone A, Priestley GV, Bartelmez SH. In vivo and in vitro characterization of long-term repopulating primitive hematopoietic cells isolated by sequential Hoechst 33342-rhodamine 123 FACS selection. Experimental hematology 1993;21:614-22.

121. Zhou S, Schuetz JD, Bunting KD, Colapietro AM, Sampath J, Morris JJ, Lagutina I, Grosveld GC, Osawa M, Nakauchi H, Sorrentino BP. The ABC transporter Bcrp1/ABCG2 is expressed in a wide variety of stem cells and is a molecular determinant of the side-population phenotype. Nature medicine 2001;7:1028-34.

122. von Furstenberg RJ, Buczacki SJ, Smith BJ, Seiler KM, Winton DJ, Henning SJ. Side population sorting separates subfractions of cycling and non-cycling intestinal stem cells. Stem cell research 2013;12:364-375.

123. Kopan R, Ilagan MX. The canonical Notch signaling pathway: unfolding the activation mechanism. Cell 2009;137:216-33.

124. Bray SJ. Notch signalling: a simple pathway becomes complex. Nature reviews. Molecular cell biology 2006;7:678-89.

125. Sasamura T, Sasaki N, Miyashita F, Nakao S, Ishikawa HO, Ito M, Kitagawa M, Harigaya K, Spana E, Bilder D, Perrimon N, Matsuno K. neurotic, a novel maternal neurogenic gene, encodes an O-fucosyltransferase that is essential for Notch-Delta interactions. Development 2003;130:4785-95.

126. Shi S, Stanley P. Protein O-fucosyltransferase 1 is an essential component of Notch signaling pathways. Proceedings of the National Academy of Sciences of the United States of America 2003;100:5234-9.

127. Rana NA, Haltiwanger RS. Fringe benefits: functional and structural impacts of O-glycosylation on the extracellular domain of Notch receptors. Current opinion in structural biology 2011;21:583-9.

128. Moran JL, Shifley ET, Levorse JM, Mani S, Ostmann K, Perez-Balaguer A, Walker DM, Vogt TF, Cole SE. Manic fringe is not required for embryonic development, and fringe family members do not exhibit redundant functions in the axial skeleton, limb, or hindbrain. Developmental

dynamics : an official publication of the American Association of Anatomists 2009;238:1803-12.

129. Kraman M, McCright B. Functional conservation of Notch1 and Notch2 intracellular domains. FASEB journal : official publication of the Federation of American Societies for Experimental Biology 2005;19:1311-3.

130. Liu Z, Chen S, Boyle S, Zhu Y, Zhang A, Piwnica-Worms DR, Ilagan MX, Kopan R. The extracellular domain of Notch2 increases its cell-surface abundance and ligand responsiveness during kidney development. Developmental cell 2013;25:585-98.

131. Logeat F, Bessia C, Brou C, LeBail O, Jarriault S, Seidah NG, Israel A. The Notch1 receptor is cleaved constitutively by a furin-like convertase. Proceedings of the National Academy of Sciences of the United States of America 1998;95:8108-12.

132. Brou C, Logeat F, Gupta N, Bessia C, LeBail O, Doedens JR, Cumano A, Roux P, Black RA, Israel A. A novel proteolytic cleavage involved in Notch signaling: the role of the disintegrin-metalloprotease TACE. Molecular cell 2000;5:207-16.

133. Parks AL, Klueg KM, Stout JR, Muskavitch MA. Ligand endocytosis drives receptor dissociation and activation in the Notch pathway. Development 2000;127:1373-85.

134. Tsai Y-H, K.L. VanDussen, E.T. Sawey, L. Shang, A.W. Wade, C. Kasper, A. Stoeck, I. Maillard, H.C. Crawford, L.C. Samuelson, P.J. Dempsey. ADAM10 Regulates Notch Function in Intestinal Stem Cells (Under revision for Gastroenterology).

135. Fortini ME. Gamma-secretase-mediated proteolysis in cell-surface-receptor signalling. Nature reviews. Molecular cell biology 2002;3:673-84.

136. Kovall RA. More complicated than it looks: assembly of Notch pathway transcription complexes. Oncogene 2008;27:5099-109.

137. Fryer CJ, White JB, Jones KA. Mastermind recruits CycC:CDK8 to phosphorylate the Notch ICD and coordinate activation with turnover. Molecular cell 2004;16:509-20.

138. Le Borgne R. Regulation of Notch signalling by endocytosis and endosomal sorting. Current opinion in cell biology 2006;18:213-22.

139. Chitnis A. Why is delta endocytosis required for effective activation of notch? Developmental dynamics : an official publication of the American Association of Anatomists 2006;235:886-94.

140. Chastagner P, Israel A, Brou C. AIP4/Itch regulates Notch receptor degradation in the absence of ligand. PloS one 2008;3:e2735.

141. Kandachar V, Roegiers F. Endocytosis and control of Notch signaling. Current opinion in cell biology 2012;24:534-40.

142. Bray S. Notch signalling in Drosophila: three ways to use a pathway. Seminars in cell & developmental biology 1998;9:591-7.

143. Iso T, Kedes L, Hamamori Y. HES and HERP families: multiple effectors of the Notch signaling pathway. Journal of cellular physiology 2003;194:237-55.

144. Kazanjian A, Noah T, Brown D, Burkart J, Shroyer NF. Atonal homolog 1 is required for growth and differentiation effects of notch/gamma-secretase inhibitors on normal and cancerous intestinal epithelial cells. Gastroenterology 2010;139:918-28, 928 e1-6.

145. van Es JH, de Geest N, van de Born M, Clevers H, Hassan BA. Intestinal stem cells lacking the Math1 tumour suppressor are refractory to Notch inhibitors. Nat Commun 2010;1:1-5.

146. Georgia S, Soliz R, Li M, Zhang P, Bhushan A. p57 and Hes1 coordinate cell cycle exit with self-renewal of pancreatic progenitors. Developmental biology 2006;298:22-31.

147. Monahan P, Rybak S, Raetzman LT. The notch target gene HES1 regulates cell cycle inhibitor expression in the developing pituitary. Endocrinology 2009;150:4386-94.

148. Kim TH, Shivdasani RA. Genetic evidence that intestinal Notch functions vary regionally and operate through a common mechanism of Math1 repression. The Journal of biological chemistry 2011;286:11427-33.

149. Weng AP, Millholland JM, Yashiro-Ohtani Y, Arcangeli ML, Lau A, Wai C, Del Bianco C, Rodriguez CG, Sai H, Tobias J, Li Y, Wolfe MS, Shachaf C, Felsher D, Blacklow SC, Pear WS, Aster JC. c-Myc is an important direct target of Notch1 in T-cell acute lymphoblastic leukemia/lymphoma. Genes & development 2006;20:2096-109.

150. Palomero T, Lim WK, Odom DT, Sulis ML, Real PJ, Margolin A, Barnes KC, O'Neil J, Neuberg D, Weng AP, Aster JC, Sigaux F, Soulier J, Look AT, Young RA, Califano A, Ferrando AA. NOTCH1 directly regulates c-MYC and activates a feed-forward-loop transcriptional network promoting leukemic cell growth. Proceedings of the National Academy of Sciences of the United States of America 2006;103:18261-6.

151. Wang H, Zang C, Taing L, Arnett KL, Wong YJ, Pear WS, Blacklow SC, Liu XS, Aster JC. NOTCH1-RBPJ complexes drive target gene expression through dynamic interactions with superenhancers. Proceedings of the National Academy of Sciences of the United States of America 2014;111:705-10.

152. Schroder N, Gossler A. Expression of Notch pathway components in fetal and adult mouse small intestine. Gene Expr Patterns 2002;2:247-50.

153. Sander GR, Powell BC. Expression of notch receptors and ligands in the adult gut. The journal of histochemistry and cytochemistry : official journal of the Histochemistry Society 2004;52:509-16.

154. Milano J, McKay J, Dagenais C, Foster-Brown L, Pognan F, Gadient R, Jacobs RT, Zacco A, Greenberg B, Ciaccio PJ. Modulation of notch processing by gamma-secretase inhibitors causes intestinal goblet cell metaplasia and induction of genes known to specify gut secretory lineage differentiation. Toxicological sciences : an official journal of the Society of Toxicology 2004;82:341-58.

155. Wu Y, Cain-Hom C, Choy L, Hagenbeek TJ, de Leon GP, Chen Y, Finkle D, Venook R, Wu X, Ridgway J, Schahin-Reed D, Dow GJ, Shelton A, Stawicki S, Watts RJ, Zhang J, Choy R, Howard P, Kadyk L, Yan M, Zha

J, Callahan CA, Hymowitz SG, Siebel CW. Therapeutic antibody targeting of individual Notch receptors. Nature 2010;464:1052-7.

156. Vooijs M, Ong CT, Hadland B, Huppert S, Liu Z, Korving J, van den Born M, Stappenbeck T, Wu Y, Clevers H, Kopan R. Mapping the consequence of Notch1 proteolysis in vivo with NIP-CRE. Development 2007;134:535-44.

157. Penton AL, Leonard LD, Spinner NB. Notch signaling in human development and disease. Seminars in cell & developmental biology 2012;23:450-7.

158. Zheng X, Tsuchiya K, Okamoto R, Iwasaki M, Kano Y, Sakamoto N, Nakamura T, Watanabe M. Suppression of hath1 gene expression directly regulated by hes1 via notch signaling is associated with goblet cell depletion in ulcerative colitis. Inflammatory bowel diseases 2011;17:2251-60.

159. Gersemann M, Becker S, Kubler I, Koslowski M, Wang G, Herrlinger KR, Griger J, Fritz P, Fellermann K, Schwab M, Wehkamp J, Stange EF. Differences in goblet cell differentiation between Crohn's disease and ulcerative colitis. Differentiation; research in biological diversity 2009;77:84-94.

160. Reedijk M, Odorcic S, Zhang H, Chetty R, Tennert C, Dickson BC, Lockwood G, Gallinger S, Egan SE. Activation of Notch signaling in human colon adenocarcinoma. International journal of oncology 2008;33:1223-9.

161. Meng RD, Shelton CC, Li YM, Qin LX, Notterman D, Paty PB, Schwartz GK. gamma-Secretase inhibitors abrogate oxaliplatin-induced activation of the Notch-1 signaling pathway in colon cancer cells resulting in enhanced chemosensitivity. Cancer research 2009;69:573-82.

162. Jubb AM, Turley H, Moeller HC, Steers G, Han C, Li JL, Leek R, Tan EY, Singh B, Mortensen NJ, Noguera-Troise I, Pezzella F, Gatter KC, Thurston G, Fox SB, Harris AL. Expression of delta-like ligand 4 (Dll4) and markers of hypoxia in colon cancer. British journal of cancer 2009;101:1749-57.

163. Wong SY, Chiam KH, Lim CT, Matsudaira P. Computational model of cell positioning: directed and collective migration in the intestinal crypt epithelium. Journal of the Royal Society, Interface / the Royal Society 2010;7 Suppl 3:S351-63.

164. Meineke FA, Potten CS, Loeffler M. Cell migration and organization in the intestinal crypt using a lattice-free model. Cell proliferation 2001;34:253-66.

165. De Matteis G, Graudenzi A, Antoniotti M. A review of spatial computational models for multi-cellular systems, with regard to intestinal crypts and colorectal cancer development. Journal of mathematical biology 2012.

166. Buske P, Galle J, Barker N, Aust G, Clevers H, Loeffler M. A comprehensive model of the spatio-temporal stem cell and tissue organisation in the intestinal crypt. PLoS computational biology 2011;7:e1001045.

167. Pin C, Watson AJ, Carding SR. Modelling the spatio-temporal cell dynamics reveals novel insights on cell differentiation and proliferation in the small intestinal crypt. PloS one 2012;7:e37115.

168. Johnston MD, Edwards CM, Bodmer WF, Maini PK, Chapman SJ. Mathematical modeling of cell population dynamics in the colonic crypt and in colorectal cancer. Proceedings of the National Academy of Sciences of the United States of America 2007;104:4008-13.

169. Paulus U, Potten CS, Loeffler M. A model of the control of cellular regeneration in the intestinal crypt after perturbation based solely on local stem cell regulation. Cell proliferation 1992;25:559-78.

170. Itzkovitz S, Blat IC, Jacks T, Clevers H, van Oudenaarden A. Optimality in the development of intestinal crypts. Cell 2012;148:608-19.

171. Potten CS, Loeffler M. A comprehensive model of the crypts of the small intestine of the mouse provides insight into the mechanisms of cell migration and the proliferation hierarchy. Journal of theoretical biology 1987;127:381-91.

172. Society AC. Cancer Facts & Figures 2012. Atlanta: American Cancer Society, 2012.

173. Cairns J. Mutation selection and the natural history of cancer. Nature 1975;255:197-200.

174. Fearon ER, Vogelstein B. A genetic model for colorectal tumorigenesis. Cell 1990;61:759-67.

175. Tsao JL, Tavare S, Salovaara R, Jass JR, Aaltonen LA, Shibata D. Colorectal adenoma and cancer divergence. Evidence of multilineage progression. The American journal of pathology 1999;154:1815-24.

176. Tsao JL, Yatabe Y, Salovaara R, Jarvinen HJ, Mecklin JP, Aaltonen LA, Tavare S, Shibata D. Genetic reconstruction of individual colorectal tumor histories. Proceedings of the National Academy of Sciences of the United States of America 2000;97:1236-41.

177. Ribba B, Colin T, Schnell S. A multiscale mathematical model of cancer, and its use in analyzing irradiation therapies. Theoretical biology & medical modelling 2006;3:7.

178. Tomlinson IP, Bodmer WF. Failure of programmed cell death and differentiation as causes of tumors: some simple mathematical models. Proceedings of the National Academy of Sciences of the United States of America 1995;92:11130-4.

179. Artyomov MN, Meissner A, Chakraborty AK. A model for genetic and epigenetic regulatory networks identifies rare pathways for transcription factor induced pluripotency. PLoS computational biology 2010;6:e1000785.

180. Yeung TM, Gandhi SC, Bodmer WF. Hypoxia and lineage specification of cell line-derived colorectal cancer stem cells. Proceedings of the National Academy of Sciences of the United States of America 2011;108:4382-7.

181. Blagoev KB. Organ aging and susceptibility to cancer may be related to the geometry of the stem cell niche. Proceedings of the National Academy of Sciences of the United States of America 2011;108:19216-21.

182. Lenaerts T, Pacheco JM, Traulsen A, Dingli D. Tyrosine kinase inhibitor therapy can cure chronic myeloid leukemia without hitting leukemic stem cells. Haematologica 2010;95:900-7.

183. Churnratanakul S, Wirzba B, Lam T, Walker K, Fedorak R, Thomson AB. Radiation and the small intestine. Future perspectives for preventive therapy. Digestive diseases 1990;8:45-60.

184. Ijiri K, Potten CS. The circadian rhythm for the number and sensitivity of radiation-induced apoptosis in the crypts of mouse small intestine. International journal of radiation biology 1990;58:165-75.

185. Geng L, Potten CS. Changes after irradiation in the number of mitotic cells and apoptotic fragments in growing mouse hair follicles and in the width of their hairs. Radiation research 1990;123:75-81.

186. Sato F, Muramatsu S, Tsuchihashi S, Shiragai A, Hiraoka T, Inada T, Kawashima K, Matsuzawa H, Nakamura W, Trucco E, Sacher GA. Radiation effects on cell populations in the intestinal epithelium of mice and its theory. Cell and tissue kinetics 1972;5:227-35.

187. Chwalinski S, Potten CS. Radiation-induced mitotic delay: duration, dose and cell position dependence in the crypts of the small intestine in the mouse. International journal of radiation biology and related studies in physics, chemistry, and medicine 1986;49:809-19.

188. Betschinger J, Knoblich JA. Dare to be different: asymmetric cell division in Drosophila, C. elegans and vertebrates. Current biology : CB 2004;14:R674-85.

189. Clevers H. Stem cells, asymmetric division and cancer. Nature genetics 2005;37:1027-8.

190. Morrison SJ, Kimble J. Asymmetric and symmetric stem-cell divisions in development and cancer. Nature 2006;441:1068-74.

191. Al-Nafussi AI, Wright NA. Cell kinetics in the mouse small intestine during immediate postnatal life. Virchows Archiv. B, Cell pathology including molecular pathology 1982;40:51-62.

192. Clayton E, Doupe DP, Klein AM, Winton DJ, Simons BD, Jones PH. A single type of progenitor cell maintains normal epidermis. Nature 2007;446:185-9.

193. Kirk D. Optimal Control Theory: An Introduction. Courier Dover Publications, 2004.

194. Schmidt GH, Winton DJ, Ponder BA. Development of the pattern of cell renewal in the crypt-villus unit of chimaeric mouse small intestine. Development 1988;103:785-90.

195. Macevicz SaO, G. Modeling social insect populations II: optimal reproductive strategies in annual eusocial insect colonies. Behav. Ecol. Sociobiol. 1976;1:265–282.

196. Perelson AS, Mirmirani M, Oster GF. Optimal strategies in immunology. I. B-cell differentiation and proliferation. Journal of mathematical biology 1976;3:325-67.

197. Hu Z, Fu YX, Greenberg AJ, Wu CI, Zhai W. Age-dependent transition from cell-level to population-level control in murine intestinal homeostasis revealed by coalescence analysis. PLoS genetics 2013;9:e1003326.
198. Wynn ML, Consul N, Merajver SD, Schnell S. Logic-based models in systems biology: a predictive and parameter-free network analysis method. Integrative biology : quantitative biosciences from nano to macro 2012;4:1323-37.
199. Dehmer JJ, Garrison AP, Speck KE, Dekaney CM, Van Landeghem L, Sun X, Henning SJ, Helmrath MA. Expansion of intestinal epithelial stem cells during murine development. PloS one 2011;6:e27070.

CHAPTER 2

NOTCH1 IS THE PRIMARY RECEPTOR REGULATING INTESTINAL STEM CELL HOMEOSTASIS

2.1: SUMMARY

The Notch signaling pathway controls intestinal epithelial differentiation, proliferation, and stem cell maintenance. Two Notch receptors, Notch1 (N1) and Notch2 (N2), are expressed in the epithelium, but the contribution of each receptor for these functions is unclear. In this study we use pan-epithelial genetic deletion of *N1* and *N2* to show that loss of *N1* alone results in secretory cell hyperplasia and decreased LGR5$^+$ stem cells. Interestingly, the secretory cell hyperplasia of the *N1* deleted intestine almost completely normalizes by two months; however, *N1* deletion renders the intestine incapable of post-irradiation recovery. Finally, we examine the combined roles of N1 and N2 on intestinal homeostasis. Our results suggest that N1 is the primary receptor involved in secretory cell fate decisions and stem cell maintenance, and that N2 plays a small role in differentiation, but a larger role in regulating proliferation. These results are critical for the continued understanding of intestinal stem cell regulation as well as potential complications with therapeutic Notch receptor blockade.

2.2: INTRODUCTION

In order to provide efficient digestive and barrier functions to the gut, the intestinal epithelium requires constant renewal of all of its absorptive and secretory cell populations, a process that is fueled by a highly proliferative intestinal stem cell compartment and regulated differentiation process.

The Notch signaling pathway is required for proper regulation of intestinal epithelial cell fate. Active Notch signaling is essential for specification of the most common cell type in the epithelium, the absorptive enterocyte[1-3]. Inhibition of the pathway by pharmacologic or genetic means leads to formation of secretory cell types such as mucin-producing goblet cells, hormone-secreting enteroendocrine cells, and antimicrobial peptide-secreting Paneth cells, at the expense of absorptive cells[4-7]. Notch signaling, in addition to Wnt, has been shown to be crucial for maintenance of proliferating progenitors[1, 3, 5, 8], and we previously determined that Notch was necessary for stem cell survival[4].

Expression of the 4 known Notch receptors (N1-4) and 5 ligands (Dll1, 3, 4 and Jag1 and 2) is temporally and spatially controlled for proper development and homeostasis of many tissues. N1 and N2 are both expressed in the adult intestinal epithelium[9-11], but individual roles for each receptor is not well understood.

Previous studies investigating N1 and N2 function utilizing humanized inhibitory antibodies suggested a role for N1 in regulating intestinal homeostasis, as α-N1 treatment showed a mild secretory cell hyperplasia[12] and decreased intestinal proliferation and toxicity when paired with irradiation damage[13] (see Appendix 1). Specific intestinal epithelial genetic deletion studies, in contrast, reported that N1 and N2 single deletions had no phenotype, and thus N1 and N2 were thought to be fully functionally redundant in the gut[14]. Due to the important therapeutic implications of intestinal Notch regulation, it is critically important to reconcile these disparate findings.

In this study we use a genetic deletion model to definitively show that N1 is the predominantly active Notch receptor in the intestinal epithelium, as *N1* deletion results in secretory cell transformation and impaired stem cell

maintenance and repair function. Furthermore, we investigate the dynamic regulation of lost N1 signal and expand on the understanding of how N1 and N2 function together to regulate proliferation and differentiation in the intestine.

2.3: MATERIALS AND METHODS

Mice

Floxed-*Notch1* (*N1^(F/F)*)[15] (Jackson Lab, no. 007181), floxed-*Notch2* (*N2^(F/F)*)[16] (Jackson Lab, no. 010525), floxed-*Rbpjκ* (*Rbpj^(F/F)*)[17] (gift from T. Honjo), *Rosa-LSL-NICD-IRES-nGFP* (*NICD*)[18] (Jackson Lab, no. 008159), *Villin-CreER^(T2)* [19] (gift from S. Robine) and *Lgr5-GFP-IRES-CreER^(T2)* (*Lgr5-GFP*)[20] (Jackson Lab, no. 008875) alleles were verified by PCR genotyping with the primers listed in Supplementary Table 2-1. All crosses were maintained on a C57BL/6 strain background. Mice were housed in ventilated and automated watering cages with a 12-hour light cycle under specific pathogen-free conditions. Protocols for mouse usage were approved by the University of Michigan Committee on Use and Care of Animals.

Animal treatment protocols and tissue collection

To activate CreER recombination, mice were injected intraperitoneally with 100mg/kg tamoxifen (Sigma) once per day for 5 days and tissue was collected on day 6 unless otherwise noted. To induce intestinal injury, animals were exposed to one dose of 12Gy whole body irradiation from a ^{137}Cs source. Animals were fasted overnight and injected intraperitoneally with 25 mg/kg 5-ethynyl-2′-deoxyuridine (EdU) (Life Technologies) 2 hours prior to tissue collection. Intestinal tissue was harvested and fixed in 4% paraformaldehyde overnight as previously described[4]. Tissue prepared for frozen sections was fixed in 4% PFA for 1 hour and incubated in 30% sucrose overnight before embedding in OCT (Tissue-Tek).

Immunohistochemistry

5µm paraffin sections were stained with Periodic acid Schiff and Alcian Blue (PAS/AB) (Newcomer Supply) and Alkaline Phosphatase (Vector Laboratories) to visualize mucin-containing goblet cells and enterocytes respectively. EdU-Click-it (Life Technologies) was used to evaluate proliferating cell number. Immunostaining with rat α-MMP7 (1:400, Vanderbilt Antibody and Protein Resource), rabbit α-MUC2 (1:200, Santa Cruz) and rabbit α-Ki67 (1:200, Thermo) was performed as described[21]. GFP transgene expression was visualized on 5µm frozen sections without antibody staining. Images were captured on a Nikon E800 microscope with Olympus DP controller software. Presented images are representative sections from terminal ileum unless otherwise noted.

Quantitative morphometric analysis

All slides were blinded for cell counting. Goblet cell hyperplasia was measured as the number of crypts that displayed increased goblet cells over total crypts per section. EdU morphometrics was achieved by counting the total number of epithelial EdU$^+$ cells per well-oriented crypt and averaged per animal. EdU counts were performed by two individuals.

Crypt isolation and flow cytometry

Crypt isolation was performed on proximal jejunum: centimeters 4-8 for crypt RNA and 9-15 for flow cytometry as measured from the pylorus. Tissue was incubated in 15mM EDTA (Sigma) in DPBS (Gibco) at 4°C for 35 minutes, vortexed for 2 minutes, and filtered through a 70µm cell strainer (BD Bioscience). Prior to processing for RNA isolation, crypts were gravity-settled twice for 10 minutes to remove single cells and fragments. To obtain a single cell suspension for flow cytometry, crypts were resuspended in TrypLE Express (Gibco), shaken at 37°C for 10-12 minutes, and 0.1mg/ml DNase I (Roche) and 10% fetal bovine serum (FBS) were added. Cells were passed through a 40µm cell strainer (BD Bioscience), pelleted at 400xG, resuspended in 2% FBS, 0.05% sodium azide

(Sigma), 2mM EDTA in DPBS and stained unfixed as follows. All cells were blocked with rat α-mouse CD16/CD32 (1:100, BD Bioscience), lymphocytes were excluded with CD45.2-PerCP-Cy5.5 (1:80, LifeTechnologies), epithelial cells were visualized with EpCAM-APC (1:80, eBioscience), and dead cells were excluded by DAPI incorporation. Cells were analyzed on a BD FACSCanto II and interpreted with FlowJo software (Treestar). GFP$^+$ cells were sequentially gated for size, singlets, DAPI$^-$, CD45.2$^-$, and EpCAM$^+$.

Gene expression analysis

RNA from full-thickness ileum was isolated by Trizol (Invitrogen) extraction followed by the RNeasy Mini kit (Qiagen) with DNAseI treatment. RNA from crypts was directly processed with the RNeasy Mini kit. cDNA was reverse transcribed with the iScript cDNA synthesis kit (BioRad) using 1μg of total RNA. Quantitative RT-PCR was performed as described[21] with the primers listed in Supplementary Table 2-2. Assays were run in triplicate and normalized to glyceraldehyde-3-phosphate dehydrogenase (*Gapdh*) as an internal control.

Statistical analyses

All experiments were performed with 3-6 biological replicates per group unless otherwise noted. Quantitative data are presented as mean + SEM, with all experimental groups normalized to time-matched tamoxifen-treated controls. Comparisons between two groups were conducted with unpaired two-tailed Student *t* tests. Comparisons between 3 or more groups were analyzed by one-way ANOVA with Tukey's or Dunett's post-tests as noted. Significance is reported as * ($P<0.05$), **($P<0.01$), ***($P<0.001$), and ****($P<0.0001$). Prism software (Graphpad) was used for statistical analyses.

2.4: RESULTS

Weight loss and secretory cell hyperplasia in N1-deleted intestine

To conditionally delete N1 in the intestinal epithelium, we crossed the $N1^{F/F}$ [15] allele to the tamoxifen-regulated *Villin-CreER*^{T2} [19]. After tamoxifen

treatment *Villin-CreER^{T2}; N1^{F/F}* (*N1^{Δ/Δ}*) mice transiently lost weight with a nadir (92% of initial weight) occurring at day 8 (Figure 2-1A). Although *N1^{Δ/Δ}* animals began to gain weight after day 8, they remained significantly lighter than controls until day 35.

As increased secretory cell differentiation is a hallmark of Notch inhibition, we assessed secretory cell populations in *N1^{Δ/Δ}* intestines to determine if single receptor deletion was sufficient to induce aberrant secretory cell differentiation. PAS/AB staining for mucin-containing cells revealed a striking increase in goblet cell abundance in the *N1^{Δ/Δ}* terminal ileum (Figure 2-1) and all other regions of the intestine (Supplementary Figure 2-1) one day after completion of tamoxifen treatment.   To determine if the abnormal goblet cell differentiation was maintained long-term, we analyzed *N1^{Δ/Δ}* animals on days 8, 19, and 60 after the start of tamoxifen induction. Interestingly, while goblet cell hyperplasia was observed in over 80% of crypts on day 8, the number of aberrant crypts significantly declined at later timepoints (Figure 2-1, Supplementary Figure 2-1). By day 60, only 6% of crypts still maintained evidence of goblet cell hyperplasia (Figure 2-1F), consistent with the stabilization of *N1^{Δ/Δ}* weights (Figure 2-1A).

To investigate if other secretory cell types were increased in *N1^{Δ/Δ}* mice, we stained for the Paneth cell marker MMP7. There was a marked increase in MMP7 staining (Supplementary Figure 2-2), as well as the presence of MUC2/MMP7 co-stained cells. MUC2 is a marker of goblet cells, and co-staining of the two markers indicates the presence of intermediate cells, a cell type that is also observed in pharmacological pan-Notch inhibition[4]. This finding was most striking in the colon, where only rare co-staining cells were observed in control tissue (Figure 2-1H, arrow). *N1^{Δ/Δ}* colon, in contrast, contained abundant MUC2/MMP7 co-stained cells, which persisted for more than 60 days (Figure 2-1I).

Analysis of secretory cell transcription factors and differentiated cell mRNA paralleled the observed secretory cell hyperplasia in the *N1^{Δ/Δ}* intestine as well as the time-dependent phenotype regression (Figure 2-2). *Atoh1*, which drives the differentiation of all secretory cell types[22, 23], was increased 3.3-fold on
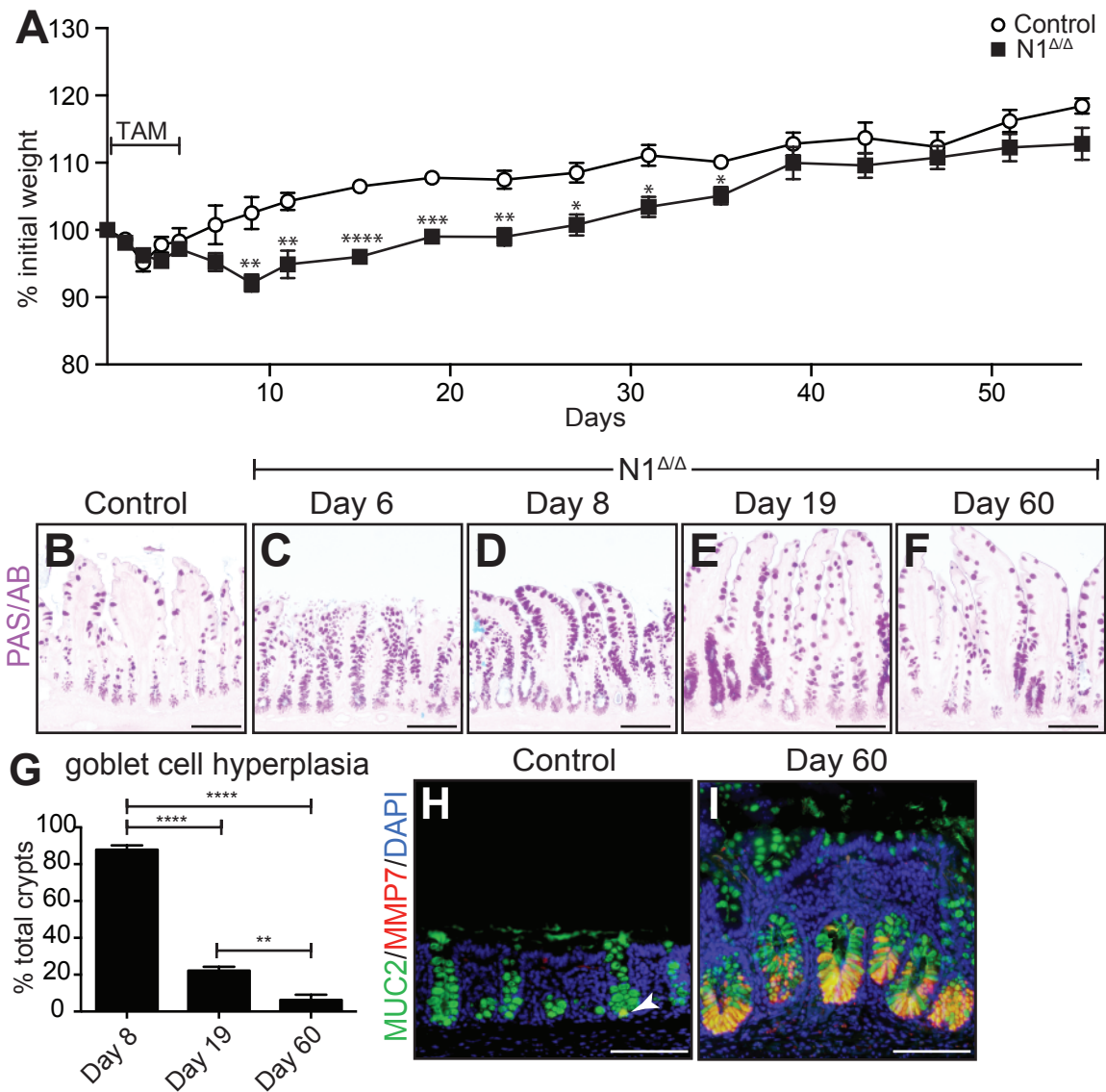
Figure 2-1. Intestinal epithelial N1 deletion leads to weight loss and aberrant secretory cell differentiation. (A) Weight curve of control and *Villin-CreER[T2]; N1[F/F]* (N1[Δ/Δ]) animals treated with 5 days of 100mg/kg tamoxifen. Bar represents duration of tamoxifen (TAM) treatment. Weights are compared with student *t* tests. (B-F) PAS/AB stained goblet cells in control (B) or N1[Δ/Δ] ileum (C-F) at the time points indicated. (G) Quantification of ileal goblet cell hyperplasia. Data are presented as percent total crypts and analyzed by ordinary one-way ANOVA with Tukey's multiple comparisons test. (H-I) Colon sections are immunostained for goblet cell marker MUC2 (green) and Paneth cell marker MMP7 (red) from control (H) and N1[Δ/Δ] (I) animals 60 days after tamoxifen treatment. White arrowhead marks a single co-staining cell. N = 3-6 animals for all groups. Scale bar = 100μm.
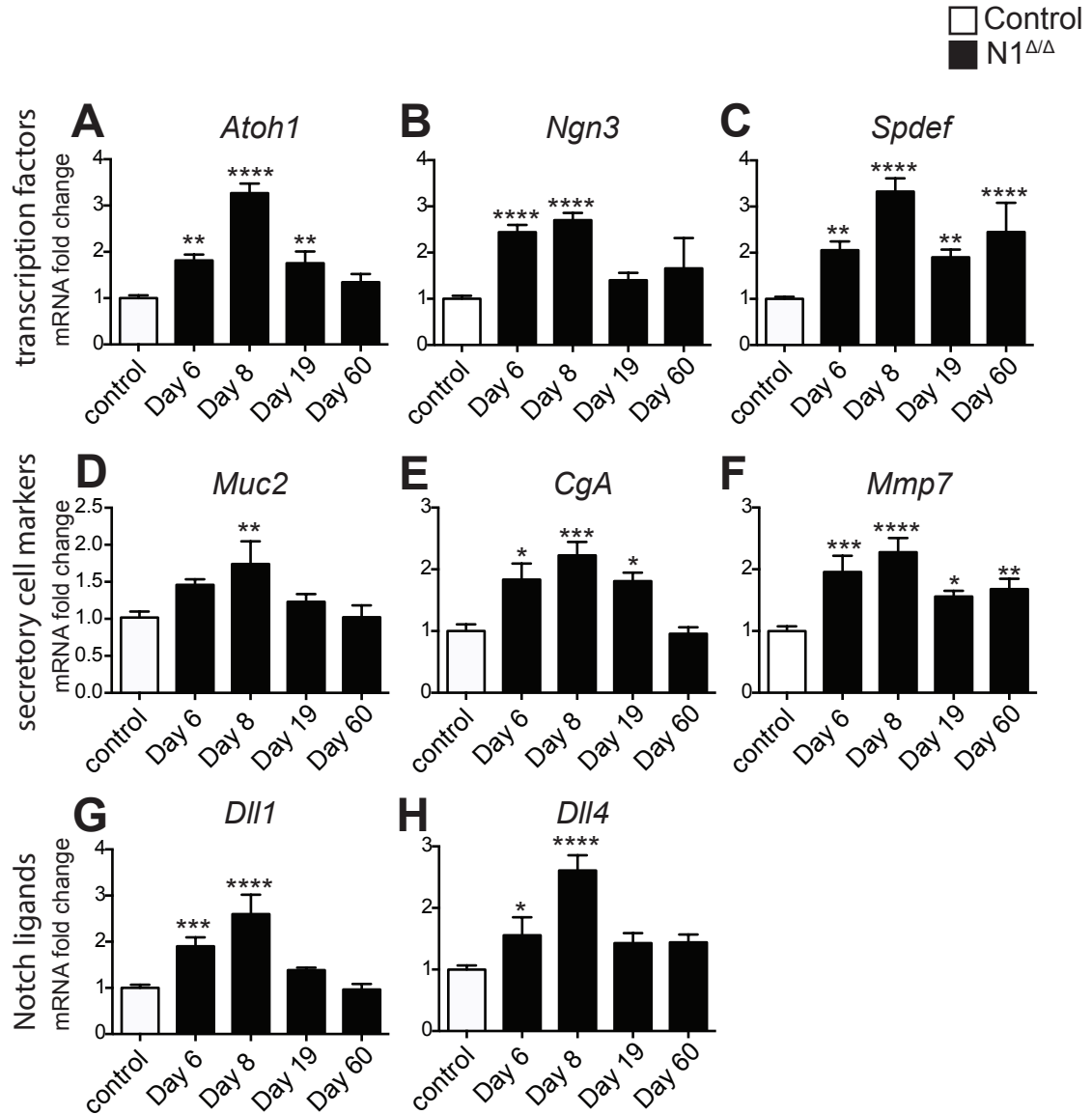
Figure 2-2. Secretory cell markers and Notch ligands are transiently upregulated in N1$^{\Delta/\Delta}$ intestine. Quantitative RT-PCR analysis of secretory cell transcription factors (A-C), differentiated secretory cell markers (D-F) and Notch ligands (G-H) in control and N1$^{\Delta/\Delta}$ animals at the time points indicated. RNA was isolated from full-thickness ileum. All values were normalized to *Gapdh* expression level and reported as fold change compared to control. Data were compared with ordinary one-way ANOVA with Dunnett's post-test. N = 3-6 animals/group.

day 8. *Ngn3* which is expressed in early endocrine cell precursors[24] was likewise increased 2.7-fold at this time point. Expression of these factors returned to baseline by day 60. *Spdef*, which is important for the terminal differentiation of goblet and Paneth cells[25,26], remained amplified 2.4-fold on day 60 (Figure 2-2C), consistent with the persistent expression of Paneth cell markers. Expression of *Muc2* and *CgA*, markers of differentiated goblet and endocrine cells, respectively, peaked at day 8 and normalized by day 60. Similar to *Spdef*, *Mmp7* expression remained elevated 1.7-fold on day 60, in agreement with the sustained MMP7 staining (Figure 2-2F). These results suggest that *N1* deletion promotes the formation of all secretory cell lineages. Differentiated goblet and endocrine cells are transiently increased after *N1* deletion while increased Paneth cell markers, presumably expressed in Paneth/goblet intermediate cells, remained for at least 2 months.

Dynamic regulation of Notch ligands

Overexpression of Notch ligands is one mechanism that could account for epithelial recovery in $N1^{\Delta/\Delta}$ intestine. DLL1 and DLL4 have been shown to be the primary ligands regulating the intestinal stem and progenitor compartment[7]. To this effect, we analyzed transcript levels of *Dll1* and *Dll4* in $N1^{\Delta/\Delta}$ intestine. Expression of both ligands was elevated 2.6-fold compared to control on day 8 (Figure 2-2G-H).

To determine whether the changes in *Dll1* and *Dll4* expression were directly linked to Notch signal, we took advantage of a Notch activation model. Previous use of such models has demonstrated the positive regulation of *Hes1*[3] and *Olfm4*[4] as well as the negative regulation of *Atoh1* and *Ngn3*[3]. For our experiment, we crossed *Villin-CreER^T2* to *Rosa26-LSL-NICD-IRES-nGFP*[17], which results in overexpression of stabilized N1 intracellular domain (NICD). Pan-epithelial activation of NICD leads to an immediate increase in epithelial proliferation, decreased secretory cell abundance, as well as decreased absorptive cell number (Supplementary Figure 2-3). Essentially, Notch activation transforms the intestinal epithelium into undifferentiated proliferative cells, rather

than absorptive cells as previously suggested[1]. In NICD-activated samples, both *Dll1* and *Dll4* expression was significantly decreased, mirroring the findings in the *N1[Δ/Δ]* intestine (Supplementary Figure 2-3J-K).

Importantly, the overexpression of *Dll1* and *Dll4* in *N1[Δ/Δ]* animals subsided over time, similar to the secretory cell markers discussed above, suggesting that the ligands are expressed on the aberrant secretory cells, and that increased ligand presentation is limited to the secretory cell expansion period.

N1-deletion does not lead to intestinal epithelial proliferation changes

In addition to secretory cell differentiation, Notch signaling controls intestinal epithelial proliferation[1, 3, 5]. Thus, we analyzed whether intestinal epithelial deletion of *N1* alone led to a proliferative defect. Interestingly, *N1[Δ/Δ]* intestine showed no decrease in proliferation at any time point as measured by morphometric counting of EdU^{+} cells (not shown). Flow cytometry for epithelial EdU^{+} cells also showed no change at 6 days after initiation of tamoxifen treatment (Supplementary Figure 2-4).

Loss of CBC stem cells in N1 deletion

We have previously shown that Notch signaling is critical for maintenance of the LGR5^{+} crypt base columnar (CBC) stem cell population[4], and thus questioned whether the secretory cell changes in the *N1[Δ/Δ]* intestine were coupled with altered stem cell homeostasis. To address this, we first analyzed mRNA transcripts of the CBC markers *Lgr5* and *Olfm4*. Expression of both genes was markedly depleted in the *N1[Δ/Δ]* intestine (not shown).

To further validate the N1-dependence of CBC stem cells, we crossed the *Villin-CreER[T2]; N1[F/F]* mice to *Lgr5-GFP*[20] to allow visualization of LGR5^{+} stem cells by GFP expression. In this experiment, control animals were tamoxifen-treated *Lgr5-GFP* mice with wild type *N1* alleles. After tamoxifen induction, we noted that the *N1[Δ/Δ]* mice appeared to have fewer GFP^{+} cells (data not shown). To quantify this change we employed flow cytometry on single cells isolated from *N1[Δ/Δ]* and control crypts. As there is a gradient of GFP expression in Lgr5-GFP

crypts[27] (Figure 2-3A), we gated for GFP^{HI} cells to explicitly measure changes in LGR5$^+$ CBCs (Figure 2-3C-D). In controls, 30% of total GFP$^+$ cells were GFP^{HI}, while N1$^{\Delta/\Delta}$ mice retained only 14% GFP^{HI} cells, a 53% reduction from baseline.

*Quiescent stem cell markers are not directly regulated by Notch*

To determine if stem cell depletion was specific to CBC stem cells, or if it was generalizable to proposed quiescent stem cell (QSC) populations, we assessed mRNA transcript levels of *Bmi1*, *Lrig1*, and *Hopx*. While we observed no change in *Bmi1* or *Lrig1* transcripts, there was a 2.3-fold increase in *Hopx* expression in *N1$^{\Delta/\Delta}$* intestine (Supplementary Figure 2-5). To our knowledge there is no established association between *Hopx* and Notch signaling, and indeed we saw no change in any of these markers in NICD activated tissues.

N1 is required for post-irradiation recovery

Since *N1* deletion results in changes in both differentiated and CBC stem cell populations, we investigated whether loss of N1 also limits intestinal repair functions. To assess this, we treated control and *N1$^{\Delta/\Delta}$* animals with tamoxifen and then administered 12Gy of whole body irradiation. The *N1$^{\Delta/\Delta}$* group quickly lost weight and had to be euthanized 3 days post-irradiation (Figure 2-4). It should be noted that while the control group also lost weight, a parallel experiment demonstrated that 12 Gy-irradiated control mice survive at least 8 days post-irradiation before succumbing to bone marrow insufficiency (data not shown). PAS/AB staining showed increased goblet cells in the *N1$^{\Delta/\Delta}$* group (Figure 2-4C), consistent with the phenotype observed in non-irradiated animals at this time point (Figure 2-1D). Normal intestine experiences a proliferative surge 3 days post-irradiation as part of the recovery response. This surge is mainly attributed to the expansion of QSC populations, as the majority of CBCs are destroyed by irradiation[28-30]. To evaluate this, we analyzed EdU incorporation in control and *N1$^{\Delta/\Delta}$* intestine. While control animals did display a visible increase in number of EdU$^+$ cells compared to non-irradiated intestine, the *N1$^{\Delta/\Delta}$* tissue was almost completely devoid of proliferative cells. The CBC compartment is not
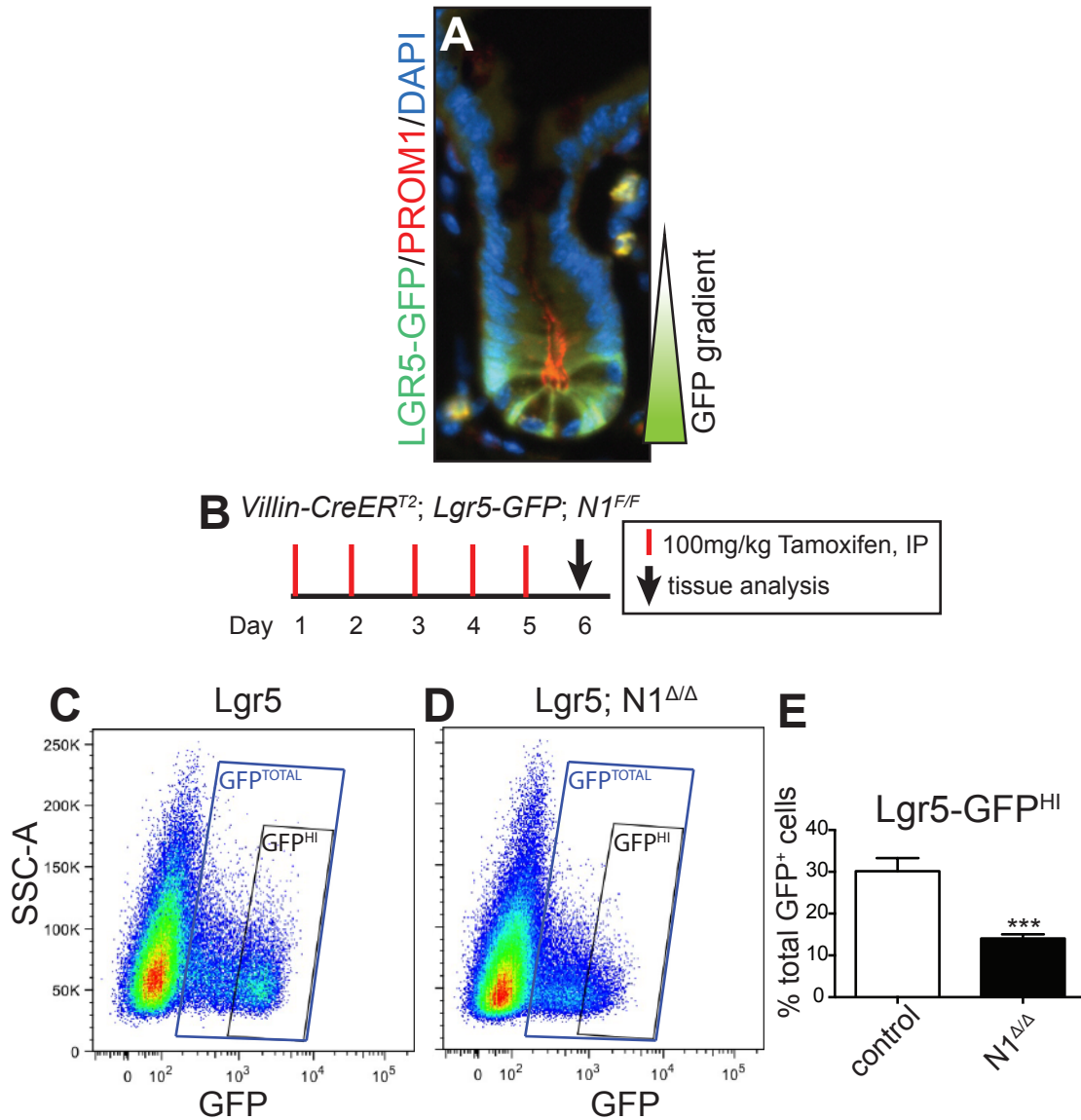
Figure 2-3. LGR5^{+} stem cells are depleted with N1 deletion. (A) Lgr5-GFP[+] crypt shows a gradient of GFP expression which is highest in the CBCs. (B) Control and *Villin-CreERT2; Lgr5-GFP; N1F/F* animals were injected with 100mg/kg tamoxifen daily for 5 days and harvested on day 6. (C-D) Scatter plots of GFP expression in single, live, CD45.2- EpCAM+ crypt epithelial cells in control (C) and N1$^{\Delta/\Delta}$ (D) animals. Gates indicate GFP[HI] populations and GFP[TOTAL] populations. (E) Quantification of GFP[HI] cells. Data are presented as percentage of GFP[TOTAL] cells. N = 3-4 animals/group.
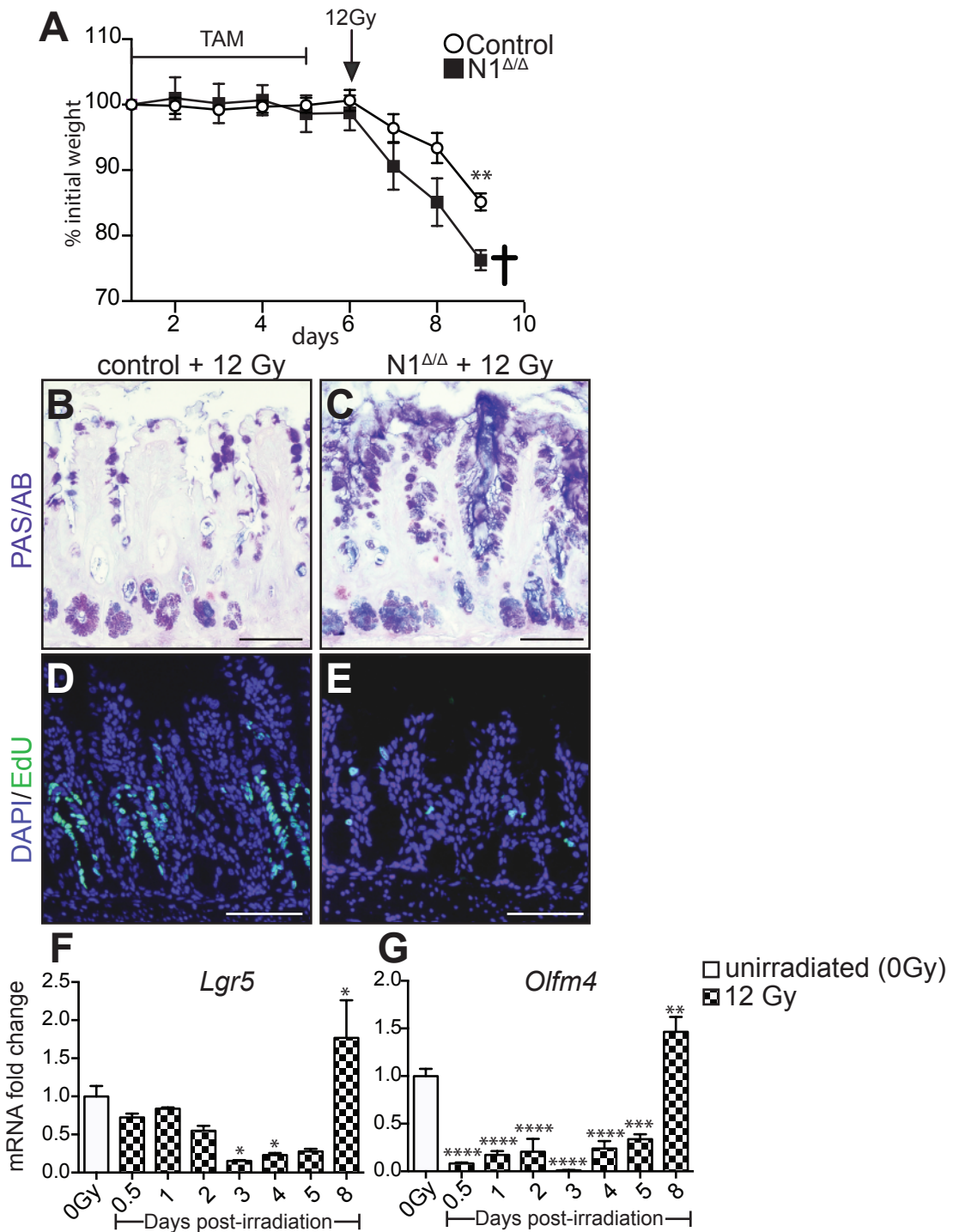
Figure 2-4. N1 is required for post-irradiation intestinal recovery. (A) Control and N1$^{\Delta/\Delta}$ animals were administered 12Gy of whole body irradiation on day 6 and harvested on day 9 when the N1$^{\Delta/\Delta}$ group had lost more than 20% body weight and was moribund (†). (B-C) PAS/AB staining for goblet cells in control (B) and N1$^{\Delta/\Delta}$ (C) intestine. (D-E) Proliferation was assessed by EdU incorporation in control (D) and N1$^{\Delta/\Delta}$ (E) animals. (F-G) Quantitative RT-PCR analysis of the CBC markers *Lgr5* and *Olfm4* in nontransgenic control mice treated with 0 or 12 Gy whole body irradiation. Scale bar =100μm.

expected to recover before approximately 1 week post-irradiation[29]. In fact, expression of CBC markers *Lgr5* and *Olfm4* do not recover until 8 days post-exposure to 12Gy (Figure 2-4F-G). Thus the failed proliferation in irradiated $N1^{\Delta/\Delta}$ intestine is likely independent from the loss of CBCs discussed above. Although *N1* deletion did not directly deplete QSC markers in non-irradiated tissue, the absence of N1 receptor may inhibit QSC activation when challenged with injury.

N2-deleted intestine shows no change in differentiation

Since our $N1^{\Delta/\Delta}$ results identified previously unrecognized phenotypes of intestinal epithelial *N1* deletion, we analyzed *N2* deletion to determine if loss of this receptor led to any unappreciated epithelial changes as well. To achieve specific intestinal epithelial deletion we crossed *Villin-CreERT2* to the $N2^{F/F}$ [16] allele. In contrast to $N1^{\Delta/\Delta}$, tamoxifen-treated *Villin-CreERT2; $N2^{F/F}$* ($N2^{\Delta/\Delta}$) animals did not lose any weight post-treatment (data not shown), and no goblet cell changes were evident in $N2^{\Delta/\Delta}$ intestine (Figure 2-5). Furthermore, no transcriptional changes were observed in any secretory cell transcription factors, differentiated cell markers, Notch ligands, or stem cell markers.

Cooperation of N1 and N2 receptors

Although *N2*-deleted intestine had no overt phenotype on its own, double deletion of *N1* and *N2* receptors is known to be lethal. Since $N1^{\Delta/\Delta}$ animals survived and partially recovered, we aimed to compare the extent of the $N1^{\Delta/\Delta}$ secretory cell phenotype with full Notch receptor deletion. Indeed $N1^{\Delta/\Delta};N2^{\Delta/\Delta}$ animals had a more profound goblet cell hyperplasia compared to $N1^{\Delta/\Delta}$ alone (Figure 2-6). Secretory cell transcription factors and differentiated markers were significantly higher in $N1^{\Delta/\Delta};N2^{\Delta/\Delta}$ compared to the $N1^{\Delta/\Delta}$ animals. This suggests that N1 and N2 function synergistically rather than redundantly to regulate epithelial differentiation.

To better understand this relationship, we assessed whether *N2* deletion sensitized the intestine to partial loss of *N1*. For this, we analyzed $N1^{\Delta/+};N2^{\Delta/\Delta}$ animals. Interestingly, while we found that the secretory cell response was only
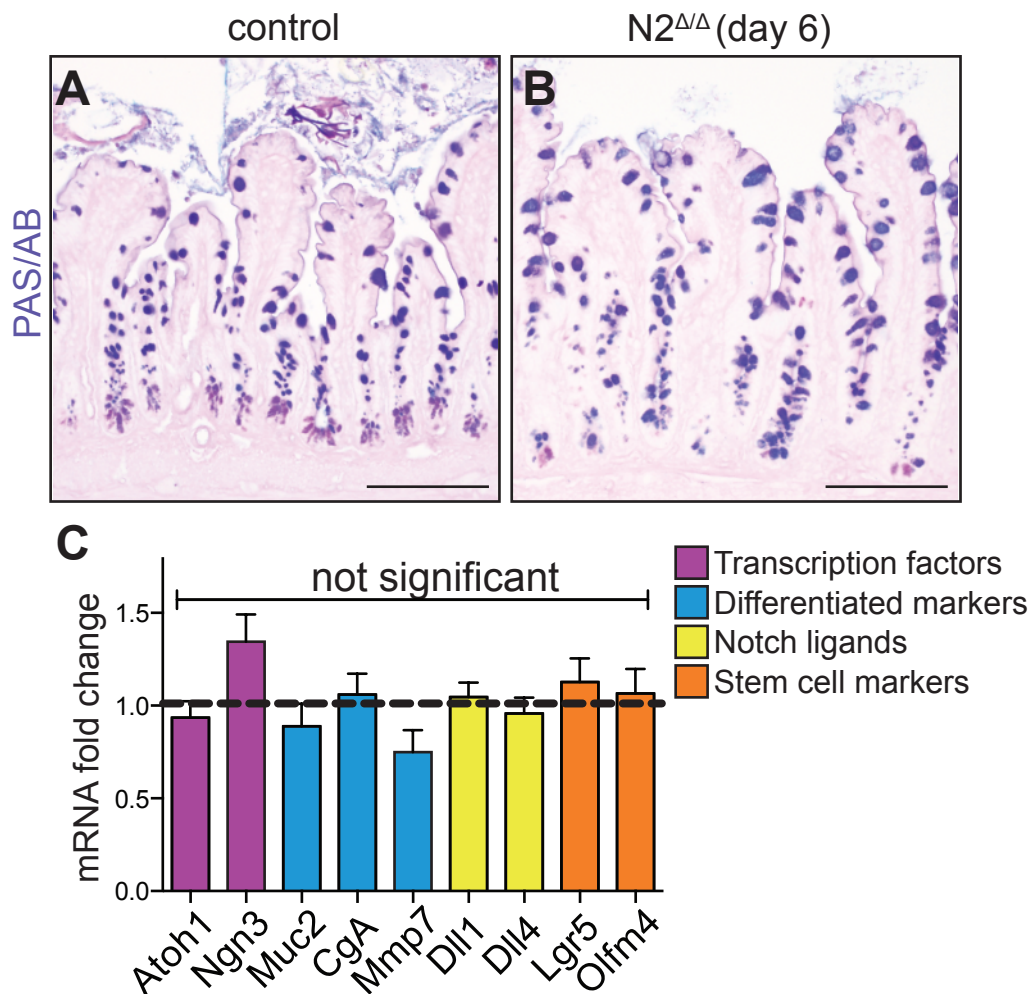
Figure 2-5. N2 deletion in the intestinal epithelium does not result in secretory cell changes. Control or *Villin-CreER^T2; N2^F/F* animals were treated with 100mg/kg tamoxifen daily for 5 days (N2^Δ/Δ) and harvested on day 6. (A-B) PAS/AB staining for goblet cells in control (A) and N2^Δ/Δ (B) intestine. No marked increases in goblet cells were observed in the N2^Δ/Δ animals. (C) qRT-PCR analysis of secretory transcription factors (purple), differentiated secretory cell markers (blue), Notch ligands (yellow) and stem cell markers (orange). Data are presented as mRNA fold-change compared to control, which was normalized to 1 (dashed line). No significant changes were observed for any marker gene. (Ngn3, P=0.1364; Mmp7, P=0.1760). N = 3-6. Scale bar =100μm.
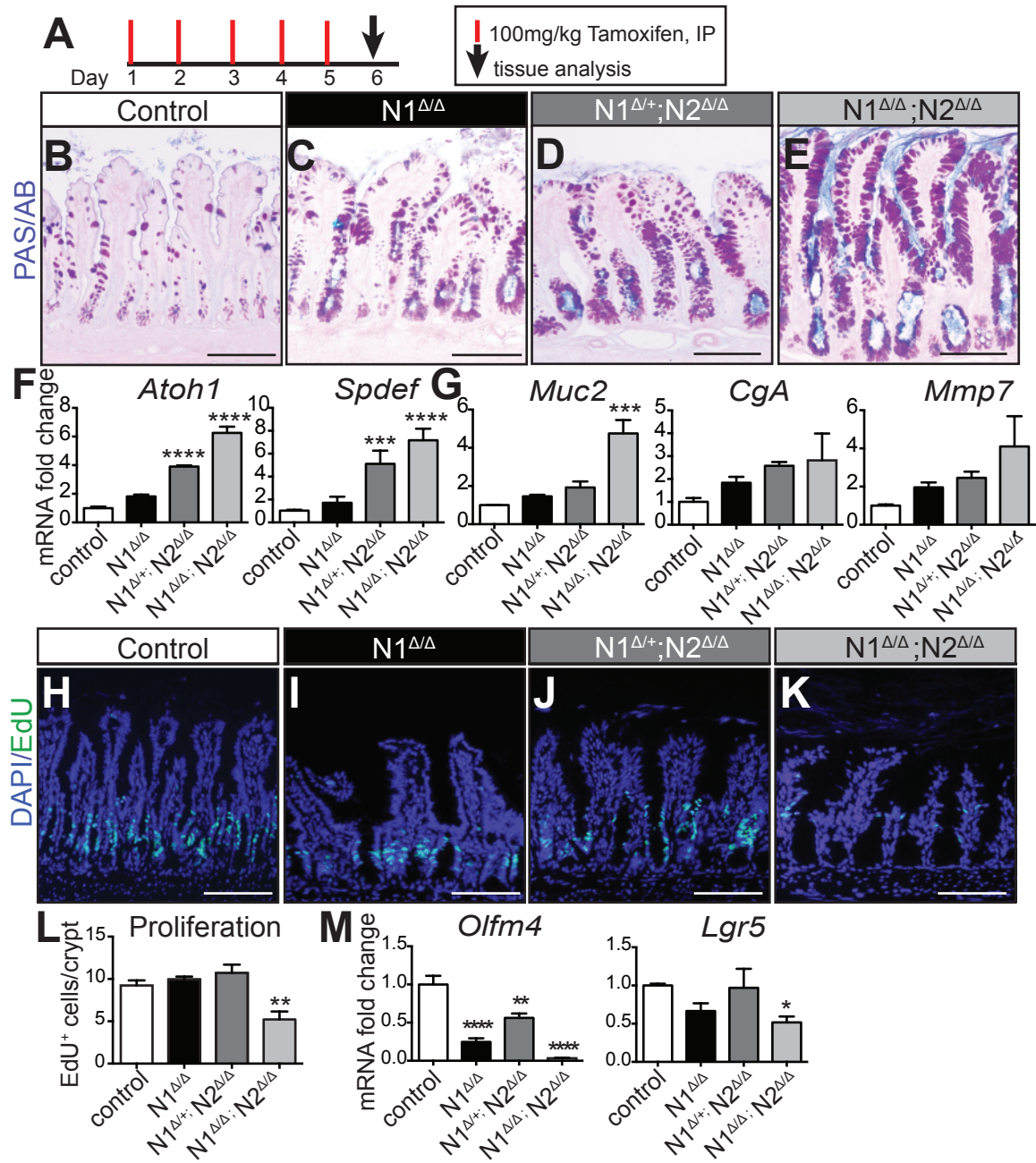
Figure 2-6. Synergistic and redundant functions of N1 and N2 in the intestinal epithelium. (A) All animals were injected with 100mg/kg tamoxifen daily for 5 days and harvested on day 6. (B-E) PAS/AB staining for goblet cells in control (B), N1$^{\Delta/\Delta}$ (C), N1$^{\Delta/+}$; N2$^{\Delta/\Delta}$ (D), N1$^{\Delta/\Delta}$; N2$^{\Delta/\Delta}$ (E) ileum. (F-G) Quantitative RT-PCR analysis for secretory cell transcription factors (F) and differentiated secretory cell markers (G) in all groups. (H-K) Representative images of ileal proliferation as visualized by EdU uptake in all groups. (L) Quantification of proliferative cells. Data are presented as average EdU$^+$ cells/crypt. Control group is pooled day 6 and day 8 controls, which were shown to the same. (M) Quantitative RT-PCR analysis for CBC stem cell markers in all groups. Quantitative data are compared with ordinary one-way ANOVA and Dunnett's post-test. N = 3-5 animals/group. Scale bar =100μm.

mildly more severe than $N1^{\Delta/\Delta}$ (Figure 2-6C, D), expression of secretory cell transcription factors was significantly increased in this group compared to $N1^{\Delta/\Delta}$ alone.

One crucial component of Notch epithelial regulation that was not appreciated in the $N1^{\Delta/\Delta}$ samples was disruption of overall epithelial proliferation. Interestingly, $N1^{\Delta/+};N2^{\Delta/\Delta}$ intestine also showed no change in proliferation (Figure 2-6J, L). Only full Notch receptor deletion resulted in decreased proliferation, suggesting that N1 and N2 function fully redundantly for this process.

Finally, we compared transcript levels of *Olfm4* and *Lgr5* in all three groups. Interestingly, while $N1^{\Delta/\Delta};N2^{\Delta/\Delta}$ animals had the highest suppression of CBC markers, $N1^{\Delta/\Delta}$ had a greater depletion of transcript levels than $N1^{\Delta/+};N2^{\Delta/\Delta}$ (Figure 2-6M). This indicates N1 is the primary receptor functioning in this stem cell population.

2.5 DISCUSSION

We present here evidence that the N1 receptor plays an important role in intestinal epithelial cell fate and stem cell maintenance. Epithelial deletion of *N1* results in a transient secretory cell hyperplasia, with overproduction of all secretory cell types. Overexpression of goblet and endocrine cell markers resolve by 2 months after *N1* deletion, but Paneth cell markers and the presence of Paneth/goblet intermediate cells persist in $N1^{\Delta/\Delta}$ animals. Additionally, our study used the *Lgr5-GFP* mouse model in combination with *N1* deletion to show that loss of *N1* very acutely impacts CBC stem cell homeostasis. Furthermore, *N1* deletion renders the intestine highly susceptible to irradiation injury, such that $N1^{\Delta/\Delta}$ animals die 3 days post-irradiation. Finally, our results further clarify the relationship between N1 and N2. We validate previous work that showed intestinal epithelial N2 deletion showed no obvious phenotype[6], and report new evidence that N1 and N2 work redundantly to regulate proliferation, but work synergistically in regulating differentiated cell fate.

Previous studies implicated that N1 is important for stem cells since its expression was found to be highest in CBCs compared to other crypt cells[31, 32].

Additionally, *N1*-expressing cells[11] as well as cells undergoing active N1 cell-surface cleavage[33] have been shown to lineage trace, the gold-standard for defining stem cells *in vivo*. To our knowledge, though, only one other study has investigated the <u>function</u> of N1 in intestinal stem cells. Vooijs et al.[33] used a chimeric *N1* deletion mouse model to conclude that while N1 was active in stem cells, it was not required for stem cell maintenance since LacZ expression from deleted cells was still observed in adult chimeras. Our results are not in direct conflict with this study, as the sheer presence of crypts with goblet cell hyperplasia after 60 days demonstrates that at least some N1-deficient stem cells have survived. Indeed, we did not observe a <u>complete</u> loss of *Lgr5* transcript or LGR5-GFP^{HI} stem cells in *N1*$^{\Delta/\Delta}$ intestine. Rather, our data favors a model where N1-deficient stem cells are at a great disadvantage compared to normal stem cells. N1-deficient stem cells can survive if necessary, but this is the exception, not the rule.

Our study is the first to show the dynamic regulation of *N1* deletion, as the epithelium almost completely normalizes within 2 months. This finding could be due to compensation for N1 loss by another Notch receptor or by competition with non-recombined cells. The *N1* deletion efficiency in our tissues started at 95% (data not shown), and since *N1*$^{\Delta/\Delta}$ stem cells are at a disadvantage, they could conceivably be outcompeted by neighboring unrecombined cells. This would lead to a patchy recovery over time as observed in both our *N1* deletion time course as *Rbpj* partial deletion model (Supplementary Figure 2-6).

Although goblet and endocrine cell populations subsided during the period analyzed, Paneth cell markers continued to be expressed. While it is agreed that Paneth cells are much longer lived than other differentiated intestinal epithelial cells, the exact length of the Paneth cell lifespan is disputed, with estimates from 18-60 days [34, 35]. Interestingly, the Paneth cells produced in *N1*$^{\Delta/\Delta}$ animals co-express goblet cell markers. The continued presence of these cells after 60 days suggests that once cells are specified as expressing both Paneth and goblet cell markers, that they do so for the duration of their life span. Of note, *Dll1* and *Dll4* have both previously been shown to be expressed in Paneth cells[36, 37] and *Dll1*

expression has additionally been demonstrated in secretory progenitors and to a lesser extent differentiated secretory cells[37]. Our results extend this finding to expression in Paneth/goblet intermediate cells as well.

Different approaches have been used to investigate the role of intestinal N1 in the past, but these published results are inconsistent. While our study bolsters the secretory cell findings reported with N1-inhibitory antibody treatment[12] and chimeric *N1*-deleted intestine[33], another study using the same model system we have employed in our experiments found that *Villin-CreER^{T2}; N1$^{\Delta/\Delta}$* mice had no phenotype[14]. Since this study used juvenile mice, we questioned whether the role of N1 in regulating differentiated cell populations was specific to fully mature intestine. When we repeated our experiment in juvenile mice, secretory hyperplasia was evident (Supplementary Figure 2-7). Thus we conclude that the differences between the previously published report and our own data may be due to tamoxifen treatment concentrations and chase times post-treatment, which were not made clear in the previous study, or variation in recombination frequencies due to using different *floxed-N1* and *N2* lines.

Finally, we previously discovered that N1-inhibitory antibody-treated animals were susceptible to irradiation injury[13]. Because the antibody was administered systemically, however, it was not clear if the intestinal epithelial cell findings were the primary cause of animal death, or it was a secondary phenotype produced from an off-target pathology like vasculopathy. Since *N1* deletion in the current study was limited to intestinal epithelial cells, we have strong evidence that intestinal N1 is required for injury response. The significance of this finding is self-evident. Since Notch receptors are promising pharmacological targets for cancer treatment and most successful therapeutic schemes are combined with injury-inducing chemotherapies or radiation, dual treatment with N1 inhibition could be deleterious.

In conclusion, N1 receptor plays a primary role in regulating intestinal epithelial cell fate and stem cell maintenance. Genetic deletion of the receptor leads to eventual epithelial recovery, but targeted inhibition of N1 should be

handled with caution due to the important role this receptor plays in intestinal epithelial homeostasis.

2.6: ACKNOWLEDGMENTS

Genotyping primer sequences

Allele	Forward primer sequence	Reverse primer sequence
Villin-CreER[T2]	ACAGGCACTAAGGGAGCCAATG	GTTCTTGCGAACCTCATCACT
Lgr5-GFP	CTGCTCTCTGCTCCCAGTCT	GAACTTCAGGGTCAGCTTGC
Floxed-N1	CCAACTGCACTCTTCTCCCAGTAATCGAAG	TGCCTCAGTTCAAACACAAGATACGAGGGG
Floxed-N2	ACCCTGTCAGAAAGTTGGCTGGTCAGGTTT	TAGAGGACGCACTGACTGCTCATCTGACAA
Rosa-LSL-NICD	AAAGTCGCTCTGAGTTGTTAT	GAAAGACCGCGAAGAGTTTG
Floxed-Rbpj	CTTGATAATTCTGTAAAGAGA	ACATTGCATTTTCACATAAAAAAGC

Primer sequences for genes analyzed by quantitative RT-PCR

Gene	Forward primer sequence	Reverse primer sequence
Ascl2	CCTCTCTCGGACCCTCTCTCAG	CAGTCAAGGTGTGCTTCCATGC
Atoh1	GCCTTGCCGGACTCGCTTCTC	TCTGTGCCATCATCGCTGTTAGGG
Bmi1	TATAACTGATGATGAGATAATAAGC	CTGGAAAGTATTGGGTATGTC
CgA	AAGAAGAGGAGGAGGAAGAGG	TCCATCCACTGCCTGAGAG
Dll1	CTGAGGTGTAAGATGGAAGCG	CAACTGTCCATAGTGCAATGG
Dll4	TCGTCGTCAGGGACAAGAATAGC	CTCGTCTGTTCGCCAAATCTTACC
Hopx	GAGGACCAGGTGGAGATCCT	TCCGTAACAGATCTGCATTCC
Lgr5	CGAGCCTTACAGAGCCTGATACC	TTGCCGTCGTCTTTATTCCATTGG
Lrig1	GTGAACAGTGGCTCCCTCTATGG	ACTCCGCTAGACTCTCCTCATCC
Mmp7	CAGACTTACCTCGGATCGTAGTGG	GTTCACTCCTGCGTCCTCACC
Muc2	AGAACGATGCCTACACCAAG	CATTGAAGTCCCCGCAGAG
Ngn3	ACCCTATCCACTGCTGCTTGTC	CGGGAAAAGGTTGTTGTGTCTCTG
Olfm4	GCCACTTTCCAATTTCAC	GAGCCTCTTCTCATACAC
Spdef	GGACGGACGACTCTTCTGACAG	GCTCCTGATGCTGCCTTCTCC

control   N1$^{\Delta/\Delta}$ (Day 6)

duodenum — A, E

jejunum — B, F

ileum — C, G

colon — D, H

PAS/AB

I   goblet cell hyperplasia duodenum
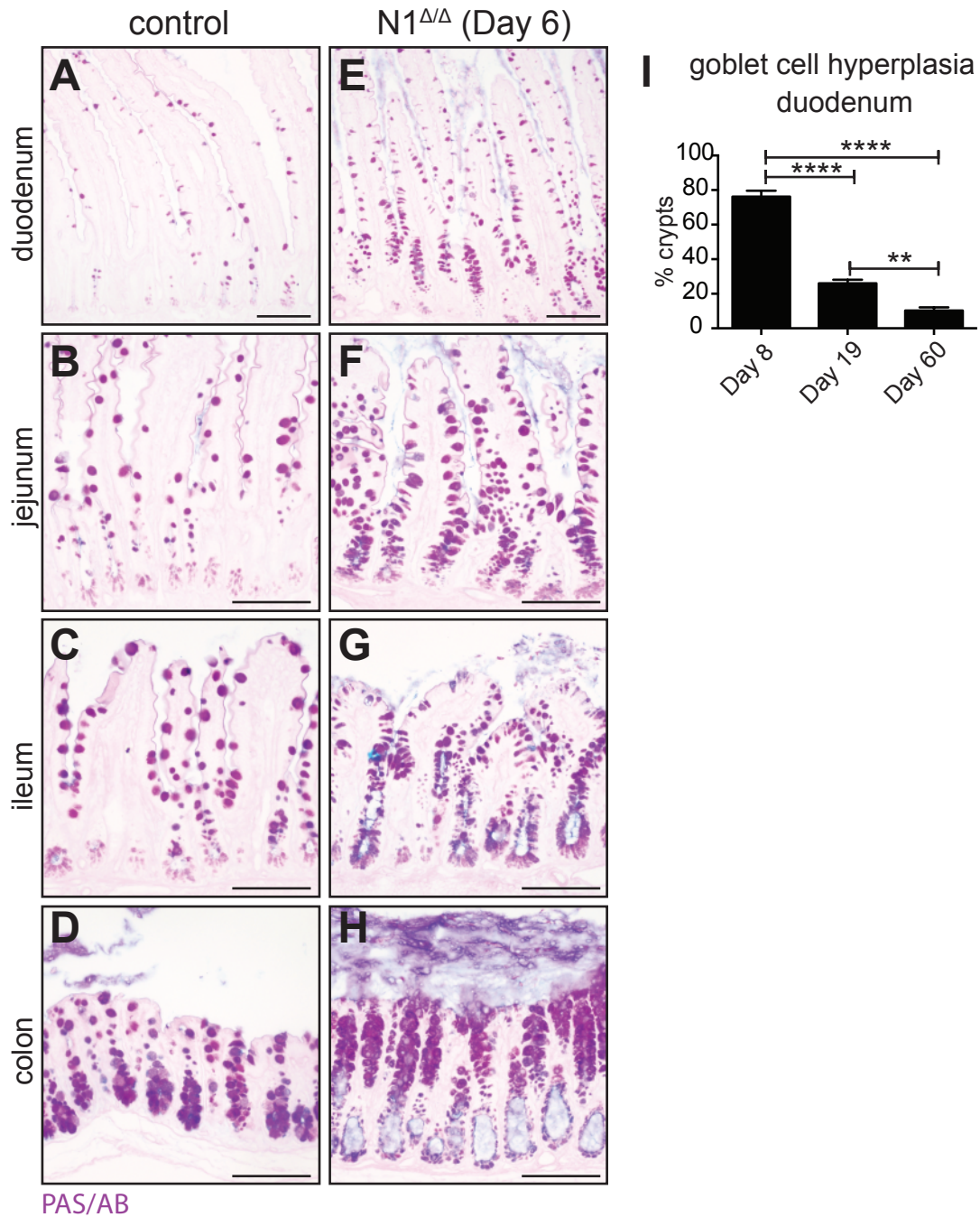
Supplementary Figure 2-1. N1 deletion in the intestinal epithelium results in increased goblet cells throughout the intestine. (A-H) PAS/AB staining for goblet cells is shown for control (A-D) and N1$^{\Delta/\Delta}$ (E-H) tissue harvested on day 6 after initiating tamoxifen treatment. Representative paraffin sections are shown from duodenum (A, E), jejunum (B, F), ileum (C, G), and proximal colon (D, H). Goblet cell hyperplasia is observed in all segments of N1$^{\Delta/\Delta}$ intestine. (I) Quantification of goblet cell hyperplasia in the duodenum shows phenotype regression over time with similar kinetics as observed in the ileum (see Figure 2-1). Data are presented as percent total crypts and compared using one-way ANOVA with Tukey's multiple comparisons test. N = 4. Scale bar =100µm.
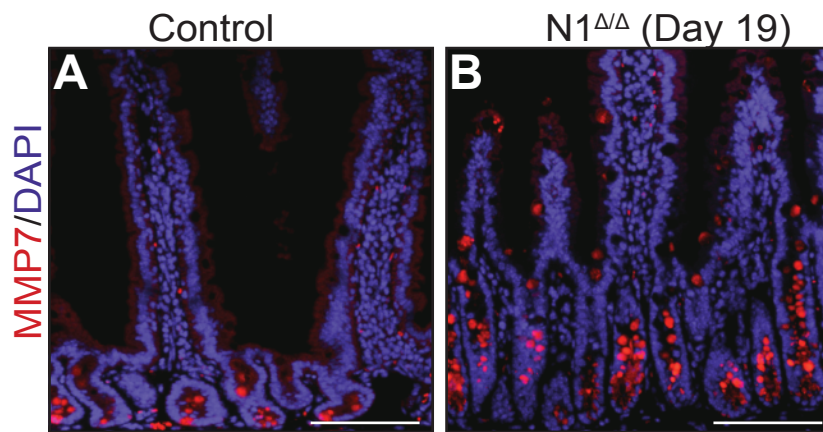
Supplementary Figure 2-2. Paneth cells are increased with N1 deletion. (A-B) MMP7 staining for Paneth cells in control (A) and N1$^{\Delta/\Delta}$ (B) duodenum on day 19 after the start of tamoxifen induction. Increased numbers MMP7$^+$ cells as well as expansion of the zone of cellular localization is observed in N1$^{\Delta/\Delta}$ intestine. Duodenum is displayed since the change is especially striking in proximal intestine where there are normally few Paneth cells, although increased MMP7 staining was observed in all parts of the intestine. N = 6. Scale bar =100μm.
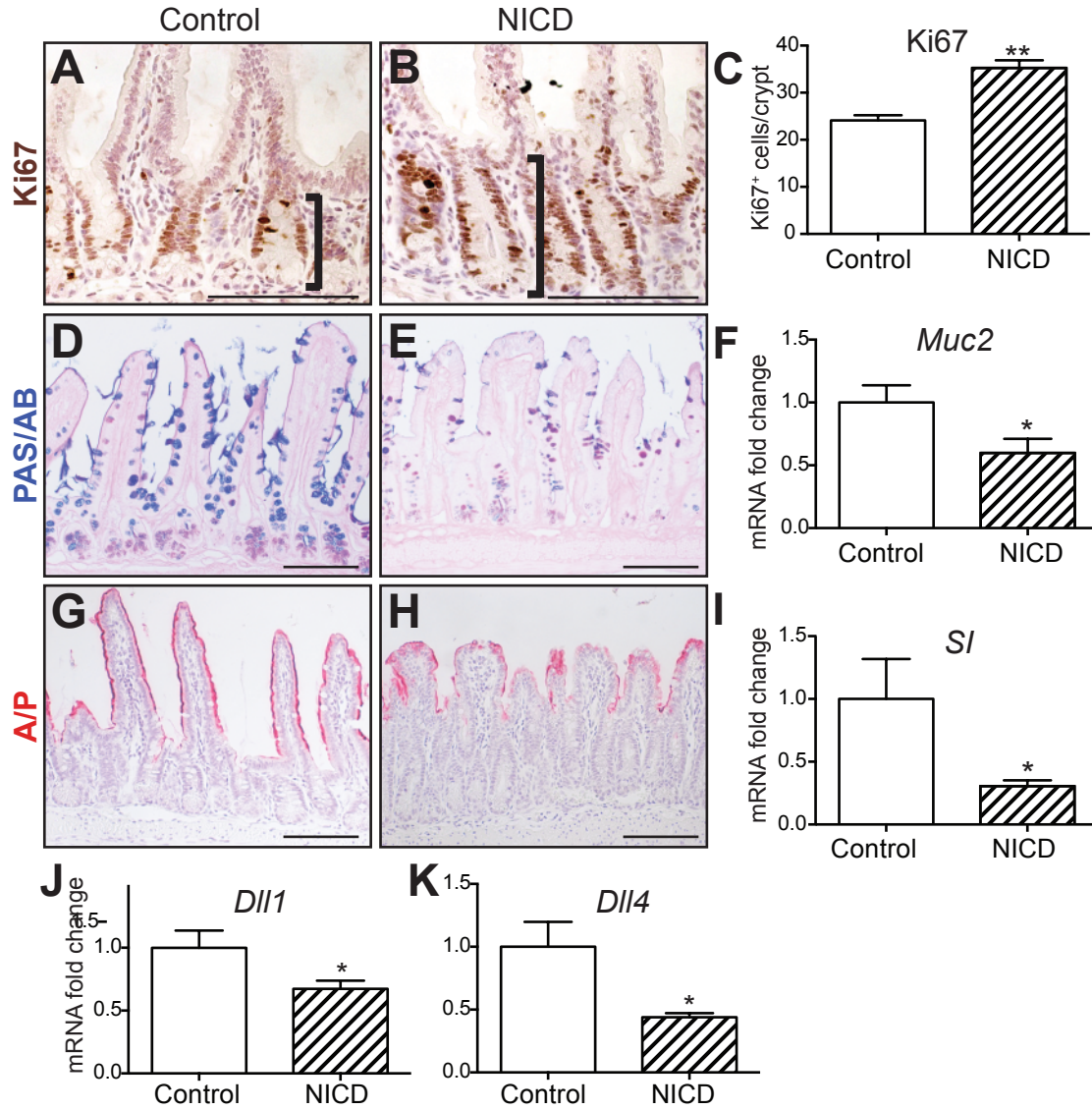
Supplementary Figure 2-3. NICD overexpression results in production of undifferentiated proliferative cells. Control or V*illin-CreERT2; Rosa-LSL-NICD* mice were treated with 5 days of 100mg/kg tamoxifen and tissues were harvested on day 6. (A-C) Proliferation in control and NICD ileum as visualized by Ki67 immunostaining and quantified in (C). Data are presented as average number of Ki67+ cells per crypt. A significant increase in proliferative cells was observed in NICD intestine. (D-E) PAS/AB staining for goblet cells in control and NICD ileum. Goblet cell number was significantly decreased in NICD intestine. (quantification not shown). (F) Expression of the goblet cell marker *Muc2* was also decreased in NICD animals. (G-H) Alkaline Phosphatase (A/P) staining for brush border enzymes marks enterocytes. A/P+ surface area is greatly decreased in NICD animals. (I) Expression of the enterocyte marker sucrose isomaltase (*SI*) is also significantly decreased in NICD intestine. (J-K) Expression of Notch ligands Dll1 and Dll4 are decreased in NICD intestine. Comparisons were made with Student's *t* test. Scale bar =100μm. Data in collaboration with Nichole Zayan.
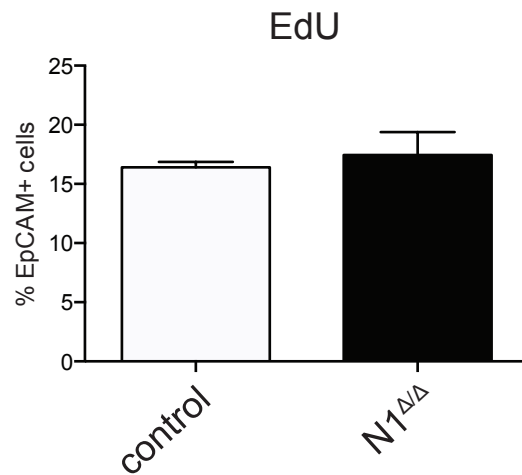
Supplementary Figure 2-4. No change in proliferation is observed in N1$^{\Delta/\Delta}$ intestine. Singly isolated control and N1$^{\Delta/\Delta}$ epithelial cells were assessed for proliferation via EdU incoroporation and flow cytometry analysis. No change in proliferation was observed. Data are presented as % total EpCAM+ cells that were Edu+. N = 4 animals/group.
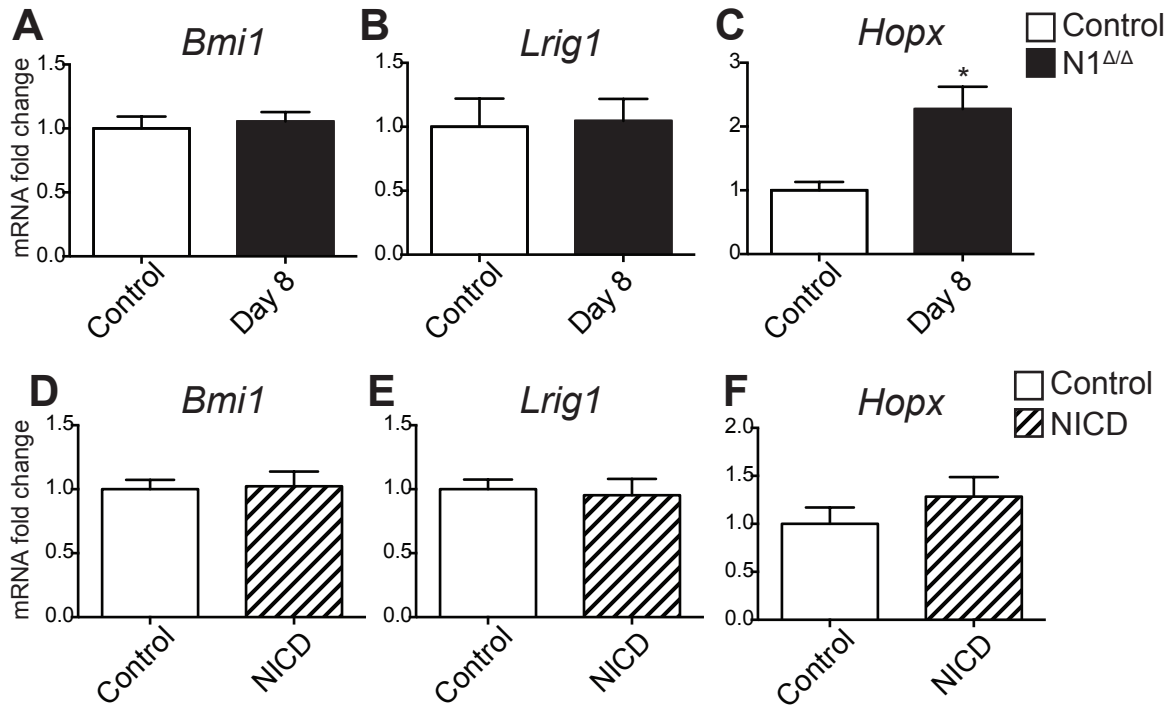
Supplementary Figure 2-5. Quiescent stem cell markers are not Notch-regulated. (A-F) Quantitative RT-PCR analysis of quiescent stem cell markers in N1$^{\Delta/\Delta}$ (A-C) or NICD-overexpressing (D-F) intestine. RNA was isolated from full-thickness ileum. N = 3-4 animals/group.
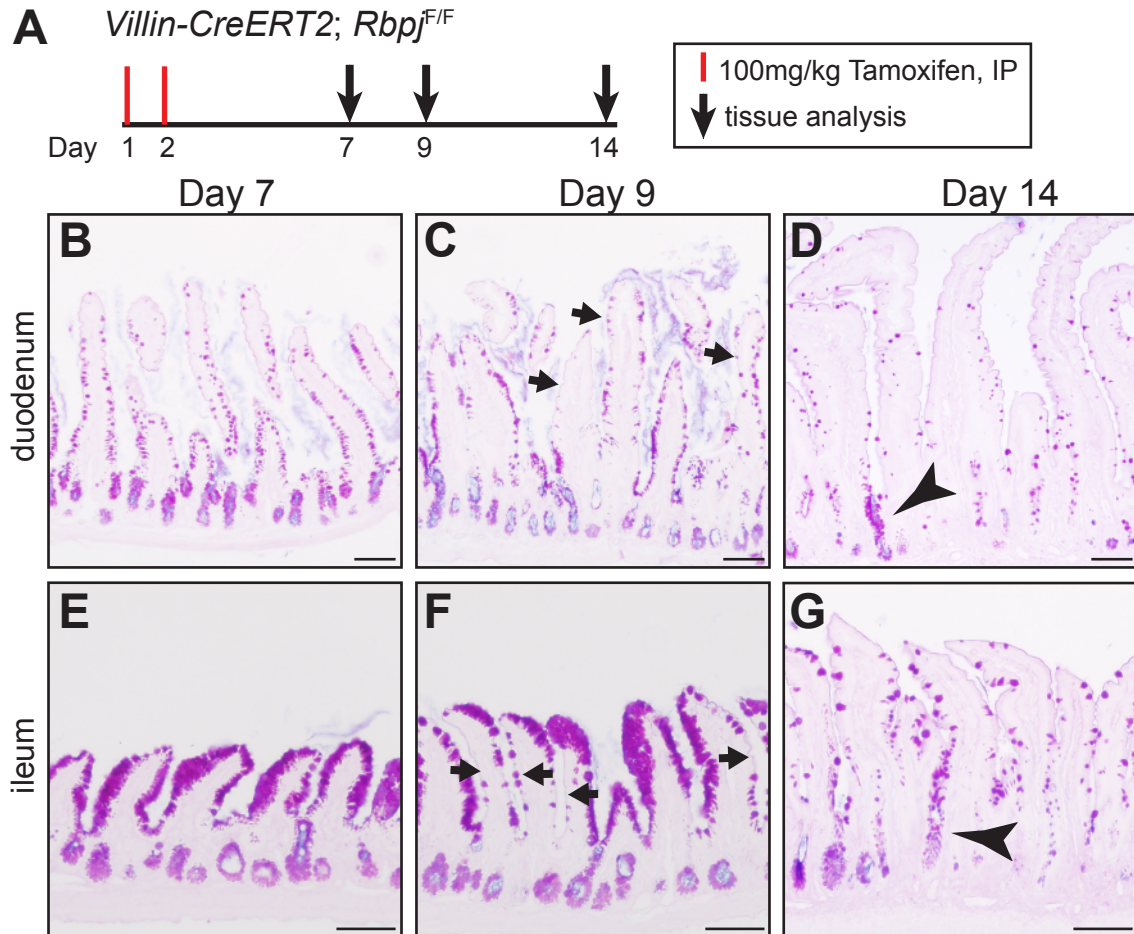
Supplementary Figure 2-6. Complete blockade of Notch signaling by Rbpj deletion results in goblet cell hyperplasia that normalizes over time. (A) Villin-CreERT2; Rbpj$^{F/F}$ mice were treated with two doses of 100mg/kg tamoxifen and tissues were harvested on day 7, 9, and 14. (B-G) PAS/AB staining for goblet cells in duodenum (B-D) and ileum (E-G) at the time points indicated. Arrows indicate patches of villi that lack goblet cells. Arrowheads denote crypts that maintain goblet cell hyperplasia. N=1 per time point. Scale bar =100μm.

A P10 *Villin-CreERT2*; *N1^{F/F}*

| 100mg/kg Tamoxifen, IP
↓ tissue analysis

Day 1 2 3 4 5 6

Control   N1^{Δ/Δ}

B duodenum   **C**

D ileum   **E**
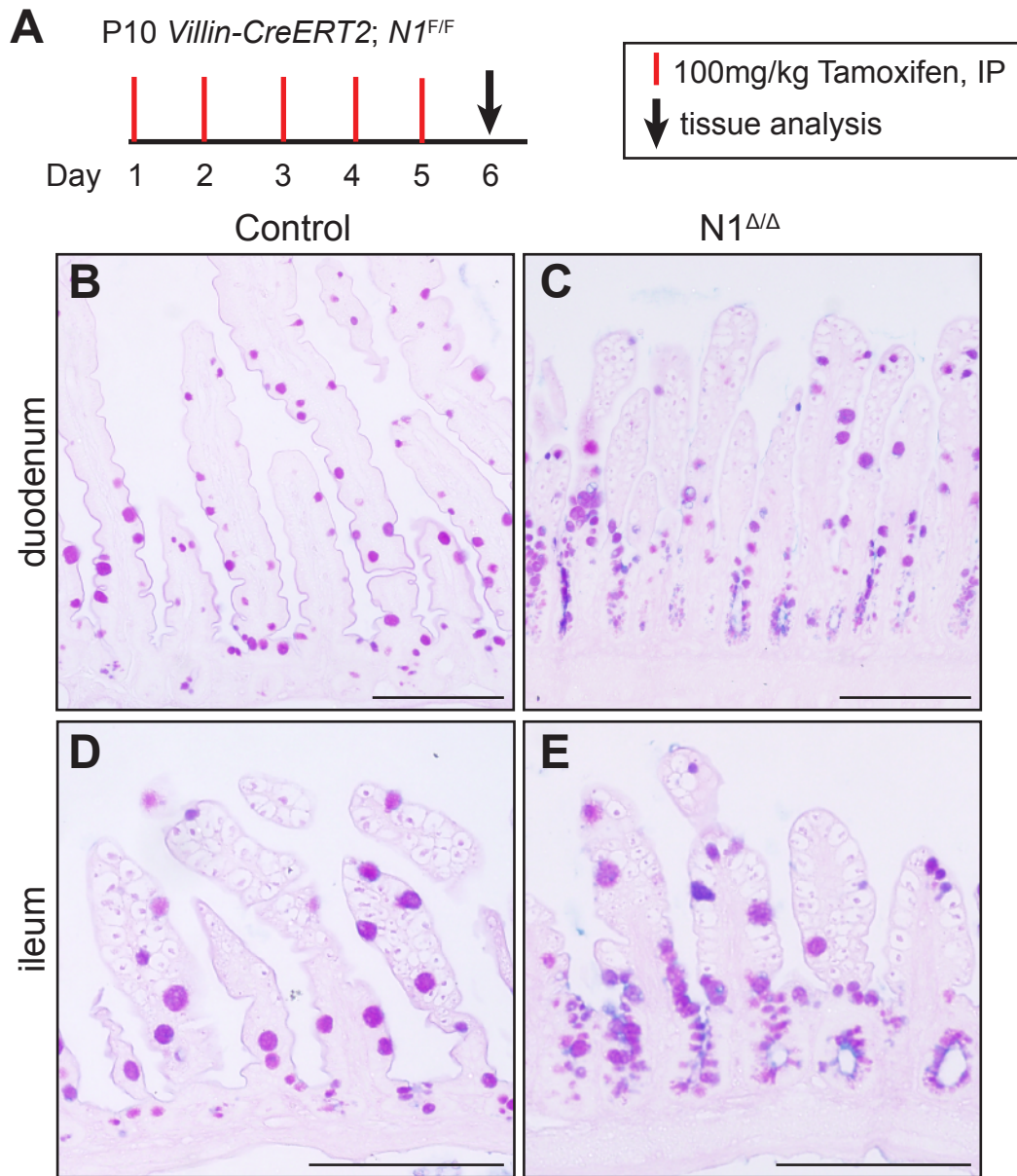
Supplementary Figure 2-7. N1 deletion in juvenile mice has a mild but apparent secretory cell phenotype. (A) 10-day old control or *Villin-CreER^{T2}; N1^{F/F}* animals were treated with 100mg/kg tamoxifen for 5 days and tissues were harvested on day 6. (B-E) PAS/AB staining for goblet cells in control (B, D) and N1^{Δ/Δ} (C,E) intestine. Increased goblet cell abundance is observed in both duodenum (C) and ileum (E) of juvenile N1^{Δ/Δ} intestine. Interestingly N1^{Δ/Δ} mice also appear to have more developed crypts than controls, which may be due to the altered differentiation program. N=1 control, 2 N1^{Δ/Δ}. Scale bar =100μm.

REFERENCES

1. Stanger BZ, Datar R, Murtaugh LC, Melton DA. Direct regulation of intestinal fate by Notch. Proc Natl Acad Sci U S A 2005;102:12443-8.
2. Jensen J, Pedersen EE, Galante P, Hald J, Heller RS, Ishibashi M, Kageyama R, Guillemot F, Serup P, Madsen OD. Control of endodermal endocrine development by Hes-1. Nat Genet 2000;24:36-44.
3. Fre S, Huyghe M, Mourikis P, Robine S, Louvard D, Artavanis-Tsakonas S. Notch signals control the fate of immature progenitor cells in the intestine. Nature 2005;435:964-8.
4. VanDussen KL, Carulli AJ, Keeley TM, Patel SR, Puthoff BJ, Magness ST, Tran IT, Maillard I, Siebel C, Kolterud A, Grosse AS, Gumucio DL, Ernst SA, Tsai YH, Dempsey PJ, Samuelson LC. Notch signaling modulates proliferation and differentiation of intestinal crypt base columnar stem cells. Development 2012;139:488-97.
5. van Es JH, van Gijn ME, Riccio O, van den Born M, Vooijs M, Begthel H, Cozijnsen M, Robine S, Winton DJ, Radtke F, Clevers H. Notch/gamma-secretase inhibition turns proliferative cells in intestinal crypts and adenomas into goblet cells. Nature 2005;435:959-63.
6. Riccio O, van Gijn ME, Bezdek AC, Pellegrinet L, van Es JH, Zimber-Strobl U, Strobl LJ, Honjo T, Clevers H, Radtke F. Loss of intestinal crypt progenitor cells owing to inactivation of both Notch1 and Notch2 is accompanied by derepression of CDK inhibitors p27Kip1 and p57Kip2. EMBO reports 2008;9:377-83.
7. Pellegrinet L, Rodilla V, Liu Z, Chen S, Koch U, Espinosa L, Kaestner KH, Kopan R, Lewis J, Radtke F. Dll1- and dll4-mediated notch signaling are required for homeostasis of intestinal stem cells. Gastroenterology 2011;140:1230-1240 e7.
8. Korinek V, Barker N, Moerer P, van Donselaar E, Huls G, Peters PJ, Clevers H. Depletion of epithelial stem-cell compartments in the small intestine of mice lacking Tcf-4. Nature genetics 1998;19:379-83.
9. Sander GR, Powell BC. Expression of notch receptors and ligands in the adult gut. J Histochem Cytochem 2004;52:509-16.
10. Schroder N, Gossler A. Expression of Notch pathway components in fetal and adult mouse small intestine. Gene Expr Patterns 2002;2:247-50.
11. Fre S, Hannezo E, Sale S, Huyghe M, Lafkas D, Kissel H, Louvi A, Greve J, Louvard D, Artavanis-Tsakonas S. Notch lineages and activity in intestinal stem cells determined by a new set of knock-in mice. PloS one 2011;6:e25785.
12. Wu Y, Cain-Hom C, Choy L, Hagenbeek TJ, de Leon GP, Chen Y, Finkle D, Venook R, Wu X, Ridgway J, Schahin-Reed D, Dow GJ, Shelton A, Stawicki S, Watts RJ, Zhang J, Choy R, Howard P, Kadyk L, Yan M, Zha

J, Callahan CA, Hymowitz SG, Siebel CW. Therapeutic antibody targeting of individual Notch receptors. Nature 2010;464:1052-7.

13. Tran IT, Sandy AR, Carulli AJ, Ebens C, Chung J, Shan GT, Radojcic V, Friedman A, Gridley T, Shelton A, Reddy P, Samuelson LC, Yan M, Siebel CW, Maillard I. Blockade of individual Notch ligands and receptors controls graft-versus-host disease. The Journal of clinical investigation 2013;123:1590-604.

14. Riccio O, van Gijn ME, Bezdek AC, Pellegrinet L, van Es JH, Zimber-Strobl U, Strobl LJ, Honjo T, Clevers H, Radtke F. Loss of intestinal crypt progenitor cells owing to inactivation of both Notch1 and Notch2 is accompanied by derepression of CDK inhibitors p27Kip1 and p57Kip2. EMBO Rep 2008;9:377-83.

15. Yang X, Klein R, Tian X, Cheng HT, Kopan R, Shen J. Notch activation induces apoptosis in neural progenitor cells through a p53-dependent pathway. Developmental biology 2004;269:81-94.

16. McCright B, Lozier J, Gridley T. Generation of new Notch2 mutant alleles. Genesis 2006;44:29-33.

17. Tanigaki K, Han H, Yamamoto N, Tashiro K, Ikegawa M, Kuroda K, Suzuki A, Nakano T, Honjo T. Notch-RBP-J signaling is involved in cell fate determination of marginal zone B cells. Nature immunology 2002;3:443-50.

18. Murtaugh LC, Stanger BZ, Kwan KM, Melton DA. Notch signaling controls multiple steps of pancreatic differentiation. Proceedings of the National Academy of Sciences of the United States of America 2003;100:14920-5.

19. el Marjou F, Janssen KP, Chang BH, Li M, Hindie V, Chan L, Louvard D, Chambon P, Metzger D, Robine S. Tissue-specific and inducible Cre-mediated recombination in the gut epithelium. Genesis 2004;39:186-93.

20. Barker N, van Es JH, Kuipers J, Kujala P, van den Born M, Cozijnsen M, Haegebarth A, Korving J, Begthel H, Peters PJ, Clevers H. Identification of stem cells in small intestine and colon by marker gene Lgr5. Nature 2007;449:1003-7.

21. Lopez-Diaz L, Hinkle KL, Jain RN, Zavros Y, Brunkan CS, Keeley T, Eaton KA, Merchant JL, Chew CS, Samuelson LC. Parietal cell hyperstimulation and autoimmune gastritis in cholera toxin transgenic mice. American journal of physiology. Gastrointestinal and liver physiology 2006;290:G970-9.

22. Yang Q, Bermingham NA, Finegold MJ, Zoghbi HY. Requirement of Math1 for secretory cell lineage commitment in the mouse intestine. Science 2001;294:2155-8.

23. Shroyer NF, Helmrath MA, Wang VY, Antalffy B, Henning SJ, Zoghbi HY. Intestine-specific ablation of mouse atonal homolog 1 (Math1) reveals a role in cellular homeostasis. Gastroenterology 2007;132:2478-88.

24. Jenny M, Uhl C, Roche C, Duluc I, Guillermin V, Guillemot F, Jensen J, Kedinger M, Gradwohl G. Neurogenin3 is differentially required for endocrine cell fate specification in the intestinal and gastric epithelium. The EMBO journal 2002;21:6338-47.

25. Gregorieff A, Stange DE, Kujala P, Begthel H, van den Born M, Korving J, Peters PJ, Clevers H. The ets-domain transcription factor Spdef promotes maturation of goblet and paneth cells in the intestinal epithelium. Gastroenterology 2009;137:1333-45 e1-3.

26. Noah TK, Kazanjian A, Whitsett J, Shroyer NF. SAM pointed domain ETS factor (SPDEF) regulates terminal differentiation and maturation of intestinal goblet cells. Experimental cell research 2010;316:452-65.

27. Sato T, Vries RG, Snippert HJ, van de Wetering M, Barker N, Stange DE, van Es JH, Abo A, Kujala P, Peters PJ, Clevers H. Single Lgr5 stem cells build crypt-villus structures in vitro without a mesenchymal niche. Nature 2009;459:262-5.

28. Van Landeghem L, Santoro MA, Krebs AE, Mah AT, Dehmer JJ, Gracz AD, Scull BP, McNaughton K, Magness ST, Lund PK. Activation of two distinct Sox9-EGFP-expressing intestinal stem cell populations during crypt regeneration after irradiation. American journal of physiology. Gastrointestinal and liver physiology 2012;302:G1111-32.

29. Yan KS, Chia LA, Li X, Ootani A, Su J, Lee JY, Su N, Luo Y, Heilshorn SC, Amieva MR, Sangiorgi E, Capecchi MR, Kuo CJ. The intestinal stem cell markers Bmi1 and Lgr5 identify two functionally distinct populations. Proceedings of the National Academy of Sciences of the United States of America 2012;109:466-71.

30. Takeda N, Jain R, LeBoeuf MR, Wang Q, Lu MM, Epstein JA. Interconversion between intestinal stem cell populations in distinct niches. Science 2011;334:1420-4.

31. Sato T, van Es JH, Snippert HJ, Stange DE, Vries RG, van den Born M, Barker N, Shroyer NF, van de Wetering M, Clevers H. Paneth cells constitute the niche for Lgr5 stem cells in intestinal crypts. Nature 2010.

32. Munoz J, Stange DE, Schepers AG, van de Wetering M, Koo BK, Itzkovitz S, Volckmann R, Kung KS, Koster J, Radulescu S, Myant K, Versteeg R, Sansom OJ, van Es JH, Barker N, van Oudenaarden A, Mohammed S, Heck AJ, Clevers H. The Lgr5 intestinal stem cell signature: robust expression of proposed quiescent '+4' cell markers. The EMBO journal 2012;31:3079-91.

33. Vooijs M, Ong CT, Hadland B, Huppert S, Liu Z, Korving J, van den Born M, Stappenbeck T, Wu Y, Clevers H, Kopan R. Mapping the consequence of Notch1 proteolysis in vivo with NIP-CRE. Development 2007;134:535-44.

34. Cheng H, Merzel J, Leblond CP. Renewal of Paneth cells in the small intestine of the mouse. The American journal of anatomy 1969;126:507-25.

35. Ireland H, Houghton C, Howard L, Winton DJ. Cellular inheritance of a Cre-activated reporter gene to determine Paneth cell longevity in the murine small intestine. Developmental dynamics : an official publication of the American Association of Anatomists 2005;233:1332-6.

36. Sato T, van Es JH, Snippert HJ, Stange DE, Vries RG, van den Born M, Barker N, Shroyer NF, van de Wetering M, Clevers H. Paneth cells

constitute the niche for Lgr5 stem cells in intestinal crypts. Nature 2011;469:415-8.

37. van Es JH, Sato T, van de Wetering M, Lyubimova A, Nee AN, Gregorieff A, Sasaki N, Zeinstra L, van den Born M, Korving J, Martens AC, Barker N, van Oudenaarden A, Clevers H. Dll1+ secretory progenitor cells revert to stem cells upon crypt damage. Nature cell biology 2012;14:1099-104.

CHAPTER 3

NOTCH REGULATION OF STEM CELL DYNAMICS

3.1: SUMMARY

The Notch signaling pathway is an important regulator of intestinal stem and progenitor cells. It has been previously shown that chronic blockade of Notch signaling leads to a marked reduction of proliferation, increased secretory cell formation, and decreased stem cell number. In this study, we show that acute inhibition of Notch signaling results in an unexpected increase in proliferation while maintaining robust secretory cell changes. Transient blockade of Notch is sufficient to rapidly decrease the expression of the Notch-specific stem cell marker *Olfm4*, indicating that the stem cell compartment is targeted. Additionally, flow cytometry for GFP in *Lgr5-GFP* mice shows a shift from GFP^{HI} to GFP^{INT}, suggesting that loss of stem cells is due to flow from the stem cell compartment to the transit-amplifying (TA) cell compartment. Compartmental modeling of the intestinal crypt was used to test the hypothesis that symmetric division of stem cells into TA cells could account for the increased proliferation observed with acute DBZ treatment. Modeling supported the symmetric division hypothesis in the context of a Notch-regulated repopulation of the stem cell compartment. Acute DBZ in the post-irradiation setting suggests that Notch regulates repopulation by allowing crypt base columnar stem cell specification rather than directly regulating quiescent stem cell populations.

3.2: INTRODUCTION

The intestinal epithelium is one of the most rapidly renewing tissues in the human body, with an estimated 17 billion cells turning over each day[1]. This startling replenishment rate is fueled by highly active stem and progenitor cell compartments. Historically, a single population of intestinal stem cells (ISCs) was thought to direct this renewal. ISCs divide once per day, leading to both stem cell self-renewal as well as delivering cells to the transit-amplifying (TA) cell compartment[2]. TA cells subsequently divide approximately every 12 hours, undergoing several rounds of division, greatly augmenting the number of cells in the crypt[3-5]. Regulated differentiation of TA cells results in the formation of mature, differentiated intestinal cells: either absorptive enterocytes, the most common cell in the epithelium, or one of several secretory cell populations, including mucin-secreting goblet cells, hormone-secreting enteroendocrine cells, and antimicrobial peptide-secreting Paneth cells[6].

The location and identity of the ISC has been debated for decades, with some favoring the crypt base columnar cell (CBCC) intercalated between the Paneth cells at the base of the crypt[7], and others supporting the "+4 cell", cells located on average 4 cells above the base of the crypt[2, 3]. A number of recent discoveries suggest that perhaps both of these populations are bona-fide ISCs. First, LGR5^{+} CBCCs were shown to actively cycle and produce all of the differentiated populations of the intestine *in vivo*[8] and *in vitro*[9]. Second, several +4 cell markers (*Bmi1*[10], *Lrig1*[11], *Hopx*[12], *mTert*[13], and others) were discovered, and cells expressing these markers were shown to be capable of producing all types of mature intestinal epithelial cells. The +4 cells cycle much less frequently than CBCCs[10-13] and are thus thought to represent quiescent stem cells (QSCs), which can replace CBCCs during times of injury and repair[12, 14, 15]. To further complicate this system, TA cells have also been shown to possess potential stem cell function during times of injury[3, 16, 17] and QSCs markers have been shown to overlap with CBCCs as well as being diffusely expressed throughout the crypt[18].

The Notch signaling pathway is one of many pathways crucial for intestinal epithelial homeostasis: regulating proliferation, differentiation and stem cell

maintenance[19-24]. Notch regulation of intestinal proliferation has been shown through both pathway activation and inhibition, as blocking Notch reduces proliferation[21, 25] and Notch overactivation results in increased proliferating cell numbers[20, 22]. Notch is required for specification of enterocytes, as pharmacologic inhibition or genetic deletion of pathway components leads to a profound secretory cell hyperplasia[19, 21, 23, 24]. Finally, both pharmacological Notch inhibition as well as deletion of the Notch ligands *Dll1* and *Dll4* result in loss of CBCC stem cells[19, 24]. Although Notch inhibition showed reduced stem cell proliferation and function[19], the mechanism behind these findings was unknown.

One of the functions of Notch signaling in stem cells in other tissues has been regulation of stem cell division asymmetry[26]. Asymmetric cell division occurs when the daughter cells of a division event assume different fates, i.e. one stem cell and one TA cell. This process is believed to be mediated by asymmetric inheritance of the Notch signaling pathway inhibitor NUMB in daughter cells[26-28]. The daughter cell that inherits NUMB turns Notch signaling off and becomes a TA cells, and the daughter that does not inherit NUMB continues to have active Notch signaling and remains a stem cell[26-28]. Studies in the *Drosophila* midgut[29] and in human colon cancer cell lines[30] suggest that NUMB might also function to inhibit Notch signaling in the intestine. The concept of NUMB-mediated asymmetric stem cell division in the intestine, however, has been contested by studies on neutral drift theory, the property that intestinal crypts become monoclonal over time[31, 32]. These reports contend that CBCC division does not occur asymmetrically, but rather symmetrically, forming two cells that are both capable of becoming either stem or TA cells[31, 32]. If this is the case, the role for Notch in regulating CBCCs remains unknown.

This study aims to further understand Notch intestinal epithelial function, specifically addressing the question *how does Notch regulate CBCC maintenance?* Combining *in vivo* experimentation with *in silico* modeling techniques, we provide evidence for a role for Notch in regulating CBCC-TA cell dynamics. We further probe the function of Notch in regulating QSC-CBCC

dynamics and determine that Notch functions permissively for CBCC specification.

3.3: MATERIALS AND METHODS

Mice

Floxed-*Rbpjκ* (*Rbpj*$^{F/F}$)[33] (gift from T. Honjo), *Villin-CreER*^{T2} [34] (gift from S. Robine), *Bmi1-CreER*[10] (Jackson Lab, no. 010531) and *Lgr5-GFP-IRES-CreER*^{T2} (*Lgr5-GFP*)[8] (Jackson Lab, no. 008875) alleles were verified by PCR genotyping with the primers listed in Supplementary Table 3-1. All crosses were maintained on a C57BL/6 strain background except Bmi1 crosses, which were on a mixed strain. Mice were housed in ventilated and automated watering cages with a 12-hour light cycle under specific pathogen-free conditions. Protocols for mouse usage were approved by the University of Michigan Committee on Use and Care of Animals.

Animal treatment protocols and tissue collection

Mice were injected intraperitoneally with 30µmol/kg Dibenzazepine (DBZ)[21] (SYNCOM) for 1-5 days and tissue was harvested at the time points indicated. Mice in experiments using *Bmi1-CreER* were treated with 100mg/kg tamoxifen (Sigma) intraperitoneally or by oral gavage once per day for 5-8 days as noted. To induce intestinal injury, animals were exposed to one dose of 12Gy whole body irradiation from a ^{137}Cs source. Animals were fasted overnight and injected intraperitoneally with 25 mg/kg 5-ethynyl-2´-deoxyuridine (EdU) (Life Technologies) 2 hours prior to tissue collection. Intestinal tissue was harvested and fixed in 4% paraformaldehyde overnight as previously described[19]. Tissue prepared for frozen sections was fixed in 4% PFA for 1 hour and incubated in 30% sucrose overnight before embedding in OCT (Tissue-Tek).

Immunohistochemistry

Paraffin sections (5µm) were stained with Periodic acid Schiff and Alcian Blue (PAS/AB) (Newcomer Supply) to visualize mucin-containing goblet cells. EdU-Click-it (Life Technologies) was used to identify proliferating cells. Immunostaining with rat α-MMP7 (1:400, Vanderbilt Antibody and Protein Resource), rabbit α-MUC2 (1:200, Santa Cruz), goat α-CGA (1:10, Santa Cruz) and rabbit α-Ki67 (1:200, Thermo) was performed as described[35]. GFP transgene expression was visualized on 5µm frozen sections. Images were captured on a Nikon E800 microscope with Olympus DP controller software.

In Situ Hybridization

Briefly, slides were deparaffinized, hydrated, and treated with 0.2N HCl for 15 minutes at room temperature. Tissues were treated with Proteinase K for 30 minutes at 37°C, post-fixed in 4% PFA for 10 minutes, acetylated for 10 minutes, incubated with hybridization buffer for 1 hour, then with *Olfm4* probe diluted in hybridization buffer at 68°C overnight. The next day tissues were washed, incubated in blocking solution for 1 hour, then with anti-DIG antibody (Roche) diluted in blocking solution overnight at 4°C. The next day slides were washed then developed with NBT/BCIP solution (Roche).

Quantitative morphometric analyses

Ki67 morphometrics were performed by counting the number of Ki67+ cells on both sides of well-oriented crypts. At least 10 crypts were counted per animal for all analyses, and counts were average per animal. EdU morphometrics on irradiated tissue was accomplished by counting Edu+ epithelial cells per crypt area as measured from the base of the crypt to the crypt villus junction. EdU counts were summed over 8-15 images and averaged over the entire measured tissue area. Nuclei per crypt were counted on both sides of well-oriented crypts on H+E images. Crypt depth measurements were performed on H+E images measuring from the crypt villus junction to the base of the crypt along the crypt

center. Morphometric analyses were completed using ImageJ software (http://imagej.nih.gov/ij/).

Crypt isolation and flow cytometry

Crypt isolation for flow cytometry was from the jejunum, centimeters 9-15 as measured from the pylorus. Tissue was incubated in 15mM EDTA (Sigma) in DPBS (Gibco) at 4°C for 35 minutes, vortexed for 2 minutes, and filtered through a 70µm cell strainer (BD Bioscience). To obtain a single cell suspension for flow cytometry, crypts were resuspended in TrypLE Express (Gibco), shaken at 37°C for 10-12 minutes, and 0.1mg/ml DNase I (Roche) and 10% fetal bovine serum (FBS) were added. Cells were passed through a 40µm cell strainer (BD Bioscience), pelleted at 400xG, resuspended in 2% FBS, 0.05% sodium azide (Sigma), 2mM EDTA in DPBS and stained unfixed as follows. All cells were blocked with rat α-mouse CD16/CD32 (1:100, BD Bioscience), lymphocytes were excluded with CD45.2-PerCP-Cy5.5 (1:80, LifeTechnologies), epithelial cells were visualized with EpCAM-APC (1:80, eBioscience), and dead cells were excluded by DAPI incorporation. Cells were analyzed on a BD FACSCanto II and interpreted with FlowJo software (Treestar). GFP$^+$ cells were sequentially gated for size, singlets, DAPI$^-$, CD45.2$^-$, and EpCAM$^+$.

Enteroid culture

Purified crypts from the first 6cm of duodenum were instilled in Matrigel (BD Biosciences) overlaid with DMEM + GlutaMAX (LifeTechnologies) with 5% each Wnt3a[36] and Rspo2[37] conditioned medias. Additional growth factors included 2% B27 (Invitrogen), 1% N2 (Invitrogen), 100ng/ml Noggin (Peprotech), 50 ng/ml EGF (R&D Systems), and 10 µM Y-27632 (Sigma, used for initial plating only). Enteroids were grown and passaged several times prior to assaying. For proliferation assays, enteroids were passaged at the indicated time and treated with 25µM DAPT in DMSO (EMD4Biosciences) or 100% DMSO as vehicle. Living enteroids were imaged with a Leica DMIRB Inverted Microscope and an Olympus DB30BW camera with Olympus DP Controller software. EdU was

introduced at 10nM for 2 hours prior to cell harvest. Experimental time points were completed in triplicate with quadruplicate wells pooled together as one replicate. Single cell isolation of enteroids was accomplished by resuspending the enteroids and Matrigel in 15mM EDTA in DPBS. Enteroids were pelleted and resuspended in 2ml TrypLE Express and incubated at 37°C for 2 minutes. 500ml of DMEM was added to each sample and enteroids were mechanically dissociated into single cells by pipetting 40 times. 5ml of additional DMEM was added to each sample, cells were pelleted, and washed with 1% BSA in DPBS. Staining for EdU was completed with the Click-it EdU flow cytometry kit (Invitrogen) as per manufacturer's instructions.

Gene expression analysis

RNA from full-thickness ileum was isolated by Trizol (Invitrogen) extraction followed by the RNeasy Mini kit (Qiagen) with DNAseI treatment. RNA from crypts was directly processed with the RNeasy Mini kit. cDNA from full tissue and crypts was reverse transcribed with the iScript cDNA synthesis kit (BioRad) using 1μg of total RNA. Quantitative RT-PCR was performed as described[35] with the primers listed in Supplementary Table 3-2. Assays were run in triplicate and normalized to glyceraldehyde-3-phosphate dehydrogenase (*Gapdh*) as an internal control.

Statistical analyses

All experiments were performed with 3-6 biological replicates per group unless otherwise noted. Quantitative data are presented as mean + SEM. Comparisons between two groups were conducted with unpaired two-tailed Student *t* tests. Comparisons between 3 or more groups were analyzed by one-way ANOVA with Dunett's post-test. Significance is reported as * ($P<0.05$), **($P<0.01$), ***($P<0.001$), and ****($P<0.0001$). Prism software (Graphpad) was used for statistical analyses.
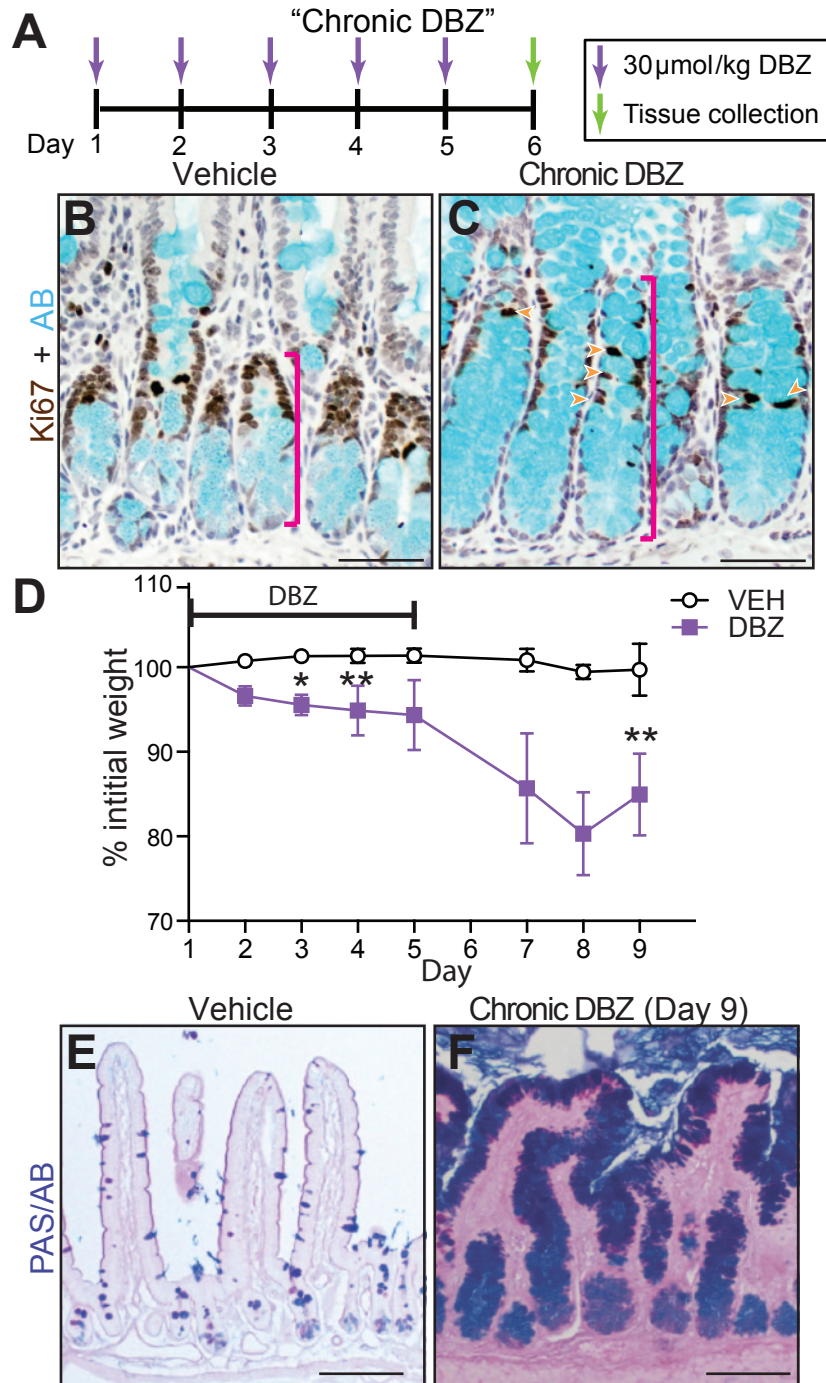
3.4: RESULTS

*Chronic Notch inhibition is lethal*

Pharmacological intervention with the gamma-secretase complex inhibitor Dibenzazepine (DBZ) has been widely used to probe Notch function in the intestine. A common treatment regimen, 5 daily doses of DBZ (referred to as "chronic DBZ" hereafter), results in a profound secretory cell hyperplasia as well as decreased epithelial proliferation (Figure 3-1). Previously, our lab determined that chronic DBZ also led to lost CBCC number[19], implicating Notch in the maintenance of this stem cell population. Both the mechanism of Notch-related CBCC loss as well as the possibility of CBCC recovery, however, remained unknown. To probe the question if epithelial recovery was possible after Notch inhibition, mice were treated with chronic DBZ and monitored over time. Chronic DBZ led to weight loss and rapid animal lethality; with all animals succumbing 3-4 days post treatment (Figure 3-1D). PAS/AB staining for goblet cells at the time of animal death revealed that the secretory hyperplasia had not resolved, suggesting that epithelial recovery was not possible after sustained Notch inhibition.

Acute DBZ results in increased intestinal epithelial proliferation

Since animals treated with chronic DBZ did not live long enough to investigate the dynamics of Notch restoration and epithelial recovery, a milder treatment regimen was implemented. With "acute DBZ" treatment, only a single dose of DBZ was administered to transiently inhibit Notch activity. Animals tolerated this treatment and survived at least 2 weeks with no apparent ill effects. To pinpoint the timing of inhibition and recovery, animals were harvested at numerous time points post acute DBZ treatment (Figure 3-2A). Tissues were first assessed for changes in intestinal epithelial proliferation. Although all previous studies associated Notch inhibition with decreased proliferation[19, 21, 38], acute DBZ treatment surprisingly resulted in a marked increase in intestinal epithelial proliferation, as measured by immunostaining for the proliferation marker Ki67 (Figure 3-2). Significant increases in Ki67$^+$ cells were observed as early as 2

Figure 3-1. Chronic DBZ results in lethal secretory cell hyperplasia and reduced proliferation. (A) Animals were administered 5 daily doses of 30μ mol/kg Dibenzazepine (DBZ) for "chronic DBZ" treatment. (B-C) Co-staining for proliferation (Ki67) and mucin-containing cells (AB) in vehicle- (B) or chronic DBZ-treated (C) intestine. Pink bars show expanded crypt depth, orange arrows mark Ki67+ nuclei in chronic DBZ intestine. (D) Weight curve of animals post-chronic DBZ treatment. Statistical comparisons were made by upaired Student *t* test. N = 4 animals per group. (E-F) PAS/AB staining for goblet cells in vehicle (E) or 3 days after chronic DBZ (F) treatment. Scale bar = 100μm.
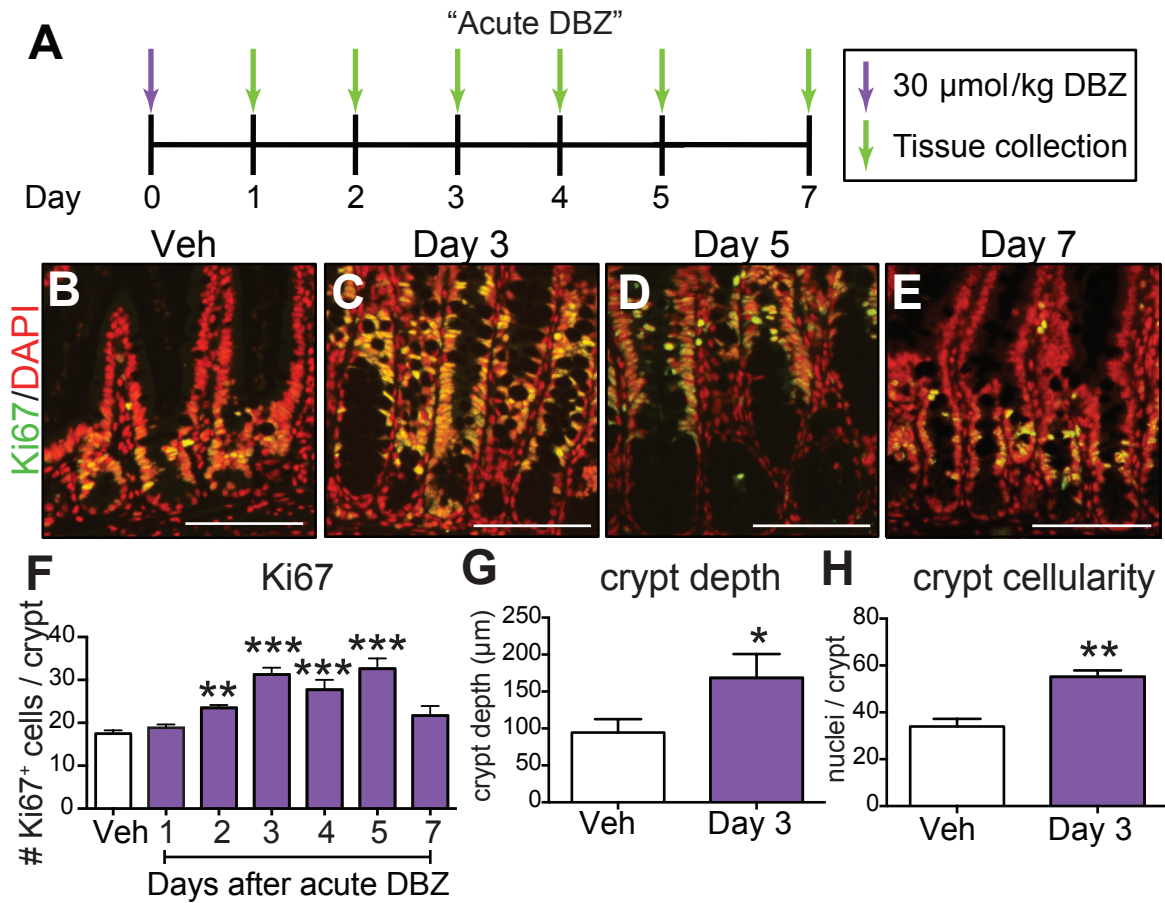
Figure 3-2. Acute DBZ leads to transiently increased intestinal epithelial proliferation and crypt expansion. (A) Animals treated with "acute DBZ" were administered one 30μmol/kg dose of DBZ and harvested at the time points indicated. (B-E) Proliferation was assessed by immunostaining for Ki67 in vehicle-treated (B) or acute DBZ-treated mice (C-E). (F) Quantification of Ki67 staining. Data are presented as number of Ki67$^+$ nuclei per ileal crypt compared with One-way ANOVA and Dunnett's post-test. Crypt depth (G) and number of cells per crypt (H) were measured in vehicle and 3 days post-acute DBZ ileum. Comparisons for G-H were made with unpaired Student t tests. N= 3-6 animals per group. Scale bar = 100μm.

days post-acute DBZ. The proliferative surge continued on days 3-5, with a 1.7 fold increase in proliferating cells compared to vehicle-treated samples on day 3. Proliferation normalized by day 7. Increased proliferation was accompanied by crypt expansion, which was increased 1.8-fold on Day 3 (Figure 3-2G). Total cells per crypt was increased 1.6-fold as well, suggesting that crypt expansion was due to hyperplasia (Figure 3-2H).

Acute DBZ leads to the production of long-lasting secretory progenitors

Since acute DBZ treatment resulted in an unexpected increase in proliferation *in vivo*, we probed other hallmarks of Notch inhibition to determine if the DBZ dosage scheme was effective in adequately blocking the pathway. Staining with PAS/AB showed a progressive increase in goblet cells after acute DBZ (Figure 3-3), consistent with the secretory cell hyperplasia observed with chronic DBZ treatment. Goblet cells were detected in both the villus and crypt regions and present in all parts of the intestine (Supplementary Figure 3-1). Additionally, CGA^{+} enteroendocrine cells were greatly increased at the base of acute DBZ-treated crypts (Figure 3-3F) as were cells co-expressing the Paneth and goblet cell markers MMP7 and MUC2 (Figure 3-3H). These co-staining cells were also previously observed with chronic DBZ treatment[19]. The increased abundance of all of these secretory cell markers suggests that committed secretory progenitors are formed with only very short interruptions in Notch signaling and that they persist for several days after Notch signaling is re-established.

Interestingly, both the appearance and the resolution of the secretory cell hyperplasia aligned with the timing of the crypt hyperproliferation. Co-staining with the mucin-marker AB and Ki67 showed both markers occupying the same crypt location (Supplementary Figure 3-2), suggesting that the proliferating cells are secretory progenitors. These data are consistent with a recent publication that described increased abundance of Ki67^{+} ATOH1^{+} cells 38 hours after DBZ treatment, and determined that Notch inhibition led to the expansion of the proliferating secretory progenitor compartment[39].
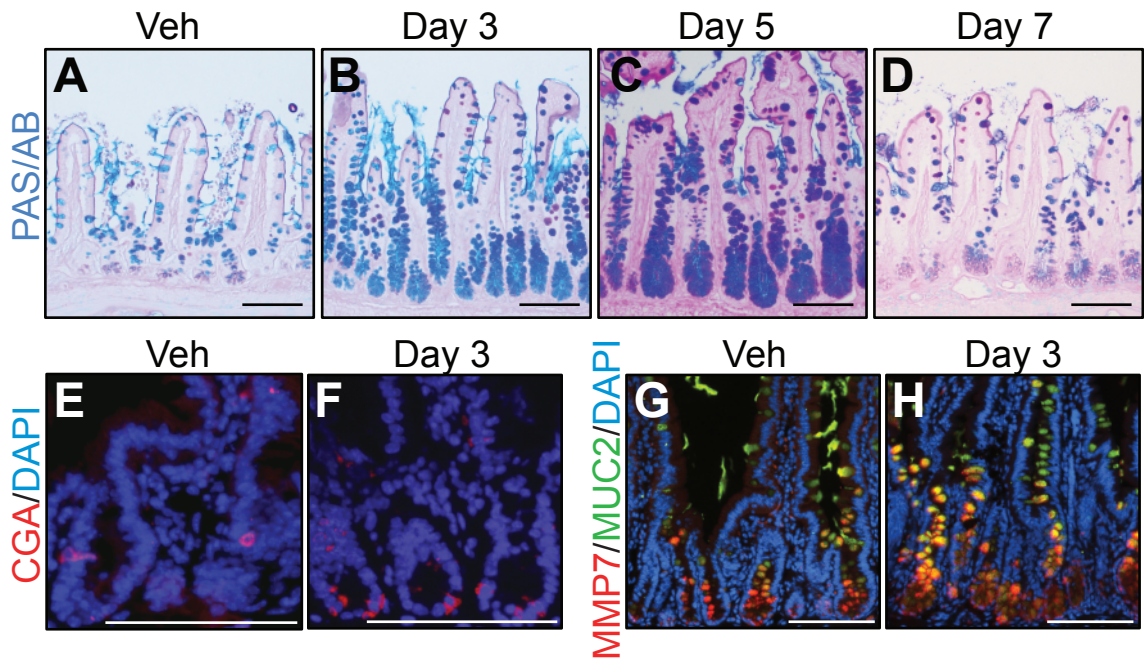
**Figure 3-3. Acute DBZ results in a transient multi-lineage secretory cell surge.** (A-D) PAS/AB staining for goblet cells at the timepoints indicated. (E-F) CGA immunostaining for endocrine cells in vehicle (E) or 3 days post-acute DBZ treatment (F). (G-H) Co-immunostaining for goblet cell marker MUC2 and Paneth cell marker MMP7 in vehicle (G) or 3 days post-acute DBZ treatment (H). N = 3-6 animals per group. Scale bar = 100μm.

Acute DBZ targets the stem cell compartment

To investigate if stem cells were affected by short interruption of Notch signaling, *in situ* hybridization was performed for the CBCC marker *Olfm4*. In addition to marking stem cells, *Olfm4* is an exquisitely sensitive intestinal Notch target gene[19], thus changes in *Olfm4* indicate that Notch has been blocked specifically in CBCCs. Indeed, Acute DBZ led to complete loss of *Olfm4* signal as early as 12 hours post acute DBZ treatment (Supplementary Figure 3-3). Such rapid control of *Olfm4* was also observed in DAPT-treated human colon cancer cells *in vitro*. In the proximal intestine *Olfm4* expression approached baseline levels by day 3 (Figure 3-4). To determine if this effect was limited to *Olfm4* transcript changes or indicated a loss in CBCC number, acute DBZ was administered to *Lgr5-GFP* mice[8] which express GFP in CBCCs. A progressive loss in GFP expression was observed during the period of *Olfm4* decline, with many fewer visible GFP$^+$ cells on Day 2 after acute DBZ (not shown).

Loss of GFP^{HI} cells are linked to increased numbers of GFP^{INT} cells

To quantify the change of CBCCs, flow cytometry was used to analyze cells marked by varying GFP levels in single cell isolates of acute DBZ-treated intestine. Since GFP expression occurs in a gradient in the crypts of *Lgr5-GFP* mice, cellular identity can be implied from the level of GFP expression. For our study, 3 levels of GFP were assessed: GFP^{HI}, GFP^{INT}, and GFP^{LOW}, where GFP^{HI} are CBCCs, GFP^{INT} represent early TA progenitors (likely T1-T2, Figure 1-3), and GFP^{LOW} are later divisions of TA cells. Altered levels of GFP^{HI} and GFP^{INT} were observed with DBZ treatment (Figure 3-4E). GFP^{HI} cells were decreased to 40% control levels on Day 2. Interestingly, GFP^{HI} loss was coupled with a 1.5-fold increase in GFP^{INT} cells at this time point. As a TA cell population, increased GFP^{INT} levels are consistent with the increased crypt proliferation observed with acute DBZ. Although not significant, similar trend decreases in GFP^{HI} and increases in GFP^{INT} were observed on Day 1, suggesting that the population changes occur together and that the process leading to these changes start early after acute DBZ treatment.
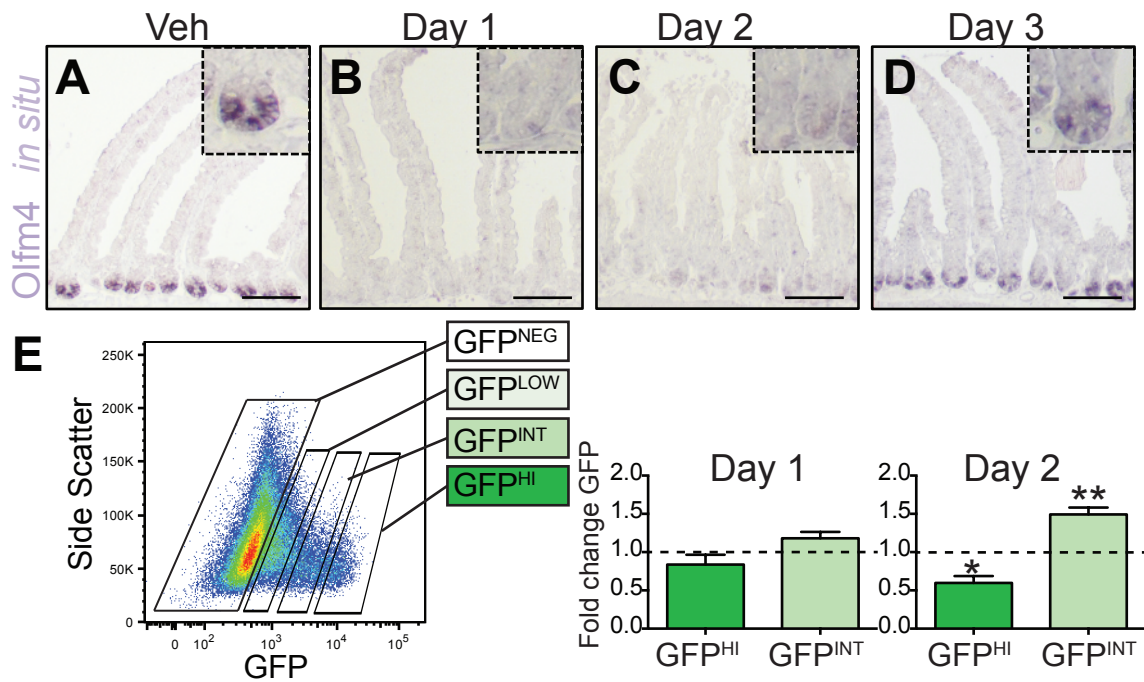
Figure 3-4. CBCCs are decreased with acute DBZ treatment. (A-D) *In situ* hybridization for crypt base columnar cell (CBCC) stem cell marker *Olfm4* in vehicle- (A) or acute DBZ-treated (C-D) mice at the times indicated. Insets are 3x original magnification. (E) Scatter plot of GFP expression by flow cytometry analysis of vehicle-treated cells. Plot is sequentially gated for single, live, CD45.2$^-$, EpCAM$^+$ cells. Boxes represent gates used to assess GFP^{HI}, GFP^{INT}, and GFP^{LOW} populations. Bar graphs display GFP^{HI} and GFP^{INT} as percent total GFP$^+$ cells on Day 1 and Day 2 after acute DBZ normalized to vehicle treated levels which were set to 1 (dashed lines). Comparisons were made with unpaired Student *t* tests compared to vehicle controls. N=3-4 animals/group. Scale bars = 100μm

Compartmental modeling of the crypt reveals a role for Notch in regulating stem cell division symmetry

Considering GFP^{HI} cells were decreased as GFP^{INT} cells were increased with acute DBZ treatment, an appealing hypothesis was that Notch inhibition led to direct shunting of CBCCs into the TA progenitor cell compartment. We questioned whether such a mechanism could explain the different proliferation trends observed in acute vs. chronic Notch inhibition.

To test this hypothesis, we turned to *in silico* modeling. As described in greater detail in Chapter 4, a theoretical compartmental model of the crypt was designed and used to identify a singular mechanism that could reconcile the proliferation differences observed between acute and chronic DBZ. (Figure 3-5A). Modeling generated several conclusions: first, increased TA cell proliferation is linked with stem cell division (see Chapter 4). That is, shunting CBCCs into the TA compartment via differentiation in the absence of stem cell division would lead to decreased CBCCs but no overall increase in proliferation. Stem cell division, specifically symmetric stem cell division where both daughter cells of a stem cell division event become TA cells, is the other mechanism that results in CBCC to TA shunting.

The compartment model was used to test if symmetric stem cell division during Notch inhibition would result in the stem and TA cell numbers expected from the *in vivo* acute and chronic DBZ experiments. Simulated results showed that Notch regulation of stem cell symmetry alone would not result in the increased proliferation of acute DBZ and decreased proliferation of chronic DBZ. Instead, only a mechanism where Notch regulates both the symmetry of stem cell division as well as the repopulation of the CBCC compartment from another source (a QSC or de-differentiating TA cell) would result in the expected proliferation results (Figure 3-5B).

With this framework in place, the model qualitatively predicted the behavior of both acute and chronic DBZ treatment modalities: a transient increase in TA cell population after acute DBZ and a severe drop in stem cell number and TA cell population after chronic DBZ (Figure 3-5C-D). The model
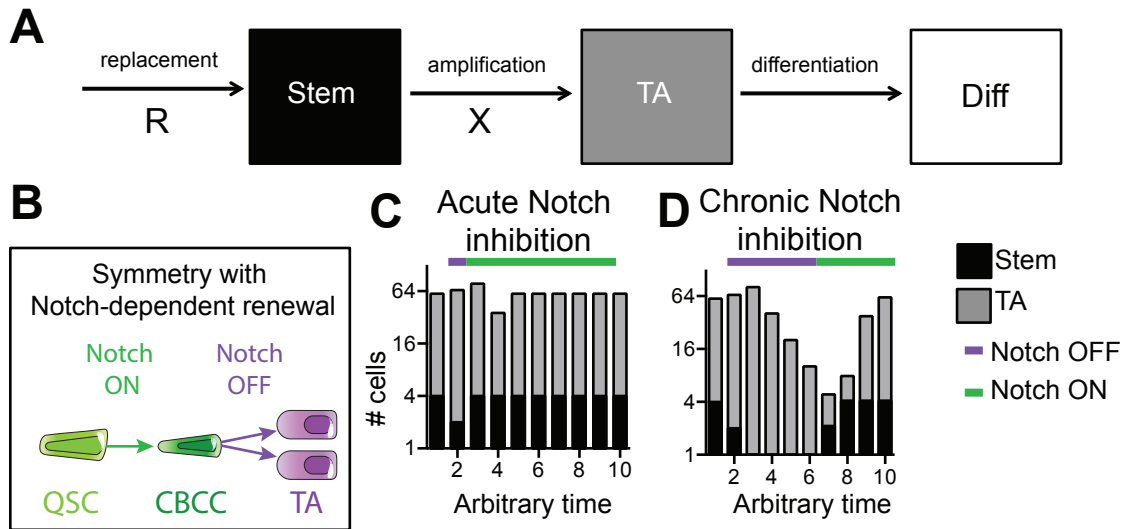
Figure 3-5. Modeling Notch-regulated stem cell symmetry. (A) Schematic diagram of the discrete compartmental model of the intestinal crypt. Compartments include stem (S), TA (T), and Differentiated (D) cell compartments. X functions to regulate stem cell symmetry. X can range from 0-2 and determines whether stem cells divide asymmetrically producing 1 stem cell and 1 TA cells, or symmetrically, forming either 2 stem cells or 2 TA cells. R is a gain or loss parameter that allows for repopulation of the stem cell compartment. (B) Diagram of hypothesis that Notch regulates stem cell symmetry as well as stem cell replacement. When Notch signaling is OFF, CBCCs divide symmetrically to form 2 TA cells, resulting in lost CBCC number. Only when Notch is turned back on can quiescent stem cells (QSCs) repopulate the CBCC compartment (C) Simulated data from testing the hypothesis in (B) To model a shift toward symmetric division, X = 1.5 for 1 day (acute Notch inhibition) or 5 days (chronic Notch inhibition) during the periods indicated (purple bars). X is returned to 1 (asymmetric division) after treatment (green bar). Notch-dependent stem cell replacement uses R = 2 after the DBZ treatment window until $S_t = S_0$.

made two additional important predictions: 1) increased TA cell number would always occur after the initiation of Notch inhibition even with additional doses of DBZ and 2) stem and TA cell recovery should occur post-chronic DBZ (Figure 3-5D).

*Validating compartmental model predictions in vivo*

The first prediction of the model suggests that the increased proliferation observed 2 days after acute DBZ is a direct result of Notch inhibition rather than a post-DBZ recovery effect and thus, a similar proliferative response should be observed even with additional doses of DBZ. To test this hypothesis, animals were administered 2-4 daily doses of DBZ and assessed for proliferation 24 hours later by Ki67 immunostaining (Figure 3-6). Interestingly, increased abundance of Ki67$^+$ cells were observed after 2 doses of DBZ when compared to vehicle, consistent with the model prediction. A progressive decline in proliferation, however, was observed with subsequent doses of DBZ.

Flow cytometry of singly isolated cells from *Lgr5-GFP* mice was used to probe stem and TA cell levels after two doses of DBZ. When compared to vehicle, GFP^{HI} CBCCs were decreased 0.6-fold while GFP^{INT} TA cells were increased 1.5-fold. Of note, the same magnitude of change was observed in these values on day 2 after acute DBZ.

The second model prediction suggested that recovery of both stem and TA cell populations should occur post-chronic DBZ treatment. Although a recovery in differentiated cell populations did not occur at the time of animal death post-chronic DBZ (Figure 3-1F), both Ki67$^+$ proliferative cells as well as GFP$^+$ CBCCs were observed at this time (Figure 3-7). Interestingly, GFP$^+$ cells were found to be displaced more highly in the crypt in these tissues (Figure 3-7C, orange arrowheads), suggesting that the stem cell niche was altered.

Role of Notch in quiescent stem cell activation

Having validated these two predictions, more credence was given to the hypothesis underlying the qualitative behavior of the model: Notch regulates both
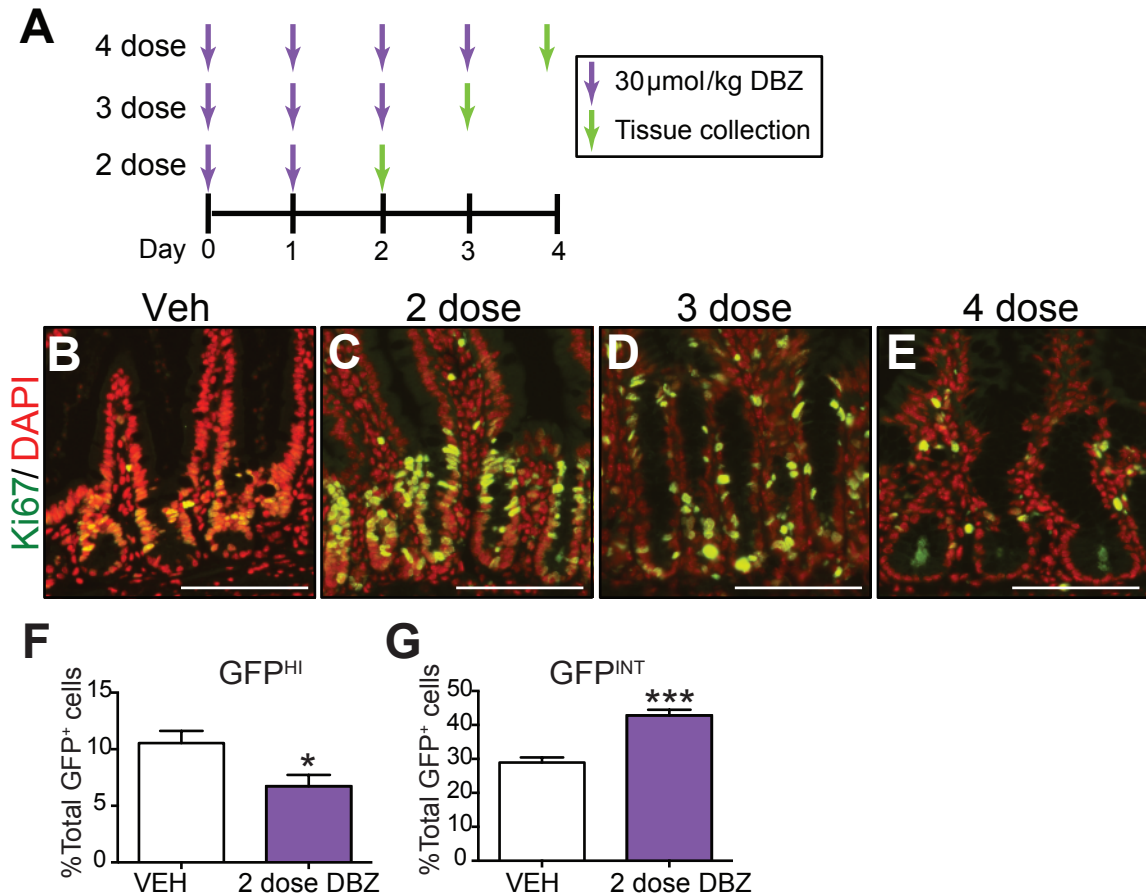
Figure 3-6. 2 doses of DBZ results in a proliferative surge and altered stem cell dynamics. (A) Animals were administered 2-4 doses of 30μmol/kg DBZ and harvested 24 hours later. (B-E) Ki67 staining for proliferation in vehicle- (B) or DBZ-treated (C-E) mice. (F-G) Flow cytometry for GFP[HI] (F) and GFP[INT] after 2 doses of DBZ. Data are presented as percent total GFP^{+} cells. Comparisons were made by unpaired Student t test compared to vehicle. N=4 animals/group. Scale bars = 100μm.
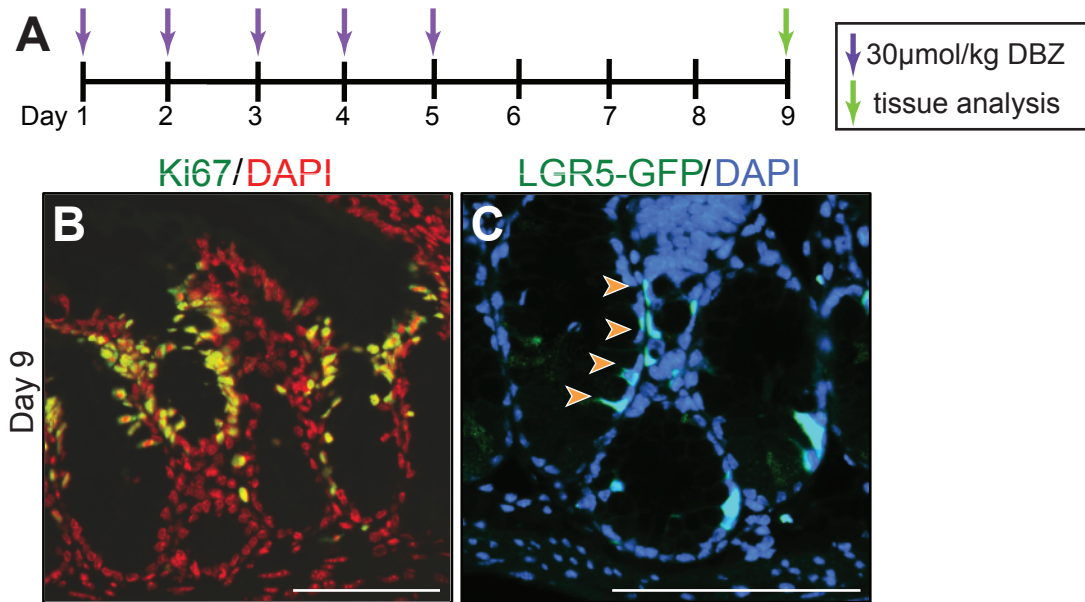
Figure 3-7. Stem and progenitor cells recover post-chronic DBZ. (A) Lgr5-GFP mice were treated with chronic DBZ and harvested on day 8-9 when moribund. (B) Proliferating cells were visualized by Ki67 immunostaining. (C) CBCCs were visualized by GFP transgene expression. Orange arrows mark upward displaced stem cells. N=4. Scale bars = 100μm.

stem cell symmetry as well as stem cell repopulation. Notch-regulated stem cell repopulation could occur via two means 1) Notch could directly regulate the activity of QSCs much like its regulation of CBCCs or 2) Notch could be required for QSCs to become CBCCs. To differentiate between these roles, an irradiation injury model was utilized. Irradiation has been shown to cause both CBCC depletion as well QSC activation, which are then primed to repopulate the voided CBCC compartment[12, 14, 15]. If Notch is indeed required for QSC activation, DBZ treatment in the irradiation setting should prevent the post-irradiation proliferative response. To test this, acute DBZ was administered post-12Gy whole body irradiation (Figure 3-8). Strikingly, post-irradiation DBZ treatment led to a dramatic loss of intestinal architecture including villus blunting, as well as decreased goblet cell differentiation. When assessed for proliferation via EdU uptake, however, abundant proliferation was observed in both vehicle and DBZ treated animals, suggesting that Notch is not required for the post-irradiation proliferative surge.

To further assess if active Notch is directly required in QSCs, a genetic mouse model was used in which Notch function was disrupted by conditional deletion of the *Rbpj* gene, the DNA binding protein essential for Notch pathway activation (see Figure 1-5). *Rbpj*-floxed mice were bred to the tamoxifen-inducible *Bmi1-CreER* mouse to delete Notch signaling in the QSCs expressing this marker. Treatment with tamoxifen results in deletion of *Rbpj* in BMI$^+$ QSCs (referred to as *Bmi1; Rbpj$^{\Delta/\Delta}$*). Littermates with deletion of a single copy of *Rbpj* were used as controls (*Bmi1; Rbpj$^{\Delta/+}$*).

Although BMI1$^+$ cells are not thought to contribute very much to homeostatic intestinal epithelial populations, some baseline lineage tracing is observed from cells expressing this marker[10, 14, 15]. To look at the effect and specificity of inhibiting Notch in this cell population, *Bmi1; Rbpj$^{\Delta/\Delta}$* intestine was assessed for secretory cell changes. A modest but evident increase in PAS/AB$^+$ cells was observed in *Bmi1; Rbpj$^{\Delta/\Delta}$* compared to *Bmi1; Rbpj$^{\Delta/+}$* (Supplementary Figure 3-4), suggesting a small percentage of BMI$^+$ cells contribute to the TA pool and loss of Notch in these cells leads to specification of secretory

120
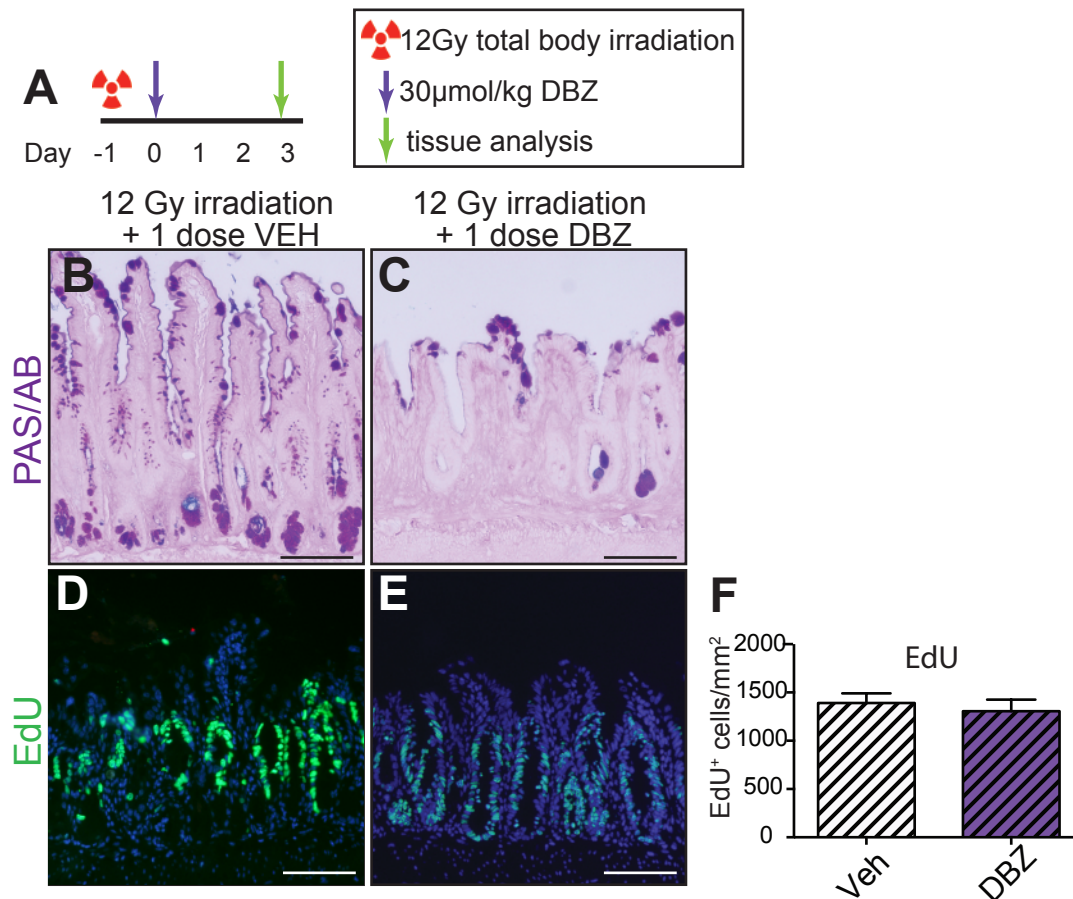
Figure 3-8. Notch is not required for post-irradiation hyperproliferation. (A) Animals were exposed to 12Gy whole body irradiation, treated with one dose of 30 µmol/kg DBZ, and euthanized three days later. (B-C) PAS/AB staining for mucin-containing goblet cells reveals decreased goblet cells as well as altered epithelial structure in DBZ-treated (C) irradiated intestine. (D-E) Proliferating cells were visualized by EdU incorporation. (F) Quantification of EdU staining. Data are presented as mean epithelial EdU$^+$ cells per crypt area in mm^2. Groups were compared with unpaired Student t test, no significant change was observed between groups. N = 3 animals/group. Scale bar = 100µm.

progenitors. This is in line with other studies that have described BMI1^{+} cell contribution to the TA pool[14]. Since *Bmi1* and *Lgr5* markers have been shown to overlap cell populations[18, 40, 41] quantitative RT-PCR was used to evaluate the transcript levels of *Bmi1* and *Olfm4* in these animals to determine if *Rbpj* was deleted in CBCCs. Interestingly while *Bmi1* transcript was significantly decreased in Rbpj$^{\Delta/\Delta}$ mice, *Olfm*4 was not changed, suggesting that Notch signaling is not being inactivated in CBCCs in this model (Supplementary Figure 3-4E).

   Bmi1; Rbpj$^{\Delta/\Delta}$ mice were exposed to 12Gy irradiation to directly determine if Notch was required for post-irradiation activation of these cells. Similar to the post-irradiation DBZ experiment, no apparent change in the post-irradiation proliferative surge was observed in *Bmi1; Rbpj$^{\Delta/\Delta}$*, suggesting that Notch blockade in BMI1^{+} cells does not limit the proliferative capacity of this cell population.

3.5: DISCUSSION

   In this study, we have used short-term Notch inhibition to investigate stem and TA cell dynamics in the intestinal epithelium. As opposed to chronic Notch inhibition, which results in <u>decreased proliferation</u>, increased secretory cells, stem cell loss and animal death, acute DBZ treatment leads to <u>increased proliferation</u> and increased secretory cells. Co-localization of these phenotypes was consistent with an overall increase in proliferative secretory progenitor cells. These histological findings were coupled with decreased LGR5-GFP[+] CBCCs as well as increased GFP[INT] TA cells. The progressive nature of these changes suggested that CBCC loss is actually due to shunting CBCCs into the TA cell compartment, and compartmental mathematical modeling was used to test this hypothesis.

   A model where Notch regulates both the symmetry of stem cell division as well as repopulation of the CBCC compartment was consistent with the stem cell and proliferation findings of both acute and chronic Notch inhibition. We validated this model *in vivo* by determining that increased proliferation is observed after

two doses of DBZ and that stem and TA cell recovery occurs post-chronic DBZ treatment as predicted.

Finally, we tested the hypothesis that Notch is required for CBCC repopulation by inhibiting Notch in the post-irradiation setting. In these experiments, QSC activation post-injury was found to be Notch-independent. This suggests that if Notch truly regulates CBCC repopulation, that it occurs during CBCC specification rather than directly regulating QSC activity.

Thus, our model suggests that when Notch signaling is active CBCCs divide asymmetrically and when Notch is inhibited CBCCs divide symmetrically to form TA cells. Although asymmetric stem cell division is known to occur in many tissues[42-44], several elegant studies in the intestine have suggested that this type of division may not actually occur[31, 32]. These studies suggest, rather, that CBCC division results in the formation of two equipotential cells that either form CBCCs or TA cells depending on niche availability[31, 32]. In this system, homeostasis is achieved when the average result of a stem cell division results in specification of 1 CBCC and 1 TA cell, rather than specific stem cell division asymmetry.

Our data are not inherently in conflict with these findings. Describing our system in this context, Notch inhibition would lead to disruption of the CBCC niche, mandating TA specification of all equipotential cells. In fact, this niche-specific model also aligns with the apparent Notch-independent activation of QSCs, as limited niche availability would not prevent QSC expansion but would only inhibit QSC transformation into CBCCs. Together, these ideas support a model where active Notch signaling is required for CBCC specification during both homeostasis and repair (Figure 3-9).

As the Notch pathway requires cell-to-cell contact for signaling activation, the majority of the intestinal Notch regulation is expected to occur within the epithelium. However, Notch receptors and ligands are also expressed in the underlying intestinal mesenchyme[45], and Notch inactivation in these cells could conceivably lead to secondary effects on the epithelium. To determine if the increased proliferation observed with acute DBZ was epithelial-specific, we assessed acute Notch inhibition in an *in vitro* intestinal enteroid system. This
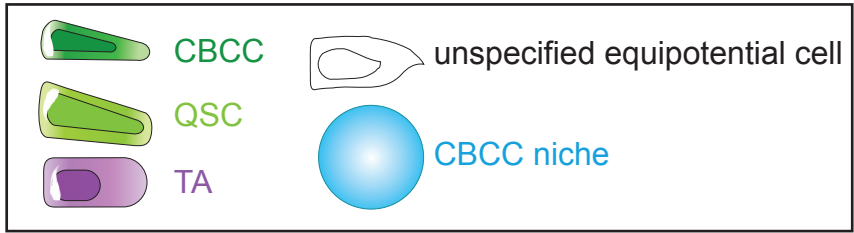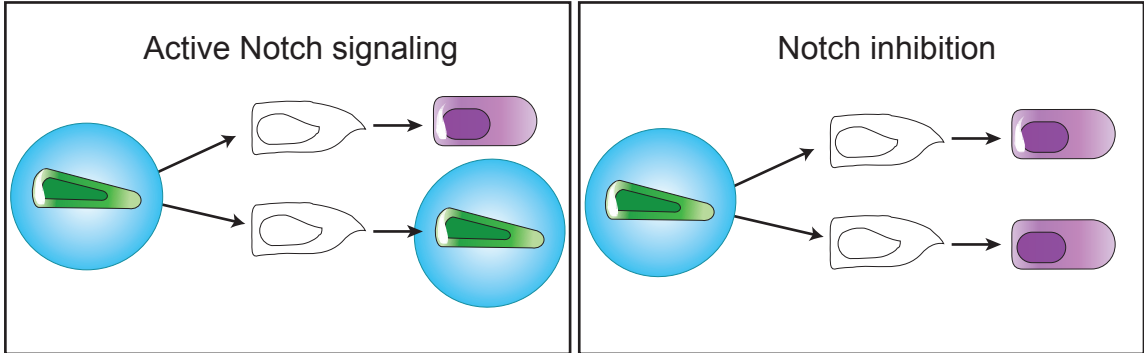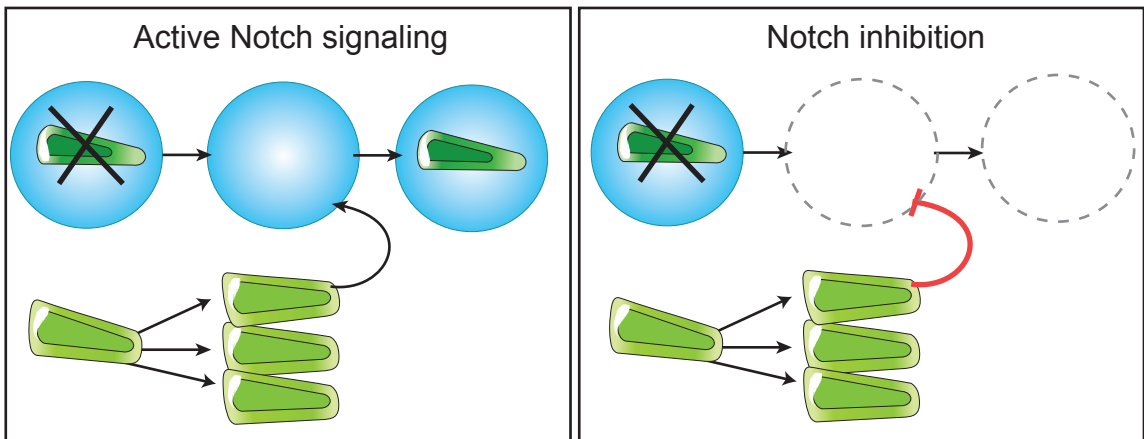
Figure 3-9. A model for Notch regulation of the CBCC niche during homeostasis and injury.

system, adapted from the Sato method[9], contains only intestinal epithelial cells and no mesenchymal component. Surprisingly, increased proliferation was not observed at any of the time points tested (Supplementary Figure 3-5). At this time, it is unclear if this discrepancy indicates that the proliferative surge observed with acute DBZ treatment is not an epithelial-specific phenomenon, or if the current enteroid culturing system does not faithfully represent *in vivo* conditions. More work will be needed to confirm that the Notch component of the ISC niche is entirely epithelial.

Our study is the first to investigate Notch regulation of QSCs. We found that QSCs may not be as Notch-sensitive as CBCCs, as specific deletion of *Rbpj* in BMI1^{+} cells results in a mild increase in secretory cells, but no deficit in post-irradiation activation of Rbpj-deficient BMI^{+} cells. Interestingly, Yan et al.[15] showed that BMI1^{+} and LGR5^{+} cells responded differently to Wnt signaling[15]. Our study suggests that these cell populations may respond differently to Notch, and perhaps other components of the CBCC niche.

Although our modeling favors the concept of increased TA cell specification as the mechanism for the increased proliferation observed in acute DBZ treatment, an alternate hypothesis for this finding could be Notch over-activation as part of a post-treatment recovery response. Notch over-activation is associated with increased proliferation[20, 22], and as DBZ is thought to be metabolized within 24 hours[46], this type of activity is feasible within the timeline investigated. Such activity has been demonstrated in T cell systems where DBZ treatment led to a build-up of pre-cleaved Notch receptor on cell membranes[47, 48]. In our studies, we observed no increase in Notch target gene expression during the proliferative surge, which would indicate that Notch signaling had not rebound activated. Indeed, a decrease in both *Olfm4* and *Hes1* expression was observed during this period (data not shown). Further evidence that this mechanism was not responsible for the proliferative surge was that similar increases in proliferation and altered GFP[HI]/GFP[INT] levels were observed both 1 day after 2 doses of DBZ and 2 days after a single dose of DBZ (i.e. both groups were analyzed on day 3 after the initiation of DBZ treatment, but were analyzed 24

hours apart after termination of treatment). If the proliferative response was due to rebound Notch activation we would expect to see altered proliferative outcomes dependent on the time post-DBZ treatment.

Finally, our results shed light on the requirement of Notch signaling for overall intestinal function. Although acute DBZ led to dramatic stem, progenitor, and differentiated cell changes, these changes were transient and animals fully recovered. Chronic DBZ treatment, however, led to animal death within 4 days after drug removal. Our mathematical modeling and *in vivo* findings that stem and TA cells recover post-chronic Notch inhibition suggest that the lethality associated with chronic DBZ is not due to stem cell compartment collapse. This lethality is more likely a failure in epithelial barrier function. A recent report showed that Notch inhibition by genetic deletion of *Rbpj* resulted in bacterial and FITC-dextran translocation across the epithelium[49], which is highly supportive of this hypothesis. Barrier malfunction is also likely involved with the rapid lethality of Notch inhibition in the irradiation setting. Thus, preventing barrier malfunction or implementing prophylactic antibiotic treatment may help prevent intestinal toxicity in therapeutic treatment regimes that combine irradiation injury and Notch inhibition.

In conclusion, we propose a revised model of Notch activity in the intestinal epithelium. Notch is critical for CBCC niche specification and any interruption of Notch signaling leads to CBCC division and TA cell production. This results in an increased number of TA cells, leading to a transient proliferative surge. Notch activity is required for repopulation of the CBCC compartment, thus extended Notch inhibition results in TA cell compartment exhaustion resulting in a progressive reduction in epithelial proliferation. These studies underline the importance for Notch in CBCC maintenance as well as shine new light on the dynamic relationship between CBCCs, TA cells, and QSCs.

3.6: ACKNOWLEDGMENTS

Supplentary Table 3-1.

Genotyping primer sequences

Allele	Forward primer sequence	Reverse primer sequence
Villin-CreER[T2]	ACAGGCACTAAGGGAGCCAATG	GTTCTTGCGAACCTCATCACT
Lgr5-GFP	CTGCTCTCTGCTCCCAGTCT	GAACTTCAGGGTCAGCTTGC
Bmi1-CreER	ACCAGCAACAGCCCCAGTGC	AAAGACCCCTAGGAATGCTC
Floxed-Rbpj	CTTGATAATTCTGTAAAGAGA	ACATTGCATTTTCACATAAAAAAGC

Primer sequences for genes analyzed by quantitative RT-PCR

Gene	Forward primer sequence	Reverse primer sequence
Bmi1	TATAACTGATGATGAGATAATAAGC	CTGGAAAGTATTGGGTATGTC
Hes1	GCTCACTTCGGACTCCATGTG	GCTAGGGACTTTACGGGTAGCA
Olfm4	GCCACTTTCCAATTTCAC	GAGCCTCTTCTCATACAC
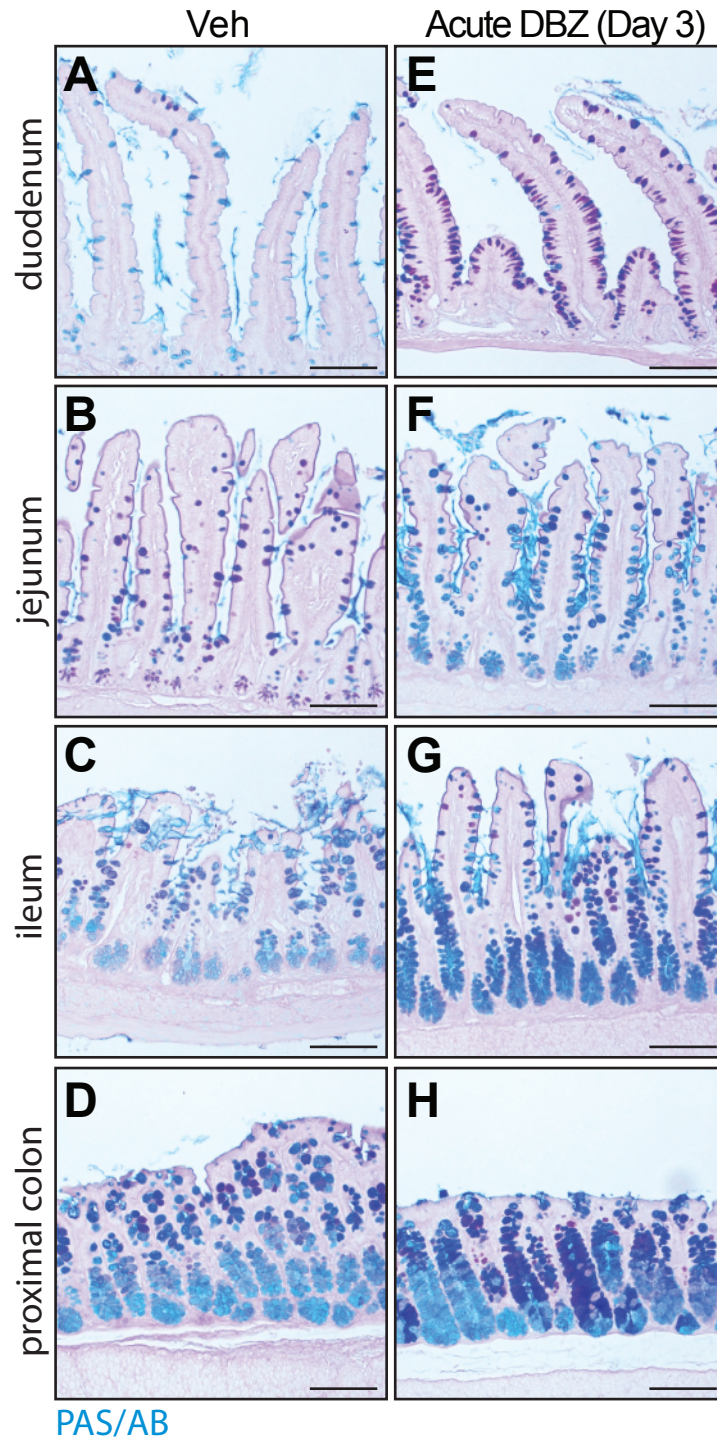
Supplementary Figure 3-1. Cell fate changes in acute DBZ model are consistent throughout the small and large intestine. PAS/AB staining for goblet cells shows that there are increased goblet cells in all parts of the intestine 3 days after acute DBZ treatment (E-H) compared to vehicle (A-D). N = 6 animals per group. Scale bar = 100μm

	Veh	Acute DBZ (Day 5)

Ki67 / AB

A

B
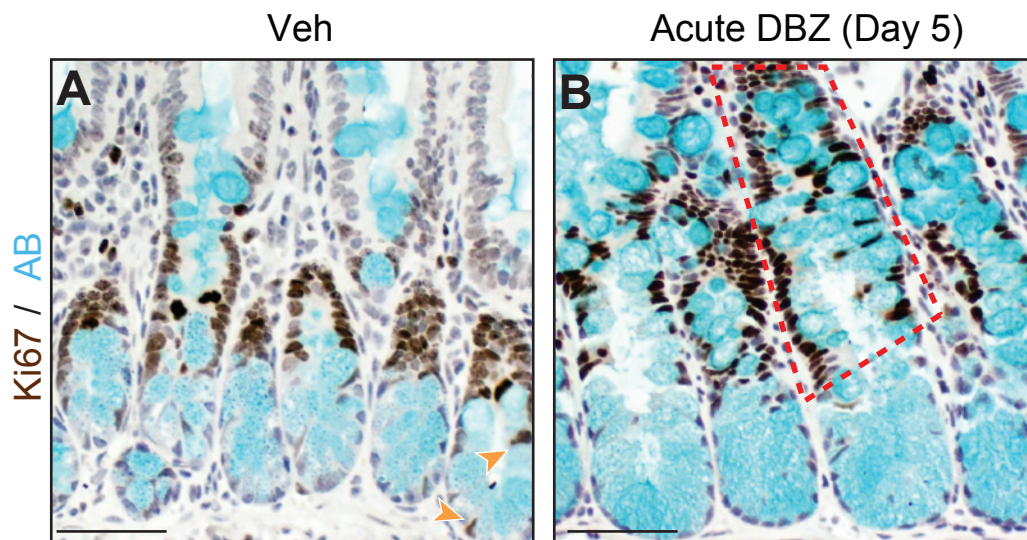
Supplementary Figure 3-2. Secretory cells and proliferating cells occupy the same crypt location. Co-staining with the mucin-marker AB and the proliferation marker Ki67 show abundant expansion of AB$^+$ and Ki67$^+$ cells in acute DBZ treated intestine compared to vehicle. Co-localization of the markers is observed in the upper two thirds of the crypt (red dashed box). Although some Ki67+ cells are observed at the base of the crypt in vehicle treated intestine (orange arrowheads), the proliferative zone is shifted upward in acute DBZ treated animals.
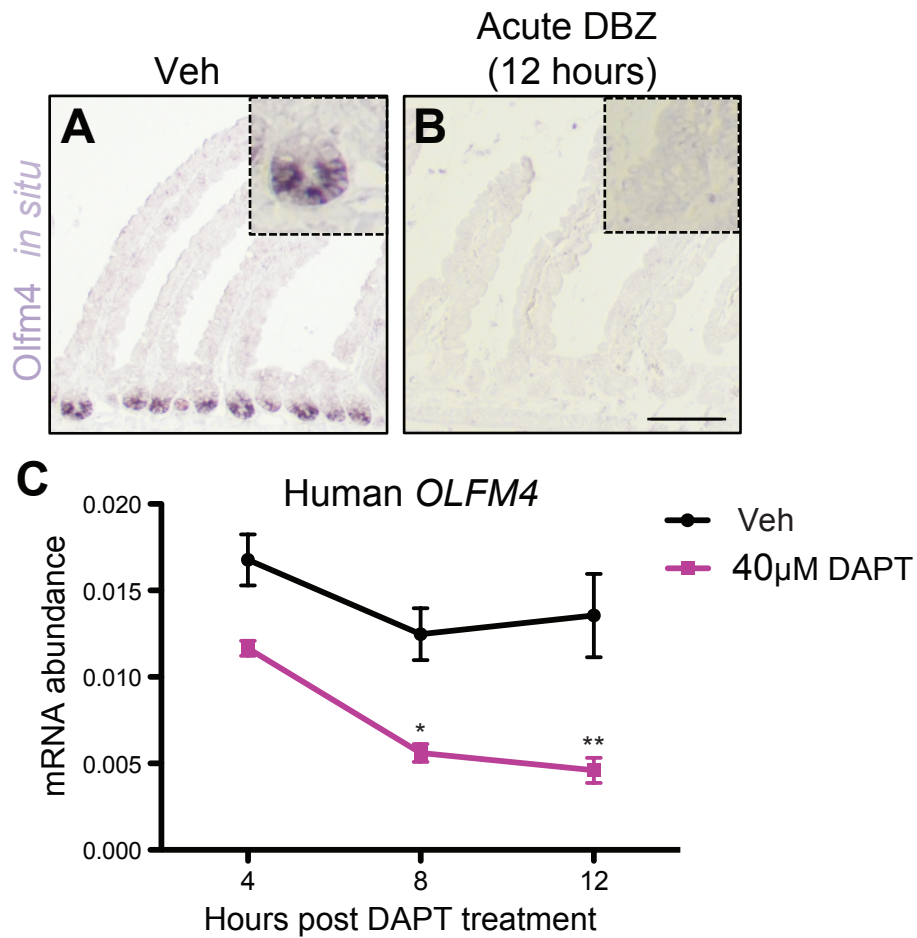
Supplementary Figure 3-3. *Olfm4* mRNA is very rapidly decreased after Notch inhibition. (A-B) *Olfm4 in situ* hybridization 12 hours after acute DBZ treatment shows a complete loss of *Olfm4* signal in duodenal crypts. (C) Quantitative RT-PCR for human *OLFM4* various time points after LS174T colon cancer cells were treated with 40µM DAPT or vehicle. DAPT results in decreased *OLFM4* expression as early as 8 hours after treatment. comparisons are made with student's *t* test. N = 3 per group.
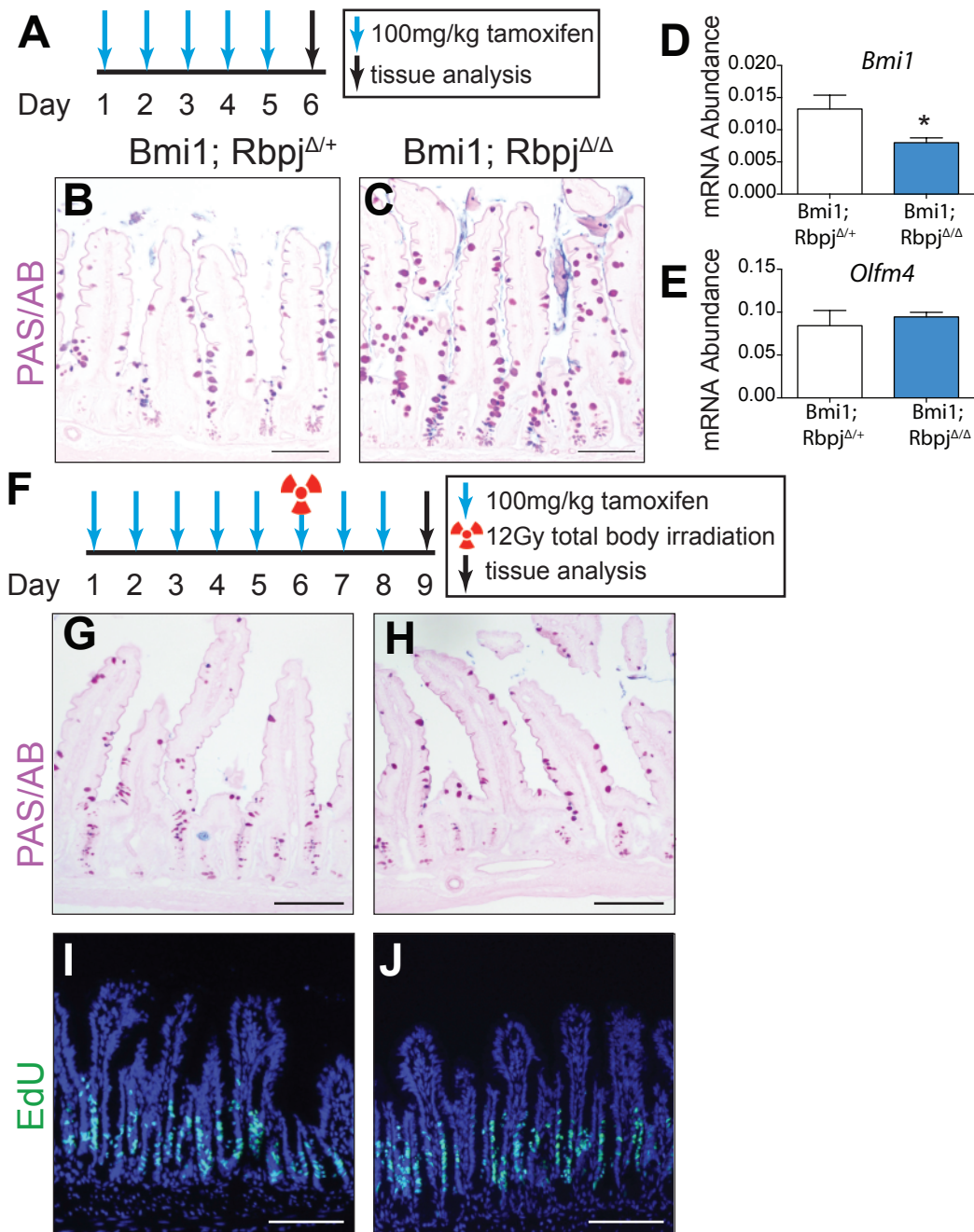
Supplementary Figure 3-4. Notch inhibition in BMI1+ cells does not prevent irradiation-induced proliferative surge. Bmi1; Rbpj[F/+] and Bmi1;Rbpj[F/F] animals were treated with tamoxifen and either euthanized on day 6 (A) or exposed to 12Gy irradiation and euthanized on day 9 after continued tamoxifen treatment (F). (B-C) PAS/AB staining shows increased goblet cells in Rbpj[Δ/Δ] compared to Rbpj[Δ/+] animals suggestive of effective Notch deletion on day 6. (D-E) Quantitative RT-PCR for *Bmi1* and *Olfm4* suggest specificity of *Rbpj* deletion in BMI1+ cells and not Olfm4+ CBCCs. (G-J) Differences in goblet cells and proliferation via EdU staining were not observed in Rbpj[Δ/Δ] intestine, suggesting that Notch deletion in these cells does not prevent post-irradiation induced proliferative surge. N=3-4 animals/group. Scale bar =100 μm.
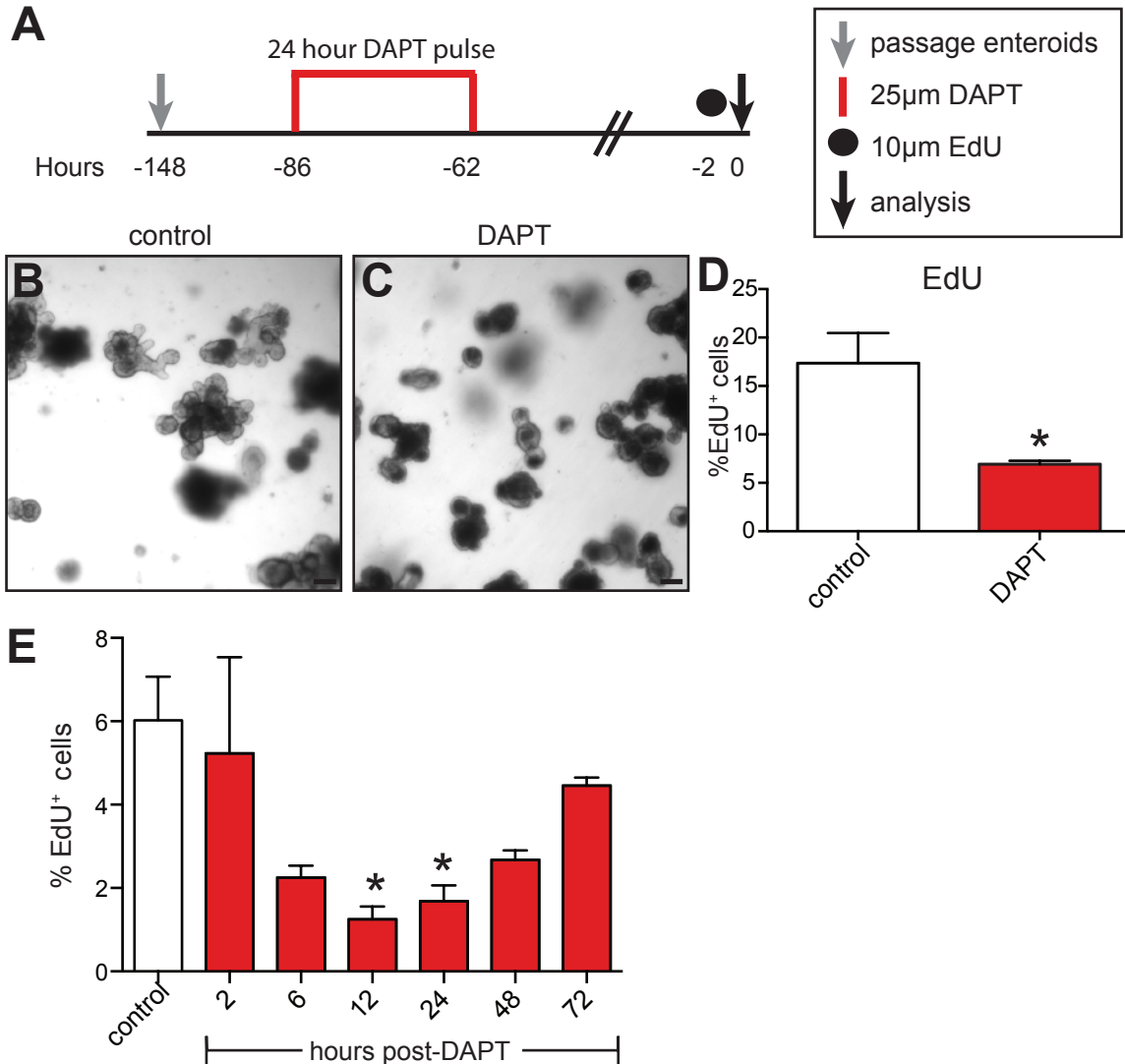
Supplementary Figure 3-5. Acute Notch inhibition in enteroids does not lead to increased proliferation. (A) Acute DAPT treatment: enteroids were treated with a 24-hour pulse of 25µm DAPT or vehicle. Media was changed to DAPT-free media and harvested 62 hours later after 2-hour incubation with EdU. (B-C) Live images of enteroids immediately prior to harvest. DAPT-treated enteroids appeared smaller with fewer budding structures. Scale bar = 100µm. (D) Proliferation as measured by flow cytometry for EdU+ cells showed decreased proliferation in the acute DAPT treated enteroids. Comparison was made with Student's t test. (E) To ensure that a time window of increased proliferation had not been missed, enteroids were treated with DAPT at various times prior to harvest as indicated. Proliferation was significantly decreased 12 and 24 hours after DAPT treatment, but no time point showed increased EdU uptake compared to vehicle. Comparisons were made with One-way ANOVA and Dunnett's post-test. Experiments were performed in triplicate with pooled quadruplicate treated wells.

REFERENCES

1. Khurana I. Textbook of Medical Physiology. Elsevier Health Sciences, 2005.
2. Potten CS, Gandara R, Mahida YR, Loeffler M, Wright NA. The stem cells of small intestinal crypts: where are they? Cell proliferation 2009;42:731-50.
3. Potten CS. Stem cells in gastrointestinal epithelium: numbers, characteristics and death. Philosophical transactions of the Royal Society of London. Series B, Biological sciences 1998;353:821-30.
4. Cheng H, Leblond CP. Origin, differentiation and renewal of the four main epithelial cell types in the mouse small intestine. I. Columnar cell. The American journal of anatomy 1974;141:461-79.
5. Barker N, van de Wetering M, Clevers H. The intestinal stem cell. Genes & development 2008;22:1856-64.
6. Crosnier C, Stamataki D, Lewis J. Organizing cell renewal in the intestine: stem cells, signals and combinatorial control. Nat Rev Genet 2006;7:349-59.
7. Cheng H, Leblond CP. Origin, differentiation and renewal of the four main epithelial cell types in the mouse small intestine. V. Unitarian Theory of the origin of the four epithelial cell types. The American journal of anatomy 1974;141:537-61.
8. Barker N, van Es JH, Kuipers J, Kujala P, van den Born M, Cozijnsen M, Haegebarth A, Korving J, Begthel H, Peters PJ, Clevers H. Identification of stem cells in small intestine and colon by marker gene Lgr5. Nature 2007;449:1003-7.
9. Sato T, Vries RG, Snippert HJ, van de Wetering M, Barker N, Stange DE, van Es JH, Abo A, Kujala P, Peters PJ, Clevers H. Single Lgr5 stem cells build crypt-villus structures in vitro without a mesenchymal niche. Nature 2009;459:262-5.
10. Sangiorgi E, Capecchi MR. Bmi1 is expressed in vivo in intestinal stem cells. Nature genetics 2008;40:915-20.
11. Powell AE, Wang Y, Li Y, Poulin EJ, Means AL, Washington MK, Higginbotham JN, Juchheim A, Prasad N, Levy SE, Guo Y, Shyr Y, Aronow BJ, Haigis KM, Franklin JL, Coffey RJ. The pan-ErbB negative regulator Lrig1 is an intestinal stem cell marker that functions as a tumor suppressor. Cell 2012;149:146-58.
12. Takeda N, Jain R, LeBoeuf MR, Wang Q, Lu MM, Epstein JA. Interconversion between intestinal stem cell populations in distinct niches. Science 2011;334:1420-4.
13. Montgomery RK, Carlone DL, Richmond CA, Farilla L, Kranendonk ME, Henderson DE, Baffour-Awuah NY, Ambruzs DM, Fogli LK, Algra S, Breault DT. Mouse telomerase reverse transcriptase (mTert) expression

marks slowly cycling intestinal stem cells. Proceedings of the National Academy of Sciences of the United States of America 2011;108:179-84.

14. Tian H, Biehs B, Warming S, Leong KG, Rangell L, Klein OD, de Sauvage FJ. A reserve stem cell population in small intestine renders Lgr5-positive cells dispensable. Nature 2011;478:255-9.

15. Yan KS, Chia LA, Li X, Ootani A, Su J, Lee JY, Su N, Luo Y, Heilshorn SC, Amieva MR, Sangiorgi E, Capecchi MR, Kuo CJ. The intestinal stem cell markers Bmi1 and Lgr5 identify two functionally distinct populations. Proceedings of the National Academy of Sciences of the United States of America 2012;109:466-71.

16. van Es JH, Sato T, van de Wetering M, Lyubimova A, Nee AN, Gregorieff A, Sasaki N, Zeinstra L, van den Born M, Korving J, Martens AC, Barker N, van Oudenaarden A, Clevers H. Dll1+ secretory progenitor cells revert to stem cells upon crypt damage. Nature cell biology 2012;14:1099-104.

17. Buczacki SJ, Zecchini HI, Nicholson AM, Russell R, Vermeulen L, Kemp R, Winton DJ. Intestinal label-retaining cells are secretory precursors expressing Lgr5. Nature 2013;495:65-9.

18. Munoz J, Stange DE, Schepers AG, van de Wetering M, Koo BK, Itzkovitz S, Volckmann R, Kung KS, Koster J, Radulescu S, Myant K, Versteeg R, Sansom OJ, van Es JH, Barker N, van Oudenaarden A, Mohammed S, Heck AJ, Clevers H. The Lgr5 intestinal stem cell signature: robust expression of proposed quiescent '+4' cell markers. The EMBO journal 2012;31:3079-91.

19. VanDussen KL, Carulli AJ, Keeley TM, Patel SR, Puthoff BJ, Magness ST, Tran IT, Maillard I, Siebel C, Kolterud A, Grosse AS, Gumucio DL, Ernst SA, Tsai YH, Dempsey PJ, Samuelson LC. Notch signaling modulates proliferation and differentiation of intestinal crypt base columnar stem cells. Development 2012;139:488-97.

20. Fre S, Huyghe M, Mourikis P, Robine S, Louvard D, Artavanis-Tsakonas S. Notch signals control the fate of immature progenitor cells in the intestine. Nature 2005;435:964-8.

21. van Es JH, van Gijn ME, Riccio O, van den Born M, Vooijs M, Begthel H, Cozijnsen M, Robine S, Winton DJ, Radtke F, Clevers H. Notch/gamma-secretase inhibition turns proliferative cells in intestinal crypts and adenomas into goblet cells. Nature 2005;435:959-63.

22. Stanger BZ, Datar R, Murtaugh LC, Melton DA. Direct regulation of intestinal fate by Notch. Proc Natl Acad Sci U S A 2005;102:12443-8.

23. Riccio O, van Gijn ME, Bezdek AC, Pellegrinet L, van Es JH, Zimber-Strobl U, Strobl LJ, Honjo T, Clevers H, Radtke F. Loss of intestinal crypt progenitor cells owing to inactivation of both Notch1 and Notch2 is accompanied by derepression of CDK inhibitors p27Kip1 and p57Kip2. EMBO Rep 2008;9:377-83.

24. Pellegrinet L, Rodilla V, Liu Z, Chen S, Koch U, Espinosa L, Kaestner KH, Kopan R, Lewis J, Radtke F. Dll1- and dll4-mediated notch signaling are required for homeostasis of intestinal stem cells. Gastroenterology 2011;140:1230-1240 e7.

25. Crosnier C, Vargesson N, Gschmeissner S, Ariza-McNaughton L, Morrison A, Lewis J. Delta-Notch signalling controls commitment to a secretory fate in the zebrafish intestine. Development 2005;132:1093-104.

26. Bray SJ. Notch signalling: a simple pathway becomes complex. Nature reviews. Molecular cell biology 2006;7:678-89.

27. Reichardt I, Knoblich JA. Cell biology: Notch recycling is numbed. Current biology : CB 2013;23:R270-2.

28. Zhou Y, Atkins JB, Rompani SB, Bancescu DL, Petersen PH, Tang H, Zou K, Stewart SB, Zhong W. The mammalian Golgi regulates numb signaling in asymmetric cell division by releasing ACBD3 during mitosis. Cell 2007;129:163-78.

29. Goulas S, Conder R, Knoblich JA. The Par complex and integrins direct asymmetric cell division in adult intestinal stem cells. Cell stem cell 2012;11:529-40.

30. Yang Y, Zhu R, Bai J, Zhang X, Tian Y, Li X, Peng Z, He Y, Chen L, Ji Q, Chen W, Fang D, Wang R. Numb modulates intestinal epithelial cells toward goblet cell phenotype by inhibiting the Notch signaling pathway. Experimental cell research 2011;317:1640-8.

31. Snippert HJ, van der Flier LG, Sato T, van Es JH, van den Born M, Kroon-Veenboer C, Barker N, Klein AM, van Rheenen J, Simons BD, Clevers H. Intestinal crypt homeostasis results from neutral competition between symmetrically dividing Lgr5 stem cells. Cell 2010;143:134-44.

32. Lopez-Garcia C, Klein AM, Simons BD, Winton DJ. Intestinal stem cell replacement follows a pattern of neutral drift. Science 2010;330:822-5.

33. Tanigaki K, Han H, Yamamoto N, Tashiro K, Ikegawa M, Kuroda K, Suzuki A, Nakano T, Honjo T. Notch-RBP-J signaling is involved in cell fate determination of marginal zone B cells. Nature immunology 2002;3:443-50.

34. el Marjou F, Janssen KP, Chang BH, Li M, Hindie V, Chan L, Louvard D, Chambon P, Metzger D, Robine S. Tissue-specific and inducible Cre-mediated recombination in the gut epithelium. Genesis 2004;39:186-93.

35. Lopez-Diaz L, Hinkle KL, Jain RN, Zavros Y, Brunkan CS, Keeley T, Eaton KA, Merchant JL, Chew CS, Samuelson LC. Parietal cell hyperstimulation and autoimmune gastritis in cholera toxin transgenic mice. American journal of physiology. Gastrointestinal and liver physiology 2006;290:G970-9.

36. Barker N, Huch M, Kujala P, van de Wetering M, Snippert HJ, van Es JH, Sato T, Stange DE, Begthel H, van den Born M, Danenberg E, van den Brink S, Korving J, Abo A, Peters PJ, Wright N, Poulsom R, Clevers H. Lgr5(+ve) stem cells drive self-renewal in the stomach and build long-lived gastric units in vitro. Cell stem cell 2010;6:25-36.

37. Bell SM, Schreiner CM, Wert SE, Mucenski ML, Scott WJ, Whitsett JA. R-spondin 2 is required for normal laryngeal-tracheal, lung and limb morphogenesis. Development 2008;135:1049-58.

38. Riccio O, van Gijn ME, Bezdek AC, Pellegrinet L, van Es JH, Zimber-Strobl U, Strobl LJ, Honjo T, Clevers H, Radtke F. Loss of intestinal crypt

progenitor cells owing to inactivation of both Notch1 and Notch2 is accompanied by derepression of CDK inhibitors p27Kip1 and p57Kip2. EMBO reports 2008;9:377-83.

39.   Kim TH, Li F, Ferreiro-Neira I, Ho LL, Luyten A, Nalapareddy K, Long H, Verzi M, Shivdasani RA. Broadly permissive intestinal chromatin underlies lateral inhibition and cell plasticity. Nature 2014;506:511-5.

40.   Itzkovitz S, Lyubimova A, Blat IC, Maynard M, van Es J, Lees J, Jacks T, Clevers H, van Oudenaarden A. Single-molecule transcript counting of stem-cell markers in the mouse intestine. Nature cell biology 2012;14:106-14.

41.   van der Flier LG, van Gijn ME, Hatzis P, Kujala P, Haegebarth A, Stange DE, Begthel H, van den Born M, Guryev V, Oving I, van Es JH, Barker N, Peters PJ, van de Wetering M, Clevers H. Transcription factor achaete scute-like 2 controls intestinal stem cell fate. Cell 2009;136:903-12.

42.   Bielen H, Houart C. The Wnt cries many: Wnt regulation of neurogenesis through tissue patterning, proliferation, and asymmetric cell division. Developmental neurobiology 2014.

43.   Sun SC, Kim NH. Molecular mechanisms of asymmetric division in oocytes. Microscopy and microanalysis : the official journal of Microscopy Society of America, Microbeam Analysis Society, Microscopical Society of Canada 2013;19:883-97.

44.   Betschinger J, Knoblich JA. Dare to be different: asymmetric cell division in Drosophila, C. elegans and vertebrates. Current biology : CB 2004;14:R674-85.

45.   Sander GR, Powell BC. Expression of notch receptors and ligands in the adult gut. J Histochem Cytochem 2004;52:509-16.

46.   Milano J, McKay J, Dagenais C, Foster-Brown L, Pognan F, Gadient R, Jacobs RT, Zacco A, Greenberg B, Ciaccio PJ. Modulation of notch processing by gamma-secretase inhibitors causes intestinal goblet cell metaplasia and induction of genes known to specify gut secretory lineage differentiation. Toxicological sciences : an official journal of the Society of Toxicology 2004;82:341-58.

47.   Weng AP, Nam Y, Wolfe MS, Pear WS, Griffin JD, Blacklow SC, Aster JC. Growth suppression of pre-T acute lymphoblastic leukemia cells by inhibition of notch signaling. Molecular and cellular biology 2003;23:655-64.

48.   Weng AP, Millholland JM, Yashiro-Ohtani Y, Arcangeli ML, Lau A, Wai C, Del Bianco C, Rodriguez CG, Sai H, Tobias J, Li Y, Wolfe MS, Shachaf C, Felsher D, Blacklow SC, Pear WS, Aster JC. c-Myc is an important direct target of Notch1 in T-cell acute lymphoblastic leukemia/lymphoma. Genes & development 2006;20:2096-109.

49.   Obata Y, Takahashi D, Ebisawa M, Kakiguchi K, Yonemura S, Jinnohara T, Kanaya T, Fujimura Y, Ohmae M, Hase K, Ohno H. Epithelial cell-intrinsic Notch signaling plays an essential role in the maintenance of gut immune homeostasis. Journal of immunology 2012;188:2427-36.

CHAPTER 4

COMPARTMENTAL MODELING OF THE INTESTINAL CRYPT

4.1: SUMMARY

This chapter describes mathematical modeling approaches used to tackle the question posed in Chapter 3: *Does Notch inhibition lead to symmetric division of stem cells into two transit-amplifying (TA) cells?* I first tested the compartmental model of the intestinal crypt published by Johnston et al.[1], and determined that a differential equation system was unsuitable for replicating the short timing and rapidly changing dynamics of intestinal Notch inhibition. Next, a discrete compartmental model was built and calibrated to simply describe stem and TA cell dynamics. Finally, the model was implemented by testing several hypotheses that could explain the proliferation findings of *in vivo* Notch inhibition including: forced differentiation, symmetric stem cell division, and apoptosis. A model where Notch inhibition results in symmetric division followed by Notch-dependent stem cell repopulation most closely matched our experimental findings.

4.2: INTRODUCTION

Mathematical and computational models are powerful instruments in the scientific toolbox. Modeling can take what has been learned from experimental observations and derive new knowledge without the confines of experimental constraints or limited sample size. Synergistically, these insights can be taken

back to the bench in the form of testable hypotheses allowing more informed and focused investigation. In the intestine, modeling has been used for discovery-making for decades: examining steady-state crypt proliferation[2, 3], crypt cell migration rates[4, 5], intestinal epithelial differentiation[6-9], neutral drift dynamics[10, 11], and tumorigenesis[1, 12-14]. Confronted with the question of how Notch regulates stem and progenitor cell number, modeling was a natural avenue to take.

In Chapter 3 I found that chronic Notch inhibition with the gamma secretase inhibitor Dibenzazepine (DBZ) resulted in decreased proliferation and decreased stem cell number[15] while acute DBZ resulted in increased proliferation and decreased stem cells. Since these experiments produced data in the form of broadly categorized stem and proliferating progenitor cell counts, this intriguing dichotomy lent itself well to a compartmental modeling approach. As discussed in detail in Chapter 1, compartmental modeling is a particular type of mathematical model that focuses on the flux between different types of cells, grouped into discrete compartments. In the intestine this usually comprises stem, progenitor or transit-amplifying (TA), and differentiated cell compartments, although any number of compartments or subcompartments could be created depending on the question.

In 2007, Johnston et al.[1] revised a simple compartmental model of the crypt that had been initiated by Tomlinson and Bodmer[13] in 1995. The Johnston model[1] utilizes an ordinary differential equation system to describe the rates of flows between stem, TA, and differentiated cell compartments and incorporates feedback into the model to make the system more stable. Their model[1] was shown to accurately describe the crypt during both homeostasis and tumorigenesis, and thus was the perfect starting point for this project.

For this study I aimed to find a singular mechanism that would explain the timing-dependent proliferation outcomes post-Notch inhibition. Since we observed an apparent shift from GFP[HI] stem cells to GFP[INT] TA cells (Chapter 3), the concept of Notch regulation of stem cell division symmetry was a key hypothesis I wished to test *in silico*.

4.3: METHODS

Simulations for the Johnston et al.[1] model were run in XPPAUT (v.6). Discrete compartmental model simulations were performed in Microsoft Excel and plotted in Graphpad Prism.

4.4: RESULTS AND DISCUSSION

Johnston et al. model of the crypt does not replicate limited TA cell lifespan

To test the hypothesis of Notch regulation of stem cell symmetry in the context of the Johnston et al.[1] model, I started by modulating parameters in the system to approximate bulk movement from the stem cell compartment to the TA cell compartment. As discussed in Chapter 1.3, the Johnston et al.[1] model divides the crypt into three compartments: stem cells (N_0), "semi-differentiated cells" (TA cells) (N_1), and fully-differentiated cells (N_2) (Figure 4-1). Fluxes out of N_0 and N_1 include death, differentiation, and renewal (α_1, α_2, α_3 and β_1, β_2, β_3 respectively). Flux out of N_2 is cell removal (sloughing off) (γ). The ordinary differential equation system of the saturating feedback model are reproduced below in **Eq 1-3**[1], where k_0, k_1, m_0, and m_1 are rate constants.

$$\frac{dN_0}{dt} = (\alpha_3 - \alpha_1 - \alpha_2)N_0 - \frac{k_0 N_0^2}{1 + m_0 N_0} \qquad \text{[1]}$$

$$\frac{dN_1}{dt} = (\beta_3 - \beta_1 - \beta_2)N_1 - \frac{k_1 N_1^2}{1 + m_1 N_1} + \alpha_2 N_0 + \frac{k_0 N_0^2}{1 + m_0 N_0} \qquad \text{[2]}$$

$$\frac{dN_2}{dt} = -\gamma N_2 + \beta_2 N_1 + \frac{k_1 N_1^2}{1 + m_1 N_1} \qquad \text{[3]}$$

Since I was interested in using this model to look at stem cell division symmetry in the context of Notch inhibition, the most relevant parameters were α_2 and α_3, the rates controlling differentiation from stem cells to TA cells and
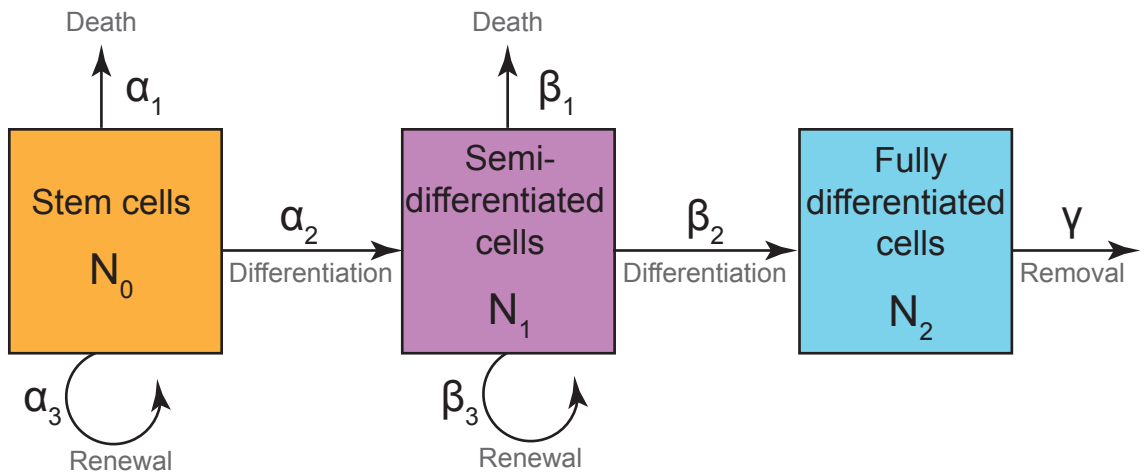
Figure 4-1. Compartmental model of the crypt by Johnston et al.[1]. Cells are distributed into 3 populations: stem cells (N_0), semi-differentiated cells (N_1), and fully-differentiated cells (N_2). Parameters governing flows between the compartments include cell death (α_1, β_1), differentiation (α_2, β_2), self-renewal (α_3, β_3) and cell removal (γ).

stem cell self-renewal, respectively. Thus to effectively model symmetric division from 1 stem cell to 2 TA cells, α_2 would increase while α_3 would decrease. I performed several simulations testing the bounds of α_2 and α_3 modulation in the context of acute (1 day) or chronic (5 days) Notch inhibition and found that alteration of these parameters led to very mild increases in the N_1 population when changed for either acute or chronic periods, but neither change led to any decrease in N_1 or N_2 number, which would be expected after the stem cell compartment had been fully depleted (Figure 4-2A,B).

Interestingly I found that even with an initial value for N_0 of 0 stem cells, populations remained in the N_1 and N_2 compartments (not shown). It became clear that the N_1 cell compartment in this model acts independently as another stem cell compartment since the parameter β_3 allowed for indefinite N_1 cell renewal. This is counter to the traditional view that TA cells possess limited self-renewal, dividing 4-6 times prior to differentiating[16-18].

To circumvent this issue, I simulated Notch inhibition such that contribution of β_3 was eliminated during the time of α_2 elevation, preventing unlimited TA self-renewal. Despite the fact that increased α_2 should lead to a bolus of extra cells in the TA cell compartment leading to a transient increase in N_1 cell number, loss of the unlimited TA cell self-renewal prevented any increase in this population (Figure 4-2C,D).

One of the strengths of the Johnston et al. model[1] is that it provides ample feedback to prevent small changes in compartmental populations from destabilizing steady state populations. While this is ideal for analysis of crypt homeostasis over long periods of time, it leads to inability to describe short-term dynamics. To adequately test our hypothesis I needed to devise a crypt model were the TA cell compartment was not an independent entity, but very much dependent on the stem cell population and the outcome of stem cell division symmetry.
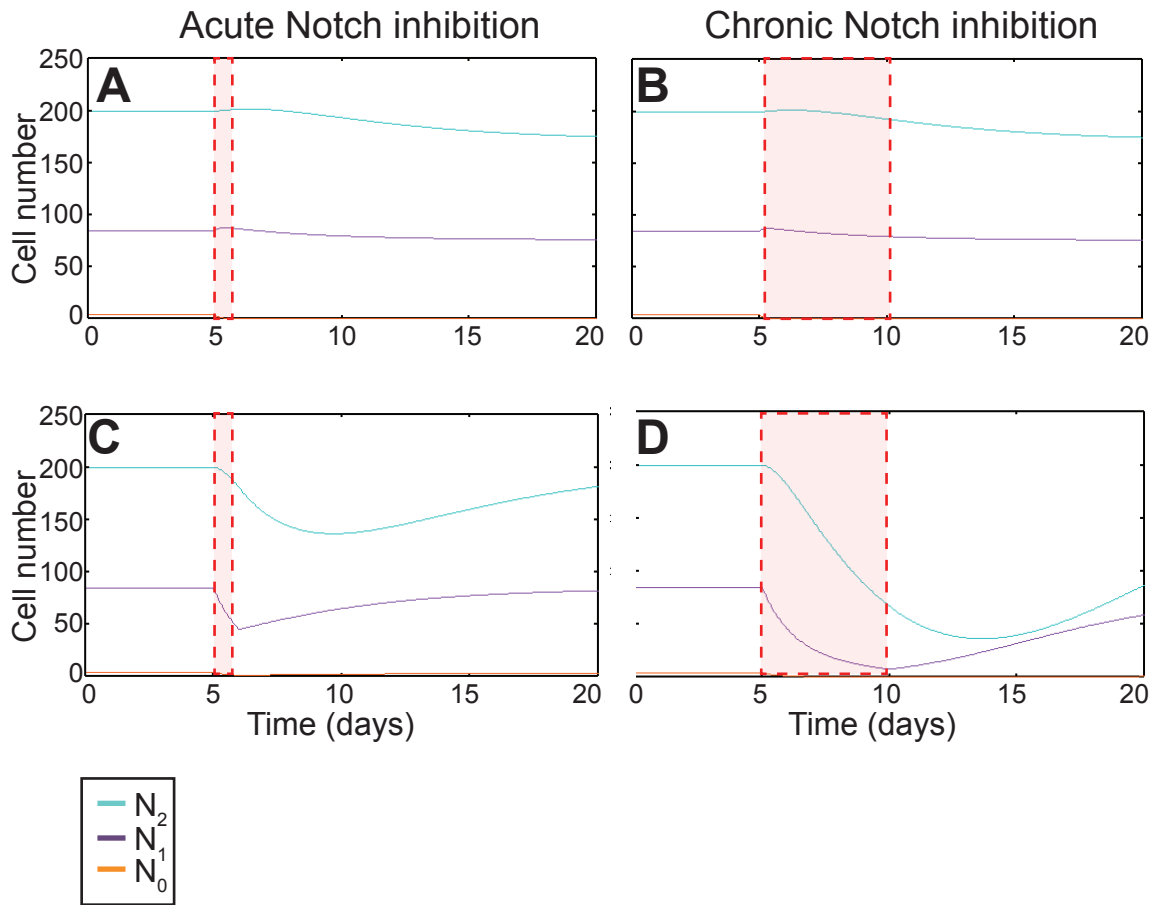
Figure 4-2. Johnston et al. model[1] does not replicate short-term crypt dynamics. (A-B) Approximating symmetric stem cell division by increasing α_2 (α_2 = 5) and decreasing α_3 to (α_3 = 0.001) during the period of "Notch inhibition" (red shaded boxes). Acute Notch inhibition is estimated as parameter changes for 1 day prior to normalization. Chronic Notch inhibition is parameter changes for 5 days prior to normalization. (C-D) Analysis of N_1 self-renewal removal. The self-renewal parameter β_3 was decreased to 0 during the period of Notch inhibition. Symmetric cell division was estimated by increasing α_2 to 1 during this period. Homeostatic parameter values are α = 0.286, α_2 = 0.3, α_3 = 0.586, β = 0.432, β_2 = 0.2, β_3 = 0.732, γ = 0.323, k_0 = 0.1, m_0 = 0.1, k_1 = 0.01, and m_1 = 0.01, as described in Johnston et al.[1] where $\alpha = \alpha_3 - \alpha_1 - \alpha_2$ and $\beta = \beta_3 - \beta_1 - \beta_2$ except during the Notch inhibition intervals as noted above.

Discrete compartmental model

Since a differential equation system did not allow the flexibility of observing compartmental changes due to small, transient fluctuations in cell numbers, I switched to a discrete (difference equation) modeling approach. Like the Tomlinson and Bodmer[13] and Johnston et al.[1] models, my model also contains, in essence, 3 compartments: stem (S), TA (T), and differentiated (D) cells, although compartment D is not directly assessed in the following analyses. Instead of cell division fueled by intrinsic cell cycle rates, compartment population numbers are determined by amplification from the previous compartment. To accurately amplify the TA compartment I started with a number of T compartments to be consistent with the idea of 4-6 rounds of TA cell division (Figure 4-3). I thus crafted the following set of difference equations **Eq 4-8**.

$$S_{(t+1)} = S_{(t)} + (1 - X)S_{(t)} + R \tag{4}$$

$$T_{1(t+1)} = S_{(t)}X \tag{5}$$

$$T_{2(t+1)} = 2T_{1(t)} \tag{6}$$

$$T_{n(t+1)} = 2T_{n-1(t)} \tag{7}$$

$$D_{(t+1)} = D_{(t)} + T_{n-1(t)} - G \tag{8}$$

where $S_{(t)}$ is the population of stem cells at time t. X is the parameter that governs stem cell division. Thus if $X = 1$ an equal amount of stem cell and TA cells are produced from each stem cell division event, the definition of asymmetric stem cell division. When $X = 0$, stem cell division is symmetric but produces only stem-like daughter cells, and when $X = 2$, stem cell division produces only 2 TA cells (Figure 4-3B). R is a net gain or loss parameter. $T_{n(t)}$ is the population in any one of several TA cell compartments at time t for n>1.
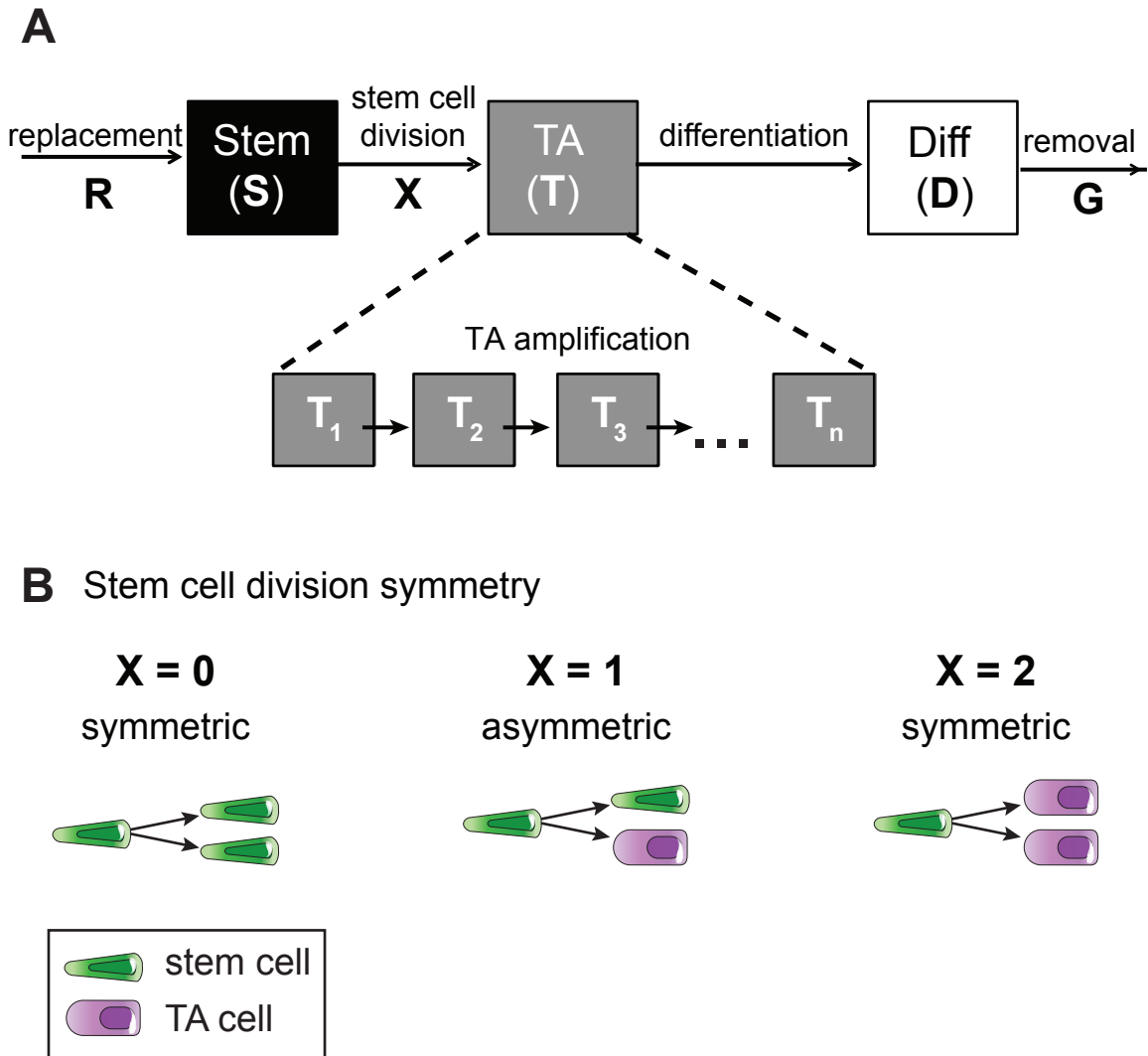
Figure 4-3. Discrete compartmental model of the intestinal crypt. (A) Schematic diagram of compartmental model. Compartments include stem (S), TA (T), and Differentiated (D) cell compartments. Multiple TA cell divisions are listed in subcompartments where n = 4-6 divisions. (B) X functions to regulate stem cell division symmetry. X can be 0, 1, or 2 and determines whether stem cells divide asymmetrically producing 1 stem cell and 1 TA cells, or symmetrically, forming either 2 stem cells or 2 TA cells.

T compartment population is calculated by simply doubling the population of the previous compartment and n is the total number TA divisions. Finally, $D_{(t)}$ is the population in the differentiated cell compartment at time t and G is the number of cells removed from D due to sloughing off at any time.

Calibration of cell division timing

First, I addressed the dissimilarity in cell cycle times intrinsic to various cell populations. Stem cells are thought to divide on average once per day[10, 19], while TA cells divide approximately every 12 hours[16, 17]. Johnston et al.[1] determined that age-matching cells was not necessary and that continuously averaging the population was sufficient for compartment analysis. It was unclear, however, how important the scale of time step t was for system dynamics in an iterative model of the crypt.

To assess this, I first set t = 12 hours to be on scale with TA cell divisions, but only allowed stem cell division every other time step. Not surprisingly, this resulted in periodic gaps in TA cell compartments leading to oscillation in total T population (Figure 4-4A). I then compared this outcome with t = 1 day, with both stem and TA cell divisions occurring every time step (Figure 4-4B). Notably, summation over a 24-hour period in the 12-hour time step model gave the same outcome for total T population as the 1 day time step. These simulations were performed in the setting of asymmetric stem cell division (X = 1) but identical conclusions were made with other values of X (not shown).

The oscillations in the 12-hour time step model are an artifact caused by the inherent assumption that cell division is synchronized. In an actual crypt, cell division is asynchronous and thus no gap in S to T transition would ever truly occur. Because the overall T population numbers were identical between the two timescales when summed over a 24-hour period, and as the comparable experimental data was collected on a daily basis, the model was scaled to a 1 day time step.
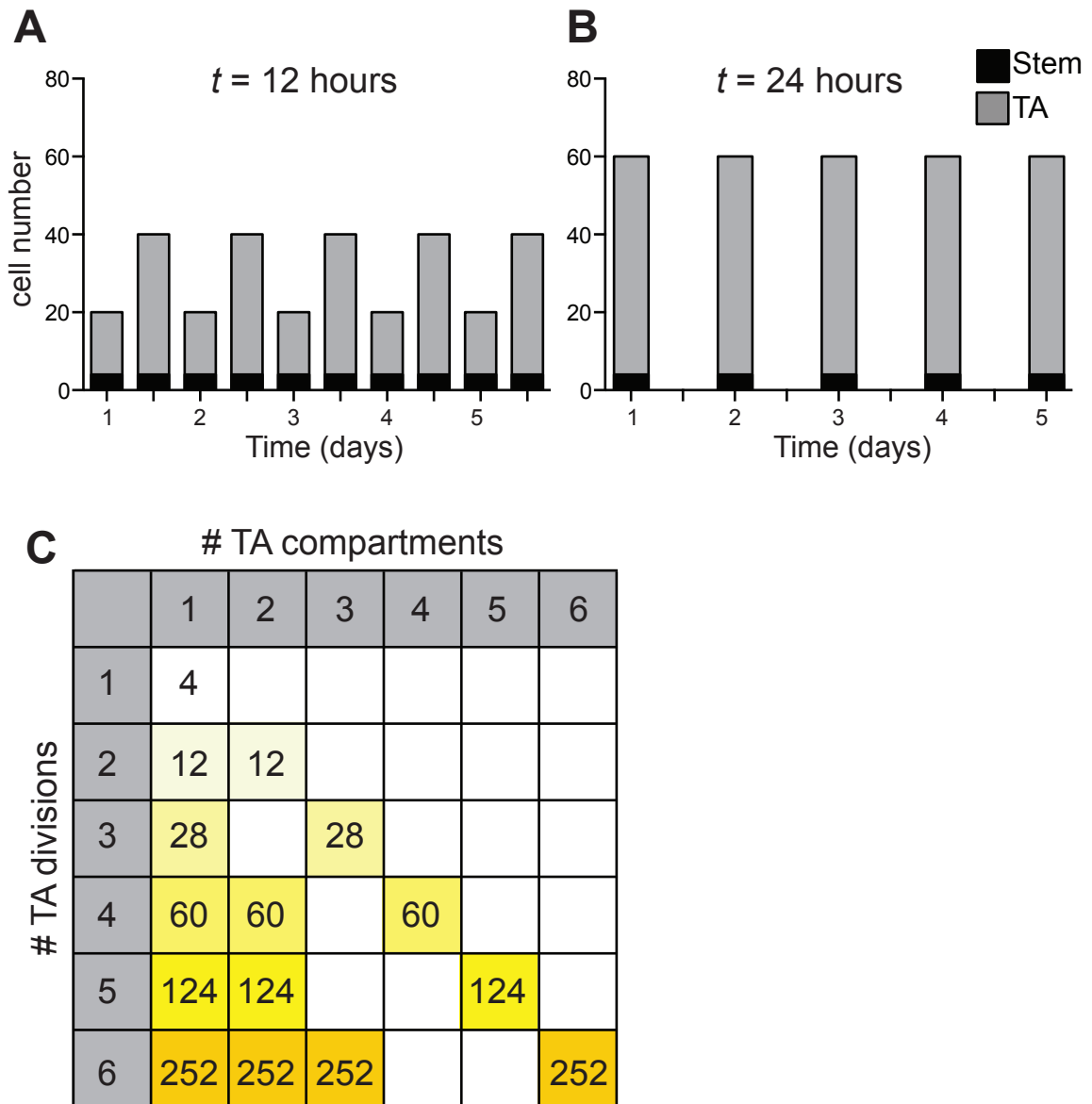
Figure 4-4. Compartmental model calibrations. (A,B) Simulated data for the discrete compartmental model with iterations run every 12 hours with stem cell division occurring every other iteration (A) or iterations run every 24 hours with stem cell division occur every iteration (B). (C) Comparison of total TA cell counts derived when various combinations of TA compartment number and rounds of division are used. Only combinations with # of divisions that were divisible by compartment number were used. Identical population values are shaded with the same color. Initial values for all calculations were S = 4, T_1 = 4, X = 1, R = 0.

TA cell compartments can be lumped

Next, I aimed to determine if multiple TA cell compartments were necessary to accurately describe an amplifying system. To test this I condensed multiple TA compartments into larger compartments and calculated whether the resulting total TA population differed than if the amplifications had occurred in individual compartments. The results are plotted in Figure 4-4C. In summary, it does not matter computationally how many compartments the TA cells are spread between, only the number of divisions affect overall TA cell population. Thus, the **Eq 5-7** can be simplified as **Eq 9**:

$$T_{(t+1)} = \omega S_{(t)} X \qquad\qquad \textbf{[9]}$$

where ω is an amplification constant dependent on the number of TA divisions. (For example, when $n = 4$, $\omega = 15$ and when $n = 6$, $\omega = 63$).

Forced differentiation versus symmetric stem cell division

I favored a hypothesis that symmetric stem cell division could explain the increased proliferation and decreased stem cells observed with acute DBZ treatment, because such a division event would inherently decrease the number of stem cells and would increase the amount of TA cells primed for amplification. I questioned, however, if stem cell division was even necessary to lead to this outcome. In our experimental system this would indicate that Notch inhibition led to the <u>differentiation</u> of stem cells into TA cells rather than <u>division</u> of stem cells into TA cells. To test this, I compared whether simply moving the entire S compartment into T_1 would result in increased TA cell number (Figure 4-5A). Strikingly, without stem cell division, no amplification above initial T population is observed. As expected, with loss of the stem cells, TA cells become depleted over time. When symmetric stem cell division is implemented however ($X = 2$), a robust doubling in population is observed over initial TA levels (Figure 4-5B). Without stem cells, this too is depleted over time, but the increased population is observed for several days prior to crypt collapse. Through this comparison,
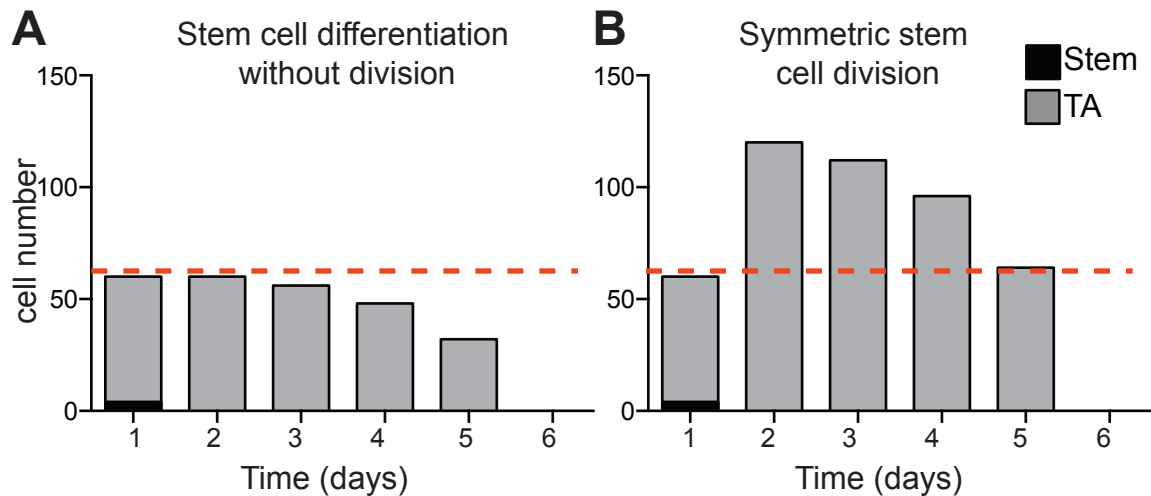
Figure 4-5. Stem cell differentiation versus symmetric division. (A) Stem and TA cell populations resulting from S compartment shift to T_1 compartment in the absence of stem cell division. Initial values: S = 4, T_1 = 4, R = 0, X = 1, ω=15 (B) Simulation of discrete compartmental model with symmetric stem cell division. Initial values: S = 4, T_1 = 4, R = 0, X = 2, ω=15.

I concluded that although differentiation of stem cells into TA cells moves cells into the proper compartment, without stem cell division no amplification is observed.

Utilizing non-integer values of X

Having determined that symmetric stem cell division (X = 2) can lead to decreased stem cells and a transient increase in TA cells (Figure 4-5B), I was encouraged that this was a viable mechanism to test in our Notch inhibition model. I noted, however, that the stem cell population number was completely depleted after a single round of division when X=2. Since our experimental findings did not suggest that the <u>entire</u> stem cell compartment is lost after DBZ treatment, I considered relaxing the stringency of stem cell symmetry in our model, allowing non-integer values of X. This removes the strict definition of asymmetric versus symmetric symmetry from the model, but allows description of stem cell progeny on a population level. Any value of X between 1 and 2 (I used X = 1.5) would indicate a greater likelihood of TA cell specification. Thus Notch inhibition could lead to more, but not all, stem cell progeny becoming TA cells.

Hypothesis-testing: Stem cell symmetry in acute and chronic Notch inhibition

The first hypothesis I wanted to test was if change in stem cell <u>symmetry alone</u> could account for the differing proliferation outcomes observed in acute and chronic Notch inhibition. To test this, we started our simulations with "homeostasis" such that X = 1, R = 0. During the period of Notch inhibition X was set at 1.5 to simulate preference for TA cell production over stem cell production. X was increased for 1 day (acute Notch inhibition) or 5 days (chronic Notch inhibition). The results of this simulation are shown in Figure 4-6A. As observed in our experimental data obtained after acute Notch inhibition with DBZ, the simulation showed a transient increase in TA cell population while stem cells were decreased. Both populations return to homeostasis after treatment, but, notably, at lower than initial value levels. Chronic Notch inhibition shows the same trends, although the stem cell compartment is completely depleted and TA
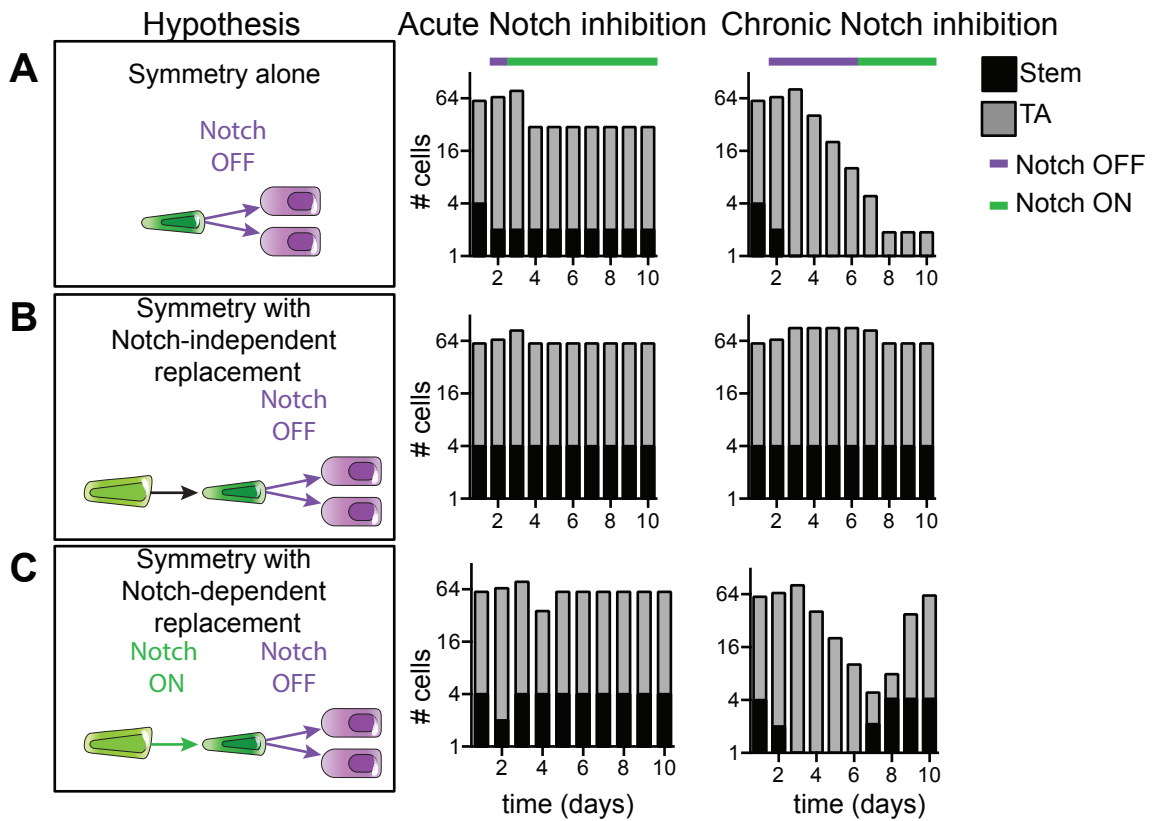
Figure 4-6. Hypothesis testing with the discrete compartmental model. The effect of Notch-regulated stem cell symmetry in the context of acute and chronic Notch inhibition is evaluated in three scenarios. To model a shift toward symmetric division X = 1.5 for 1 day (acute) or 5 days (chronic) during the periods indicated (purple bars). X is returned to 1 after treatment (green bar). Symmetry is tested alone (A), with Notch-independent stem cell replacement (B), and with Notch-dependent stem cell replacement (C). Notch independent stem cell replacement is accomplished by $R = S_0 - S_t$ during Notch inhibition window. Notch-dependent stem cell replacement uses $R = 2$ after the Notch inhibition window until $S_t = S_0$. Initial values: S = 4, T = 60, R = 0, X = 1, ω=15.

cell populations progressively decline before reaching much lower resting levels. While the chronic Notch inhibition outcomes resemble the decreased stem and proliferating cell findings we observed experimentally, the acute Notch inhibition simulation did not mirror our results since experimental proliferation returned to baseline by 7 days, rather than remaining lowered post-treatment.

Hypothesis-testing: Stem cell symmetry with Notch-independent stem cell replacement

Since the decreased homeostatic resting levels observed above were fueled from a persistent loss in stem cell number, I probed the idea of stem cell replacement in conjunction with altered stem cell symmetry. Numerous studies have shown that lost or damaged crypt base columnar stem cells can be replaced by quiescent or facultative stem cell populations[20-23]. Thus repopulation of the S compartment is possible independent from stem cell symmetry and self-renewal. The model takes this into account with the net gain or loss parameter, R. Positive R values function to allow repopulation of S, presumably by a quiescent stem cell.

In Figure 4-6B, I simulated Notch-regulated stem cell symmetry as above, but allowed for replacement of lost stem cells throughout the Notch inhibition window. Constant stem cell replacement was determined by **Eq. 10**:

$$R = S_0 - S_t \qquad\qquad \textbf{[10]}$$

where S_0 is the initial stem cell population and S_t is the decreased stem cell population at time t. With these parameters, stem cell populations remained unchanged throughout the entire test window in both acute and chronic Notch inhibition conditions. TA populations increased during the period of treatment and normalized after restoration of Notch signaling. Neither of these scenarios reflected the stem cell trends observed in our experimental system. Notch-independent stem cell replacement showed no loss in TA cell number in the

chronic Notch inhibition model, which did not at all reflect the significant loss in proliferating TA cells observed with chronic DBZ treatment experimentally.

Hypothesis-testing: Stem cell symmetry with Notch-<u>dependent</u> stem cell replacement

Finally, I tested Notch-regulated stem cell symmetry with <u>Notch-regulated stem cell replacement</u> (Figure 4-6C). In this simulation, R was altered only after Notch restoration. In the post-Notch inhibition window R was arbitrarily set at 2 until S_t returned to S_0 levels. In acute Notch inhibition this resulted in transiently decreased stem cells and transiently increased TA cell population, both of which returned to baseline homeostatic levels, although a transient decrease in TA cell number was observed prior to normalization. With chronic Notch inhibition, this resulted in a complete loss of stem cells and a marked reduction in TA cell number. After Notch restoration, a slow but complete recovery of both populations is observed.

In comparing these simulations with our experimental findings, the stem cell symmetry with Notch-dependent stem cell replacement is the best approximation thus far reconciling both acute and chronic DBZ results. Although I did not directly observe a dip in TA cell number prior to restoration with experimental acute DBZ, all other aspects of this simulation closely resembled the stem and proliferating cell profiles obtained in those experiments. The lack of this TA cell dip could be because I did not directly measure TA cell number, or it could have occurred transiently at a time point I did not analyze.

If this system is a rough approximation of what actually occurs with crypt dynamics in the setting of Notch inhibition, then the chronic Notch inhibition simulation provides several interesting testable outcomes. First, increased TA cells are observed prior to decreased TA cells. Second, stem and TA cells eventually recover post-Notch inhibition. As discussed in Chapter 3, both of these outcomes were tested in our *in vivo* system and were found to closely resemble these predictions, an encouraging validation of the model.

Apoptosis: an alternate hypothesis

To avoid being short-sighted in my consideration of possible mechanisms, I used the model to test an obvious alternate mechanism of stem cell loss, apoptosis. In our *in vivo* system, I did not find a significant increase in cleaved caspase^{+} cells in the crypts after acute DBZ. I questioned, however, whether I had simply missed a narrow window of apoptosis as other stem cell damage models have shown a wave of apoptosis ending within 6 hours post-injury[24]. Since decreased stem cell number was observed with both acute and chronic DBZ, apoptosis can be modeled with a negative R value in both scenarios. Apoptosis alone results in total crypt collapse (not shown), so replication of the proliferative cell expansion observed in acute DBZ would require either independent increased TA cell replication or a rebound increase in stem cell number. I modeled the latter hypothesis in Figure 4-7. Although the general trends are similar to our experimental data there are several key differences. First, increased TA cell proliferation is greatly delayed from the time of Notch inhibition and only appears after a transient decrease in TA cell number. Neither of these findings were observed in our experimental setting. Second, the chronic Notch inhibition simulation showed no transient increase in TA cell number, which we have now established occurs prior to decreased proliferation. These discrepancies in addition to the absence of *in vivo* evidence of increased apoptosis make this an unlikely mechanism regulating Notch-dependent proliferation changes.

4.5: CONCLUSIONS AND FUTURE DIRECTIONS

I devised and implemented a simple compartmental model of the intestinal crypt to test the hypothesis that Notch inhibition results in symmetric division of intestinal stem cells. I found that Notch-regulated stem cell symmetry did approximate our *in vivo* findings of stem and TA cell number with acute and chronic Notch DBZ treatment, but only in the context of Notch-regulated stem cell replacement. These findings provided important predictions such as increased TA cell number after multiple doses of DBZ and recovery of both the stem and
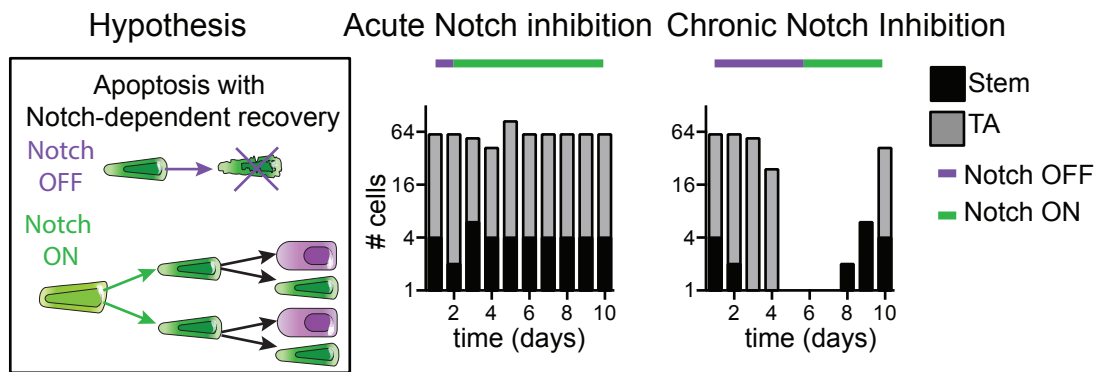
Figure 4-7. Testing apoptosis and Notch-dependent stem cell recovery as a mechanism of differential proliferation outcomes. Apoptosis is modeled by R = -2 during the Notch inhibition window (purple bar) and R = 4 immediately after Notch restoration (green bar). Initial values: S = 4, T = 60, R = 0, X = 1, ω=15.

TA cell compartments post-chronic DBZ that I was able to take back to the bench to test directly for model validation.

This discrete compartmental model is composed of a very simple framework, which makes it approachable for non-experts of mathematical and computational biology, and thus ideal for interfacing with experimental efforts. The limited parameters and assumption of synchronized cell division inherent in the model, however, also limits its predictive power, allowing only general qualitative behavior to be assessed. To garner more quantitative simulated data, I would need to generate a model with more precise parameters such as cell cycle times and rates of flow between compartments. An ordinary differential equation system could be employed to model average rates, but this system would need to ensure that the TA cell compartment remained dependent on stem cell number. Alternatively, a probabilistic agent-based model could be employed to individually track cells moving through crypt compartments.

Future revisions to the model could include a more explicit investigation of stem cell replacement. In the simulations above, R was a bulk gain or loss parameter. I arbitrarily chose a value for stem cell replacement ($R = 2$) in my Notch-dependent stem cell replacement model, which assumes that only two new stem cells can be added to the compartment each day either by quiescent stem cell division or de-differentiation. More precise testing of timing and amplitude of R modulation could determine if the dip in TA cells observed in that simulation is a necessity of the system or an artifact of timing. Furthermore, some studies suggest that TA cells can de-differentiate to repopulate the stem cell pool[23, 25]. Addition of a term that would allow movement from the TA compartment back into the stem cell compartment would allow investigation of this process in the context of Notch inhibition.

In conclusion, mathematical models do not need to be particularly complex to be extremely useful in *in silico* hypothesis testing and hypothesis generation. The data that we generated in these simulations proved to be very helpful for directing the next phases of our experimental work. These types of models can be tailored to address many aspects of ISC biology.

4.6: ACKNOWLEDGMENTS

REFERENCES

1. Johnston MD, Edwards CM, Bodmer WF, Maini PK, Chapman SJ. Mathematical modeling of cell population dynamics in the colonic crypt and in colorectal cancer. Proceedings of the National Academy of Sciences of the United States of America 2007;104:4008-13.
2. Loeffler M, Stein R, Wichmann HE, Potten CS, Kaur P, Chwalinski S. Intestinal cell proliferation. I. A comprehensive model of steady-state proliferation in the crypt. Cell and tissue kinetics 1986;19:627-45.
3. Johnston MD, Edwards CM, Bodmer WF, Maini PK, Chapman SJ. Examples of mathematical modeling: tales from the crypt. Cell cycle 2007;6:2106-12.
4. Kaur P, Potten CS. Circadian variation in migration velocity in small intestinal epithelium. Cell and tissue kinetics 1986;19:591-9.
5. Meineke FA, Potten CS, Loeffler M. Cell migration and organization in the intestinal crypt using a lattice-free model. Cell proliferation 2001;34:253-66.
6. Paulus U, Loeffler M, Zeidler J, Owen G, Potten CS. The differentiation and lineage development of goblet cells in the murine small intestinal crypt: experimental and modelling studies. Journal of cell science 1993;106 (Pt 2):473-83.
7. Gerike TG, Paulus U, Potten CS, Loeffler M. A dynamic model of proliferation and differentiation in the intestinal crypt based on a hypothetical intraepithelial growth factor. Cell proliferation 1998;31:93-110.
8. Pin C, Watson AJ, Carding SR. Modelling the spatio-temporal cell dynamics reveals novel insights on cell differentiation and proliferation in the small intestinal crypt. PloS one 2012;7:e37115.
9. Buske P, Galle J, Barker N, Aust G, Clevers H, Loeffler M. A comprehensive model of the spatio-temporal stem cell and tissue organisation in the intestinal crypt. PLoS computational biology 2011;7:e1001045.
10. Snippert HJ, van der Flier LG, Sato T, van Es JH, van den Born M, Kroon-Veenboer C, Barker N, Klein AM, van Rheenen J, Simons BD, Clevers H. Intestinal crypt homeostasis results from neutral competition between symmetrically dividing Lgr5 stem cells. Cell 2010;143:134-44.
11. Lopez-Garcia C, Klein AM, Simons BD, Winton DJ. Intestinal stem cell replacement follows a pattern of neutral drift. Science 2010;330:822-5.
12. d'Onofrio A, Tomlinson IP. A nonlinear mathematical model of cell turnover, differentiation and tumorigenesis in the intestinal crypt. Journal of theoretical biology 2007;244:367-74.
13. Tomlinson IP, Bodmer WF. Failure of programmed cell death and differentiation as causes of tumors: some simple mathematical models. Proceedings of the National Academy of Sciences of the United States of America 1995;92:11130-4.

14. Sasikumar R, Rejitha JR, Binumon PK, Manoj M. Role of heterozygous APC mutation in niche succession and initiation of colorectal cancer--a computational study. PloS one 2011;6:e22720.

15. VanDussen KL, Carulli AJ, Keeley TM, Patel SR, Puthoff BJ, Magness ST, Tran IT, Maillard I, Siebel C, Kolterud A, Grosse AS, Gumucio DL, Ernst SA, Tsai YH, Dempsey PJ, Samuelson LC. Notch signaling modulates proliferation and differentiation of intestinal crypt base columnar stem cells. Development 2012;139:488-97.

16. Potten CS. Stem cells in gastrointestinal epithelium: numbers, characteristics and death. Philosophical transactions of the Royal Society of London. Series B, Biological sciences 1998;353:821-30.

17. Cheng H, Leblond CP. Origin, differentiation and renewal of the four main epithelial cell types in the mouse small intestine. I. Columnar cell. The American journal of anatomy 1974;141:461-79.

18. Barker N, van de Wetering M, Clevers H. The intestinal stem cell. Genes & development 2008;22:1856-64.

19. Barker N, van Es JH, Kuipers J, Kujala P, van den Born M, Cozijnsen M, Haegebarth A, Korving J, Begthel H, Peters PJ, Clevers H. Identification of stem cells in small intestine and colon by marker gene Lgr5. Nature 2007;449:1003-7.

20. Tian H, Biehs B, Warming S, Leong KG, Rangell L, Klein OD, de Sauvage FJ. A reserve stem cell population in small intestine renders Lgr5-positive cells dispensable. Nature 2011;478:255-9.

21. Takeda N, Jain R, LeBoeuf MR, Wang Q, Lu MM, Epstein JA. Interconversion between intestinal stem cell populations in distinct niches. Science 2011;334:1420-4.

22. Yan KS, Chia LA, Li X, Ootani A, Su J, Lee JY, Su N, Luo Y, Heilshorn SC, Amieva MR, Sangiorgi E, Capecchi MR, Kuo CJ. The intestinal stem cell markers Bmi1 and Lgr5 identify two functionally distinct populations. Proceedings of the National Academy of Sciences of the United States of America 2012;109:466-71.

23. van Es JH, Sato T, van de Wetering M, Lyubimova A, Nee AN, Gregorieff A, Sasaki N, Zeinstra L, van den Born M, Korving J, Martens AC, Barker N, van Oudenaarden A, Clevers H. Dll1+ secretory progenitor cells revert to stem cells upon crypt damage. Nature cell biology 2012;14:1099-104.

24. Zhu Y, Huang YF, Kek C, Bulavin DV. Apoptosis differently affects lineage tracing of Lgr5 and Bmi1 intestinal stem cell populations. Cell stem cell 2013;12:298-303.

25. Buczacki SJ, Zecchini HI, Nicholson AM, Russell R, Vermeulen L, Kemp R, Winton DJ. Intestinal label-retaining cells are secretory precursors expressing Lgr5. Nature 2013;495:65-9.

CHAPTER 5

CONCLUSIONS AND FUTURE DIRECTIONS

The research undertaken for this thesis has advanced the field of intestinal stem cell (ISC) biology by furthering our understanding of how the Notch signaling pathway regulates ISC dynamics. I have tackled this question with two broad approaches: (1) determining the specificity for Notch receptors in regulating intestinal epithelial homeostasis, and (2) probing the relationships between stem and progenitor compartments in the context of Notch inhibition.

In this chapter, I will put my research in the context of the field and discuss some questions that my work raises. I present some preliminary data and discuss experimentation that can be undertaken to address these questions regarding intestinal Notch signaling and ISC regulation.

Notch1 is the primary receptor regulating intestinal epithelial differentiation

In Chapter 2, I discovered a specific role for the Notch1 (N1) receptor in controlling differentiation in the intestinal epithelium, as deletion of *N1* alone results in a dramatic secretory cell hyperplasia. The role of N1 in regulating intestinal epithelial differentiation has been contested in the literature. Previous work using specific Notch inhibitory antibodies showed a mild secretory cell defect with α-N1 antibody treatment[1] as did chimeric deletion of *N1*[2]. In contrast, Riccio et al.[3] used the *Villin-CreER^{T2}* Cre driver to conditionally delete *N1* and *N2* in the intestinal epithelium. This study[3] found that neither single deletion had any phenotype, and only double deletion of *N1* and *N2* resulted in secretory cell

161

hyperplasia. The conclusion that N1 and N2 are functionally redundant in the gut has since propagated throughout the literature.

My work also took advantage of the *Villin-CreER*^{T2} mouse model to conditionally delete *N1* and *N2* specifically in the intestinal epithelium. While it is unclear why the Riccio et al.[3] study did not uncover the $N1^{\Delta/\Delta}$ secretory cell phenotype, my study provides definitive evidence that N1 is indeed required for proper intestinal epithelial cell fate decisions.

N1 is the primary receptor for stem cell maintenance

Our lab discovered that pan-Notch inhibition with the gamma-secretase inhibitor Dibenzazepine (DBZ) resulted in a loss of crypt base columnar stem cell (CBCC) number and function, suggesting a role for Notch in CBCC survival[4]. Additional work from the Radtke lab[5] demonstrated that dual deletion of the Notch ligands *Dll1* and *Dll4* also leads to stem cell loss, bolstering our finding that Notch is required for CBCC maintenance.

In Chapter 2, I utilize the *Lgr5-GFP* mouse model, which marks CBCCs with GFP, in conjunction with *Villin-CreER*^{T2}-mediated *N1* deletion. In this system, I showed that deletion of *N1* is sufficient to reduce GFP^{HI} CBCC levels to below 50% of baseline levels. Only one other report[2] previously assessed a specific role for N1 in stem cell maintenance. Vooijs et al.[2] used a chimeric mouse model where N1-deficient cells were marked by expression of LacZ. Although N1 had been missing from these cells since development, some LacZ^{+} crypt/villus units were observed in adult animals[2]. These LacZ^{+} cells also contained an increased proportion of secretory cells compared to normal, suggesting that a N1-deficient ISC was capable of survival and production of progeny[2].

Together, these data suggest that *N1* deletion results in an initial loss of some (~50%) of CBCCs, but not all. This raises the question of why some stem cells would be susceptible to *N1* deletion but others are not. One explanation is that not all stem cells, even CBCCs, are created equal and thus might have different requirements for Notch receptor activation. A recent study utilizing

intravital imaging of stem cell division has separated the LGR5^{+} CBCC compartment into two functional groups "central cells" which occupied the lower positions in the crypt and "border cells" which occupied positions 3-4, adjacent to TA cells[6]. As an aside, the presence of two functional CBCC groups might explain why the Winton group recently found that the number of functionally active stem cells was likely to be 6 per crypt[7], despite LGR5-GFP counts showing 14-16 cells per crypt[8, 9]. Although both central and border cells can function as stem cells, central cells were shown to have a "survival advantage," which might be linked to niche exposure[10]. Since Notch is a critical component of the niche, cells that require more niche signals might be at a selective disadvantage with *N1* is deleted.

Our finding that the secretory cell hyperplasia in $N1^{\Delta/\Delta}$ intestine almost completely disappears by 2 months is consistent with N1-deficient stem cells having a selective disadvantage. These cells could be slowly replaced by normal, unrecombined stem cells over time. The Vooijs et al. study[2] discussed above did not disclose the age of animals at the time of analysis, but based on my results I would expect that the number of LacZ[+] crypts would reduce as the mice aged.

LGR5^{+} stem cells are intolerant of Notch modulation

The observation of decreased CBCCs with *N1* deletion is consistent with a number of findings that stem cells are exquisitely sensitive to loss of Notch. In data that I did not present in this thesis, I used the *LGR5-GFP-CreERT2* mouse model to investigate deletion or activation of Notch signaling components specifically in CBCCs. In these experiments, I expected to see secretory cell hyperplasia as evidence of Notch inhibitory phenotype in a patchy nature due to the mosaic nature of the Cre driver. Instead I observed no visible phenotype when *Lgr5-GFP-CreERT2* was crossed to Rbpj[F/F], DNMAML[F/F], or combined N1[F/F];N2[F/F].

Interestingly, a similar finding was observed even with Notch activation. In Chapter 2, I used a Notch activation model to understand how constitutive Notch signaling affects the intestinal epithelial proliferation and differentiation profiles.

To assess this I utilized the *Villin-CreER^{T2}* ; *Rosa26-LSL-NICD-nGFP* model, which leads to expression of activated NICD in the intestinal epithelium. In this system I found that proliferation is increased, and that all types of differentiated cells are decreased. This is important since earlier works suggested that Notch activation results in an increase in the absorptive lineage at the expense of secretory cells[11, 12].

Since Notch activation resulted in an undifferentiated phenotype and Notch is activated in a number of cancers, we were interested in determining if Notch activation specifically in CBCCs could induce intestinal adenoma formation. To study this we utilized the *Lgr5-GFP-CreER^{T2}* mouse crossed to *Rosa26-LSL-NICD-nGFP*. Interestingly, while NICD activation in LGR5$^+$ cells in the stomach led to formation of antral polyps (Figure 5-1, Demitrack et al., unpublished), no polyps were observed in the intestine.

Our hypothesis is that modulation of Notch signaling, either activation or inhibition, in CBCCs is deleterious such that these cells are at a competitive disadvantage compared to normal neighbors. This may explain why Notch signaling is not thought to be an <u>inducing</u> force for intestinal and colonic neoplasias. The fact that this phenomenon does not appear to occur in the same manner in the stomach introduces important questions of how LGR5$^+$ cells may be differentially regulated by Notch in the stomach and intestine.

Compensation versus loss of N1 deletion

While selective disadvantage would be consistent with the above findings and would result in the secretory cell hyperplasia disappearance observed in the intestinal epithelium of $N1^{\Delta/\Delta}$ animals, an obvious alternate hypothesis is that compensation by another Notch component or alternate pathway occurs leading to restoration of the tissue. We have utilized both *in situ* hybridization as well as quantitative RT-PCR for *N1* transcript to try to determine if N1 deletion rates change throughout our timecourse. At this point, both arms of the study are inconclusive, although it appears that at least a partial restoration of N1 occurs.
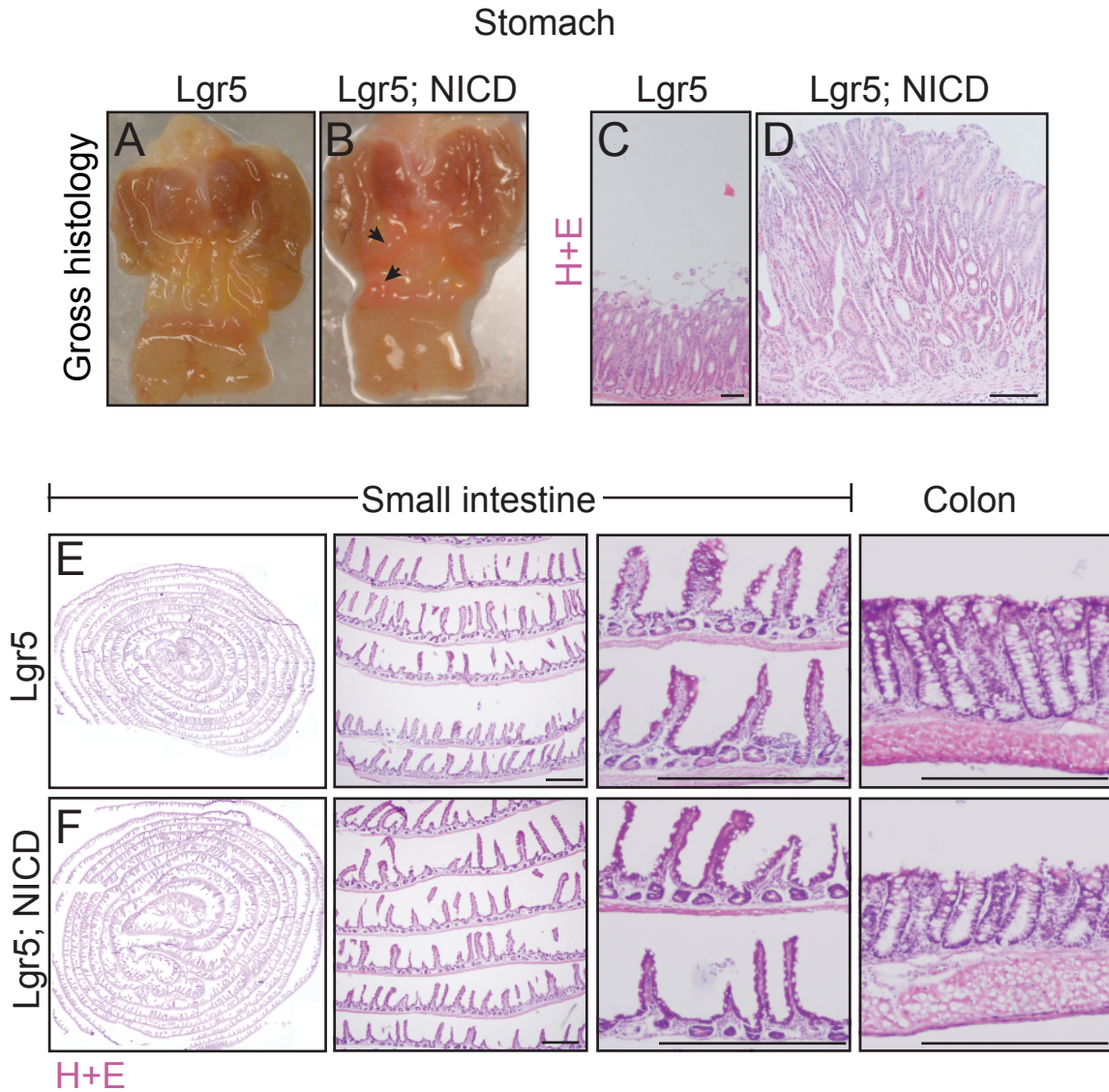
Figure 5-1. NICD activation in LGR5+ cells results in polyp formation in the stomach but not intestine. (A-B) Gross histology of Lgr5 and Lgr5; NICD stomachs 6 months after tamoxifen activation. Large antral polyps are visible in NICD stomachs (arrows) (C-D) H+E staining shows epithelial hypertrophy and glandular dysplasia in NICD polyps. (E-F) No abnormalities were observed along the entire length of the small and large intestine. Scale bars, 100 μm. (Stomach data aquired by Elise Demitrack, unpublished)

Future optimization of N1-antibody staining would help these efforts in pinpointing the extent of N1 recovery.
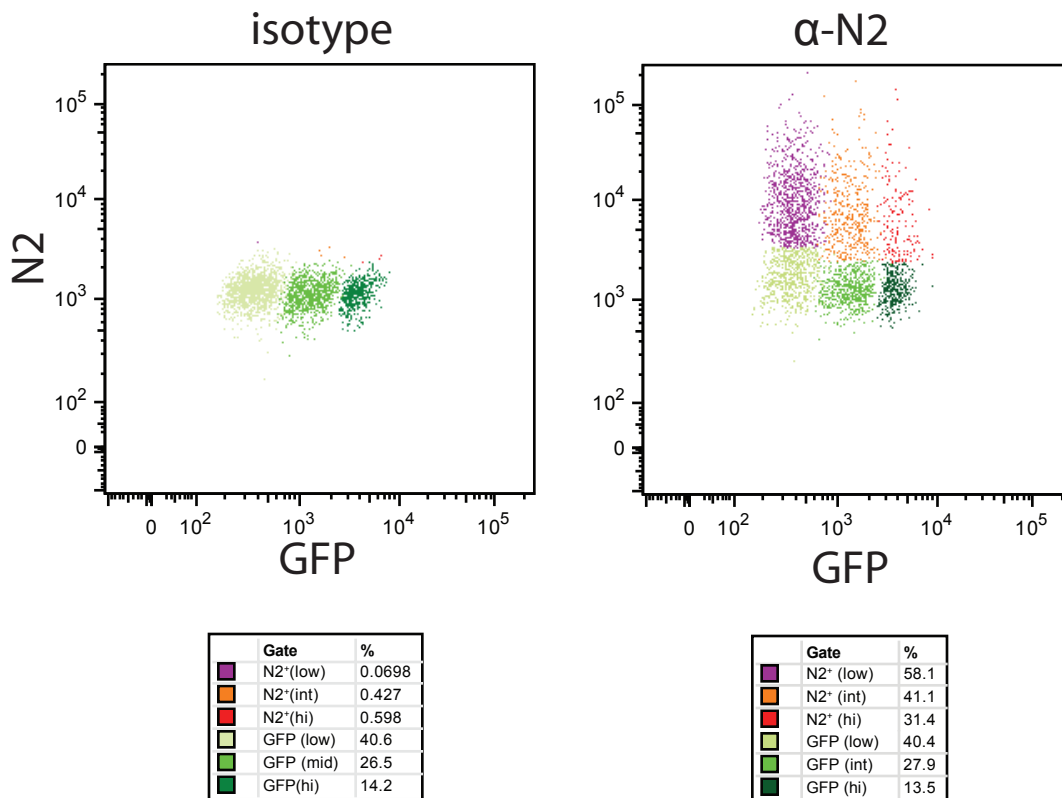
In terms of compensation, while we did observe increased expression of *Dll1* and *Dll4*, these genes returned to baseline over time and are thus not likely for the long-term normalization of $N1^{\Delta/\Delta}$. N2 is the most likely candidate for long-term compensation of N1, although we did not observe an increase in *N2* expression transcriptionally. Since much of Notch receptor activity occurs post-translationally, however, a more informative approach would be to look at changes in N2 surface expression in $N1^{\Delta/\Delta}$ animals. Preliminary flow cytometry data staining for N2 suggests that this is a feasible approach to take in the future (Figure 5-2).

A specific role for N2?

In Chapter 2, deletion of *N2* appeared to have no secretory cell phenotype, consistent with previously published results[1, 3]. By combining different combinations of *N1* and *N2* deletion I show that N1 and N2 are synergistic for epithelial differentiation and redundant for proliferation.

Previous *in situ* hybridization studies reported a range of N2 expression in the crypt, from a few cells[13] to the entire crypt[14], and a transgenic mouse model which expresses Cre in cells expressing N2 showed rare lineage tracing[14]. The reason for the rarity of the tracing is unknown, and could be due to mosaic expression of the transgene, or that N2 is functionally active on TA cells, and that lineage-traced crypts had TA cells that sporadically de-differentiated into the stem cell compartment.

My preliminary flow cytometry data discussed above (Figure 5-2) suggest that N2 is membrane-associated for all GFP^{+} cells in the crypt which would include stem and TA cells. Future work requires better-controlled trials to be confident that this staining is legitimate. In any case, moving in the direction of assessing membrane protein expression is the right path to obtaining a better understanding of Notch signaling in the intestine.

	Gate	%
■	N2+(low)	0.0698
■	N2+(int)	0.427
■	N2+(hi)	0.598
■	GFP (low)	40.6
■	GFP (mid)	26.5
■	GFP(hi)	14.2

	Gate	%
■	N2+ (low)	58.1
■	N2+ (int)	41.1
■	N2+ (hi)	31.4
■	GFP (low)	40.4
■	GFP (int)	27.9
■	GFP (hi)	13.5

Figure 5-2. Preliminary N2 staining of intestinal epithelial cells. Singly isolated cells from Lgr5-GFP jejunum were stained with anti-N2 antibody or isotype control. Cells were sequentially gated for size, singlets, DAPI$^-$, CD45.2$^-$, EpCAM$^+$, and GFP$^+$. Low background staining is observed in isotype-stained control, but N2 staining is observed in GFP^{HI}, GFP^{INT}, and GFP^{LOW} populations suggesting that N2 has surface expression on a subset of all stem and TA cells. This is a promising technique to investigate compensation of N2 in N1-deleted intestine.

Acute Notch inhibition leads to increased proliferation and shifted stem cells

In Chapter 3, I turn back to a pharmacologic inhibition model with DBZ to understand what happens to a stem cell once Notch signaling is turned off. Since chronic Notch inhibition is typically associated with decreased proliferation and increased secretory cells, I was surprised to find that a single (acute) dose of DBZ led to both <u>increased proliferation</u> and increased secretory cell production.

Exploiting the gradient GFP expression in the crypts of the *Lgr5-GFP-CreER^{T2}* mouse model, I used flow cytometry to analyze GFP^{HI} and GFP^{INT} cells which are expected to be CBCCs and first level TA progenitors, respectively. With this technique I found that acute DBZ treatment led to a decrease in GFP^{HI} cells that was always associated with an increase in GFP^{INT} cells, consistent with a bulk shift from the stem to progenitor cell compartments.

I used mathematical modeling (discussed below) to test the hypothesis that the increased proliferation of acute DBZ is caused by symmetric stem cell division and determined that Notch was also involved in CBCC replacement, presumably by a QSC population.

Notch regulation of CBCC replacement

To test the role of Notch in CBCC repopulation, I performed acute DBZ in the post-irradiation setting. Since irradiation leads to CBCC death[15-17] this model aimed to block Notch signaling in the remaining QSCs. Increased QSC abundance is observed after irradiation[15, 18, 19], and indeed increased overall epithelial proliferation was observed in our post-irradiation DBZ animals, despite intestinal architecture collapse. This suggests that Notch is not required for QSC activation. Additional experiments using the *Bmi1-Cre^{ER}*; *Rbpj$^{F/F}$* model in the irradiation setting resulted in similar results, as proliferative cell expansion was observed despite inactivation of Notch signaling.

These experiments are admittedly difficult to interpret. Timing of DBZ treatment and tamoxifen induction with the timing of irradiation injury could have major effects on the outcome. For instance, we administered DBZ 24 hours after 12Gy irradiation. Studies have shown that BMI1^{+} cells are more proliferative by 2

days after 12 Gy[15]. It is possible, however, that this process starts within 24 hours after irradiation exposure and that the DBZ was administered too late to effectively block activation. Additionally, acute DBZ itself led to increased proliferation. Since division of CBCCs into TA cells is thought to be the source of the increased proliferation in acute DBZ, and CBCCs are killed by irradiation, it is likely that the proliferative cells are QSC-derived rather than CBCC-derived. Including a lineage trace reporter gene or utilizing the *Bmi1-GFP* transgenic mouse[20] would help to differentiate between these possibilities. The fact that the post-irradiation DBZ led to rapid lethality and total epithelial collapse despite a proliferative surge is another interesting avenue that needs to be followed up.

Notch is required for post-irradiation recovery

       I have shown that various means of Notch inhibition render the intestine incapable of irradiation recovery: N1-deletion (Chapter 2), α-N1 inhibitory antibody treatment[21], and DBZ treatment in the post-irradiation setting (Chapter 3 and Tran et al.[21]). While the cause of death is not clear in these animals, it is clear that combination of irradiation and Notch inhibition is deleterious. This is one of the most striking and important findings in my thesis, as it implies that potential Notch-inhibiting cancer drugs should not be used in combination regimes with therapeutic or palliative radiation treatment.   Interestingly, Notch inhibition in the post-irradiation setting (post-irradiation DBZ or inhibitory antibodies) appears to lead to decreased secretory cell determination, the exact opposite of Notch inhibition on its own. Additionally, in Chapter 2, I found that the Notch target gene *Olfm4* is markedly reduced immediately after irradiation treatment. This gene is expected to decline since it is a CBCC marker, and CBCCs are killed by irradiation, but its loss of expression precedes the loss of *Lgr5*, suggesting that Notch may be directly inhibited by irradiation damage. If this is the case, it will be important to determine if intestinal epithelial Notch is required for recovery from other injury modalities or if this extreme sensitivity is specific to irradiation treatment.

Compartmental mathematical modeling of the intestinal crypt

Part of my thesis work has been devoted to understanding the state-of-the-art in terms of compartmental mathematical modeling of the intestinal crypt. I published a review[22] in a journal geared to integrate biological and computational themes to educate both sides of the community about models that have successfully described intestinal homeostasis and tumorigenesis, post-irradiation recovery, and crypt development. I have outlined methods that could be undertaken to use compartmental modeling in conjunction with experimentation to answer several of the lingering questions that remain in the ISC field such as: How is stem cell number regulated? Are ISCs completely defined by the niche? Is there a dedicated QSC population? What is the nature of the TA compartment?

In Chapter 4, I directly take advantage of compartmental mathematical modeling to test my hypothesis: *Does Notch regulate the symmetry of stem cell division?* In this chapter, I first exploit one of the most valuable aspects of *in silico* work; the ability to use previously published models to test new hypotheses. I used the ordinary differential equation model of crypt homeostasis and tumorigenesis by Johnston et al.[23] to test my Notch regulation of stem cell symmetry hypothesis. I found that while this model is suitable for evaluating stem, TA, and differentiated cell populations averaged over long periods of time, it was not appropriate to look at short-term changes like those expected during Notch inhibition.

I then designed my own discrete compartmental mathematical model of the crypt to test my hypothesis. With this model I was able to obtain qualitative predictions of stem and TA cell numbers where inhibition of Notch results in symmetric stem cell division resulting in formation of 2 TA progenitors. I found that alteration of symmetry alone did not replicate the restoration of homeostasis observed in acute Notch inhibition. Rather, I found that my experimental findings of increased TA cells/decreased stem cells with acute DBZ and decreased TA

cells/decreased stem cells with chronic DBZ were replicated by a mechanism where Notch regulates symmetry as well as CBCC replacement.

This approach allowed me to test some of my modeling predictions *in vivo*, but future revisions of the model integrating robust cell counting data as well as accurate cell division rates would allow for more quantitative predictions. Importantly, my work demonstrates a simple scaffold that can be adapted to test many other signaling pathways that may be involved in regulating stem cells.

Asymmetric stem cell division in the ISC

Although the concept of stem cell division asymmetry is commonplace for other tissue stem cells[24-27], the idea is controversial in ISCs. This is due to neutral drift dynamics studies that determined that ISCs divide symmetrically to form equipotential cells, which are equally capable of becoming stem cells or TA cells depending on niche availability[9, 28]. A revision of this model now suggests that stem cells can either become a central CBCC, a border CBCC, or a TA cell, and that there is priority in central CBCCs staying in the stem cell compartment[10]. These authors[10] still contend that these decisions are based off of niche availability rather than any intrinsic asymmetry of division.

Interestingly, asymmetric stem cell division was directly observed during crypt development[29]. Either ISCs lose the ability to divide asymmetrically with maturity or these studies are incapable of adequately visualizing asymmetric stem cell division. A study in adult drosophila ISCs showed localization of Par complex and integrins on the spindle to position NUMB for successful asymmetric stem cell division[30]. Many drosophila ISC findings have been replicated in mammals, so it is disconcerting that such a stark difference exists in the method of stem cell division. A better evaluation of NUMB and other proteins associated with asymmetric stem cell division is required before eliminating this as a possibility for adult mammalian ISCs. Whether ISCs truly divide asymmetrically or not, my data suggests that Notch plays an important role in eventual population asymmetry of crypt.

In conclusion, the Notch signaling pathway is important for many aspects of intestinal epithelial homeostasis. My thesis work has illustrated an important role for the N1 receptor in regulating epithelial cell fate and stem cell maintenance, especially in the post-irradiation setting. Additionally, I have shown that loss of Notch signaling leads to CBCC removal from the stem cell compartment by division into the TA cell compartment. Prolonged Notch inhibition results in TA cell collapse since CBCC replacement can only occur with active Notch signaling providing a CBCC niche.

REFERENCES

1. Wu Y, Cain-Hom C, Choy L, Hagenbeek TJ, de Leon GP, Chen Y, Finkle D, Venook R, Wu X, Ridgway J, Schahin-Reed D, Dow GJ, Shelton A, Stawicki S, Watts RJ, Zhang J, Choy R, Howard P, Kadyk L, Yan M, Zha J, Callahan CA, Hymowitz SG, Siebel CW. Therapeutic antibody targeting of individual Notch receptors. Nature 2010;464:1052-7.
2. Vooijs M, Ong CT, Hadland B, Huppert S, Liu Z, Korving J, van den Born M, Stappenbeck T, Wu Y, Clevers H, Kopan R. Mapping the consequence of Notch1 proteolysis in vivo with NIP-CRE. Development 2007;134:535-44.
3. Riccio O, van Gijn ME, Bezdek AC, Pellegrinet L, van Es JH, Zimber-Strobl U, Strobl LJ, Honjo T, Clevers H, Radtke F. Loss of intestinal crypt progenitor cells owing to inactivation of both Notch1 and Notch2 is accompanied by derepression of CDK inhibitors p27Kip1 and p57Kip2. EMBO Rep 2008;9:377-83.
4. VanDussen KL, Carulli AJ, Keeley TM, Patel SR, Puthoff BJ, Magness ST, Tran IT, Maillard I, Siebel C, Kolterud A, Grosse AS, Gumucio DL, Ernst SA, Tsai YH, Dempsey PJ, Samuelson LC. Notch signaling modulates proliferation and differentiation of intestinal crypt base columnar stem cells. Development 2012;139:488-97.
5. Pellegrinet L, Rodilla V, Liu Z, Chen S, Koch U, Espinosa L, Kaestner KH, Kopan R, Lewis J, Radtke F. Dll1- and dll4-mediated notch signaling are required for homeostasis of intestinal stem cells. Gastroenterology 2011;140:1230-1240 e7.
6. Ritsma L, Ellenbroek SI, Zomer A, Snippert HJ, de Sauvage FJ, Simons BD, Clevers H, van Rheenen J. Intestinal crypt homeostasis revealed at single-stem-cell level by in vivo live imaging. Nature 2014;507:362-5.
7. Kozar S, Morrissey E, Nicholson AM, van der Heijden M, Zecchini HI, Kemp R, Tavare S, Vermeulen L, Winton DJ. Continuous clonal labeling reveals small numbers of functional stem cells in intestinal crypts and adenomas. Cell stem cell 2013;13:626-33.
8. Barker N, van Es JH, Kuipers J, Kujala P, van den Born M, Cozijnsen M, Haegebarth A, Korving J, Begthel H, Peters PJ, Clevers H. Identification of stem cells in small intestine and colon by marker gene Lgr5. Nature 2007;449:1003-7.
9. Snippert HJ, van der Flier LG, Sato T, van Es JH, van den Born M, Kroon-Veenboer C, Barker N, Klein AM, van Rheenen J, Simons BD, Clevers H. Intestinal crypt homeostasis results from neutral competition between symmetrically dividing Lgr5 stem cells. Cell 2010;143:134-44.
10. Ritsma L, Ellenbroek SI, Zomer A, Snippert HJ, de Sauvage FJ, Simons BD, Clevers H, van Rheenen J. Intestinal crypt homeostasis revealed at single-stem-cell level by in vivo live imaging. Nature 2014.

11. Fre S, Huyghe M, Mourikis P, Robine S, Louvard D, Artavanis-Tsakonas S. Notch signals control the fate of immature progenitor cells in the intestine. Nature 2005;435:964-8.

12. Stanger BZ, Datar R, Murtaugh LC, Melton DA. Direct regulation of intestinal fate by Notch. Proc Natl Acad Sci U S A 2005;102:12443-8.

13. Sander GR, Powell BC. Expression of notch receptors and ligands in the adult gut. J Histochem Cytochem 2004;52:509-16.

14. Fre S, Hannezo E, Sale S, Huyghe M, Lafkas D, Kissel H, Louvi A, Greve J, Louvard D, Artavanis-Tsakonas S. Notch lineages and activity in intestinal stem cells determined by a new set of knock-in mice. PloS one 2011;6:e25785.

15. Yan KS, Chia LA, Li X, Ootani A, Su J, Lee JY, Su N, Luo Y, Heilshorn SC, Amieva MR, Sangiorgi E, Capecchi MR, Kuo CJ. The intestinal stem cell markers Bmi1 and Lgr5 identify two functionally distinct populations. Proceedings of the National Academy of Sciences of the United States of America 2012;109:466-71.

16. Potten CS, Hendry JH. Differential regeneration of intestinal proliferative cells and cryptogenic cells after irradiation. International journal of radiation biology and related studies in physics, chemistry, and medicine 1975;27:413-24.

17. Zhu Y, Huang YF, Kek C, Bulavin DV. Apoptosis differently affects lineage tracing of Lgr5 and Bmi1 intestinal stem cell populations. Cell stem cell 2013;12:298-303.

18. Van Landeghem L, Santoro MA, Krebs AE, Mah AT, Dehmer JJ, Gracz AD, Scull BP, McNaughton K, Magness ST, Lund PK. Activation of two distinct Sox9-EGFP-expressing intestinal stem cell populations during crypt regeneration after irradiation. American journal of physiology. Gastrointestinal and liver physiology 2012;302:G1111-32.

19. Takeda N, Jain R, LeBoeuf MR, Wang Q, Lu MM, Epstein JA. Interconversion between intestinal stem cell populations in distinct niches. Science 2011;334:1420-4.

20. Hosen N, Yamane T, Muijtjens M, Pham K, Clarke MF, Weissman IL. Bmi-1-green fluorescent protein-knock-in mice reveal the dynamic regulation of bmi-1 expression in normal and leukemic hematopoietic cells. Stem cells 2007;25:1635-44.

21. Tran IT, Sandy AR, Carulli AJ, Ebens C, Chung J, Shan GT, Radojcic V, Friedman A, Gridley T, Shelton A, Reddy P, Samuelson LC, Yan M, Siebel CW, Maillard I. Blockade of individual Notch ligands and receptors controls graft-versus-host disease. The Journal of clinical investigation 2013;123:1590-604.

22. Carulli AJ, Samuelson LC, Schnell S. Unraveling intestinal stem cell behavior with models of crypt dynamics. Integrative biology : quantitative biosciences from nano to macro 2014;6:243-57.

23. Johnston MD, Edwards CM, Bodmer WF, Maini PK, Chapman SJ. Mathematical modeling of cell population dynamics in the colonic crypt

and in colorectal cancer. Proceedings of the National Academy of Sciences of the United States of America 2007;104:4008-13.

24. Betschinger J, Knoblich JA. Dare to be different: asymmetric cell division in Drosophila, C. elegans and vertebrates. Current biology : CB 2004;14:R674-85.

25. Bielen H, Houart C. The Wnt cries many: Wnt regulation of neurogenesis through tissue patterning, proliferation, and asymmetric cell division. Developmental neurobiology 2014.

26. Morrison SJ, Kimble J. Asymmetric and symmetric stem-cell divisions in development and cancer. Nature 2006;441:1068-74.

27. Sun SC, Kim NH. Molecular mechanisms of asymmetric division in oocytes. Microscopy and microanalysis : the official journal of Microscopy Society of America, Microbeam Analysis Society, Microscopical Society of Canada 2013;19:883-97.

28. Lopez-Garcia C, Klein AM, Simons BD, Winton DJ. Intestinal stem cell replacement follows a pattern of neutral drift. Science 2010;330:822-5.

29. Itzkovitz S, Blat IC, Jacks T, Clevers H, van Oudenaarden A. Optimality in the development of intestinal crypts. Cell 2012;148:608-19.

30. Goulas S, Conder R, Knoblich JA. The Par complex and integrins direct asymmetric cell division in adult intestinal stem cells. Cell stem cell 2012;11:529-40.